





THE UNIVERSITY of ADELAIDE

# Analysis of MADS-box genes and heat stress in barley (*Hordeum vulgare*)

**by Cindy CALLENS, MSc**

Thesis submitted to the University of Nottingham and the University of Adelaide for the degree of Doctor of Philosophy, September 2019

# Table of contents

**Table of contents** ..... **I**

**Acknowledgements** ..... **III**

**List of Figures** ..... **IV**

**List of Tables** ..... **VI**

**Abstract** ..... **VII**

**Chapter 1: Introduction** ..... **1**
1.1 Abstract ..... 2
1.2 Introduction ..... 2
1.3 The MADS-box protein f ..... 4
1.4 MADS-box protein structure is conserved between diverse plant species ..... 4
1.5 The role of MIKCc-type MADS-box proteins in the ABCDE model of flower development ..... 5
1.6 The ABCDE model in monocots ..... 5
*1.6.1 A-class genes* ..... *6*
*1.6.2 B-class genes* ..... *10*
*1.6.3 C- and D-class genes* ..... *14*
*1.6.4 E-class genes* ..... *17*
*1.6.5 AGL6-like genes* ..... *20*
1.7 Conclusions and perspectives ..... 22
1.8 Acknowledgements ..... 23
1.9 References ..... 23

**Chapter 1: Supplementary files** ..... **28**

**Aims and objectives** ..... **36**

**Chapter 2: Expression analysis and protein-protein interactions of the DEF/GLO-like MADS-box genes in barley (*Hordeum vulgare*)** ..... **37**
2.1 Introduction ..... 40
*2.1.1 Expression patterns of ABCDE MADS-box genes in grasses* ..... *40*
*2.1.2 Protein-protein interactions of B-class MADS-box genes in grasses* ..... *45*
2.2 Materials and methods ..... 47
*2.2.1 Plant materials, growth conditions and sample preparation* ..... *47*
*2.2.2 Quantitative reverse transcription PCR (qRT-PCR)* ..... *48*
*2.2.3 Clustering analysis* ..... *49*
*2.2.4 In Situ Hybridization* ..... *51*
2.3 Results ..... 51
*2.3.1 Expression analysis of the ABCDE MADS-box genes in barley* ..... *51*
2.4 Discussion ..... 60
2.5 References ..... 65

**Chapter 3: Functional analysis of the DEF/GLO-like MADS-box genes in barley (*Hordeum vulgare*)** ..... **70**
3.1 Introduction ..... 73
3.2 Materials and methods ..... 74
*3.2.1 Design of SRDX pBract214 dominant repression constructs* ..... *74*
*3.2.2 Agrobacterium-mediated barley transformation* ..... *75*
*3.2.3 Plant materials and growth conditions* ..... *76*
*3.2.4 Genotyping* ..... *77*
*3.2.5 Phenotyping* ..... *77*
*3.2.6 Pollen viability assay with Fluorescein Diacetate (FDA) stain* ..... *77*

*3.2.8 Quantitative reverse transcription (qRT) PCR* ..... *78*
*3.2.9 Evaluation of sterility in barley transformants expressing pUBI:HvBM2-SRDX* *78*
3.3 Results ..... 78
*3.3.1 Barley transformants expressing pUBI:HvBM2-SRDX* ..... *78*
*3.3.2 Barley transformants expressing pUBI:HvBM4-SRDX* ..... *79*
*3.3.3 Barley transformants expressing pUBI:HvBM16-SRDX* ..... *83*
*3.3.4 Embryos transformed with pUBI:HvBM2-SRDX, pUBI:HvBM4-SRDX and pUBI:HvBM16-SRDX* ..... *83*
3.4 Discussion ..... 89
3.5 References ..... 91

**Chapter 4: Effects of heat stress on reproductive development in three European barley varieties ..... 94**
4.1 Abstract ..... 98
4.2 Introduction ..... 98
4.3 Materials and methods ..... 100
*4.3.1 Plant materials and growth conditions* ..... *100*
*4.3.2 Pollen viability assay* ..... *101*
*4.3.3 Immunolabelling* ..... *102*
*4.3.4 3D X-ray imaging* ..... *102*
*4.3.5 Phenotyping* ..... *102*
*4.3.6 Evaluation of sterility* ..... *103*
4.4 Results ..... 103
*4.4.1 Anther morphology in barley varieties after heat stress* ..... *103*
*4.4.2 Carpel morphology in barley varieties after heat stress* ..... *107*
*4.4.3 Male fertility after heat stress* ..... *107*
*4.4.4 Seed set after heat stress* ..... *110*
4.5 Discussion ..... 111
4.6 Conclusions ..... 113
4.7 Acknowledgements ..... 114
4.8 References ..... 115

**Chapter 4: Supplementary files ..... 119**

**Chapter 5: Discussion ..... 126**
5.1 Expression of the A-, Bsister-like, C-, D-, E- and AGL6-like MADS-box genes in barley ..... 127
5.2 Expression and protein-protein interactions of the B-class MADS-box genes in barley ..... 130
5.3 Function of the B-class genes in flower development in barley ..... 131
5.4 MADS-box genes and abiotic stress ..... 135
5.5 Conclusions and future work ..... 140
5.6 References ..... 143

# Acknowledgements

It's quite astonishing that four years of my life fit into 150 pages, but here it is. The friends and knowledge I've gained and the experiences I was privileged enough to have in those four years would probably need several hundred more pages.
I am incredibly grateful for the opportunity I got with this PhD. I still remember the day I got the offer. I was sitting in a hotel lobby in Italy, ready for a weekend of volunteering at the first IQA European Games. I screamed and laughed and marvelled at the fact that I would be doing a PhD. Not only that, I'd be doing a PhD in the UK and in Australia! My quidditch friends joined me in celebration. Quidditch is the sort of warm community that makes sure you have a family in every country. That was very much true in Australia where I was welcomed with open arms by the Adelaide team. They will forever be my Adelaide family. But childhood friends are that other rare kind of family. The family you choose. My two best friends have been there for me for over a decade and I would be absolutely lost without them. They have always believed in me and supported me, even when I failed. My parents deserve a big thank you too, as they (reluctantly) said goodbye to me for four years to go off on my adventure abroad. They are everything to me.

I owe a lot to my mentor in the lab, Dr. Jose Fernandez. He taught me everything I know and guided me through the pitfalls of molecular biology even when I was across the world. The friends I made in the lab, both in Nottingham and in Adelaide, have been so valuable to me. Dr. Debbie Devis kept me sane and was an incredible friend to me in a country where I didn't know anyone. Dr. Jonathan Atkinson and Dr. Lorna McAusland are two of the kindest people I know and have been amazing. They are always there to listen and make me feel better.
All the people in the Wilson lab have been absolutely fantastic, helping whenever I needed it. They are all part of this thesis.

I could never have succeeded without my supervisor Prof. Zoe Wilson. Always available when I was having a tough time, having my back and providing me with invaluable advice. Thank you also to my supervisors in Adelaide, Prof. Dabing Zhang and A/Prof. Matthew Tucker, for all the support and guidance during the two years I was in Adelaide and beyond.

# List of Figures

**Figure 1.1** Rice, maize, wheat, barley, orchid and lily floral structures.
**Figure 1.2** Structure of MIKC-type MADS-box proteins.
**Figure 1.3** The ABCDE model in rice florets. The model depicts the pattern of gene expression required for normal whorl development.
**Figure 1.4** Phylogenetic analysis of ABCDE MADS-box genes from *Arabidopsis, Amborella trichopoda, Populus trichocarpa*, rice, maize, wheat, barley, orchid and lily.
**Figure 1.5** Sequence alignment and expression patterns of A-class MADS-box genes in *Arabidopsis, Amborella trichopoda, Populus trichocarpa*, rice, maize, barley, wheat, orchid and lily.
**Figure 1.6** Sequence alignment and expression patterns of B-class MADS-box genes in *Arabidopsis, Amborella trichopoda, Populus trichocarpa*, rice, maize, barley, wheat, orchid and lily.
**Figure 1.7** Sequence alignment and expression patterns of $B_{sister}$-class MADS-box genes in *Arabidopsis, Amborella trichopoda, Populus trichocarpa*, rice, maize, barley, wheat, orchid and lily.
**Figure 1.8** Sequence alignment and expression patterns of C-class MADS-box genes in *Arabidopsis, Amborella trichopoda, Populus trichocarpa*, rice, maize, wheat, barley, orchid and lily.
**Figure 1.9** Sequence alignment and expression patterns of D-class MADS-box genes in *Arabidopsis, Amborella trichopoda, Populus trichocarpa*, rice, maize, wheat, barley, orchid and lily.
**Figure 1.10** Sequence alignment and expression patterns of E-class MADS-box genes in *Arabidopsis, Amborella trichopoda, Populus trichocarpa*, rice, maize, wheat, barley, orchid and lily.
**Figure 1.11** Sequence alignment and expression patterns of AGL6-like MADS-box genes in *Arabidopsis, Amborella trichopoda, Populus trichocarpa*, rice, maize, wheat, barley, orchid and lily.
**Figure 2.1** Structure of the K-box domain in $MIKC^c$ MADS-box genes.
**Figure 2.2** B-class genes HvBM2 and HvBM4 on the reverse strand and the presence of Receptor Kinase 2 and 3 on the forward strand.
**Figure 2.3** Heat map showing expression patterns of the ABCDE MADS-box genes in barley.
**Figure 2.4** Real-time quantitative PCR expression analysis of A-class and B-class MADS-box genes.
**Figure 2.5** Real-time quantitative PCR expression analysis of B-class, $B_{sister}$-like, C-class and D-class MADS-box genes.
**Figure 2.6** Real-time quantitative PCR expression analysis of AGL6-like MADS-box genes and changes in expression between biological replicates in stages LFE2 and LFE4.
**Figure 2.7** Heat map showing hierarchical clustering of the relative expression values of the ABCDE MADS-box genes in barley.
**Figure 2.8** mRNA in situ hybridization of the *HvBM2* transcript.
**Figure 2.9** Schematic overview of potential interacting ABCDE MADS-box proteins in development of floral tissues at different developmental stages.
**Figure 3** Schematic representation of the SRDX mode of action.

**Figure 3.1** Phenotype of carpel, stamens and lodicules in barley transformants expressing *pUBI:HvBM2-SRDX* compared to control florets.
**Figure 3.2** Pollen viability of barley transformants expression *pUBI:HvBM2-SRDX*, *pUBI:HvBM4-SRDX* or *pUBI:HvBM16-SRDX* compared to control.
**Figure 3.3** Sterility in barley transformants expressing *pUBI:HvBM2-SRDX*
**Figure 3.4** Phenotype of carpel, stamens and lodicules in barley transformants expressing *pUBI:HvBM4-SRDX* compared to control florets.
**Figure 3.5** Phenotype of carpel, stamens and lodicules in barley transformants *pUBI:HvBM16-SRDX* compared to control florets.
**Figure 3.6** Phenotype of carpel, stamens and lodicules in barley transformants expressing a combination of *pUBI:HvBM2-SRDX* and *pUBI:HvBM16-SRDX* (Line C) constructs compared to control florets.
**Figure 3.7** Phenotype of carpel, stamens and lodicules in barley transformants expressing a combination of *pUBI:HvBM4-SRDX* and *pUBI:HvBM16-SRDX* (Line C) constructs compared to control florets.
**Figure 3.8** Expression analysis of the *pUBI:HvBM2-SRDX* (A) and *pUBI:HvBM4-SRDX* (B) constructs in plants exhibiting a phenotype.
**Figure 3.9** Phenotype of carpel, stamens and lodicules in barley transformants expressing a combination of *pUBI:HvBM4-SRDX* and *pUBI:HvBM16-SRDX* (Line E) constructs compared to control florets.
**Figure 4.1** Anther development in barley cultivars Optic, Moonshine and RGT Planet.
**Figure 4.2** X-ray CT images of (A) anther and (B) carpel development in control and heat stress conditions for Optic and Planet.
**Figure 4.3** X-ray CT images of anther and carpel development in control and heat stress conditions for Moonshine.
**Figure 4.4** Immunolabelling of cell wall components in anthers and ovules in Optic, Moonshine and Planet.
**Figure 5.1** Hypothetical ABCDE model in barley based on expression analysis, hierarchical clustering and functional analysis of the B-class genes.

# List of Tables

**Table 1.1** The ABCDE genes in *Arabidopsis* and monocot species.
**Table 2.1** Developmental staging and spike size for samples collected from *Hordeum vulgare cv. Golden Promise*.
**Table 2.2** Gene specific primers designed for the ABCDE MADS-box genes for Real-time quantitative PCR analysis.
**Table 3.1** Primers used for the design of *HvBM2*, *HvBM4* and *HvBM16* SRDX dominant repression constructs.
**Table 3.2** Primers designed for genotyping of the *HvBM2*, *HvBM4* and *HvBM16* SRDX pBract214 constructs in transformed barley plants.
**Table 3.3** Overview of the constructs transformed in the transgenic plants and the resulting phenotypes.
**Table 4.1** Average number of tillers per plant and seeds per spike, and number of tagged tillers for the three different varieties in control conditions, after meiosis heat treatment or after mitosis heat treatment ± standard deviation. Stars indicate a p -value <0.05.
**Table 5.1** Comparison of expression patterns in rice, maize, wheat and barley in different floral organ tissues.

## Abstract

Barley is a widely grown, economically important cereal crop used for stock feed, malting and brewing. Fundamental understanding of the underlying genetic network controlling floral organ development is essential for potential modification of floral architecture for plant breeding. ABCDE-model MADS-box proteins are a type of MADS-box family transcription factors that contain a conserved 60 amino acid MADS-box motif and that are involved in inflorescence and flower development. In the dicot model *Arabidopsis thaliana* and in crops like rice (*Oryza sativa*), maize (*Zea mays*) and wheat (*Triticum aestivum*) most of the ABCDE-model MADS-box flowering genes have been identified. In barley (*Hordeum vulgare*) however, only a select number of MADS-box flowering genes have been investigated. Identifying the role and structure of the ABCDE-model MADS-box genes in barley floral development could shed a light on the evolutionary differences between barley and closely related crops and the development of their inflorescences and flower morphogenesis. In this thesis I aimed to identify the expression patterns of the ABCDE-model MADS-box genes in barley by qRT-PCR and in situ hybridization. To investigate the function of the B-class genes in barley the CRES-T dominant repression system, also known as SRDX, was used. Results showed that the expression patterns of the ABCDE MADS-box genes are conserved in barley and that the B-class genes have a redundant function in stamens and lodicule development. MADS-box transcription factors have been shown to be involved in abiotic stress tolerance in several different species like tomato, rice and sheepgrass. Abiotic stresses, particularly global warming, are the major causes of crop yield losses by affecting fertility and seed set. Prior to analysis of the specific impact of abiotic stress on the MADS-box genes, it is important to understand the effects of abiotic stress on barley per se. Effects of heat stress on reproductive structures and fertility in barley have not been extensively investigated. In this thesis the effect of high temperature conditions on floral development in three commercial European spring barley varieties during two vulnerable reproductive stages, meiosis and mitosis, was examined by using fertility assays, 3-dimensional modelling, cytology and immunolabelling. Results showed that male reproductive organs are more vulnerable to heat stress than female reproductive organs and that certain varieties are more tolerant to heat stress.

# Chapter 1: Introduction

## Dissecting the role of MADS-box genes in monocot floral development and diversity

Cindy Callens[1,2], Matthew R. Tucker[2], Dabing Zhang[2,3] and Zoe A. Wilson[1]

[1] School of Biosciences, University of Nottingham, Sutton Bonington Campus, Loughborough, Leicestershire LE12 5RD, UK
[2] School of Agriculture, Food and Wine, University of Adelaide, Waite Campus, Urrbrae, SA, Australia
[3] School of Life Sciences and Biotechnology, Shanghai Jiao Tong University, Shanghai 200240, China

*Journal of Experimental Botany*
doi:10.1093/jxb/ery086

FLOWERING NEWSLETTER REVIEW

# Dissecting the role of MADS-box genes in monocot floral development and diversity

**Cindy Callens[1,2], Matthew R. Tucker[2], Dabing Zhang[2,3] and Zoe A. Wilson[1,*]**

[1] School of Biosciences, University of Nottingham, Sutton Bonington Campus, Loughborough, Leicestershire LE12 5RD, UK
[2] School of Agriculture, Food and Wine, University of Adelaide, Waite Campus, Urrbrae, SA, Australia
[3] School of Life Sciences and Biotechnology, Shanghai Jiao Tong University, Shanghai 200240, China

* Correspondence: zoe.wilson@nottingham.ac.uk

Received 15 November 2017; Editorial decision 26 February 2018; Accepted 16 March 2018

Editor: Frank Wellmer, Trinity College Dublin, Ireland

## Abstract

**Many monocot plants have high social and economic value. These include grasses such as rice (*Oryza sativa*), wheat (*Triticum aestivum*), and barley (*Hordeum vulgare*), which produce soft commodities for many food and beverage industries, and ornamental flowers such ase lily (*Lilium longiflorum*) and orchid (*Oncidium* Gower Ramsey), which represent an important component of international flower markets. There is constant pressure to improve the development and diversity of these species, with a significant emphasis on flower development, and this is particularly relevant considering the impact of changing environments on reproduction and thus yield. MADS-box proteins are a family of transcription factors that contain a conserved 60 amino acid MADS-box motif. In plants, attention has been devoted to characterization of this family due to their roles in inflorescence and flower development, which holds promise for the modification of floral architecture for plant breeding. This has been explored in diverse angiosperms, but particularly the dicot model *Arabidopsis thaliana*. The focus of this review is on the less well characterized roles of the MADS-box proteins in monocot flower development and how changes in MADS-box proteins throughout evolution may have contributed to creating a diverse range of flowers. Examining these changes within the monocots can identify the importance of certain genes and pinpoint those which might be useful in future crop improvement and breeding strategies.**

**Keywords:** Arabidopsis, barley, floral development, inflorescence, lily, MADS-box, monocots, rice, transcription factors, wheat, orchid.

## Introduction

The grass family, Poaceae, diverged from other Poales ~55–70 million years ago (Bommert *et al.*, 2005). The inflorescence morphology of grasses is one of the major determinants of yield, and is thus a key breeding target (Bommert *et al.*, 2005). Identifying genes and proteins that are involved in flower development and their behaviour in high-yielding varieties and varieties that are resistant to biotic and abiotic stresses may help to identify pathways that can be targeted for the improvement of important crops.

Much of our knowledge of flower structure, morphology, and genetics has been gained through study of the model dicotyledonous plants *Arabidopsis thaliana* and *Antirrhinum majus*. Arabidopsis flowers contain four concentric whorls of organs including four sepals, four petals, six stamens, and two fused carpels. In general, flowers in the grasses share a similar structure, but exhibit some key differences. The rice spikelet comprises a single fertile floret that contains a lemma and palea in whorl 1, two lodicules in whorl 2, six stamens in whorl 3, and a pistil in whorl 4 (Fig. 1A). In addition, there are

© The Author(s) 2018. Published by Oxford University Press on behalf of the Society for Experimental Biology. All rights reserved.
For permissions, please email: journals.permissions@oup.com

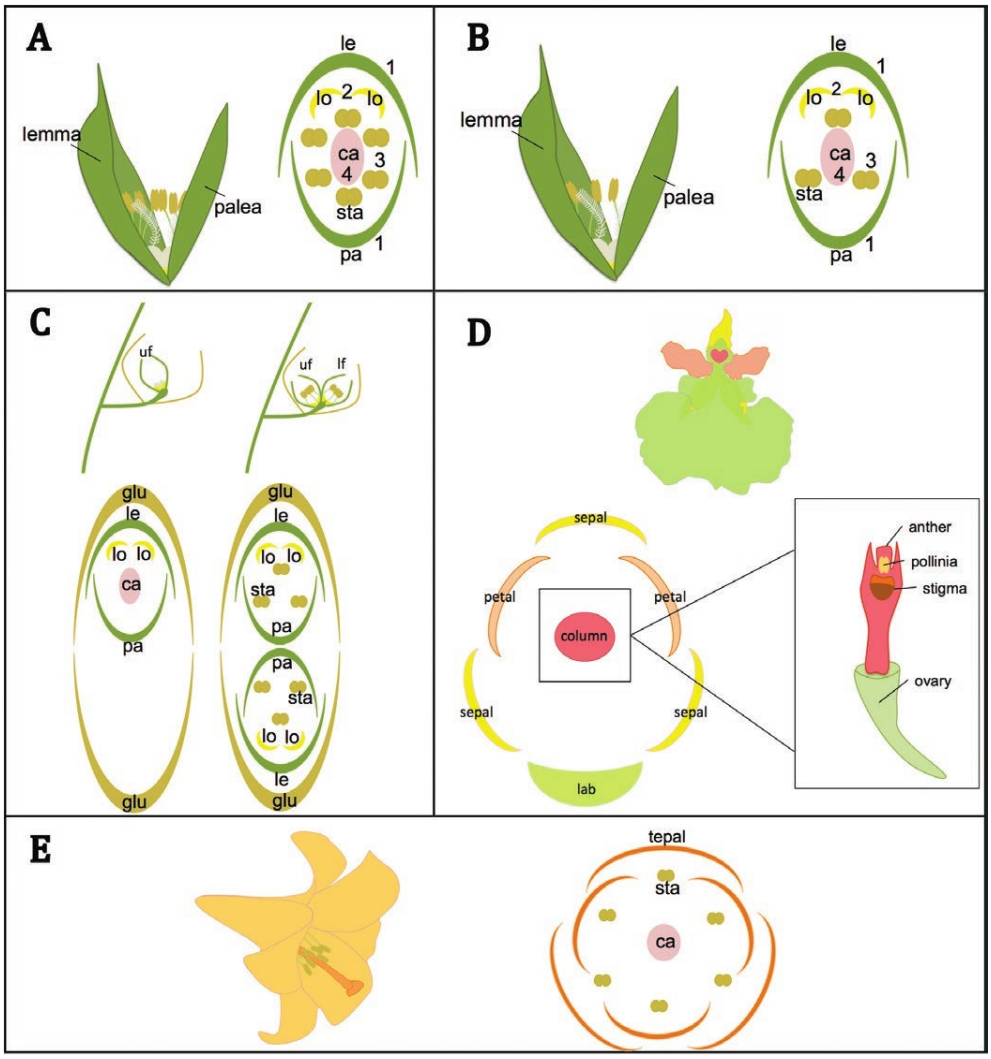



**Fig. 1.** Rice, maize, wheat, barley, orchid, and lily floral structures. (A) A rice floret has four whorls: a lemma (le) and palea (pa) in whorl 1 that protect the floret, two lodicules (lo) in whorl 2, six stamens (sta) in whorl 3, and a carpel (ca) in whorl 4. (B) Barley and wheat florets are very similar, but only have three stamens. (C) Maize has two separate inflorescences, one male (tassel) and one female (ear). Spikelets consist of a pair of florets: the upper floret (uf) and lower floret (lf). Female florets (C, left) have a lemma, palea, two lodicules, and a carpel, but no stamens. Male florets (C, right) have a lemma, palea, two lodicules, and three stamens, but no carpel. Both are protected by glumes (glu). (D) Orchids have three sepals in the first whorl and two petals and a labellum (lab) in the second whorl. The third and fourth whorl are located in the column. (E) Lily has five tepals in the first and second whorl, six stamens in the third whorl, and a carpel in the fourth whorl.

two pairs of repressed bracts: rudimentary glumes and sterile lemmas (Zhang *et al.*, 2013). The identity of the palea and lemma has caused a lot of debate (Clifford, 1987; Bell, 1991). Their morphology is very similar except for three vascular strands in the lemma compared with two in the palea (Ambrose *et al.*, 2000), and a higher density of trichomes and more stomata in the lemma compared with the palea (Ambrose *et al.*, 2000). The palea is considered a prophyll in whose axil the grass flower arises (Bell, 1991). Many mutant phenotypes support the interpretation that the palea and lemma are equivalent to the sepals of most other flowers (Bowman, 1997; Ambrose *et al.*, 2000; Kyozuka *et al.*, 2000; Prasad *et al.*, 2001; Xu *et al.*, 2017). Their function is to protect the florets and kernels from pathogen and insect attack and supply carbohydrates to the developing seeds (Zhang *et al.*, 2013). Lodicules play a role in opening the florets and aid in co-ordination of stamen extrusion, pollination, and fertilization (Bommert *et al.*, 2005; Yoshida, 2012). They are believed to be equivalent to petals in other flowers (Ambrose *et al.*, 2000; Kyozuka *et al.*, 2000; Nagasawa *et al.*, 2003). Wheat, barley, and rye have spikelets that are directly attached to the main axis (Fig. 1B), while other grasses have long, branched

inflorescences and spikelets that are attached to lateral inflorescence branches (Zhang and Yuan, 2014). A spike can contain up to 40 florets (Bommert *et al.*, 2005).

In rice, the inflorescence meristem produces several primary branch meristems and they produce secondary branch meristems. Both of these in turn produce spikelet meristems (Hoshikawa, 1989). The spikelet meristem turns into a terminal spikelet meristem and produces the flowers (Kellogg, 2007). Maize has distinct male (tassel) and female (ear) inflorescences (Zhang and Yuan, 2014) that are physically separated (Fig. 1C), and each spikelet has a pair of florets, an upper and lower one (Dreni and Zhang, 2016). The shoot apical meristem (SAM) gives rise to the terminal tassel, which has long branches and develops male flowers. The first branches that are produced by the apical meristem are long branches, which produce a large number of short branches. Each short branch produces a single lateral branch that terminates in a spikelet (Kellogg, 2007). Ears are derived from axillary shoot meristems, have no long branches, and develop female flowers (Bommert *et al.*, 2005). Male and female flowers initiate one pistil, three stamens, two lodicules, a palea, and a lemma. The carpel primordia in the male florets and the stamen primordia in the female florets are aborted after initiation to produce unisexual florets (Bommert *et al.*, 2005).

Orchids are also members of the monocotyledons, in the family Orchidaceae, but are distinct from the true grasses. Orchid flowers have a zygomorphic structure, which is very different from any of the grass floret structures, and within the orchid family there is also great diversity (Pan *et al.*, 2014). *Oncidium* Gower Ramsey, the variety that has been frequently used for floral characterization, has three types of perianth organs. In the first whorl, three small sepals can be identified, while in the second whorl, two petals and the very distinctive lip, or labellum, are found (Fig. 1D); because the sepals and petals are not significantly different in some plant species, they are often called tepals. The labellum is particularly interesting from an evolutionary perspective since it represents a unique floral structure that may indicate a shift in protein function and interactions in the highly conserved MADS-box family (Mondragón-Palomino and Theissen, 2008). It is essential for the interaction with pollinators, and different models have been proposed to describe the protein interactions leading to labellum development (Mondragón-Palomino and Theissen, 2008).

Lily (*Lilium longiflorum*) from the monocot family Liliaceae produces flowers that have three sepals in the first whorl, three petals in the second whorl, six stamens in the third whorl, and three fused carpels in the fourth whorl (Fig. 1E). In *L. longiflorum*, most parts of the sepals and petals are still connected to each other, giving the lily flowers their distinct trumpet form and distinguishing them from other lily species. Similar to orchids, the sepals and petals are almost identical, which earned them the general name tepals (Tzeng and Yang, 2001). Orchid flowers probably originated from a flower with lily-like actinomorphic perianth with undifferentiated whorls of tepals (Mondragón-Palomino and Theissen, 2008).

## The MADS-box protein family

The MADS-box acronym is derived from MCM1 (yeast), AG (Arabidopsis), DEFICIENS (Antirrhinum), and SRF (mammals), the first four proteins discovered in the transcription factor family (Shore and Sharrocks, 1995; Lawton-Rauh *et al.*, 2000). The MADS-box proteins are involved in diverse developmental processes in flowering plants, cardiac muscle development in animals, and pheromone response in yeast (Schwarz-Sommer *et al.*, 1990; Pelucchi *et al.*, 2002; Becker and Theissen, 2003).

In plants, the MADS-box genes have been proposed to be the driving force behind much floral diversity (Theissen and Saedler, 2001; Yamaguchi and Hirano, 2006). Therefore, better insight into their expression and function, and their conservation in different species is important to inform breeding strategies targeting alterations in floral architecture. The MADS-box domain is highly conserved across different species in dicots and monocots, which makes the functional diversity of the proteins extremely interesting. In this review, the expression patterns and functions of MADS-box genes relative to flower development in six different monocot species, namely barley, wheat, maize (*Zea mays*), rice, orchid, and lily, have been compared. The cereals barley, wheat, maize, and rice are mainly cultivated for food purposes, while orchid and lily have economic value as ornamental plants and flowers.

## MADS-box protein structure is conserved between diverse plant species

The MADS-box genes have been divided into two groups: Type I and Type II (Becker and Theissen, 2003). Type I genes seem to have a faster evolutionary rate than Type II genes. The number of duplications of Type I genes is higher, however, even in the shorter time frame (Gramzow and Theissen, 2013). In plants, the Type II MADS-box genes are called MIKC-type genes, an acronym of the four different domains that have been identified in all genes of this type (Becker and Theissen, 2003).

The MIKC-type MADS-box genes consist of a MADS-box domain, an intervening domain (I), a K-box (K), and a C-terminal domain (C) (Fig. 2) (Theissen *et al.*, 1996). The highly conserved MADS-box motif has 60 amino acids for a sequence-specific DNA binding activity that also plays a role in dimerization and accessory factor binding. The weakly conserved intervening domain is a regulatory determinant for formation of DNA-binding dimers. The keratin-like K-box is defined by conserved regular spacing of hydrophobic residues and can form amphipatic helices involved in protein dimerization, which mediate protein–protein interactions. The most variable domain is located at the C-terminal end. It is involved in transcriptional activation and formation of multimeric transcription factor complexes (Shore and Sharrocks, 1995; Becker and Theissen, 2003; Fornara *et al.*, 2003; Zhao *et al.*, 2006).

Dependent on the structure of the I-domain and K-box, the MIKC-type MADS-box proteins can be further subdivided into two categories: the MIKC$^{c}$-type and the MIKC*-type

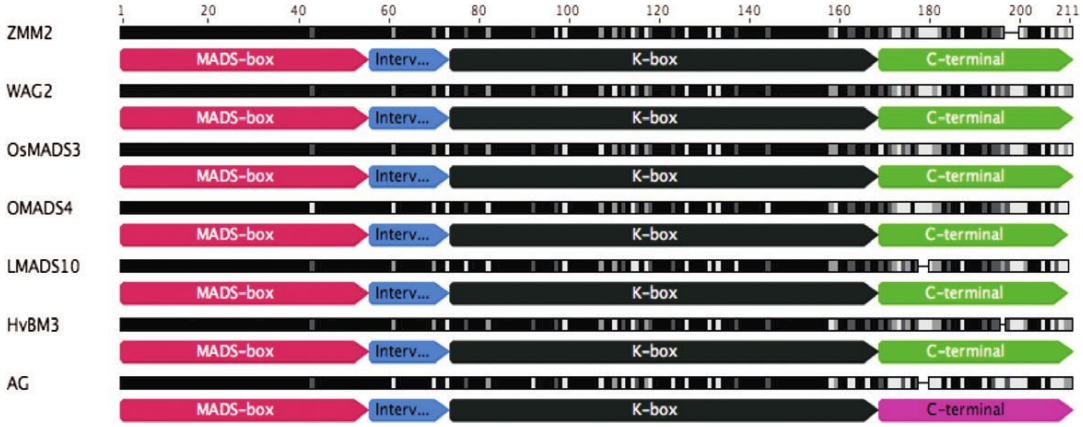



**Fig. 2.** Structure of MIKC-type MADS-box proteins. MIKC-type MADS-box proteins consist of a highly conserved MADS-box domain, responsible for DNA binding, dimerization, and accessory factor binding. The intervening domain is weakly conserved and is a regulatory determinant for the formation of DNA-binding dimers. The K-box is a keratin-like domain that mediates protein–protein interactions. The C-terminal domain is the most variable domain and is involved in transcriptional activation and formation of transcription factor complexes. As an example, MIKC-type proteins from maize (ZMM2), wheat (WAG2), rice (OsMADS3), orchid (OMADS4), lily (LMADS10), barley (HvBM3), and Arabidopsis (AG), all C-class genes, were aligned and their domains were highlighted. The C-terminal domain for AG was significantly different in sequence from that of the monocots and is therefore highlighted in a different colour. MUSCLE multiple alignment of protein sequences from the NCBI, IPK, and MSU rice databases.

proteins. The I-domain in the MIKC$^c$-type proteins is only encoded by one exon, while that in the MIKC*-type proteins is longer, with four or five exons (Becker and Theissen, 2003; Zhao *et al.*, 2006).

Gene duplication within the MADS-box gene family is believed to be a key process during flower evolution (Theissen and Saedler, 2001). After gene duplication, a gene can have several different fates. If a gene is duplicated in its entirety, this frequently leads to functional redundancy (Tautz, 1992; Pickett and Meeks-Wagner, 1995). On the other hand, one duplicated gene can retain the ancestral function, while the other acquires a mutation or a series of cumulative mutations and becomes a pseudogene. In another scenario, one gene retains the ancestral function, while the other gains a beneficial mutation that will be positively selected for, which results in a new function. Another possibility is that both genes acquire complementary loss-of-function mutations that result in the preservation of both genes as they now together retain the original functions of their single ancestor (Lynch and Force, 2000). This is also referred to as the duplication–degeneration–complementation (DDC) model (Force *et al.*, 1999; Prince and Pickett, 2002). These are called non-functionalization, neo-functionalization, and sub-functionalization, respectively (Schilling *et al.*, 2015). Most major difference in the MADS-box gene family between species are thought to have arisen from gene duplications.

## The role of MIKC$^c$-type MADS-box proteins in the ABCDE model of flower development

The floral organ identity MADS-box genes of the MIKC$^c$ type have been divided into five different classes based on their homeotic function: class A, B, C, D, and E genes (Bowman *et al.*, 1989, 1991; Coen and Meyerowitz, 1991; Weigel and Meyerowitz, 1994; Theissen, 2001). The A- and E-class protein complexes specify sepals in the first whorl (Fig. 3). Complexes of A-, B-, and E-class proteins specify petals in the second whorl (Honma and Goto, 2001). B-, C-, and E-class complexes specify stamens in the third whorl, and C- and E-class protein complexes specify carpels in the fourth whorl (Coen and Meyerowitz, 1991; Honma and Goto, 2001). D-class proteins specify ovules together with E-class genes (Fig. 3) (Colombo *et al.*, 1995; Angenent and Colombo, 1996; Theissen and Saedler, 2001; Becker and Theissen, 2003; Li *et al.*, 2011; H. Wang *et al.*, 2015). Another group of genes, phylogenetically related to the B-class genes, was identified and was named the $B_{sister}$ or $B_s$ genes (Becker *et al.*, 2002). Genes in this class are mainly expressed in female reproductive organs, especially in the ovules (Münster *et al.*, 2001; Becker *et al.*, 2002; Becker and Theissen, 2003). All of these genes also fall into separate clades, named after the first proteins identified (Fig. 4). The genes in the SQUA-clade all determine either inflorescence or floral meristem identity, and some have additional A-type functions, while genes in the DEF/GLO clade have class B functions (Theissen *et al.*, 1996). The AG-clade consists of an AG- and an AGL11 (or STK)-lineage, and the class E genes are all part of the SEP/AGL2-clade. Alignments of all proteins in the different subfamilies can be found in Supplementary Figs S1–S7 at *JXB* online

## The ABCDE model in monocots

MADS-box genes involved in flower development have been studied in a wide variety of species. In monocots, most research has been undertaken in rice, wheat, and maize. Comparing the expression patterns and functions of MADS-box floral genes in different monocot species provides information on

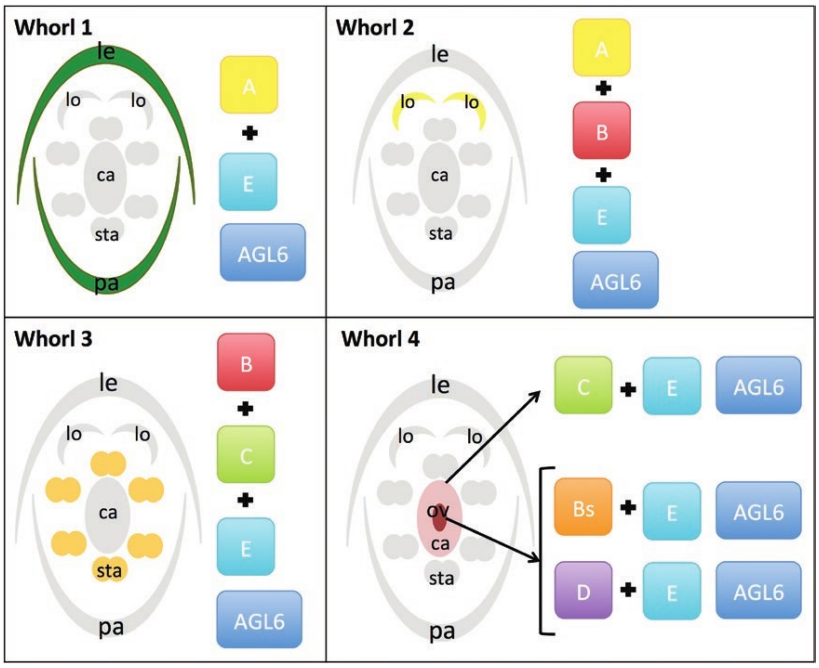



**Fig. 3.** The ABCDE model in rice florets. The model depicts the pattern of gene expression required for normal whorl development. The MIKC$^c$-type MADS-box proteins are divided into different classes: A, B, C, D, and E-class. The $B_{sister}$ proteins are classified as B-class proteins, but have a distinct function. AGL6-like proteins are often classified together with the E-class proteins because they have similar functions. These proteins form complexes to determine the identity of floral organs shown here in a rice floret: lemma (le), palea (pa), lodicules (lo), stamen (sta), carpel (ca), and ovule (ov).

the differences in their morphology and how evolution may have affected different floral structures and floral diversity among these species. While rice, wheat, and barley have a similar floral pattern, the flowers in orchid and lily are very different. The emergence of unique organs such as the labellum in orchid and the differentiation between male tassels and female ears in maize are also interesting to be elucidated. Comparing the expression and function of the ABCDE MADS-box genes within these monocot species provides an interesting opportunity to elucidate more about their role in shaping these different floral structures.

### *A-class genes*

In Arabidopsis and *Antirrhinum*, the A-class genes *AP1* and *SQUA* are responsible for the transition from vegetative to reproductive growth, determination of floral organ identity, and the regulation of fruit maturation (Fornara *et al.*, 2004). Their orthologues in monocots have some level of conservation, but there is some divergence in sequence, expression pattern, and function (Zhang and Yuan, 2014). In the core eudicots, there are two different gene clades within the class A genes: euAP1 and euFUL, which have arisen from a duplication event that coincided with the origin of this angiosperm group (Litt and Irish, 2003; Shan *et al.*, 2007). In non-core eudicots and monocots, only sequences that are similar to those of euFUL genes have been found, and these have been termed 'FUL-like' genes (Litt and Irish, 2003). The monocot FUL-like genes fall into two successively branching clades, which indicates another duplication in the gene lineage (Litt and Irish, 2003).

The FUL-like and the euFUL sequences have a highly conserved motif in the C-terminus (Fig. 5), the FUL-like or paleoAP1 motif (L/MPPWML), which has not been found in the euAP1 sequences (Litt and Irish, 2003). euAP1 sequences have two distinct conserved motifs in their C-terminus: RRNa-LaLT/NLa and CFAT/A. These motifs contain an acidic transcription activation domain and a farnesylation signal (Litt and Irish, 2003; Fornara *et al.*, 2004; Chen *et al.*, 2008). Neither of these motifs has been observed in FUL-like and euFUL sequences. It is suggested that the euAP1 motif has arisen via a translational frameshift from the euFUL/FUL-like motif. This frameshift may have resulted in different functions for the euAP1 proteins (Litt and Irish, 2003).

The rice genome contains four A-class genes, *OsMADS14*, *OsMADS15*, *OsMADS18*, and *OsMADS20*. Northern blot and *in situ* hybridization analysis showed that *OsMADS15* is expressed in the apical region of the floral meristem and subsequently accumulates in the developing lemma and palea (Kyozuka *et al.*, 2000). Expression becomes restricted to the palea, lemma, and lodicules after differentiation of the spikelet organs (Fig. 5B) (Kyozuka *et al.*, 2000), which is similar to *AP1* (Fornara *et al.*, 2003). T-DNA insertional lines that lead to loss-of-function mutants of *OsMADS15* show smaller paleas, while a single nucleotide mutation in *OsMADS15* leads to degenerative paleas and occasional pseudovivipary

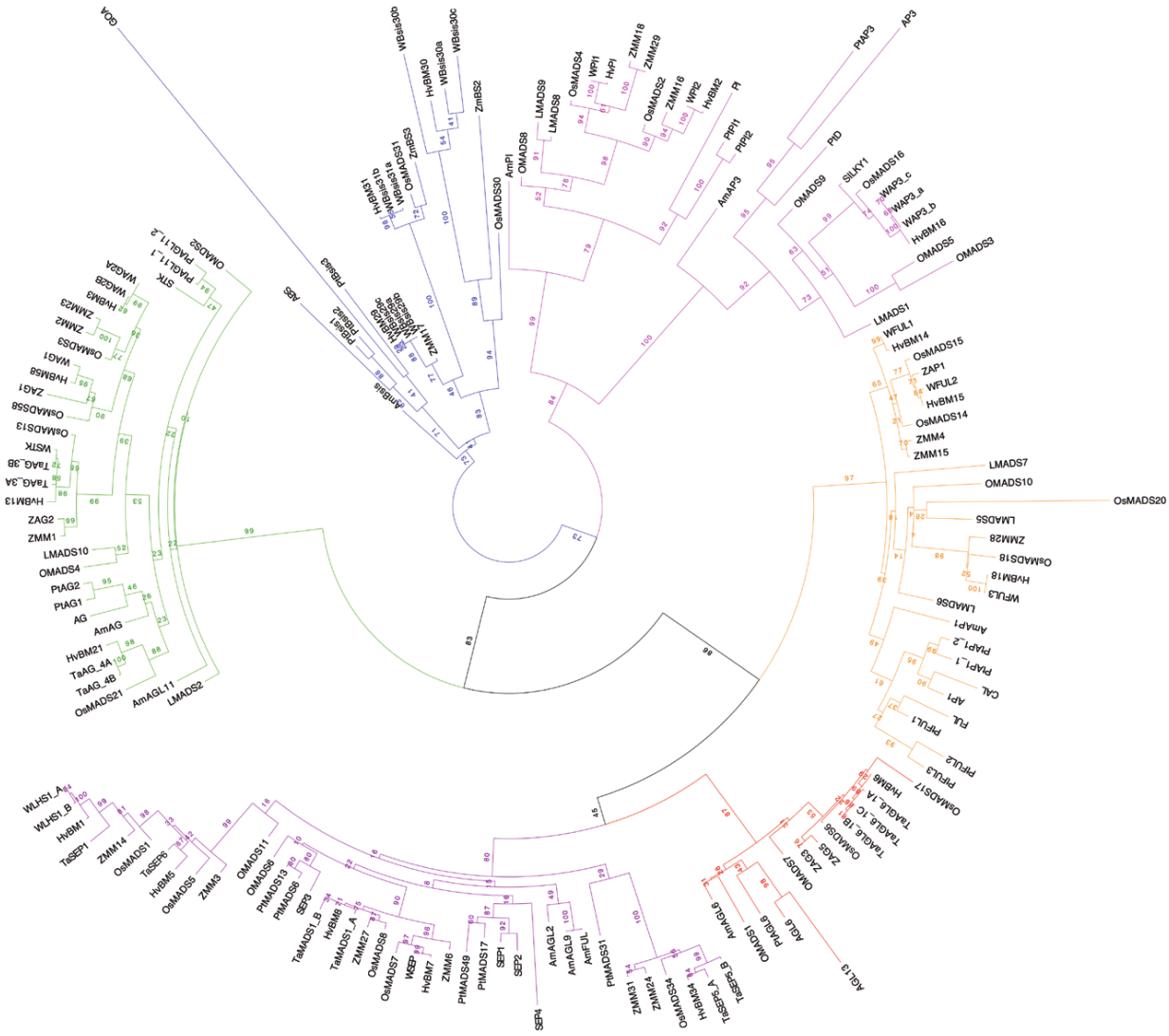
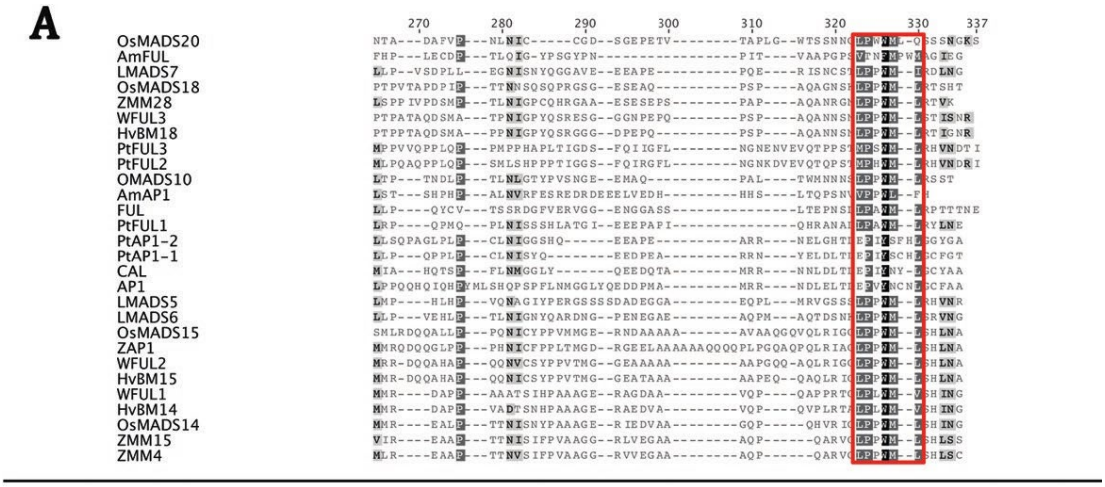



**Fig. 4.** Phylogenetic analysis of ABCDE MADS-box genes from Arabidopsis, *Amborella trichopoda*, *Populus trichocarpa*, rice, maize, wheat, barley, orchid, and lily. Phylogenetic tree obtained with RAxML tree building through Geneious version 8.0 by Biomatters. Available from http://www.geneious.com. Maximum likelihood tree from 1000 bootstrap replicates. MUSCLE multiple alignment of protein sequences from the NCBI, IPK, and MSU databases was used. BMGE clean up of the multiple aligment via Galaxy@pasteur (https://galaxy.pasteur.fr). The different subfamilies are represented by different colours: SQUA (orange), DEF/GLO (pink), GMM13 (blue), AG (green), AGL2 (purple), AGL6 (red). Alignments of all proteins in the different subfamilies can be found in Supplementary Figs S1–S7.

(Wang *et al.*, 2010; Wu *et al.*, 2017). Overexpression of *OsMADS15* causes early internode elongation, shoot-born crown root development, reduced plant height, and early flowering (Lu *et al.*, 2012). Northern blot and *in situ* hybridization analysis showed that *OsMADS14* expression is similar to that of *OsMADS15*, and is initially detectable in the whole region of the floral meristem during flower development, and subsequently becomes restricted to the primordia of glumes, lemma, and palea (Pelucchi *et al.*, 2002). In mature flowers, the expression of *OsMADS14* is detectable in the reproductive organs (Fig. 5B) (Moon *et al.*, 1999*b*; Pelucchi *et al.*, 2002). A loss-of-function T-DNA insertion mutant in *OsMADS14* showed no phenotype in the field, while ectopic expression leads to early flowering at the callus stage (Jeon *et al.*, 2000*b*; Wu *et al.*, 2017). Double mutant *osmads14osmads15* plants fail to produce secondary branches and spikelets, and only leaf-like organs are observed (Wu *et al.*, 2017). The single mutant phenotype of *OsMADS14* and that of the double mutant suggest that its function is largely redundant with other genes, such as *OsMADS15*. Analysis of heterozygous double mutants suggests that OsMADS14 and OsMADS15 went through sub-functionalization and acquired partially




**B**

Class A

| Tissue / Species | Rice | Maize | Barley | Wheat | Orchid | Lily |
|---|---|---|---|---|---|---|
| Inflorescence meristem | | | | WFUL1, -2, -3 | | LMADS7 |
| Spikelet meristem | | | | WFUL1, -2, -3 | | |
| Floral meristem | OsMADS14, -15, -18 | | | WFUL1, -2, -3 | | |
| Sepal/Lemma-Palea | OsMADS14, -15, -18 | ZMM4, -15, ZAP1 | HvBM14, -15, -18 | WFUL1, -2, -3 | | |
| Petal/Lodicules | OsMADS14, -15 | ZMM4, -15, ZAP1 | HvBM14, -15, -18 | WFUL1, -2, -3 | | |
| Labellum | | | | | OMADS10 | |
| Stamen | OsMADS14, -18 | | HvBM14, -15, -18 | WFUL1, -3 | OMADS10 | |
| Carpel | OsMADS14, -18 | | HvBM14, -15, -18 | WFUL1, -3 | OMADS10 | LMADS5, -6 |
| Vegetative leaves | OsMADS18 | ZMM4, -15 | HvBM18 | WFUL1 | OMADS10 | LMADS5, -6 |
| Vegetative stem | | ZMM4, -15 | HvBM18 | | | LMADS5, -6, -7 |
| Roots | OsMADS18 | ZMM4, -15 | HvBM18 | | | |

**Fig. 5.** Sequence alignment and expression patterns of A-class MADS-box genes in Arabidopsis, *Amborella trichopoda*, *Populus trichocarpa*, rice, maize, barley, wheat, orchid, and lily. (A) The conserved FUL-like motif (LPPWML) can be found in all the monocot A-class MADS-box genes, with only minor differences. In HvBM5 and WFUL1, the proline at the third position has been substituted by a leucine, while the leucine at the sixth position has been substituted by a valine. In OsMADS20, the proline at the third position has been substituted by a tryptophan and in LMADS7 the leucine at the sixth position has been substituted by an isoleucine. (B) The expression patterns appear conserved in the grasses, with some diversity in orchid and lily. Red squares indicate that multiple genes are expressed in this tissue, while yellow indicates that only one gene is expressed in this tissue. White squares indicate that there is no expression, and grey squares indicate that no data are available regarding the expression in these tissues.

overlapping functions (Wu *et al.*, 2017). They work together in a dose-dependent manner by antagonizing C-class genes and both determine floral meristem fate (Wu *et al.*, 2017). OsMADS14 mainly regulates the identities of the lodicule and stamens, while OsMADS15 is mainly responsible for the empty glumes, palea, and lemma (Wu *et al.*, 2017). *OsMADS18* has a different expression pattern compared with the other *AP1* orthologues. Northern blot and *in situ* hybridization analysis revealed expression in roots, leaves, and flowers, with a strong signal in the inflorescence (Masiero *et al.*, 2002; Pelucchi *et al.*, 2002; Fornara *et al.*, 2003). *OsMADS18* expression levels are maximal when the plant reaches the reproductive stage (Fornara *et al.*, 2003), but are absent from the lodicules and the sterile glumes in mature flowers (Pelucchi *et al.*, 2002). Fornara *et al.* (2004) described an RNAi line of *OsMADS18* that showed no visible phenotype, while a recent RNAi line described by Wu *et al.* (2017) showed only a low seed setting rate. Overexpression of *OsMADS18* induces precocious initiation of axillary shoot meristems and early transition to flowering (Fornara *et al.*, 2004). These results suggest that OsMADS18 is possibly not required for specifying floral organ identity but may be involved in promoting the differentiation of the vegetative shoot or seed development together with OsMADS14 and OsMADS15 (Fornara *et al.*, 2004; Wu *et al.*, 2017). Yeast two-hybrid and bimolecular fluorescence complementarion (BiFC) experiments have shown that OsMADS18 forms heterodimers with OsMADS14, OsMADS15, OsMADS8, OsMADS7, OsMADS6, and OsMADS47 (Masiero *et al.*, 2002; Wu *et al.*, 2017), but does not form homodimers (Wu *et al.*, 2017), revealing a conserved aspect between monocots and dicots (Fornara *et al.*, 2004). Both OsMADS14 and OsMADS15 have been shown to interact with each other and with OsMADS1, and can also form homodimers (Lim *et al.*, 2000; Wu *et al.*, 2017). The expression of *OsMADS20* was detected in shoots and seeds by RT-PCR (Lee *et al.*, 2003*b*), but RNAi lines show no observable phenotype (Wu *et al.*, 2017). The quadruple mutant of *osmads14 osmads15 osmads18 osmads20* does not display a more severe phenotype than the double mutant *osmads14 osmads15*, suggesting that OsMADS14 and OsMADS15 are sufficient for specifying palea, lemma, and lodicule identity in rice florets (Wu *et al.*, 2017).

In maize, *ZAP1* was identified as the *AP1* orthologue because of the sequence similarities and the similar

expression pattern to Arabidopsis (Mena *et al.*, 1995). *ZAP1* mRNA was detected in male and female inflorescences and the husk leaves that surround the developing ear using northern blot analysis (Fig. 5B) (Mena *et al.*, 1995). *ZAP1* is expressed in lemma, palea, and lodicules, similar to *OsMADS14* and *OsMADS15* (Li *et al.*, 2014). *ZMM4* and *ZMM15* have also been identified as orthologues of rice *OsMADS14*; *ZMM28* is the orthologue of rice *OsMADS18* (Table 1) (Zhao *et al.*, 2011; Li *et al.*, 2014). *ZMM4* and *ZMM15* are not expressed in young tissues, but accumulate after the transition from vegetative to reproductive growth in developing apical and lateral inflorescences (Danilevskaya *et al.*, 2008). Expression of *ZMM4* and *ZMM15* was not found in any of the embryonic tissues, but low levels of expression in husk, stalk, mature leaf, and root were detected by massively parallel signature sequencing (MPSS) analysis, *in situ* hybridization, and promotor:GUS (β-glucuronidase) analysis (Danilevskaya *et al.*, 2008). The expression profile of *ZMM15* is similar to that of *ZMM4* but overall has a low expression level (Danilevskaya *et al.*, 2008). When both genes are overexpressed, only ZMM14 mediates early flowering, which may suggest that ZMM15 has a function similar to but weaker than ZMM14 (Danilevskaya *et al.*, 2008).

The expression patterns of the barley A-class genes do not correspond to those of *SQUA* and *AP1*, implying that they are not functional equivalents (Schmitz *et al.*, 2000). *In situ* hybridization, RT-PCR, and northern blot analysis showed that at the awn primordium stage, the expression of *HvBM18*

**Table 1.** *The ABCDE genes in Arabidopsis and monocot species*

| | Clade | Core eudicot clade | Arabidopsis | Monocot clade | Orchid | Lily | Grasses clade | Rice | Maize | Barley | Wheat |
|---|---|---|---|---|---|---|---|---|---|---|---|
| **SQUA** | **AP1** | **euAP1** | AP1<br>CAL | | | | | | | | |
| | **FUL** | **euFUL** | FUL | | | | | | | | |
| | **FUL-like** | **FUL-like** | | **FUL-like** | OMADS10 | LMADS5 | **FUL1** | OsMADS14 | ZMM4<br>ZMM15 | HvBM14 | WFUL1 |
| | | | | | | LMADS6 | **FUL2** | OsMADS15 | ZAP1 | HvBM15 | WFUL2 |
| | | | | | | LMADS7 | **FUL3** | OsMADS18 | ZMM28 | HvBM18 | WFUL3 |
| | | | | | | | **FUL4** | OsMADS20 | | | |
| **DEF/GLO** | **DEF** | **euAP3** | AP3 | **paleoAP3** | OMADS3<br>OMADS5<br>OMADS9<br>OMADS12 | LMADS1 | **paleoAP3** | OsMADS16 | SILKY1 | HvBM16 | WAP3 |
| | **GLO** | **GLO** | PI | **GLO** | OMADS8 | LMADS8<br>LMADS9 | **GLO** | OsMADS2<br>OsMADS4 | ZMM16<br>ZMM18<br>ZMM29 | HvBM2<br>HvBM4 | WPI2<br>WPI1 |
| **GMM13** | **$B_{sister}$** | **$B_{sister}$** | ABS<br>GOA | **$B_{sister}$** | | | **OsMADS29** | OsMADS29 | ZMM17 | HvBM29 | WBsis |
| | | | | | | | **OsMADS30** | OsMADS30 | ZmBS2 | HvBM30 | TaBS2 |
| | | | | | | | **OsMADS31** | OsMADS31 | ZmBS3 | HvBM31 | TaBS3 |
| **AG** | **AG** | **euAG** | AG | **AG** | OMADS4 | LMADS10 | **AG** | OsMADS3 | ZMM2<br>ZMM23 | HvBM3 | WAG2 |
| | | **PLENA** | SHP1<br>SHP2 | | | | | OsMADS58 | ZAG1 | HvBM58 | WAG1 |
| | **AGL11** | **AGL11** | STK | **AGL11** | OMADS2 | LMADS2 | **AGL11** | OsMADS13<br>OsMADS21 | ZAG2<br>ZMM1 | HvBM13<br>HvBM21 | WSTK<br>Ta-AG4 |
| **AGL2** | **LOFSEP** | **SEP1/2** | SEP1<br>SEP2 | **LOFSEP** | OMADS11 | LMADS4 | **OsMADS1** | OsMADS1 | ZMM14<br>ZMM8 | HvBM1 | WLHS1<br>TaSEP1 |
| | | **FBP9/23** | | | | | **OsMADS5** | OsMADS5 | ZMM3 | HvBM5 | TaSEP6 |
| | | **SEP4** | SEP4 | | | | **OsMADS34** | OsMADS34 | ZMM24<br>ZMM31 | HvBM34 | TaSEP5 |
| | **SEP3** | **SEP3** | SEP3 | **SEP3** | OMADS6 | LMADS3 | **OsMADS7** | OsMADS7 | ZMM6 | HvBM7 | WSEP |
| | | | | | | | **OsMADS8** | OSMADS8 | ZMM27 | HvBM8 | TaMADS1 |
| **AGL6** | **AGL6** | **euAGL6** | AGL6<br>AGL13 | **AGL-I** | | | **ZAG3/OsMADS6** | OsMADS6 | ZAG3<br>ZAG5 | HvBM6 | TaAGL6 |
| | | **AGL6-like** | | | | | **OsMADS17** | OsMADS17 | | | |
| | | | | **AGL-2** | | | | | | | |
| | | | | **AGL-3** | OMADS7<br>OMADS1 | | | | | | |
| | | | | **AGL-4** | | | | | | | |

Listed are the genes in the model organism Arabidopsis and the orthologues in monocots rice (*Oryza sativa*), maize (*Zea mays*), barley (*Hordeum vulgare*), wheat (*Triticum aestivum*), orchid (*Oncidium* Gower Ramsey), and lily (*Lilium longiflorum*) that have been identified to date

(also known as *BM3*) and *HvBM14* (also known as *BM5*) is hardly detectable, while *HvBM15* (also known as *BM8*) expression is strong (Schmitz *et al.*, 2000). Subsequently the three genes are expressed in all organ primordia and the vascular system of the barley floret throughout inflorescence development (Schmitz *et al.*, 2000). *HvBM14* and *HvBM15* are specific for these tissues, while *HvBM18* is also expressed in all other tissues, similar to its orthologue in rice, *OsMADS18* (Fig. 5B) (Schmitz *et al.*, 2000). *HvBM14* shows a marked increase in transcript abundance during the induction of the reproductive phase, similar to *OsMADS18* (Fornara *et al.*, 2004). *HvBM14* is the equivalent of the *VRN1* gene in other temperate cereals and is generally not expressed in non-vernalized winter barleys, but is induced by vernalization (Trevaskis *et al.*, 2003). Spring barley lines carrying dominant spring *VRN-H1* alleles or with homozygous recessive *VRN-H2* alleles have low levels of *HvBM14* expression (Trevaskis *et al.*, 2003). Trevaskis *et al.* (2003) suggest that *HvBM14* expression might be controlled by activation and repression to respond to vernalization, which has been suggested previously in wheat (Tranquilli and Dubcovsky, 2000; Yan *et al.*, 2003; Sasani *et al.*, 2009).

Orthologues of the rice genes *OsMADS14*, *OsMADS15*, and *OsMADS18* have been found in wheat and have been termed *WFUL1* (corresponding to *VRN1*), *WFUL2*, and *WFUL3*, respectively (Table 1) (Kinjo *et al.*, 2012). *In situ* hybridization, RT-PCR, and qRT-PCR determined that *WFUL3* is expressed in the spikelet primordia and throughout the spikelet meristem. *WFUL1* and *WFUL2* are only expressed in the basal part of the spikelet meristem. *WFUL1* is expressed in leaves at the vegetative phase, in young spikes, and in all floral organs after floral organ development, while the expression of *WFUL2* is reduced in stamens and undetectable in pistils (Fig. 5B) (Kinjo *et al.*, 2012). This corresponds to the expression pattern and function of *OsMADS14* and *OsMADS15* in rice and *ZAP1* in maize, indicating that this diversification of function has also occurred in the common ancestor of all the mentioned grasses (Murai, 2013). Overexpression of *WFUL1* and *WFUL2* leads to early flowering phenotypes (Adam *et al.*, 2007; Kinjo *et al.*, 2012). *WFUL1* has been suggested to have a function in phase transition in leaves and providing flowering competency (Murai *et al.*, 2003; Murai, 2013). *WFUL3* seems to have a function in floral meristem development together with *WFUL2*, while *WFUL2* has a specialized function in development of the outer floral organs (Kinjo *et al.*, 2012). Yeast two- or three-hybrid analysis showed that WFUL2 interacts with the B-class proteins WAP3 and WPI and the E-class proteins WSEP and WLHS1, while WFUL1 and WFUL2 both interact with WSEP (Kinjo *et al.*, 2012).

*OMADS10*, the *AP1* orthologue in orchid, is almost undetectable in flower buds of early developmental stages and during flower maturation, as shown by RT-PCR (Chang *et al.*, 2009). In mature flowers, *OMADS10* is expressed in the labellum, carpel, anther cap, and stigmatic cavity (Fig. 5B) (Chang *et al.*, 2009). It is also strongly detected in vegetative leaves. This expression pattern is different from those of A-function genes in Arabidopsis, *Antirrhinum*, and the grasses, but is similar to that found in the *AP1* orthologues in lily, *LMADS5* and *LMADS6* (Chang *et al.*, 2009). Ectopic expression of *OMADS10* in Arabidopsis induced an early flowering phenotype, but no homeotic conversions of floral organs (Chang *et al.*, 2009). Apart from *LMADS5* and *LMADS6*, there is one more A-class MADS-box gene in lily: *LMADS7*. Northern blot analysis showed that *LMADS5* and *LMADS6* were strongly expressed in vegetative stem, and leaves and carpels, and weakly in the other three floral organs (Chen *et al.*, 2008). *LMADS7* expression was absent in vegetative leaves and in any of the four organs of the flower, but was detected in the vegetative stem and the inflorescence meristem (Chen *et al.*, 2008). The expression pattern of *LMADS5*, *6*, and *7* is mostly different from that of other genes in the SQUA clade, with the exception of the A-class MADS-box genes in orchid (Fig. 5B). Ectopic expression of the A-class lily genes in Arabidopsis results in early flowering phenotypes and floral organ conversions such as carpelloid sepals and staminoid petals (Chen *et al.*, 2008). Functional complementation analysis showed that ectopic expression of these genes could rescue an *ap1* mutant phenotype in Arabidopsis (Chen *et al.*, 2008). Based on their expression pattern and ectopic expression analysis, it was suggested that they have a function in flower induction, initiation, and formation (Chen *et al.*, 2008).

In rice, only *OsMADS18* shows a different expression pattern compared with other A-class genes, whereas all the A-class genes in barley have a different expression pattern. There is also no *OsMADS20* orthologue in barley, maize, or wheat. In maize, there has been a duplication event resulting in *ZMM4* and *ZMM15*, and both appear to be orthologues of *OsMADS14*. In wheat, only *WFUL2* has the ascribed A-class function. *WFUL1* and *WFUL3* have a different expression pattern and function. The A-class genes in orchid and lily have a expression patterns completely different from those of their orthologues in grasses and Arabidopsis. Loss-of-function or knock-down mutants are currently missing for most of the A-class genes in maize, barley, wheat, orchid, and lily, and they could lead to a better understanding of their function.

### *B-class genes*

B-class genes determine the identity of petals and stamens in Arabidopsis (Fornara *et al.*, 2003), and increasing evidence suggests that this is an ancestral function (Becker and Theissen, 2003; Münster *et al.*, 2001). Similar to the A-class genes, the B-class genes have been shaped by a gene duplication event close to the base of the crown group angiosperms, creating two lineages: the DEF-like lineage, which consists of AP3-like proteins, and the GLO-like lineage, which consists of PI-like proteins (Fig. 6B) (Winter *et al.*, 2002*a*; Becker and Theissen, 2003; Zahn *et al.*, 2005*b*).

### *AP3-like genes*

In higher eudicots, an euAP3 motif is found in the AP3-like proteins, but is absent in non-core eudicots and non-eudicots. Instead a highly conserved paleoAP3 motif (YGxHDLRLA) is observed in their sequences (Fig. 6A)

(Kramer *et al.*, 1998). AP3-like proteins also have a highly conserved sequence motif in the K-box (Q/HYExM) (Kramer *et al.*, 1998; Tzeng and Yang, 2001). Only one DEF-like gene has been found in most monocots, so it is presumed that no gene duplication event happened here, except for orchids, where the gene duplication seems to have occurred in the DEF-clade instead of the GLO-clade (Table 1) (Chen *et al.*, 2012). The paleoAP3 motif seems to have significant sequence diversification in the GLO-like lineage after duplication, where it has been termed a PI-like motif (Fig. 6A) (Kramer *et al.*, 1998; Moon *et al.*, 1999*a*). The observation of these different motifs in the monocot B-class MADS-box genes shows that AP3 homologues were highly conserved in most monocots during evolution and that they are more closely related to the lower eudicots than to the higher eudicots (Tzeng and Yang, 2001).

In rice *OsMADS16* is a member of the DEF-clade, and expression is detected in lodicule and stamen primordia from initiation onwards, as revealed by RNA blot analysis and *in situ* hybridization (Fig. 6B) (Moon *et al.*, 1999*a*; Fornara *et al.*, 2003; Nagasawa *et al.*, 2003). DEF- and GLO-like proteins, like AP3 and PI in Arabidopsis, form obligate heterodimers, which might have originated after the gymnosperm–angiosperm split but before the monocot–eudicot split (Goto and Meyerowitz, 1994; Davies *et al.*, 1996; Winter *et al.*, 2002*b*). The interaction between proteins of the GLO- and the DEF-clade is conserved, as shown by the interaction of OsMADS16 with OsMADS4 and OsMADS2 by yeast two-hybrid analysis (Moon *et al.*, 1999*a*; Yao *et al.*, 2008). They form a heterodimer and may auto-regulate their own expression (Yadav *et al.*, 2007), similar to AP3 and PI in Arabidopsis (Krizek and Meyerowitz, 1996). The function

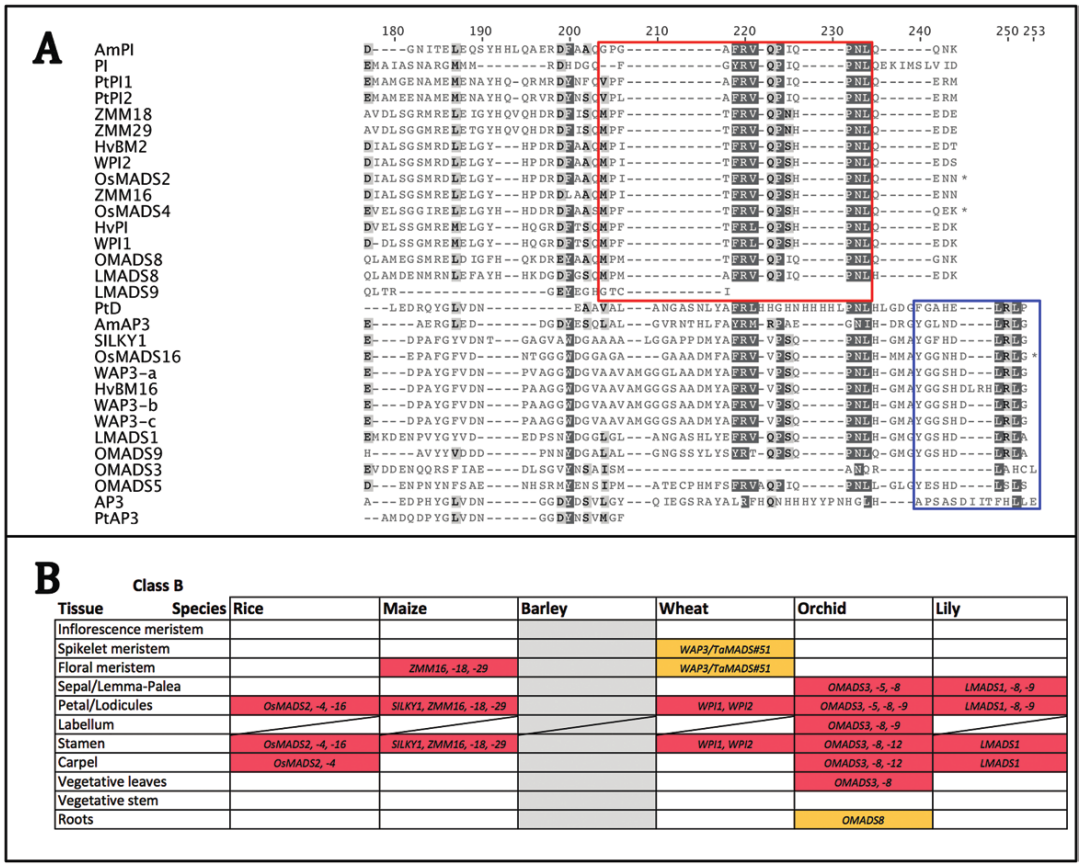



**Fig. 6.** Sequence alignment and expression patterns of B-class MADS-box genes in Arabidopsis, *Amborella trichopoda*, *Populus trichocarpa*, rice, maize, barley, wheat, orchid, and lily. The B-class genes can be subdivided into two different clades: the DEF- and the GLO-clade. (A) Multiple alignment of protein sequences from the NCBI, IPK, and MSU rice databases. Both clades have different motifs, a paleoAP3-motif (YGxHDLRLA) or a PI-motif (MPFTFRVQPSHPNL), respectively. HVPI and WPI1 have similar differences in the motif, as have LMADS8 and OMADS8. HvBM2, WPI2, OsMADS2, and ZMM16 also have similar differences, identifying them as homologues. LMADS9 is a truncated version of LMADS8 and does not have the PI-motif. All members of the monocot DEF-clade have a variation of the motif, except OMADS3. (B) The expression patterns of the grasses are conserved and have diversified in orchid and lily. Red squares indicate that multiple genes expressed in this tissue, while yellow indicates that only one gene is expressed in this tissue. White squares indicate that there is no expression, and grey squares indicate that no data are available regarding the expression in these tissues.

of *OsMADS16* seems to be well conserved between rice and Arabidopsis (Yamaguchi and Hirano, 2006). A loss-of-function mutant of *OsMADS16*, known as *spw1* (*superwoman1*), shows the homoetic transformation of stamens into carpels and lodicules into palea-like organs (Nagasawa *et al.*, 2003). Similarly, *SILKY1*, the *AP3* orthologue in maize, is required for the normal development of lodicules and stamens. *SILKY1* is expressed in the centre of the floral meristem after the lemma and palea primordia have initiated, as well as in lodicules and stamens throughout their development (Ambrose *et al.*, 2000). A loss-of-function mutation of *SILKY1* results in homeotic transformations of stamens to carpels and lodicules to lemma- or palea-like organs (Ambrose *et al.*, 2000). OsMADS16 also seems to interact with OsMADS3 (C-class), OsMADS15 (A-class), OsMADS8 (E-class), and OsMADS6 (AGL6-like) (Lee *et al.*, 2003*a*).

In wheat, two homeologous genes of *WAP3* (*TaMADS#51* and *TaMADS#82*) on chromosomes 7B and 7D, respectively, were identified as AP3-like B-class genes (Table 1) (Hama *et al.*, 2004). *WAP3*/*TaMADS#51* expression is only detected in young spikes at the floral organ development stage, while *WAP3*/*TaMADS#82* expression was lower in young spikes, but higher in spikes at the heading stage (Fig. 6B) (Hama *et al.*, 2004).

The DEF-like genes in orchid are subdivided into four different clades (Mondragón-Palomino and Theissen, 2008). *OMADS3* (clade 2), one AP3-like gene in orchid, does not contain the C-terminal motif, which differs from the other B-class genes found so far (Fig. 6) (Hsu and Yang, 2002). The conserved K-box sequence (QYQRM), however, is present (Hsu and Yang, 2002; Tsai and Chen, 2006). Its expression can be detected in all four floral organs as well as in vegetative leaves, as shown by a combination of RT-PCR and northern analysis (Hsu and Yang, 2002) which is different from other B-class genes that show specific expression in flowers (Fig. 6B). Yeast two-hybrid analysis showed that OMADS3 is able to form strong homodimers (Hsu and Yang, 2002; Tsai and Chen, 2006). Three other DEF-like genes are found in orchid; *OMADS12* (clade 4), *OMADS5* (clade 1) with expression in sepals and petals, and *OMADS9* (clade 3) which is highly expressed in petals and absent in vegetative tissues (Fig. 6B) (Chang *et al.*, 2010; Hsu *et al.*, 2015). OMADS5 and OMADS9 may play a different role in the formation of the sepal, petal, and labellum (Chang *et al.*, 2010). The difference for petal and lip formation may be due to the expression of *OMADS5* in the petal and its absence in the lip. OMADS5 may have a negative role in regulating labellum formation (Chang *et al.*, 2010), which was further supported by the reduced expression of *OMADS5* in lip-like sepals and lip-like petals of peloric orchid mutants of *O.* Gower Ramsey (Chang *et al.*, 2010). OMADS5 and OMADS9 are able to form homodimers and heterodimers with each other and with OMADS3 (Chang *et al.*, 2010). *OMADS12* is weakly expressed in stamen, but strongly expressed in the carpel (Hsu *et al.*, 2015). Its expression is completely absent in the sepal, petal, and labellum (Hsu *et al.*, 2015). This indicates that clade 4 in *O.* Gower Ramsey does not appear to affect perianth differentiation (Hsu *et al.*, 2015).

In lily, the *LMADS1* gene is the functional counterpart of *AP3* in Arabidopsis (Table 1) (Tzeng and Yang, 2001), with conserved function in regulating petal and stamen development. *LMADS1* is expressed in all four floral whorls, but the protein is only detected in petals and stamens, as revealed by western blot analysis, suggesting post-transcriptional regulation (Tzeng and Yang, 2001). *LMADS1* transcripts were also strongly detected in late-developing carpels (Tzeng and Yang, 2001). Yeast two-hybrid analysis showed that LMADS1 can form strong homodimers, similar to OMADS3 (Hsu and Yang, 2002; Tzeng *et al.*, 2004; Tzeng and Yang, 2001; Tsai and Chen, 2006). The highly conserved paleoAP3 motif (YGSHDLRLA) was found at the C-terminus of LMADS1 (Fig. 6A). Within the K-box, the highly conserved sequence (QYEKM) was also identified (Tzeng and Yang, 2001).

Briefly, wheat has two *AP3* homeologues showing different expression patterns, possibly indicating divergent functions. A series of duplication events in orchid are proposed to form four different clades of AP3-like B-class genes with functional diversification, which may contribute to the development of the unique orchid floral structure, the labellum. Unlike the A-class genes, lily AP3-like genes now show more similarity with the AP3-like genes in grasses and Arabidopsis than with those in orchid.

### *PI-like genes*

Several GLO-like genes have been identified in rice, barley, wheat, maize, and lily (Chung *et al.*, 1995; Münster *et al.*, 2001; Hama *et al.*, 2004; Chang *et al.*, 2010; Chen *et al.*, 2012); proteins of the GLO-like lineage have a conserved PI-motif in their C-terminal domain (Fig. 6).

In rice, the PI-like genes *OsMADS2* and *OsMADS4* are mainly expressed in lodicules, stamens, and carpels (Fig. 6B) (Chung *et al.*, 1995; Kyozuka *et al.*, 2000; Fornara *et al.*, 2003). The function of *OsMADS2* is similar to that of PI in Arabidopsis, based upon RNAi analysis (Prasad and Vijayraghavan, 2003; Kang and An, 2005; Yadav *et al.*, 2007; Yao *et al.*, 2008). RNAi knock-down lines of *OsMADS2* showed continued growth of the distal region of second whorl organs forming an elongated bract-like structure, but no apparent changes in stamen shape (Yadav *et al.*, 2007; Yoshida *et al.*, 2007; Yao *et al.*, 2008). *OsMADS2* is transiently expressed early in all floral tissues and later strongly expressed in early stamen primordia, as shown by *in situ* hybridization (Kyozuka *et al.*, 2000; Yadav *et al.*, 2007). Similar expression levels are detected in developing lodicules and stamens, but are later substantially reduced in differentiating stamens (Kyozuka *et al.*, 2000; Yadav *et al.*, 2007). *OsMADS4* transcription activation occurs very early and uniformly during spikelet meristem initiation (Chung *et al.*, 1995; Yadav *et al.*, 2007). During floret organ development, high levels of *OsMADS4* expression occur in the stamen and carpel, with reduced expression in differentiating lodicules (Yadav *et al.*, 2007). RNAi lines of *OsMADS4* showed no phenotypic alterations, indicating that OsMADS4 and OsMADS2 might be acting redundantly in stamen specification (Yoshida *et al.*, 2007; Yao *et al.*, 2008). Supporting this, in the double knock-down mutants of *OsMADS2* and *OsMADS4*, the

stamens were transformed into carpel-like organs (Yoshida *et al.*, 2007; Yao *et al.*, 2008). Moreover, the lodicules in these double mutants also showed a complete homeotic conversion to bract-like organs, suggesting that OsMADS4 plays a minor role in determining lodicule identity (Yoshida *et al.*, 2007; Yao *et al.*, 2008).

The *PI* orthologues *ZMM18*, *ZMM29*, and *ZMM16* in maize show an expression pattern similar to that of *OsMADS2* and *OsMADS4* (Fig. 6B) (Fornara *et al.*, 2003). *ZMM16* is the orthologue of *OsMADS2*, while *ZMM18* and *ZMM29* are orthologous to *OsMADS4* (Table 1) (Münster *et al.*, 2001). These maize genes are expressed in lodicules, stamens, and carpel primordia in male and female inflorescences and later are restricted only to the stamen and lodicules (Whipple *et al.*, 2004). *ZMM16* was also weakly detected in vegetative organs (Münster *et al.*, 2001). The observation of some different expression patterns of *ZMM16* from *ZMM18* and *ZMM29* suggest that different degrees of selection pressures led to a functional diversification of the genes (Münster *et al.*, 2001). The gene pair *ZMM18* and *ZMM29* appears to have originated by a gene duplication event (Münster *et al.*, 2001). Using an EMSA, Whipple *et al.* (2004) showed that ZMM16 forms obligate heterodimers to bind DNA. They also showed that neither SILKY1 nor ZMM16 alone could bind DNA, while SILKY1 and ZMM16 together could bind DNA, indicating that the heterodimer is necessary for DNA binding. *WPI1* and *WPI2* in wheat are orthologous to *OsMADS4* and *OsMADS2*, respectively. *WPI1* is expressed in the primordia of the stamen and lodicules, as shown by *in situ* analysis (Table 1; Fig. 6B) (Hama *et al.*, 2004). The alloplasmic wheat with a deficiency of *WPI1* showed pistillody, the change of stamens into pistil-like structures, suggesting that WPI1 plays a role in floral organ identity (Hama *et al.*, 2004).

*OMADS8* is the only GLO-like gene identified in *O.* Gower Ramsey (Table 1), with expression detected in vegetative leaves, roots, and all floral organs (Fig. 6B) (Chang *et al.*, 2010; Hsu *et al.*, 2015). OMADS8 was unable to form homodimers or heterodimers with OMADS5 or OMADS9, while it does, however, form heterodimers with OMADS3 (Chang *et al.*, 2010). Ectopic expression of *OMADS8* in Arabidopsis converted sepals into petal-like organs (Chang *et al.*, 2010). Based on these findings in *O.* Gower Ramsey, Chang *et al.* (2010) proposed that the presence of at least OMADS3/8/5 and/or OMADS9 is required for sepal and petal formation, whereas the presence of OMADS3/8/9 and the absence of OMADS5 are likely to be required for labellum formation (Chang *et al.*, 2010).

*LMADS8* and *LMADS9* were identified as the *PI* orthologues in *L. longiflorum* (Table 1) (Chen *et al.*, 2012). qRT-PCR analysis revealed that *LMADS8* is highly expressed in the first and second whorl tepals in young and mature flowers, but is absent in vegetative leaves, roots, and stem (Chen *et al.*, 2012). The expression pattern of *LMADS9* is very similar to that of *LMADS8* (Fig. 6B). As seen in Arabidopsis AP3 and PI, and OsMADS4 and OsMADS16 in rice, LMADS8 and LMADS9 are able to form heterodimers with the AP3-like LMADS1 proteins, and can also form homodimers and heterodimers with each other, as shown by yeast two-hybrid analysis (Chen *et al.*, 2012). LMADS8 and LMADS9 seem to be involved in tepal formation and to a minor extent in early stamen formation (Chen *et al.*, 2012). Interestingly, *LMADS9* is a truncated version of *LMADS8*, missing the PI-motif in the C-terminal region (Fig. 6A) (Chen *et al.*, 2012). Ectopic expression of *LMADS8* and *LMADS9* in Arabidopsis partially converts sepals into petal-like organs (Chen *et al.*, 2012). Overexpression of *LMADS8* in the *pi* mutant of Arabidopsis completely rescued the phenotype, while overexpression of *LMADS9* only partially rescued the phenotype (Chen *et al.*, 2012).

Overall, the PI-like B-class genes in the grasses seem to have a conserved expression pattern and function. Only one PI-like gene is found in orchid, with a different protein–protein interaction pattern and function, indicating that the B-class genes are essential for the unique floral structure of orchids (Chang *et al.*, 2010). Even though LMADS9 does not have the defining PI-motif at its C-terminus, it does not seem to have lost its interaction possibilities and, possibly, may have retained its function (Chen *et al.*, 2012).

### *The $B_{sister}$ genes are phylogenetically closely related to the B-class genes but have different functions*

Close relatives of B-class genes have been identified in various species including rice, maize, barley, and wheat, and have been termed the $B_{sister}$ ($B_s$) genes. They are mainly expressed in female reproductive organs, especially ovules. The two lineages were most probably generated by gene duplication (Münster *et al.*, 2001; Becker and Theissen, 2003). Compared with the B-class genes, $B_{sister}$ genes share a shorter I domain, a subterminal PI-motif-derived sequence, and in some cases a paleoAP3 motif in the C-terminal region (Fig. 7A) (Becker *et al.*, 2002). In Arabidopsis, two $B_{sister}$ genes have been identified, *ABS* and *GOA* (Becker *et al.*, 2002; Nesi *et al.*, 2002; Mizzotti *et al.*, 2012). *ABS* is expressed in the endothelial layer of the inner integuments of mature ovules and is necessary for inner integument differentiation (Nesi *et al.*, 2002). *GOA* has a broad expression pattern in ovule primordia and in ovules, which later is restricted to the outer integuments (Prasad *et al.*, 2010). It has functions in ovule outer integument development and the regulation of fruit longitudinal growth (Prasad *et al.*, 2010; Yang *et al.*, 2012).

The $B_{sister}$ genes form three subclades in monocots: OsMADS29, OsMADS30, and OsMADS31 (Yang *et al.*, 2012), which are named after the three $B_{sister}$ genes found in the rice genome (Table 1). Expression analysis showed that *OsMADS29* expression is restricted to developing seeds, while *OsMADS30* is expressed throughout all organs in the plant (Fig. 7B) (Yang *et al.*, 2012). Suppressed expression of *OsMADS29* by an antisense construct results in reduced and delayed cell degradation of the nucellar projection, abnormal endosperm development, and altered seed morphology (Yin and Xue, 2012), indicating that *OsMADS29* is important for the degradation of the nucellar projection and the nucellus. Yeast two-hybrid analysis showed that OsMADS29 interacts with all five E-class MADS-box genes and both AGL6-like MADS-box genes (Nayar *et al.*, 2014). It also interacts with

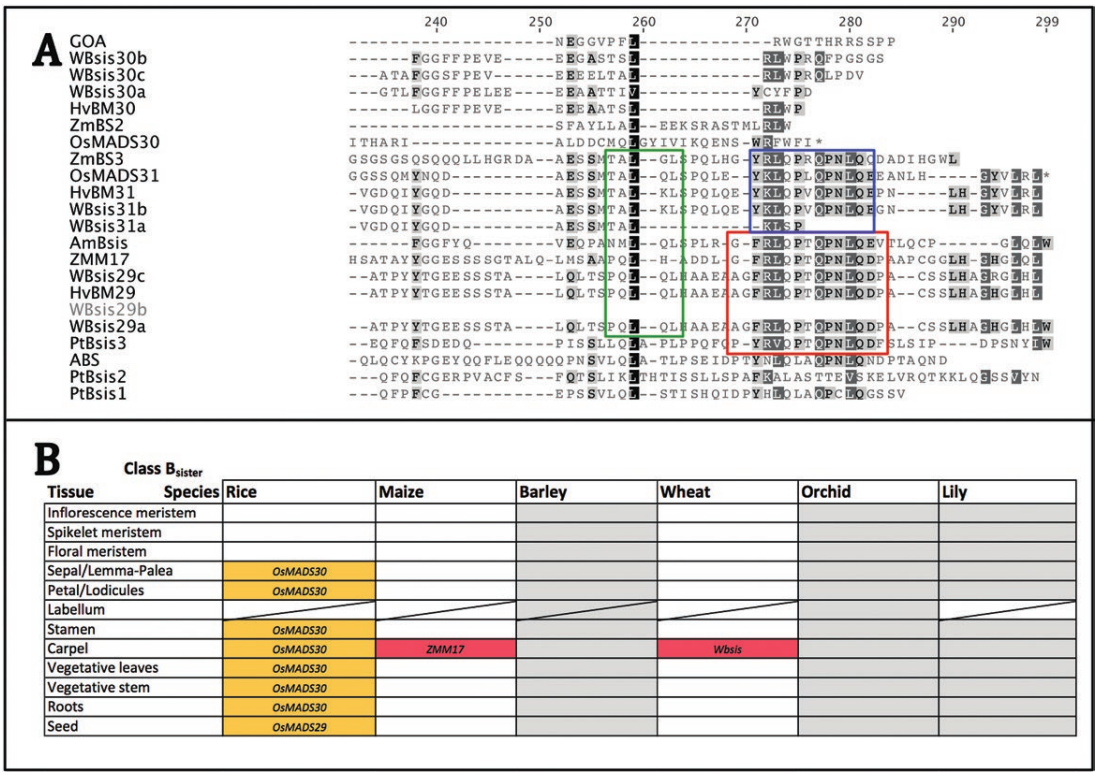



**Fig. 7.** Sequence alignment and expression patterns of $B_{sister}$-class MADS-box genes in Arabidopsis, *Amborella trichopoda*, *Populus trichocarpa*, rice, maize, barley, wheat, orchid, and lily. (A) Multiple alignment of protein sequences from the NCBI, IPK, and MSU rice databases. A conserved PI-derived motif can be found in the $B_{sister}$ genes together with another unidentified motif downstream of the PI-derived motif. Variations in the PI-derived motif seem to divide the $B_{sister}$ genes into two groups. One group consisting of ZMM17, OsMADS29, WBsis, and HvBM29 has GFRLQPTQPNLQDP as the PI-derived motif. The other group consisting of OsMADS31 and HvBM31 has YKLQPL/VQPNLQE as the PI-derived motif. An unidentified TALQL motif can be found in all monocot $B_{sister}$ genes, which is remarkably similar to the motif found in the C-class MADS-box genes (see Fig. 8). OsMADS30 contains neither of the two motifs. (B) The expression patterns of $B_{sister}$ genes that have been investigated show conservation in the female reproductive organs. Red squares indicate that multiple genes are expressed in this tissue, while yellow indicates that only one gene is expressed in this tissue. White squares indicate that there is no expression, and grey squares indicate that no data are available regarding the expression in these tissues.

A-class OsMADS14 and OsMADS18, C-class OsMADS3 and $B_{sister}$ protein OsMADS31, and forms homodimers (Nayar *et al.*, 2014). *OsMADS30* lacks the characteristic $B_{sister}$ motifs (Becker *et al.*, 2002; Yang *et al.*, 2012) and has a different C-terminus due to the insertion of a mobile element (OsME), which has an altered function and expression profile (Fig. 7A) (Schilling *et al.*, 2015). In maize, *ZMM17* has been identified as a $B_{sister}$ gene; *ZMM17* is expressed in all organ primordia of the female spikelet, but later is restricted to the ovule and the developing silk, as determined by northern hybridization analysis (Becker *et al.*, 2002; Yang *et al.*, 2012). *WBsis* was classified as a $B_{sister}$ gene and part of the *OsMADS29*-like clade in wheat because of the high sequence similarity to *OsMADS29* and *OsMADS31* (Yamada *et al.*, 2009). *WBsis* is expressed in the endothelial layer of the inner integument of the ovule, similar to *ABS* in Arabidopsis; weak expression is also detected in the nucellus and the outer integument (Yamada *et al.*, 2009; Mizzotti *et al.*, 2012; Yang *et al.*, 2012).

All $B_{sister}$ genes discussed here show a similar expression pattern, except *OsMADS30* which also has a diverged function. No $B_{sister}$ genes have been thoroughly investigated in barley, orchid, and lily.

### *C- and D-class genes*

C-class genes in eudicots specify the plant reproductive organs alone (carpels) or together with the B-class genes (stamens) (Fornara *et al.*, 2003). They also seem to be involved in the negative regulation of A-class MADS-box genes (Gustafson-Brown *et al.*, 1994; Wang *et al.*, 2015). Upon the discovery of the function of the MADS-box genes *FBP7* and *FBP11* in *Petunia* in regulating ovule organ identity, the ABC model was extended to incorporate a D function (Angenent *et al.*, 1995; Colombo *et al.*, 1995). D-gene function is involved in the determination of the identity of the central meristem, the progenitor tissue of the placenta, and the ovules (Angenent and Colombo, 1996). Both C- and D-class genes belong to the AG-like subfamily and have arisen through a gene duplication

event close to the base of the angiosperm emergence (Becker and Theissen, 2003).

C- and D-class proteins can be distinguished by the structure of the N-terminal part of the K-box. In the D-lineage, a glutamine at position 105 is conserved, while this residue is not found in the C-lineage (Figs 7, 8) (Kramer *et al.*, 2004; Dreni *et al.*, 2007). Most D-lineage proteins also have a non-polar hydrophobic residue at position 106, whereas C-lineage proteins have a polar residue at that position (Dreni *et al.*, 2007). Monocot D-lineage proteins have a specific single amino acid insertion at position 90, and at position 113 there is a histidine residue. Both of these are not present in C-lineage proteins (Dreni *et al.*, 2007). Furthermore there is a conserved AG motif I and AG motif II in the C-terminal region of AG-like proteins, which can be found in C- and D-class proteins (Kramer *et al.*, 2004). A nine amino acid motif downstream of the AG motif II is specific for D-class proteins (Hsu *et al.*, 2010) (Figs 8, 9).

In rice, two duplicated C-class genes *OsMADS3* and *OsMADS58* have partially sub-functionalized (Table 1) (Kang *et al.*, 1995; Yamaguchi *et al.*, 2006). *OsMADS3* shows high sequence and expression similarity to Arabidopsis *AG* (C-class gene). *In situ* hybridization showed that *OsMADS3* is strongly expressed in stamen primordia, while *OsMADS58* is expressed at a lower level uniformly throughout the floral meristem (Dreni *et al.*, 2011). After the differentiation of the third whorl organ, both *OsMADS3* and *OsMADS58* have a similar expression profile in the filament and the anther wall, and a stable expression level in the carpel and ovule primordia (Dreni *et al.*, 2011). *OsMADS3* plays a predominant role in stamen specification, with knock-out mutants by T-DNA insertion (*mads3-3*) exhibiting stamens completely or incompletely transformed into lodicules while carpels developed normally (Yamaguchi *et al.*, 2006; Dreni *et al.*, 2011). Even though *osmads58* insertional mutants showed no drastic phenotype (Dreni *et al.*, 2011), *osmads3-3 osmads58* double mutants showed a complete loss of reproductive organ identity and floral meristem determinacy (Dreni *et al.*, 2011). The size of the floral meristem also strongly increased, and the combination of these features resulted in an enlarged third whorl. In half of the florets, the carpel was replaced by a small green lemma/palea-like structure (Dreni *et al.*, 2011). Based on these results, it seems that OsMADS3 and OsMADS58 work redundantly, with the contribution of OsMADS3 being more important (Dreni *et al.*, 2011). OsMADS3 and OsMADS58 genetically interact with the B-class gene OsMADS16 and together they play a key role in suppressing indeterminate growth within the floral meristem in the third whorl primordia (Yun *et al.*, 2013).

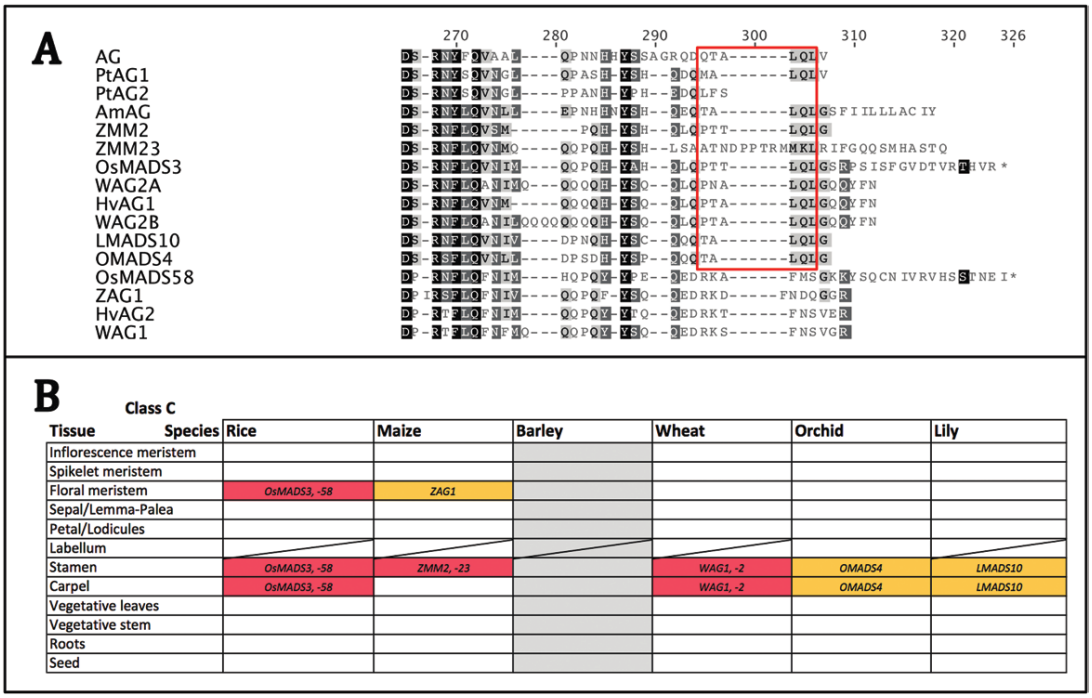



**Fig. 8.** Sequence alignment and expression patterns of C-class MADS-box genes in Arabidopsis, *Amborella trichopoda*, *Populus trichocarpa*, rice, maize, wheat, barley, orchid, and lily. (A) The C-class genes are very conserved throughout the entire sequence. A small distinction can be made at the C-terminus where the TALQL motif, that is also present in the $B_{sister}$ genes, can be found in some of the homologues. Expression of C-class genes seems to be conserved in all species. (B) The expression patterns of C-class genes are conserved across all species that have been investigated to date. Red squares indicate that multiple genes are expressed in this tissues, while yellow indicates that only one gene is expressed in this tissue. White squares indicate that there is no expression, and grey squares indicate that no data are available regarding the expression in these tissues.

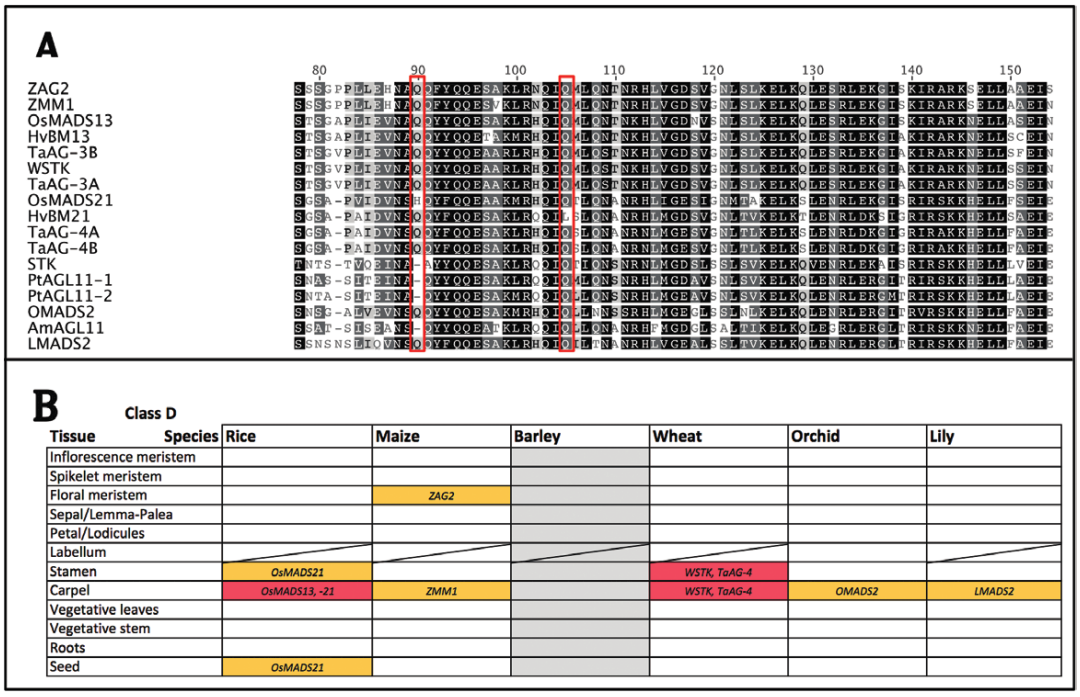



**Fig. 9.** Sequence alignment and expression patterns of D-class MADS-box genes in Arabidopsis, *Amborella trichopoda*, *Populus trichocarpa*, rice, maize, wheat, barley, orchid, and lily. (A) Multiple alignment of protein sequences from the NCBI, IPK, and MSU rice databases The C- and D-class MADS-box genes in monocots can be distinguished by a conserved glutamine at position 105 and a single amino acid insertion at position 90 in the D-lineage. Remarkably, HvBM21 does not have a glutamine, but a leucine at position 105. It seems that most monocot genes have a glutamine insertion at position 90, except OsMADS21, that has a histidine. (B) Expression of D-class genes seems to be conserved among all species. Red squares indicate that multiple genes are expressed in this tissue, while yellow indicates that only one gene is expressed in this tissue. White squares indicate that there is no expression, and grey squares indicate that no data are available regarding the expression in these tissues.

*WAG1* and *WAG2* are classified as C-function genes in *Triticum aestivum* (Table 1) (Meguro *et al.*, 2003; Zhao *et al.*, 2006; Shitsukawa *et al.*, 2007; Hirabayashi and Murai, 2009; Murai, 2013). Although they share high level sequence similarity to rice *OsMADS58* and *OsMADS3*, respectively, they have different expression patterns and functions (Wei *et al.*, 2011; Murai, 2013). Meguro *et al.* (2003) detected three homeologues of *WAG1* in the wheat genome on the group one chromosomes (1A, 1B, and 1D) by Southern blot analysis, while Wei *et al.* (2011) found three homeologues of *WAG2* on the group two chromosomes (2A, 2B, and 2D). *WAG1* expression is low during initiation of floral organ primordia, but transcripts accumulate in developing spikes at the booting to heading stage seen by northern blot analysis, suggesting that it is involved in floral organ development rather than differentiation (Meguro *et al.*, 2003). *In situ* hybridization showed that *WAG1* and *WAG2* are detected in the stamen, carpel, and ovule (Fig. 8B) (Yamada *et al.*, 2009). Ectopic expression of the *WAG1* and *WAG2* genes induced pistilloid stamens in alloplasmic wheat, which suggests they participate in ectopic ovule formation in these structures (Yamada *et al.*, 2009).

The maize orthologues of rice *OsMADS3* are *ZMM2* and *ZMM23*, and *OsMADS58* is *ZAG1* (Table 1) (Schmidt *et al.*, 1993; Theissen *et al.*, 1995; Münster *et al.*, 2002; Li *et al.*, 2014). *ZAG1* is expressed early in stamen and carpel primordia, as shown by RNA blot analysis and *in situ* hybridization (Schmidt *et al.*, 1993). *ZMM2* is mainly expressed in the anthers (Fig. 8B) (Mena *et al.*, 1996; Li *et al.*, 2014). Analysis of loss-of-function mutants showed that *ZAG1* determines the floral meristem, while *ZMM2* participates in regulating the formation of stamens and carpels (Mena *et al.*, 1996; Wei *et al.*, 2011). The orchid genes *OMADS4* and *OMADS2* are both placed in the AG-clade, with *OMADS4* having a C-class function and *OMADS2* a D-class function (Table 1) (Hsu *et al.*, 2010). qRT-PCR analysis showed that *OMADS4* is expressed in stamens, the stigmatic cavity, and the ovule (Fig. 8B) (Hsu *et al.*, 2010), which is similar to the expression pattern of *AG* in Arabidopsis (Yanofsky *et al.*, 1990). Yeast two-hybrid analysis showed that OMADS4 and OMADS2 can form homodimers and heterodimers with each other (Hsu *et al.*, 2010). *LMADS10*, the C-class gene in lily, is expressed in stamens and carpels (Hsu *et al.*, 2010). This is very similar to the expression pattern in *O.* Gower Ramsey (Fig. 8B). Ectopic expression of *LMADS10* in Arabidopsis caused early flowering and produced small, curly leaves and floral organ conversions such as carpelloid sepals (Hsu *et al.*, 2010). Overexpression of *OMADS4* in Arabidopsis only showed a moderate early flowering phenotype with no homeotic floral organ changes (Hsu *et al.*, 2010).

Rice has two duplicated D-lineage genes: *OsMADS13* and *OsMADS21* (Table 1) (Kramer *et al.*, 2004; Dreni *et al.*, 2007). *OsMADS13* is expressed in the ovule primordium and the inner cell layer of the carpel wall. Its expression persists during development of the ovule, mainly in the integuments (Lopez-Dee *et al.*, 1999). In a *Tos17* insertion mutant of *OsMADS13*, ovule primordia developed into carpelloid structures that grew out of the carpel, giving rise to ectopic styles and stigmas (Dreni *et al.*, 2007; Yamaki *et al.*, 2011). The *osmads3-3 osmads13* double mutant showed a complete loss of floral meristem determinacy inside the fourth whorl, while the *osmads13 osmads58* double mutant showed a similar but milder phenotype (Dreni *et al.*, 2011; Li *et al.*, 2011). OsMADS13 interacts with the E-class MADS-box proteins, OsMADS7 and OsMADS8, and is involved in ovule specification and floral meristem determinacy (Fornara *et al.*, 2003; Yamaguchi and Hirano, 2006; Dreni *et al.*, 2007). RT-PCR and *in situ* hybridization showed that *OsMADS21* is expressed at low levels in the inner two whorls of the flower and ovules; its expression overlaps with that of *OsMADS13* (Arora *et al.*, 2007; Dreni *et al.*, 2007). The *OsMADS21* expression is in two whorls of the flower which differs from other D-lineage genes, which are ovule specific (Fig. 9B) (Dreni *et al.*, 2007); it is also highly expressed in developing kernels (Arora *et al.*, 2007; Dreni *et al.*, 2007). T-DNA insertional mutants of *OsMADS21* show no aberrant phenotype, while os*mads13 osmads21* double mutants showed no more severe phenotypes than the *osmads13* single mutant, and up-regulation of *OsMADS21* resulted in partial complementation of the *osmads13* phenotype, but ovule development was not completely restored (Dreni *et al.*, 2007, 2011). These results suggest that *OsMADS21* has lost its function in determining ovule identity, presumably because of its redundancy with *OsMADS13* (Fornara *et al.*, 2003; Yamaguchi and Hirano, 2006; Dreni *et al.*, 2007).

The closest relative of the Arabidopsis D-function gene *STK* in wheat is *WSTK*, also known as TaAG-3 (Table 1) (Zhao *et al.*, 2006; Paolacci *et al.*, 2007). Yeast two-hybrid analysis has shown that WSTK forms a complex with the E-class protein WSEP (Shitsukawa *et al.*, 2007; Yamada *et al.*, 2009; Murai, 2013). RT-PCR assays showed that it is expressed in pistils, with strong expression in the developing ovule (Yamada *et al.*, 2009). *In situ* hybridization showed WSTK mRNA in the ectopic ovules and pistil-like stamens of alloplasmic wheat, suggesting a role in ovule formation (Yamada *et al.*, 2009). There are presumably three homeologues of *WSTK* in the wheat genome (Zhao *et al.*, 2006; Yamada *et al.*, 2009). The closest relative to *OsMADS2*1 in wheat has been identified as *TaAG-4* (Paolacci *et al.*, 2007). *TaAG-4* has weak expression in stamens and very high expression in pistils, as shown by RT-PCR (Paolacci *et al.*, 2007). *ZAG2* and *ZMM1* have been identified as D-class genes in maize (Schmidt *et al.*, 1993; Theissen *et al.*, 1995; Li *et al.*, 2014). *ZAG2* is a floral specific gene, but is expressed later in floral primordia than the C-class gene *ZAG1*. Expression of *ZAG2* is largely restricted to the developing ovules and the inner carpel face, as determined by *in situ* hybridization (Schmidt *et al.*, 1993). qRT-PCR showed that *OMADS2* in *O.* Gower Ramsey is expressed in the stigmatic cavity and the ovary, but is undetectable in sepals, petals, the labellum, and stamens (Fig. 9B) (Hsu *et al.*, 2010). Ectopic expression of *OMADS2* shows the same phenotype as *LMADS10*, except that there are no floral organ conversions (Hsu *et al.*, 2010). *LMADS2* was identified as the D-class protein in *L. longiflorum* (Tzeng *et al.*, 2002). It was exclusively expressed in the carpel, more specifically in the ovule, as seen by RNA blot analysis (Tzeng *et al.*, 2002). LMADS2 can form heterodimers with LMADS10 and both can also form homodimers, as shown by yeast two-hybrid analysis (Hsu *et al.*, 2010). Ectopic expression of *LMADS2* in Arabidopsis caused early flowering and floral organ conversion of sepals and petals to carpel- and stamen-like structures (Tzeng *et al.*, 2002).

The gene duplication event of C-class genes is also seen in some grasses, for instance in maize, leading to three different C-class genes and possible sub-functionalization (Dreni and Kater, 2014). In contrast, only one C-class gene and one D-class gene have currently been found in *O.* Gower Ramsey and *L. longiflorum*, but their expression patterns are highly conserved compared with those of Arabidopsis and rice.

### *E-class genes*

E-class genes belong to the *AGL2*-subfamily and specify flower organ identity by forming higher order protein complexes with the class A, B, or C proteins (Pelaz *et al.*, 2000; Theissen, 2001; Becker and Theissen, 2003). This ability to form tetrameric complexes also contributes to the development of floral quartets to control sepal, petal, stamen, and carpel formation or their equivalents in grasses (Theissen and Saedler, 2001; Becker and Theissen, 2003; Fornara *et al.*, 2003;). In Arabidopsis, *SEP1/2/3/4* have been identified as E-class genes (Ma *et al.*, 1991; Huang *et al.*, 1995; Mandel and Yanofsky, 1998). *SEP1*, *SEP2*, and *SEP4* are expressed in all four whorls of the flower, with SEP4 showing higher expression in the central dome (Flanagan and Ma, 1994; Savidge *et al.*, 1995; Ditta *et al.*, 2004). *SEP3* is only expressed in the inner three whorls (Mandel and Yanofsky, 1998).

*AGL2*-like genes were deduced to have undergone a gene duplication event before the origin of the extant angiosperms, and after the divergence between extant gymnosperms and angiosperms, creating the SEP3- and LOFSEP-lineages (Malcomber and Kellogg, 2005; Zahn *et al.*, 2005*a*). Furthermore, SEP3- and LOFSEP-lineages may have undergone more gene duplication events in the grasses, leading to three LOFSEP lineages: OsMADS1-, OsMADS5- and OsMADS34-clades and two SEP3-lineages: OsMADS7- and OsMADS8-clades (Malcomber and Kellogg, 2005; Zahn *et al.*, 2005*a*). In addition, two motifs (SEPI and SEPII) that consist of hydrophobic and polar residues were observed in AGL2-like proteins (Vandenbussche *et al.*, 2003; Zahn *et al.*, 2005*a*). Clade-specific changes in these motifs can be seen; for instance, the OsMADS5-clade in grasses have lost the final 12–15 amino acids within the SEPII motif, possibly caused by

a recent gene duplication followed by a frameshift mutation (Vandenbussche *et al.*, 2003; Zahn *et al.*, 2005*a*).

*LOFSEP-lineage*

*OsMADS1-clade.* *OsMADS1*, one well-characterized E-class gene in rice, plays an important role in floral meristem determination and controls the differentiation and proliferation of palea- and lemma-specific cell types (Jeon *et al.*, 2000*a*; Prasad *et al.*, 2005). The expression of *OsMADS1* is detected in the floral meristem during early flower development, and later in the palea, lemma, and weakly in the carpel, shown by northern blot analysis, RT-PCR, and *in situ* hybridization (Fig. 10B) (Chung *et al.*, 1994; Prasad *et al.*, 2001; Kobayashi *et al.*, 2010). Overexpression of *OsMADS1* caused stunted panicles, irregularly positioned branches and spikelets, and the rudimentary glumes were transformed into palea/lemma-like structures (Prasad *et al.*, 2001, 2005). Different mutants of *OsMADS1* have been investigated. Jeon *et al.* (2000*a*) reported that *lhs-1* (*leafy hull sterile1*), which contains two missense mutations in the *OsMADS1* MADS-domain, showed a loss of floral meristem determination and transformation of palea and lemma into leaf-like structures. Similarly, other *OsMADS1* mutants such as *osmads1-z* and *nsr* (*naked seed rice*) showed the transformation of the lemma, palea, and lodicules into leaf-like structures (Chen *et al.*, 2006; Gao *et al.*, 2010). OsMADS1 was shown to interact with the A-class proteins OsMADS14 and OsMADS15, the B-class protein OsMADS16, the C-class proteins OsMADS3 and OsMADS58, the D-class protein OsMADS13, the E-class proteins OsMADS7 and OsMADS8, and the AGL-like

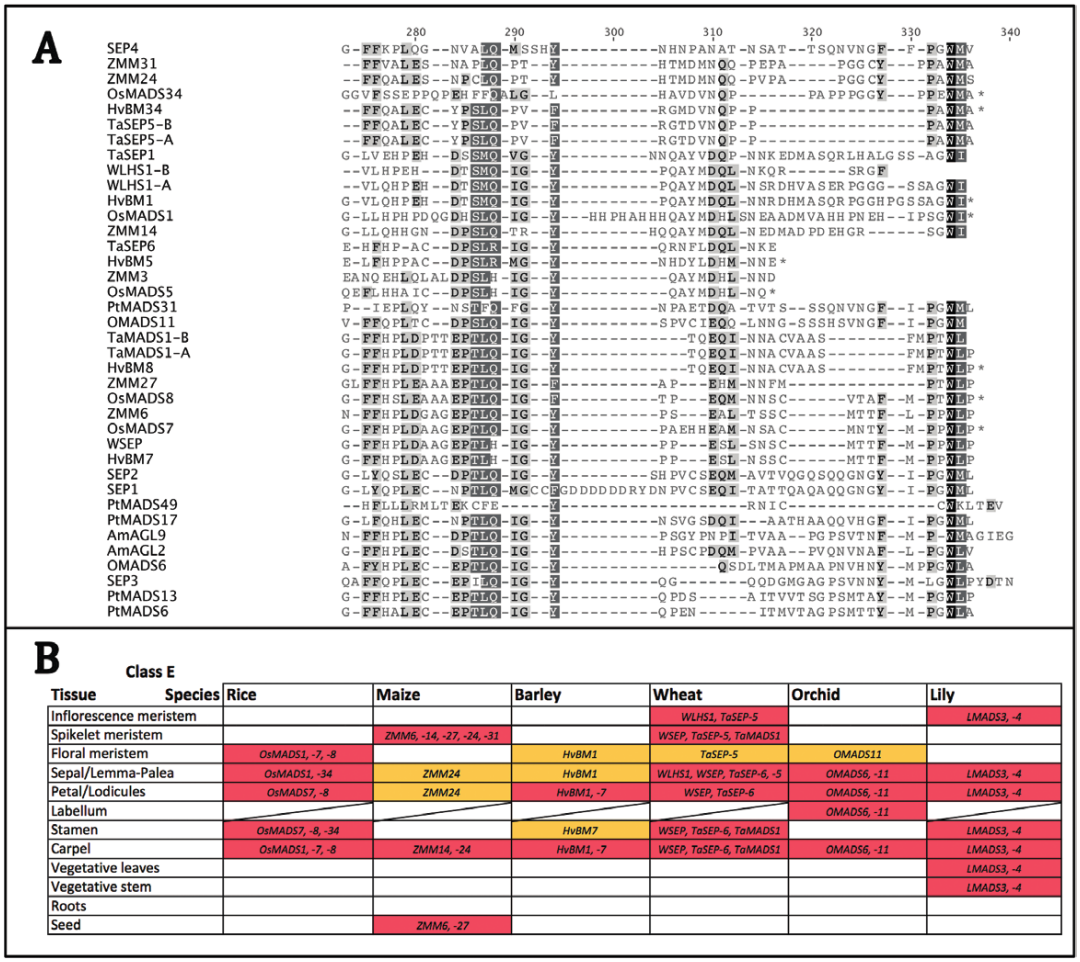



**Fig. 10.** Sequence alignment and expression patterns of E-class MADS-box genes in Arabidopsis, *Amborella trichopoda*, *Populus trichocarpa*, rice, maize, wheat, barley, orchid, and lily. (A) Multiple alignment of protein sequences from the NCBI, IPK, and MSU rice databases. The distinction between the two subgroups can clearly be seen, with the OsMADS1 group less related to the Arabidopsis SEP genes, and the OsMADS7 group more closely related to the SEP genes. (B) Expression of E-class genes in very diverse, but seems to be mostly conserved among the different species. Maize seems to have distinct genes with specified expression. Red squares indicate that multiple genes are expressed in this tissue, while yellow indicates that only one gene is expressed in this tissue. White squares indicate that there is no expression, and grey squares indicate that no data are available regarding the expression in these tissues.

protein OsMADS6 (Moon *et al.*, 1999*b*; Lim *et al.*, 2000; Cui *et al.*, 2010; Hu *et al.*, 2015). Two maize homologues of *OsMADS1*, *ZMM8* and *ZMM14*, are thought to determine the alternative identity of the upper versus the lower floret within each spikelet primordium (Cacharrón *et al.*, 1999; Becker and Theissen, 2003). Their expression was only detectable in the upper floret, but not in the lower floret of the developing spike, shown by *in situ* hybridization (Fig. 10B) (Cacharrón *et al.*, 1995, 1999). *ZMM14* expression is lower than that of *ZMM8*, and is stronger in the carpels than in the other tissues (Cacharrón *et al.*, 1999). The function of barley *HvBM1* (also known as *BM7*) remains to be elucidated. The expression of *HvBM1* is seen in the floret meristem at the distal part of the awn primordium. As floret development continues, expression is detected in the lemma and palea, in the lodicules and the ovule, but not in the anther (Schmitz *et al.*, 2000).

Wheat has three homeologues of *OsMADS1* called *WLHS1* located on chromosomes 4A, 4B, and 4C (Shitsukawa *et al.*, 2007). *In situ* hybridization analysis showed that the expression of *WLHS1* is initially detectable in the inflorescence axis at inflorescence meristem initiation (Shitsukawa *et al.*, 2007). During floral organ differentiation, their expression signals are detected in the spikelet axis at the most proximal position (Shitsukawa *et al.*, 2007). Later, their expression was observed in the glume, lemma, and palea until maturity of the floral organs (Shitsukawa *et al.*, 2007). Shitsukawa *et al.* (2007) showed that expression of *WLHS1-B* is much lower than that of *WLHS1-A* and *-D*. WLHS1-B and WLHS1-D interact with B-class WAP3 and WPI2 and all E-class genes, with the exception of WLHS1-A (Shitsukawa *et al.*, 2007). It has been suggested that the lack of interaction with WLHS1-A is due to the loss of the K-box in WLHS1-A (Davies *et al.*, 1996; Shitsukawa *et al.*, 2007). Overexpression of *WLHS1* homeologues in Arabidopsis showed no phenotype for *WLHS1-A*, and early flowering and late production of terminal flowers for *WLHS1-B* and *-D* (Shitsukawa *et al.*, 2007).

*OsMADS5-clade.* The function of the *LOFSEP* gene *OsMADS5* has remained a mystery because of no detectable phenotype in either panicles or vegetative organs in loss-of-function mutants, except for the lodicules being more tightly attached to the lemma and palea upon spikelet dissection (Agrawal *et al.*, 2005). Recent findings using genetic and molecular approaches suggest that one role of *OsMADS5* is to regulate spikelet morphogenesis together with *OsMADS1* and *OsMADS34* redundantly by positively regulating the other MADS-box floral homeotic genes. Furthermore, OsMADS1, OsMADS5, and OsMADS34 can form protein–protein interactions with other MADS-box floral homeotic members, which is a typical, conserved activity of plant SEP proteins (Wu *et al.*, 2018).

*ZMM3* (maize) was classified as a member of the OsMADS5-clade in the LOFSEP-lineage with unknown function (Malcomber and Kellogg, 2005). Paolacci *et al.* (2007) identified *TaSEP-6* as an orthologue of *OsMADS5*, located on chromosomes 7A, 7B, and 7D in the wheat genome. Northern blot analysis, RT-PCR, and qRT-PCR showed that it is expressed in all floral organs, but at very high levels in glumes, lemma, and palea (Paolacci *et al.*, 2007).

*OsMADS34-clade.* Unlike other *SEP*-like genes involved in controlling flower development, *OsMADS34* [*PANICLE PHYTOMER2* (*PAP2*)], one *LOFSEP* gene, is required for rice inflorescence and spikelet development (Gao *et al.*, 2010; Kobayashi *et al.*, 2010; Lin *et al.*, 2014). *osmads34-1* showed altered inflorescence shape with increased primary branch number and decreased secondary branch number. In addition, *osmads34-1* showed fewer spikelets and changed spikelet morphology, containing elongated sterile lemmas with lemma/palea-like features (Gao *et al.*, 2010). Recently *OsMADS34*/*PAP2* was shown to be involved in the transition from vegetative to reproductive development via specifying inflorescence meristem identity together with three *AP1*/*FUL*-like genes *OsMADS14*, *OsMADS15*, and *OsMADS18* (Kobayashi *et al.*, 2012). These findings clearly show that OsMADS34 is a positive regulator of inflorescence meristem identity and spikelet meristem identity, as well as a suppressor of elongation of the glumes (Kobayashi *et al.*, 2010, 2012).

In maize and wheat, the functions of *OsMADS34* homologues have not been elucidated, and only expression data are reported. Two maize homologues of *OsMADS34*, *ZMM24* and *ZMM31*, are expressed in early developing tassels and ears, and *ZMM24* shows high expression throughout ear development (Danilevskaya *et al.*, 2008). *TaSEP-5* was identified as the orthologue of *OsMADS34* in wheat, and its three homeologues are located on chromosomes 5A, 5B, and 5D, with a high expression level at the early spike developmental stages, which decreases, but increases again in spikes at the booting and heading stages (Paolacci *et al.*, 2007). Notably, *TaSEP-5* is highly expressed in the glumes, lemma, and palea (Paolacci *et al.*, 2007).

*Orchid and lily.* To date there is no direct genetic evidence showing the function of the *OsMADS1*-like gene *OMADS11* in orchid. *OMADS11* is highly expressed in the sepal, petal, lip, carpel, anther cap, and stigmatic cavity, and has no expression signal in vegetative leaves and stamens, as was shown by RT-PCR. Ectopic expression of *OMADS11* in Arabidopsis showed an early flowering phenotypes and smaller, curled leaves (Chang *et al.*, 2009). In lily, *LMADS3* and *LMADS4* were identified as E-class genes (Table 1) (Tzeng *et al.*, 2003). *LMADS4* is a *SEP1*/*2* orthologue, which is expressed in the inflorescence meristem, floral buds of different developmental stages, and in all four whorls of the flower (Tzeng *et al.*, 2003; Chang *et al.*, 2009). *LMADS4* is also expressed in the vegetative leaf and in the inflorescence stem (Tzeng *et al.*, 2003). Arabidopsis plants with ectopic expression of *LMADS4* were indistinguishable from the wild-type plants (Tzeng *et al.*, 2003).

*SEP3-lineage*

*OsMADS7-clade.* *OsMADS7* has a redundant function in specifying rice flower development with *OsMADS8*, as suggested by the observation that *OsMADS7* and *OsMADS8* share almost identical expression patterns (Kang *et al.*, 1997; Pelucchi *et al.*, 2002). *OsMADS7* and *OsMADS8* are expressed early in the floral meristem where the lodicule and stamen primordia develop (Kang *et al.*, 1997; Pelucchi *et al.*, 2002). Subsequently they are expressed in lodicules, developing stamen, and carpel primordia throughout floret development (Fig. 10B) (Kang *et al.*, 1997; Pelucchi *et al.*, 2002). Overexpression and knock-down of *OsMADS7* shows similar phenotypes to that of *OsMADS8* (Kang *et al.*, 1997; Jeon *et al.*, 2000*b*; Cui *et al.*, 2010). Knock-down of both *OsMADS7* and *OsMADS8* resulted in late flowering and homeotic transformation of lodicules, stamens, and carpels into palea/lemma-like structures, while knock-down of *OsMADS7* or *OsMADS8* using RNAi only showed mild phenotypes (Cui *et al.*, 2010). *In vitro* and *in vivo* assays showed that OsMADS7 interacts with OsMADS8 and OsMADS1, and can form homodimers (Cui *et al.*, 2010).

*ZMM6* in maize is weakly expressed in all organs of the upper and lower floret during inflorescence development, and is strongly expressed in the endosperm transfer cell region and the embryo during maize kernel development (Fig. 10B) (Cacharrón *et al.*, 1995, 1999; Lid *et al.*, 2004). Loss of function of *ZMM6* with a *Mutator* insertion showed no obvious developmental defects in the kernel (Lid *et al.*, 2004).

In barley, *HvBM7* (also known as *BM9*) expression has been found in anthers, but not in the lemma or palea, and later also in lodicules and the carpel (Fig. 10B) (Schmitz *et al.*, 2000). The wheat SEP-like protein WSEP has three homeologues in the wheat genome on chromosomes 7A, 7B, and 7D (Paolacci *et al.*, 2007; Shitsukawa *et al.*, 2007). Just before initiation of the lodicule, and stamen and carpel formation, *WSEP* expression was detected in whorls 2, 3, and 4 (Shitsukawa *et al.*, 2007). In all subsequent stages, expression was also detected in the palea of the floret (Fig. 10B). qRT-PCR showed that there is no difference in expression between the three homeologues (Shitsukawa *et al.*, 2007). Overexpression of *WSEP* in Arabidopsis showed early flowering and 4–5 curled leaves phenotypes for all three homeologues (Shitsukawa *et al.*, 2007). The strong expression of *WSEP* not only during floral organ differentiation but also after floral organ determination suggests that *WSEP* genes are involved in both floral organ differentiation and their subsequent development (Shitsukawa *et al.*, 2007; Chang *et al.*, 2009; Murai, 2013). WSEP interacts with the A-class WAP1, the B-class WAP3 and WPI2, the C-class WAG1 and WAG2, the D-class WSTK, and all E-class genes, except WLHS1-A (Shitsukawa *et al.*, 2007).

*OsMADS8-clade.* The expression pattern of the *OsMADS8* homologue in maize *ZMM27* is similar to that of *ZMM6*, showing weak expression during development of the inflorescence and strong expression during maize kernel development (Lid *et al.*, 2004). Further, loss of function of *ZMM27* in a *Mutator* insertional mutant did not induce obvious defects and neither did the double mutant with *ZMM6* (Lid *et al.*, 2004). *TaMADS1* was identified as the *OsMADS8* orthologue in wheat, with the three homeologues located on chromosomes 5A, 5B, and 5D (Paolacci *et al.*, 2007). Northern blot analysis and *in situ* hybridization showed that they are uniformly expressed in the spikelet primordia and later confined to the carpels and stamens (Zhao *et al.*, 2006). Overexpression of *TaMADS1* in Arabidopsis showed mild to severe phenotypes, with early flowering and abnormal floral organs (Zhao *et al.*, 2006).

*Orchid and lily.* Expression of the *OsMADS7*-like gene in orchid, *OMADS6*, is abundant in the sepal, petal, labellum, carpel, anther cap, and stigmatic cavity, and weak in the stamen, as shown by RT-PCR (Fig. 10B) (Chang *et al.*, 2009). Overexpression of *OMADS6* in Arabidopsis resulted in early flowering, 2–4 small curled leaves, terminal flowers composed of 2–3 flowers, and homeotic conversions of sepals into carpel-like structures and petals into stamen-like structures (Chang *et al.*, 2009). In lily, *LMADS3* is a *SEP3* orthologue, which shows almost identical expression to that of the *OsMADS1*-like gene in lily, *LMADS4* (Tzeng *et al.*, 2003). Northern blot analysis showed that *LMADS3* is expressed in the inflorescence meristem and later in all four floral organs, but is absent in vegetative leaves (Tzeng *et al.*, 2003). Overexpression of *LMADS3* in Arabidopsis resulted in early flowering, 2–3 small curled rosette leaves, and two curled cauline leaves (Tzeng *et al.*, 2003). Inflorescence determinacy was lost, as was production of terminal flowers at the end of the inflorescence that had 2–3 carpels.

## AGL6-*like genes*

The *AGL6* subfamily is thought to be sister to the E-class AGL2-like genes (Becker and Theissen, 2003). Rijpkema *et al.* (2009) proposed adding *AGL6*-like genes to the E-class of the ABCDE model. Arabidopsis has two AGL6-like genes: *AGL6* and *AGL13*, both of which have various divergent functions in the plant, although no loss-of-function mutants have been described so far (Dreni and Zhang, 2016). AGL6 in Arabidopsis can interact with some type I MADS proteins, which is unusual for MIKC$^c$-type MADS proteins (Dreni and Zhang, 2016). AGL6-like proteins have a C-terminus with two short, but highly conserved regions named AGL6-I and AGL6-II motifs (Ohmori *et al.*, 2009).

In monocots, the *AGL6* family has four well-defined clades: *AGL6*-I to *AGL6*-IV (Dreni and Zhang, 2016). Orchid sequences are part of the AGL6-III and AGL6-IV clade (Dreni and Zhang, 2016). The *AGL6*-I clade in grasses can be further subdivided into two branches: *ZAG3*/*OsMADS6* and *OsMADS17* (Dreni and Zhang, 2016). Li *et al.* (2010) proposed that a duplication event that gave rise to these clades may have occurred before the diversification of grasses. The *OsMADS17* clade is characterized by 25 amino acid substitutions, most of them located in the K-domain and the C-terminal domain. *OsMADS6*-like sequences in grasses have a highly conserved motif (MLGWVL) that is different in *OsMADS17*-like genes (VMGWPL) (Fig. 10A) (Reinheimer and Kellogg, 2009).

The expression pattern of *AGL6*-like genes in plants shows clear differences reflecting evolutionary changes (Reinheimer and Kellogg, 2009). Their expression in the inner integument of the ovule is ancestral, and is also seen in the gymnosperms. Expression in the floral meristem was acquired in angiosperms, and expression in the second whorl organs was acquired in monocots. Early in grass evolution, a new expression domain emerged in the palea (Reinheimer and Kellogg, 2009).

Rice has two *AGL6*-like genes, *OsMADS6* and *OsMADS17*, which have different expression patterns (Ohmori *et al.*, 2009; Reinheimer and Kellogg, 2009). RT-PCR and *in situ* hybridization showed that *OsMADS6* is expressed in the floral meristem at early stages and later in the emerging palea primordium (Li *et al.*, 2010). It is also detected in developing palea, lodicules, ovule integuments, and carpels, and weakly in lemma (Fig. 11B) (Li *et al.*, 2010; Dreni and Zhang, 2016). Mutants of *OsMADS6* (also called *mfo1*) showed disturbed palea and lodicule identities, and had extra carpels or spikelets (Ohmori *et al.*, 2009). The *mfo1 lhs1* double mutant resulted in a severe phenotype including the loss of spikelet meristem determinacy, suggesting that together with OsMADS1, OsMADS6 determines floral organ and meristem identities (Ohmori *et al.*, 2009; Li *et al.*, 2010). This also suggests that OsMADS6 has a very similar function to the E-class genes, which regulate the development of all four whorls and floral meristem determinacy (Li *et al.*, 2010). OsMADS6 can also form protein complexes with rice B-, D-, and E-class proteins in yeast two-hybrid assays, which resemble the complexes formed by E-class genes with A-, B-, and C-class proteins in Arabidopsis (Moon *et al.*, 1999*b*; Lee *et al.*, 2003*a*; Seok *et al.*, 2010). OsMADS6 also interacts with the D-class protein OsMADS13 and the $B_{sister}$-class protein OsMADS29 (Favaro *et al.*, 2002; Nayar *et al.*, 2014). Together with B-class proteins, it specifies lodicule identity (Dreni and Zhang, 2016). OsMADS6 also represses the A-class genes *OsMADS14* and *OsMADS15*. *OsMADS17* is expressed in the floral meristem and later becomes restricted to the lodicule primordia and is also detected in the anther wall (Fig. 11B) (Reinheimer and Kellogg, 2009). Suppression of *OsMADS17* by RNAi did not result in any morphological abnormalities (Ohmori *et al.*, 2009). In the *mfo1* background, however, it enhanced the *mfo1* phenotype (Ohmori *et al.*, 2009).

Maize also has two *AGL6*-like genes: *ZAG3* and *ZAG5* (Table 1) (Mena *et al.*, 1995; Reinheimer and Kellogg, 2009). It was suggested that maize had lost the AGLI/OsMADS17-clade and that both *ZAG3* and *ZAG5* are orthologues of *OsMADS6* (Dreni and Zhang, 2016). *In situ* hybridization

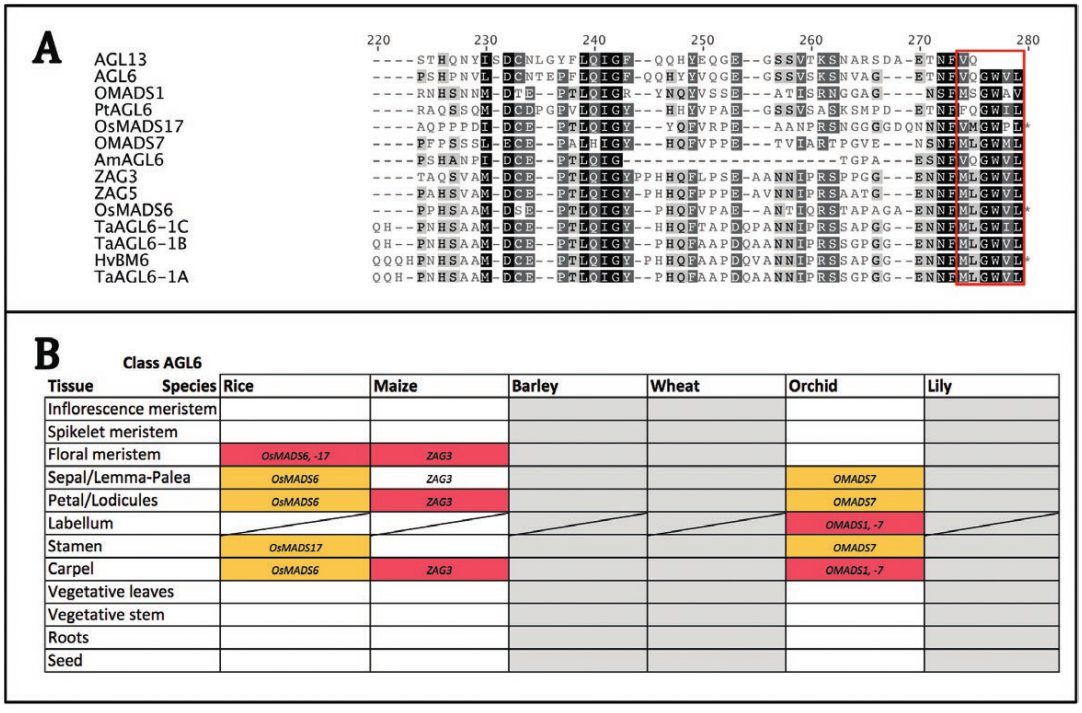



**Fig. 11.** Sequence alignment and expression patterns of AGL6-like MADS-box genes in Arabidopsis, *Amborella trichopoda*, *Populus trichocarpa*, rice, maize, wheat, barley, orchid, and lily. (A) Multiple alignment of protein sequences from the NCBI, IPK, and MSU rice databases. The AGL6-like genes are very conserved throughout the entire sequence. At the C-terminus (A), the motif for the OsMADS6-like genes (MLGWVL) can be distinguished, while the OsMADS17-like genes have a different motif (VMGWPL). (B) The expression pattern of AGL6-like genes seems to be conserved among the different species, with the exception of the labellum in orchid. Red squares indicate that multiple genes are expressed in this tissue, while yellow indicates that only one gene is expressed in this tissue. White squares indicate that there is no expression, and grey squares indicate that no data are available regarding the expression in these tissues.

showed that *ZAG3* is expressed in both the upper and lower floral meristems, but not in the lemma and stamens (Thompson *et al.*, 2009). Later in development, it was observed in developing lodicules, palea, carpel, and the inner integument of the ovule (Fig. 11B). ZAG3 interacts with the C-class protein ZAG1 (Reinheimer and Kellogg, 2009; Thompson *et al.*, 2009). Loss of function of *ZAG3*, known as the *bearded-ear* (*bde*) mutant, resulted in spikelets that produce more florets with more floral organs in the tassels (Thompson *et al.*, 2009). In the ear of the mutant, the spikelets also produce more florets, which have more palea/lemma-like organs and sterile ovaries.

Similar to rice and maize, orchid also has two AGL6-like genes: *OMADS7* and *OMADS1*. The expression pattern of *OMADS7* is extremely similar to that of the E-class gene *OMADS6* and of AGL6-like genes in other species, for example *AGL6* in Arabidopsis and *ZAG3* in maize (Chang *et al.*, 2009). Overexpression of *OMADS7* in Arabidopsis resulted in early flowering, producing small curled leaves and homeotic conversion of sepals into carpel-like structures with stigmatic papillae (Chang *et al.*, 2009). *OMADS1* shows a different expression, only in the apical meristem, the labellum, and carpel of the flowers (Hsu *et al.*, 2003). Yeast two-hybrid analysis showed that OMADS1 can interact with OMADS3 (Hsu *et al.*, 2003). Ectopic expression of *OMADS1* in Arabidopsis and tobacco resulted in reduced plant size, early flowering, and loss of inflorescence determinacy (Hsu *et al.*, 2003). Homeotic conversions of sepals into carpel-like structures and petals into staminoid structures were also observed (Hsu *et al.*, 2003).

AGL6-like genes seem to be involved in diverse processes in all four whorls, with conserved expression and function in most of the species. In orchid there seems to be a specialized function for these genes in labellum formation.

## Conclusions and perspectives

MADS-box ABCDE genes are crucial for floral development, and their evolutionary changes with gene duplication, sub-functionalization, and neo-functionalization led to novel morphological forms in plants. Understanding the function of these MADS-box genes can provide information on how different floral structures originated and identify targets for future crop improvement.

In grasses, the A-class genes underwent more gene duplications and acquired functions in specifying the grass-specific flower organs such as the palea and lodicule. Clearly the whole picture of A-class genes in grasses still remains to be elucidated.

As in other species, the function of B-class genes is relatively conserved in most grasses, even though there may has been gene duplication and sub-functionalization. Exceptionally, in orchids, two separate duplication events have led to some remarkable changes in floral structure. *OMADS3* in orchid lost the C-terminal motifs of MADS-box proteins and has the expression signal in the vegetative leaves (Hsu and Yang, 2002; Tsai and Chen, 2006). It is speculated that *LMADS1* in lily may represent an ancestral form of the B function gene, which retains the ability to form homodimers and regulates petal and stamen development (Tzeng and Yang, 2001). Notably, the *OsMADS30* $B_{sister}$ gene has gone through neo-functionalization, giving it a function in vegetative development instead of ovule and seed development (Schilling *et al.*, 2015). Until now, little is known about the $B_{sister}$ genes in most of the species described.

Despite gene duplication events the C- and D-class genes seem to have retained most of their function and expression patterns in monocots. Sub-functionalization has led to genes working redundantly, and the rice D-class gene *OsMADS21* has lost its ability to determine ovule development because of redundancy with *OsMADS13* (Fornara *et al.*, 2003; Prasad *et al.*, 2005; Yamaguchi and Hirano, 2006; Dreni *et al.*, 2007). Its higher expression in developing kernels might suggest that OsMADS21 has gone through neo-functionalization and has a function after fertilization (Arora *et al.*, 2007).

The E-class genes are more difficult to compare than the other classes of genes from the ABCDE model as they have diversified with a function in inflorescence and spikelet development during evolution. The expression of *OsMADS1* homologues in grasses varies from species to species with the developmental pattern of florets in the spikelet. *OsMADS1*-like genes may have been involved in morphological diversification of inflorescences during the evolution of grass species (Yamaguchi and Hirano, 2006).

Expression of *AGL6*-like genes in the palea is conserved in all spikelet-bearing grasses. This could indicate that AGL6-like genes might play a conserved role in palea development (Reinheimer and Kellogg, 2009). It has been proposed that AGL6-like genes may have played an important role in the evolution of unique flower features, such as the labellum in orchids (Dreni and Zhang, 2016).

Characterization of these genes, their structure, their expression pattern, and their function will give greater insight into their role in flower development. Importantly, phylogenetic analysis can sometimes be misleading, and data from functional analysis experiments are needed to confirm whether genes belong in specific clades and still retain a function in flower development. In line with this, neo-functionalization probably plays a relatively important and unexplored role in monocot floral diversity.The identification of orthologues is currently heavily reliant on sequence similarities, but, due to the many gene duplication events that have shaped the MADS-box family, some MADS-box genes in monocots have gained new roles, or lost their ancestral function. It must also be noted that most of these sequences are extracted from reference genomes, and therefore a much greater level of diversity may be present in the pangenome that is not represented here. Since flower development is one of the major determinants for yield in important crops, improving our understanding about the genes and networks involved in flower development is an essential tool to help towards devising new strategies for crop improvement.

## Supplementary data

Supplementary data are available at *JXB* online.

Fig. S1. Sequence alignment of A-class proteins in Arabidopsis, *Amborella trichopoda*, *Populus trichocarpa*, rice, maize, wheat, barley, orchid, and lily.

Fig. S2. Sequence alignment of B-class proteins in Arabidopsis, *Amborella trichopoda*, *Populus trichocarpa*, rice, maize, wheat, barley, orchid, and lily.

Fig. S3. Sequence alignment of $B_{sister}$-class proteins in Arabidopsis, *Amborella trichopoda*, *Populus trichocarpa*, rice, maize, wheat, barley, orchid, and lily.

Fig. S4 Sequence alignment of C-class proteins in Arabidopsis, *Amborella trichopoda*, *Populus trichocarpa*, rice, maize, wheat, barley, orchid, and lily.

Fig. S5. Sequence alignment of D-class proteins in Arabidopsis, *Amborella trichopoda*, *Populus trichocarpa*, rice, maize, wheat, barley, orchid, and lily.

Fig. S6. Sequence alignment of E-class proteins in Arabidopsis, *Amborella trichopoda*, *Populus trichocarpa*, rice, maize, wheat, barley, orchid, and lily.

Fig. S7. Sequence alignment of AGL6-class proteins in Arabidopsis, *Amborella trichopoda*, *Populus trichocarpa*, rice, maize, wheat, barley, orchid, and lily.

## Acknowledgements

We thank Dr Julian Schwerdt for help with the phylogenetic analysis. CC is studying for a Dual PhD Degree at The University of Nottingham and University of Adelaide, and is funded from a PhD Scholarship from the University of Nottingham. This work was supported by the Australian Research Council (DZ, DP170103352; MT, FT140100780), an Australia-China Science and Research Fund Joint Research Centre grant ACSRF48187, the National Key Technologies Research and Development Program of China, Ministry of Science and Technology (grant no. 2016YFD 0100804; 2016YFE0101000), and the National Natural Science Foundation of China (NSFC) (31230051).

## References

**Adam H, Ouellet F, Kane NA, Agharbaoui Z, Major G, Tominaga Y, Sarhan F.** 2007. Overexpression of TaVRN1 in Arabidopsis promotes early flowering and alters development. Plant and Cell Physiology **48,** 1192–1206.

**Agrawal GK, Abe K, Yamazaki M, Miyao A, Hirochika H.** 2005. Conservation of the E-function for floral organ identity in rice revealed by the analysis of tissue culture-induced loss-of-function mutants of the OsMADS1 gene. Plant Molecular Biology **59,** 125–135.

**Ambrose BA, Lerner DR, Ciceri P, Padilla CM, Yanofsky MF, Schmidt RJ.** 2000. Molecular and genetic analyses of the *silky1* gene reveal conservation in floral organ specification between eudicots and monocots. Molecular Cell **5,** 569–579.

**Angenent G, Colombo L.** 1996. Molecular control of ovule development. Trends in Plant Science **1,** 228–232.

**Angenent GC, Franken J, Busscher M, van Dijken A, van Went JL, Dons HJ, van Tunen AJ.** 1995. A novel class of MADS box genes is involved in ovule development in petunia. The Plant Cell **7,** 1569–1582.

**Arora R, Agarwal P, Ray S, Singh AK, Singh VP, Tyagi AK, Kapoor S.** 2007. MADS-box gene family in rice: genome-wide identification, organization and expression profiling during reproductive development and stress. BMC Genomics **8,** 242.

**Becker A, Kaufmann K, Freialdenhoven A, Vincent C, Li MA, Saedler H, Theissen G.** 2002. A novel MADS-box gene subfamily with a sister-group relationship to class B floral homeotic genes. Molecular Genetics and Genomics **266,** 942–950.

**Becker A, Theissen G.** 2003. The major clades of MADS-box genes and their role in the development and evolution of flowering plants. Molecular Phylogenetics and Evolution **29,** 464–489.

**Bell AD.** 1991. An illustrated guide to flowering plant morphology. New York: Oxford University Press.

**Bommert P, Satoh-Nagasawa N, Jackson D, Hirano HY.** 2005. Genetics and evolution of inflorescence and flower development in grasses. Plant and Cell Physiology **46,** 69–78.

**Bowman JL.** 1997. Evolutionary conservation of angiosperm flower development at the molecular and genetic levels. Journal of Biosciences **22,** 515–527.

**Bowman JL, Smyth DR, Meyerowitz EM.** 1989. Genes directing flower development in Arabidopsis. The Plant Cell **1,** 37–52.

**Bowman JL, Smyth DR, Meyerowitz EM.** 1991. Genetic interactions among floral homeotic genes of Arabidopsis. Development **112,** 1–20.

**Cacharrón J, Fischer A, Saedler H, Theissen G.** 1995. Expression patterns of MADS-box genes as studied by in situ hybridization. Maize Genetics Cooperation Newsletter **69,** 37–38.

**Cacharrón J, Saedler H, Theissen G.** 1999. Expression of MADS box genes ZMM8 and ZMM14 during inflorescence development of *Zea mays* discriminates between the upper and the lower floret of each spikelet. Development Genes and Evolution **209,** 411–420.

**Chang YY, Chiu YF, Wu JW, Yang CH.** 2009. Four orchid (*Oncidium* Gower Ramsey) AP1/AGL9-like MADS box genes show novel expression patterns and cause different effects on floral transition and formation in *Arabidopsis thaliana*. Plant and Cell Physiology **50,** 1425–1438.

**Chang YY, Kao NH, Li JY, Hsu WH, Liang YL, Wu JW, Yang CH.** 2010. Characterization of the possible roles for B class MADS box genes in regulation of perianth formation in orchid. Plant Physiology **152,** 837–853.

**Chen MK, Hsieh WP, Yang CH.** 2012. Functional analysis reveals the possible role of the C-terminal sequences and PI motif in the function of lily (*Lilium longiflorum*) PISTILLATA (PI) orthologues. Journal of Experimental Botany **63,** 941–961.

**Chen MK, Lin IC, Yang CH.** 2008. Functional analysis of three lily (*Lilium longiflorum*) APETALA1-like MADS box genes in regulating floral transition and formation. Plant and Cell Physiology **49,** 704–717.

**Chen ZX, Wu JG, Ding WN, Chen HM, Wu P, Shi CH.** 2006. Morphogenesis and molecular basis on naked seed rice, a novel homeotic mutation of OsMADS1 regulating transcript level of AP3 homologue in rice. Planta **223,** 882–890.

**Chung YY, Kim SR, Finkel D, Yanofsky MF, An G.** 1994. Early flowering and reduced apical dominance result from ectopic expression of a rice MADS box gene. Plant Molecular Biology **26,** 657–665.

**Chung Y-Y, Kim S-R, Kang H-G, Noh Y-S, Park MC, Finkel D, An G.** 1995. Characterization of two rice MADS box genes homologous to GLOBOSA. Plant Science **109,** 45–56.

**Clifford H.** 1987. Spikelet and floral morphology. In: Soderstrom TR, Hilu K, Campbell CS, Barkworth ME, eds. Grass systematics and evolution: an international symposium held at the Smithsonian Institution. Washington, DC: Smithsonian Institution Press, 21–30.

**Coen ES, Meyerowitz EM.** 1991. The war of the whorls: genetic interactions controlling flower development. Nature **353,** 31–37.

**Colombo L, Franken J, Koetje E, van Went J, Dons HJ, Angenent GC, van Tunen AJ.** 1995. The petunia MADS box gene FBP11 determines ovule identity. The Plant Cell **7,** 1859–1868.

**Cui R, Han J, Zhao S, *et al*.** 2010. Functional conservation and diversification of class E floral homeotic genes in rice (*Oryza sativa*). The Plant Journal **61,** 767–781.

**Danilevskaya ON, Meng X, Selinger DA, Deschamps S, Hermon P, Vansant G, Gupta R, Ananiev EV, Muszynski MG.** 2008. Involvement of the MADS-box gene ZMM4 in floral induction and inflorescence development in maize. Plant Physiology **147,** 2054–2069.

**Davies B, Egea-Cortines M, de Andrade Silva E, Saedler H, Sommer H.** 1996. Multiple interactions amongst floral homeotic MADS box proteins. EMBO Journal **15,** 4330–4343.

**Ditta G, Pinyopich A, Robles P, Pelaz S, Yanofsky MF.** 2004. The SEP4 gene of *Arabidopsis thaliana* functions in floral organ and meristem identity. Current Biology **14,** 1935–1940.

**Dreni L, Jacchia S, Fornara F, Fornari M, Ouwerkerk PB, An G, Colombo L, Kater MM.** 2007. The D-lineage MADS-box gene OsMADS13 controls ovule identity in rice. The Plant Journal **52,** 690–699.

**Dreni L, Kater MM.** 2014. MADS reloaded: evolution of the AGAMOUS subfamily genes. New Phytologist **201,** 717–732.

**Dreni L, Pilatone A, Yun D, Erreni S, Pajoro A, Caporali E, Zhang D, Kater MM.** 2011. Functional analysis of all AGAMOUS subfamily members in rice reveals their roles in reproductive organ identity determination and meristem determinacy. The Plant Cell **23,** 2850–2863.

**Dreni L, Zhang D.** 2016. Flower development: the evolutionary history and functions of the AGL6 subfamily MADS-box genes. Journal of Experimental Botany **67,** 1625–1638.

**Favaro R, Immink RG, Ferioli V, Bernasconi B, Byzova M, Angenent GC, Kater M, Colombo L.** 2002. Ovule-specific MADS-box proteins have conserved protein–protein interactions in monocot and dicot plants. Molecular Genetics and Genomics: MGG **268,** 152–159.

**Flanagan CA, Ma H.** 1994. Spatially and temporally regulated expression of the MADS-box gene AGL2 in wild-type and mutant arabidopsis flowers. Plant Molecular Biology **26,** 581–595.

**Force A, Lynch M, Pickett FB, Amores A, Yan YL, Postlethwait J.** 1999. Preservation of duplicate genes by complementary, degenerative mutations. Genetics **151,** 1531–1545.

**Fornara F, Marziani G, Mizzi L, Kater M, Colombo L.** 2003. MADS-box genes controlling flower development in rice. Plant Biology **5,** 16–22.

**Fornara F, Parenicová L, Falasca G, *et al.*** 2004. Functional characterization of OsMADS18, a member of the AP1/SQUA subfamily of MADS box genes. Plant Physiology **135,** 2207–2219.

**Gao X, Liang W, Yin C, *et al.*** 2010. The SEPALLATA-like gene OsMADS34 is required for rice inflorescence and spikelet development. Plant Physiology **153,** 728–740.

**Goto K, Meyerowitz EM.** 1994. Function and regulation of the Arabidopsis floral homeotic gene PISTILLATA. Genes and Development **8,** 1548–1560.

**Gramzow L, Theissen G.** 2013. Phylogenomics of MADS-box genes in plants—two opposing life styles in one gene family. Biology **2,** 1150–1164.

**Gustafson-Brown C, Savidge B, Yanofsky MF.** 1994. Regulation of the arabidopsis floral homeotic gene APETALA1. Cell **76,** 131–143.

**Hama E, Takumi S, Ogihara Y, Murai K.** 2004. Pistillody is caused by alterations to the class-B MADS-box gene expression pattern in alloplasmic wheats. Planta **218,** 712–720.

**Hirabayashi C, Murai K.** 2009. Class C MADS-box gene AGAMOUS was duplicated in the wheat genome. Wheat Information Service **107,** 13–16.

**Honma T, Goto K.** 2001. Complexes of MADS-box proteins are sufficient to convert leaves into floral organs. Nature **409,** 525–529.

**Hoshikawa K.** 1989. The growing rice plant—an anatomical monograph. Tokyo: Nobunkyo Press, 59–67.

**Hsu HF, Hsieh WP, Chen MK, Chang YY, Yang CH.** 2010. C/D class MADS box genes from two monocots, orchid (*Oncidium* Gower Ramsey) and lily (*Lilium longiflorum*), exhibit different effects on floral transition and formation in *Arabidopsis thaliana.* Plant and Cell Physiology **51,** 1029–1045.

**Hsu HF, Hsu WH, Lee YI, Mao WT, Yang JY, Li JY, Yang CH.** 2015. Model for perianth formation in orchids. Nature Plants **1,** 15046.

**Hsu HF, Huang CH, Chou LT, Yang CH.** 2003. Ectopic expression of an orchid (*Oncidium* Gower Ramsey) AGL6-like gene promotes flowering by activating flowering time genes in *Arabidopsis thaliana*. Plant and Cell Physiology **44,** 783–794.

**Hsu HF, Yang CH.** 2002. An orchid (*Oncidium* Gower Ramsey) AP3-like MADS gene regulates floral formation and initiation. Plant and Cell Physiology **43,** 1198–1209.

**Hu Y, Liang W, Yin C, *et al.*** 2015. Interactions of OsMADS1 with floral homeotic genes in rice flower development. Molecular Plant **8,** 1366–1384.

**Huang H, Tudor M, Weiss CA, Hu Y, Ma H.** 1995. The Arabidopsis MADS-box gene AGL3 is widely expressed and encodes a sequence-specific DNA-binding protein. Plant Molecular Biology **28,** 549–567.

**Jeon JS, Jang S, Lee S, *et al.*** 2000*a*. leafy hull sterile1 is a homeotic mutation in a rice MADS box gene affecting rice flower development. The Plant Cell **12,** 871–884.

**Jeon J-S, Lee S, Jung K-H, Yang W-S, Yi G-H, Oh B-G, An G.** 2000*b*. Production of transgenic rice plants showing reduced heading date and plant height by ectopic expression of rice MADS-box genes. Molecular Breeding **6,** 581–592.

**Kang HG, An G.** 2005. Morphological alterations by ectopic expression of the rice OsMADS4 gene in tobacco plants. Plant Cell Reports **24,** 120–126.

**Kang HG, Jang S, Chung JE, Cho YG, An G.** 1997. Characterization of two rice MADS box genes that control flowering time. Molecules and Cells **7,** 559–566.

**Kang HG, Noh YS, Chung YY, Costa MA, An K, An G.** 1995. Phenotypic alterations of petal and sepal by ectopic expression of a rice MADS box gene in tobacco. Plant Molecular Biology **29,** 1–10.

**Kellogg EA.** 2007. Floral displays: genetic control of grass inflorescences. Current Opinion in Plant Biology **10,** 26–31.

**Kinjo H, Shitsukawa N, Takumi S, Murai K.** 2012. Diversification of three APETALA1/FRUITFULL-like genes in wheat. Molecular Genetics and Genomics **287,** 283–294.

**Kobayashi K, Maekawa M, Miyao A, Hirochika H, Kyozuka J.** 2010. PANICLE PHYTOMER2 (PAP2), encoding a SEPALLATA subfamily MADS-box protein, positively controls spikelet meristem identity in rice. Plant and Cell Physiology **51,** 47–57.

**Kobayashi K, Yasuno N, Sato Y, Yoda M, Yamazaki R, Kimizu M, Yoshida H, Nagamura Y, Kyozuka J.** 2012. Inflorescence meristem identity in rice is specified by overlapping functions of three AP1/FUL-like MADS box genes and PAP2, a SEPALLATA MADS box gene. The Plant Cell **24,** 1848–1859.

**Kramer EM, Dorit RL, Irish VF.** 1998. Molecular evolution of genes controlling petal and stamen development: duplication and divergence within the APETALA3 and PISTILLATA MADS-box gene lineages. Genetics **149,** 765–783.

**Kramer EM, Jaramillo MA, Di Stilio VS.** 2004. Patterns of gene duplication and functional evolution during the diversification of the AGAMOUS subfamily of MADS box genes in angiosperms. Genetics **166,** 1011–1023.

**Krizek BA, Meyerowitz EM.** 1996. The Arabidopsis homeotic genes APETALA3 and PISTILLATA are sufficient to provide the B class organ identity function. Development **122,** 11.

**Kyozuka J, Kobayashi T, Morita M, Shimamoto K.** 2000. Spatially and temporally regulated expression of rice MADS box genes with similarity to Arabidopsis class A, B and C genes. Plant and Cell Physiology **41,** 710–718.

**Lawton-Rauh AL, Alvarez-Buylla ER, Purugganan MD.** 2000. Molecular evolution of flower development. Trends in Ecology and Evolution **15,** 144–149.

**Lee S, Jeon JS, An K, Moon YH, Lee S, Chung YY, An G.** 2003*a*. Alteration of floral organ identity in rice through ectopic expression of OsMADS16. Planta **217,** 904–911.

**Lee S, Kim J, Son JS, *et al.*** 2003*b*. Systematic reverse genetic screening of T-DNA tagged genes in rice for functional genomic analyses: MADS-box genes as a test case. Plant and Cell Physiology **44,** 1403–1411.

**Li H, Liang W, Jia R, Yin C, Zong J, Kong H, Zhang D.** 2010. The AGL6-like gene OsMADS6 regulates floral organ and meristem identities in rice. Cell Research **20,** 299–313.

**Li H, Liang W, Yin C, Zhu L, Zhang D.** 2011. Genetic interaction of OsMADS3, DROOPING LEAF, and OsMADS13 in specifying rice floral organ identities and meristem determinacy. Plant Physiology **156,** 263–274.

**Li N, Liu Y, Zhong M, Li H.** 2014. Thinking out of the box: MADS-box genes and maize spikelet development. African Journal of Biotechnology **13**.

**Lid SE, Meeley RB, Min Z, Nichols S, Olsen O-A.** 2004. Knock-out mutants of two members of the AGL2 subfamily of MADS-box genes expressed during maize kernel development. Plant Science **167,** 575–582.

**Lim J, Moon YH, An G, Jang SK.** 2000. Two rice MADS domain proteins interact with OsMADS1. Plant Molecular Biology **44,** 513–527.

**Lin X, Wu F, Du X, Shi X, Liu Y, Liu S, Hu Y, Theißen G, Meng Z.** 2014. The pleiotropic SEPALLATA-like gene OsMADS34 reveals that the 'empty glumes' of rice (*Oryza sativa*) spikelets are in fact rudimentary lemmas. New Phytologist **202,** 689–702.

**Litt A, Irish VF.** 2003. Duplication and diversification in the APETALA1/FRUITFULL floral homeotic gene lineage: implications for the evolution of floral development. Genetics **165,** 821–833.

**Lopez-Dee ZP, Wittich P, Enrico Pè M, Rigola D, Del Buono I, Gorla MS, Kater MM, Colombo L.** 1999. OsMADS13, a novel rice MADS-box gene expressed during ovule development. Developmental Genetics **25,** 237–244.

**Lu S-J, Wei H, Wang Y, Wang H-M, Yang R-F, Zhang X-B, Tu J-M.** 2012. Overexpression of a transcription factor OsMADS15 modifies plant architecture and flowering time in rice (*Oryza sativa* L.). Plant Molecular Biology Reporter **30,** 1461–1469.

**Lynch M, Force A.** 2000. The probability of duplicate gene preservation by subfunctionalization. Genetics **154,** 459–473.

**Ma H, Yanofsky MF, Meyerowitz EM.** 1991. AGL1–AGL6, an Arabidopsis gene family with similarity to floral homeotic and transcription factor genes. Genes and Development **5,** 484–495.

**Malcomber ST, Kellogg EA.** 2005. SEPALLATA gene diversification: brave new whorls. Trends in Plant Science **10,** 427–435.

**Mandel MA, Yanofsky MF.** 1998. The ArabidopsisAGL9 MADS box gene is expressed in young flower primordia. Sexual Plant Reproduction **11,** 22–28.

**Masiero S, Imbriano C, Ravasio F, Favaro R, Pelucchi N, Gorla MS, Mantovani R, Colombo L, Kater MM.** 2002. Ternary complex formation between MADS-box transcription factors and the histone fold protein NF-YB. Journal of Biological Chemistry **277,** 26429–26435.

**Meguro A, Takumi S, Ogihara Y, Murai K.** 2003. WAG, a wheat AGAMOUS homolog, is associated with development of pistil-like stamens in alloplasmic wheats. Sexual Plant Reproduction **15,** 221–230.

**Mena M, Ambrose BA, Meeley RB, Briggs SP, Yanofsky MF, Schmidt RJ.** 1996. Diversification of C-function activity in maize flower development. Science **274,** 1537.

**Mena M, Mandel MA, Lerner DR, Yanofsky MF, Schmidt RJ.** 1995. A characterization of the MADS-box gene family in maize. The Plant Journal **8,** 845–854.

**Mizzotti C, Mendes MA, Caporali E, Schnittger A, Kater MM, Battaglia R, Colombo L.** 2012. The MADS box genes SEEDSTICK and ARABIDOPSIS Bsister play a maternal role in fertilization and seed development. The Plant Journal **70,** 409–420.

**Mondragón-Palomino M, Theissen G.** 2008. MADS about the evolution of orchid flowers. Trends in Plant Science **13,** 51–59.

**Moon YH, Jung JY, Kang HG, An G.** 1999*a*. Identification of a rice APETALA3 homologue by yeast two-hybrid screening. Plant Molecular Biology **40,** 167–177.

**Moon YH, Kang HG, Jung JY, Jeon JS, Sung SK, An G.** 1999*b*. Determination of the motif responsible for interaction between the rice APETALA1/AGAMOUS-LIKE9 family proteins using a yeast two-hybrid system. Plant Physiology **120,** 1193–1204.

**Münster T, Deleu W, Wingen LU, *et al*.** 2002. Maize MADS-box genes galore. Maydica **47,** 287–301.

**Münster T, Wingen LU, Faigl W, Werth S, Saedler H, Theissen G.** 2001. Characterization of three GLOBOSA-like MADS-box genes from maize: evidence for ancient paralogy in one class of floral homeotic B-function genes of grasses. Gene **262,** 1–13.

**Murai K.** 2013. Homeotic genes and the ABCDE model for floral organ formation in wheat. Plants **2,** 379–395.

**Murai K, Miyamae M, Kato H, Takumi S, Ogihara Y.** 2003. WAP1, a wheat APETALA1 homolog, plays a central role in the phase transition from vegetative to reproductive growth. Plant and Cell Physiology **44,** 1255–1265.

**Nagasawa N, Miyoshi M, Sano Y, Satoh H, Hirano H, Sakai H, Nagato Y.** 2003. SUPERWOMAN1 and DROOPING LEAF genes control floral organ identity in rice. Development **130,** 705.

**Nayar S, Kapoor M, Kapoor S.** 2014. Post-translational regulation of rice MADS29 function: homodimerization or binary interactions with other seed-expressed MADS proteins modulate its translocation into the nucleus. Journal of Experimental Botany **65,** 5339–5350.

**Nesi N, Debeaujon I, Jond C, Stewart AJ, Jenkins GI, Caboche M, Lepiniec L.** 2002. The TRANSPARENT TESTA16 locus encodes the ARABIDOPSIS BSISTER MADS domain protein and is required for proper development and pigmentation of the seed coat. The Plant Cell **14,** 2463–2479.

**Ohmori S, Kimizu M, Sugita M, Miyao A, Hirochika H, Uchida E, Nagato Y, Yoshida H.** 2009. MOSAIC FLORAL ORGANS1, an AGL6-like MADS box gene, regulates floral organ identity and meristem fate in rice. The Plant Cell **21,** 3008–3025.

**Pan ZJ, Chen YY, Du JS, Chen YY, Chung MC, Tsai WC, Wang CN, Chen HH.** 2014. Flower development of Phalaenopsis orchid involves functionally divergent SEPALLATA-like genes. New Phytologist **202,** 1024–1042.

**Paolacci AR, Tanzarella OA, Porceddu E, Varotto S, Ciaffi M.** 2007. Molecular and phylogenetic analysis of MADS-box genes of MIKC type and chromosome location of SEP-like genes in wheat (*Triticum aestivum* L.). Molecular Genetics and Genomics **278,** 689–708.

**Pelaz S, Ditta GS, Baumann E, Wisman E, Yanofsky MF.** 2000. B and C floral organ identity functions require SEPALLATA MADS-box genes. Nature **405,** 200–203.

**Pelucchi N, Fornara F, Favalli C, Masiero S, Lago C, Pè E, Colombo L, Kater M.** 2002. Comparative analysis of rice MADS-box genes expressed during flower development. Sexual Plant Reproduction **15,** 113–122.

**Pickett FB, Meeks-Wagner DR.** 1995. Seeing double: appreciating genetic redundancy. The Plant Cell **7,** 1347–1356.

**Prasad K, Parameswaran S, Vijayraghavan U.** 2005. OsMADS1, a rice MADS-box factor, controls differentiation of specific cell types in the lemma and palea and is an early-acting regulator of inner floral organs. The Plant Journal **43,** 915–928.

**Prasad K, Sriram P, Kumar CS, Kushalappa K, Vijayraghavan U.** 2001. Ectopic expression of rice OsMADS1 reveals a role in specifying the lemma and palea, grass floral organs analogous to sepals. Development Genes and Evolution **211,** 281–290.

**Prasad K, Vijayraghavan U.** 2003. Double-stranded RNA interference of a rice PI/GLO paralog, OsMADS2, uncovers its second-whorl-specific function in floral organ patterning. Genetics **165,** 2301–2305.

**Prasad K, Zhang X, Tobón E, Ambrose BA.** 2010. The Arabidopsis B-sister MADS-box protein, GORDITA, represses fruit growth and contributes to integument development. The Plant Journal **62,** 203–214.

**Prince VE, Pickett FB.** 2002. Splitting pairs: the diverging fates of duplicated genes. Nature Reviews. Genetics **3,** 827–837.

**Reinheimer R, Kellogg EA.** 2009. Evolution of AGL6-like MADS box genes in grasses (Poaceae): ovule expression is ancient and palea expression is new. The Plant Cell **21,** 2591–2605.

**Sasani S, Hemming MN, Oliver SN, *et al*.** 2009. The influence of vernalization and daylength on expression of flowering-time genes in the shoot apex and leaves of barley (*Hordeum vulgare*). Journal of Experimental Botany **60,** 2169–2178.

**Savidge B, Rounsley SD, Yanofsky MF.** 1995. Temporal relationship between the transcription of two Arabidopsis MADS box genes and the floral organ identity genes. The Plant Cell **7,** 721–733.

**Schilling S, Gramzow L, Lobbes D, *et al*.** 2015. Non-canonical structure, function and phylogeny of the Bsister MADS-box gene OsMADS30 of rice (*Oryza sativa*). The Plant Journal **84,** 1059–1072.

**Schmidt RJ, Veit B, Mandel MA, Mena M, Hake S, Yanofsky MF.** 1993. Identification and molecular characterization of ZAG1, the maize homolog of the Arabidopsis floral homeotic gene AGAMOUS. The Plant Cell **5,** 729–737.

**Schmitz J, Franzen R, Ngyuen TH, Garcia-Maroto F, Pozzi C, Salamini F, Rohde W.** 2000. Cloning, mapping and expression analysis of barley MADS-box genes. Plant Molecular Biology **42,** 899–913.

**Schwarz-Sommer Z, Huijser P, Nacken W, Saedler H, Sommer H.** 1990. Genetic control of flower development by homeotic genes in *Antirrhinum majus*. Science **250,** 931.

**Seok HY, Park HY, Park JI, Lee YM, Lee SY, An G, Moon YH.** 2010. Rice ternary MADS protein complexes containing class B MADS heterodimer. Biochemical and Biophysical Research Communications **401,** 598–604.

**Shan H, Zhang N, Liu C, Xu G, Zhang J, Chen Z, Kong H.** 2007. Patterns of gene duplication and functional diversification during the evolution of the AP1/SQUA subfamily of plant MADS-box genes. Molecular Phylogenetics and Evolution **44,** 26–41.

**Shitsukawa N, Tahira C, Kassai K, *et al.*** 2007. Genetic and epigenetic alteration among three homoeologous genes of a class E MADS box gene in hexaploid wheat. The Plant Cell **19,** 1723–1737.

**Shore P, Sharrocks AD.** 1995. The MADS-box family of transcription factors. European Journal of Biochemistry **229,** 1–13.

**Tautz D.** 1992. Problems and paradigms: redundancies, development and the flow of information. BioEssays **14,** 263–266.

**Theissen G.** 2001. Development of floral organ identity: stories from the MADS house. Current Opinion in Plant Biology **4,** 75–85.

**Theissen G, Kim JT, Saedler H.** 1996. Classification and phylogeny of the MADS-box multigene family suggest defined roles of MADS-box gene subfamilies in the morphological evolution of eukaryotes. Journal of Molecular Evolution **43,** 484–516.

**Theissen G, Saedler H.** 2001. Plant biology. Floral quartets. Nature **409,** 469–471.

**Theissen G, Strater T, Fischer A, Saedler H.** 1995. Structural characterization, chromosomal localization and phylogenetic evaluation of two pairs of AGAMOUS-like MADS-box genes from maize. Gene **156,** 155–166.

**Thompson BE, Bartling L, Whipple C, Hall DH, Sakai H, Schmidt R, Hake S.** 2009. *bearded-ear* encodes a MADS box transcription factor critical for maize floral development. The Plant Cell **21,** 2578–2590.

**Tranquilli G, Dubcovsky J.** 2000. Epistatic interaction between vernalization genes Vrn-Am1 and Vrn-Am2 in diploid wheat. Journal of Heredity **91,** 304–306.

**Trevaskis B, Bagnall DJ, Ellis MH, Peacock WJ, Dennis ES.** 2003. MADS box genes control vernalization-induced flowering in cereals. Proceedings of the National Academy of Sciences, USA **100,** 13099–13104.

**Tsai WC, Chen HH.** 2006. The orchid MADS-box genes controlling floral morphogenesis. ScientificWorldJournal **6,** 1933–1944.

**Tzeng TY, Chen HY, Yang CH.** 2002. Ectopic expression of carpel-specific MADS box genes from lily and lisianthus causes similar homeotic conversion of sepal and petal in Arabidopsis. Plant Physiology **130,** 1827–1836.

**Tzeng TY, Hsiao CC, Chi PJ, Yang CH.** 2003. Two lily SEPALLATA-like genes cause different effects on floral formation and floral transition in Arabidopsis. Plant Physiology **133,** 1091–1101.

**Tzeng TY, Liu HC, Yang CH.** 2004. The C-terminal sequence of LMADS1 is essential for the formation of homodimers for B function proteins. Journal of Biological Chemistry **279,** 10747–10755.

**Tzeng TY, Yang CH.** 2001. A MADS box gene from lily (*Lilium longiflorum*) is sufficient to generate dominant negative mutation by interacting with PISTILLATA (PI) in *Arabidopsis thaliana*. Plant and Cell Physiology **42,** 1156–1168.

**Vandenbussche M, Theissen G, Van de Peer Y, Gerats T.** 2003. Structural diversification and neo-functionalization during floral MADS-box gene evolution by C-terminal frameshift mutations. Nucleic Acids Research **31,** 4401–4409.

**Wang H, Zhang L, Cai Q, *et al.*** 2015. OsMADS32 interacts with PI-like proteins and regulates rice flower development. Journal of Integrative Plant Biology **57,** 504–513.

**Wang K, Tang D, Hong L, Xu W, Huang J, Li M, Gu M, Xue Y, Cheng Z.** 2010. DEP and AFO regulate reproductive habit in rice. PLoS Genetics **6,** e1000818.

**Wang QH, Yang ZJ, Wei SH, Jiang ZY, Yang YF, Hu ZS, Sun QX, Peng ZS.** 2015. Molecular cloning, characterization and expression analysis of WAG-1 in the pistillody line of common wheat. Genetics and Molecular Research **14,** 12455–12465.

**Wei S, Peng Z, Zhou Y, Yang Z, Wu K, Ouyang Z.** 2011. Nucleotide diversity and molecular evolution of the WAG-2 gene in common wheat (*Triticum aestivum* L) and its relatives. Genetics and Molecular Research **34,** 606–615.

**Weigel D, Meyerowitz EM.** 1994. The ABCs of floral homeotic genes. Cell **78,** 203–209.

**Whipple CJ, Ciceri P, Padilla CM, Ambrose BA, Bandong SL, Schmidt RJ.** 2004. Conservation of B-class floral homeotic gene function between maize and Arabidopsis. Development **131,** 6083.

**Winter K-U, Saedler H, Theißen G.** 2002*a*. On the origin of class B floral homeotic genes: functional substitution and dominant inhibition in Arabidopsis by expression of an orthologue from the gymnosperm Gnetum. The Plant Journal **31,** 457–475.

**Winter KU, Weiser C, Kaufmann K, Bohne A, Kirchner C, Kanno A, Saedler H, Theissen G.** 2002*b*. Evolution of class B floral homeotic proteins: obligate heterodimerization originated from homodimerization. Molecular Biology and Evolution **19,** 587–596.

**Wu D, Liang W, Zhu W, Chen M, Ferrándiz C, Burton RA, Dreni L, Zhang D.** 2018. Loss of LOFSEP transcription factor function converts spikelet to leaf-like structures in rice. Plant Physiology **176,** 1646–1664.

**Wu F, Shi X, Lin X, Liu Y, Chong K, Theißen G, Meng Z.** 2017. The ABCs of flower development: mutational analysis of AP1/FUL-like genes in rice provides evidence for a homeotic (A)-function in grasses. The Plant Journal **89,** 310–324.

**Xu W, Tao J, Chen M, Dreni L, Luo Z, Hu Y, Liang W, Zhang D.** 2017. Interactions between FLORAL ORGAN NUMBER4 and floral homeotic genes in regulating rice flower development. Journal of Experimental Botany **68,** 483–498.

**Yadav SR, Prasad K, Vijayraghavan U.** 2007. Divergent regulatory OsMADS2 functions control size, shape and differentiation of the highly derived rice floret second-whorl organ. Genetics **176,** 283–294.

**Yamada K, Saraike T, Shitsukawa N, Hirabayashi C, Takumi S, Murai K.** 2009. Class D and B(sister) MADS-box genes are associated with ectopic ovule formation in the pistil-like stamens of alloplasmic wheat (*Triticum aestivum* L.). Plant Molecular Biology **71,** 1–14.

**Yamaguchi T, Hirano HY.** 2006. Function and diversification of MADS-box genes in rice. ScientificWorldJournal **6,** 1923–1932.

**Yamaguchi T, Lee DY, Miyao A, Hirochika H, An G, Hirano HY.** 2006. Functional diversification of the two C-class MADS box genes OSMADS3 and OSMADS58 in *Oryza sativa*. The Plant Cell **18,** 15–28.

**Yamaki S, Nagato Y, Kurata N, Nonomura K.** 2011. Ovule is a lateral organ finally differentiated from the terminating floral meristem in rice. Developmental Biology **351,** 208–216.

**Yan L, Loukoianov A, Tranquilli G, Helguera M, Fahima T, Dubcovsky J.** 2003. Positional cloning of the wheat vernalization gene VRN1. Proceedings of the National Academy of Sciences, USA **100,** 6263.

**Yang X, Wu F, Lin X, *et al.*** 2012. Live and let die—the B(sister) MADS-box gene OsMADS29 controls the degeneration of cells in maternal tissues during seed development of rice (*Oryza sativa*). PLoS One **7,** e51435.

**Yanofsky MF, Ma H, Bowman JL, Drews GN, Feldmann KA, Meyerowitz EM.** 1990. The protein encoded by the Arabidopsis homeotic gene *agamous* resembles transcription factors. Nature **346,** 35–39.

**Yao SG, Ohmori S, Kimizu M, Yoshida H.** 2008. Unequal genetic redundancy of rice PISTILLATA orthologs, OsMADS2 and OsMADS4, in lodicule and stamen development. Plant and Cell Physiology **49,** 853–857.

**Yin LL, Xue HW.** 2012. The MADS29 transcription factor regulates the degradation of the nucellus and the nucellar projection during rice seed development. The Plant Cell **24,** 1049–1065.

**Yoshida H.** 2012. Is the lodicule a petal: molecular evidence? Plant Science **184,** 121–128.

**Yoshida H, Itoh J, Ohmori S, *et al.*** 2007. *superwoman1-cleistogamy*, a hopeful allele for gene containment in GM rice. Plant Biotechnology Journal **5,** 835–846.

**Yun D, Liang W, Dreni L, Yin C, Zhou Z, Kater MM, Zhang D.** 2013. OsMADS16 genetically interacts with OsMADS3 and OsMADS58 in specifying floral patterning in rice. Molecular Plant **6,** 743–756.

**Zahn LM, Kong H, Leebens-Mack JH, Kim S, Soltis PS, Landherr LL, Soltis DE, Depamphilis CW, Ma H.** 2005*a*. The evolution of the SEPALLATA subfamily of MADS-box genes: a preangiosperm origin with multiple duplications throughout angiosperm history. Genetics **169,** 2209–2223.

**Zahn LM, Leebens-Mack J, DePamphilis CW, Ma H, Theissen G.** 2005*b*. To B or Not to B a flower: the role of DEFICIENS and GLOBOSA orthologs in the evolution of the angiosperms. Journal of Heredity **96,** 225–240.

**Zhang D, Yuan Z.** 2014. Molecular control of grass inflorescence development. Annual Review of Plant Biology **65,** 553–578.

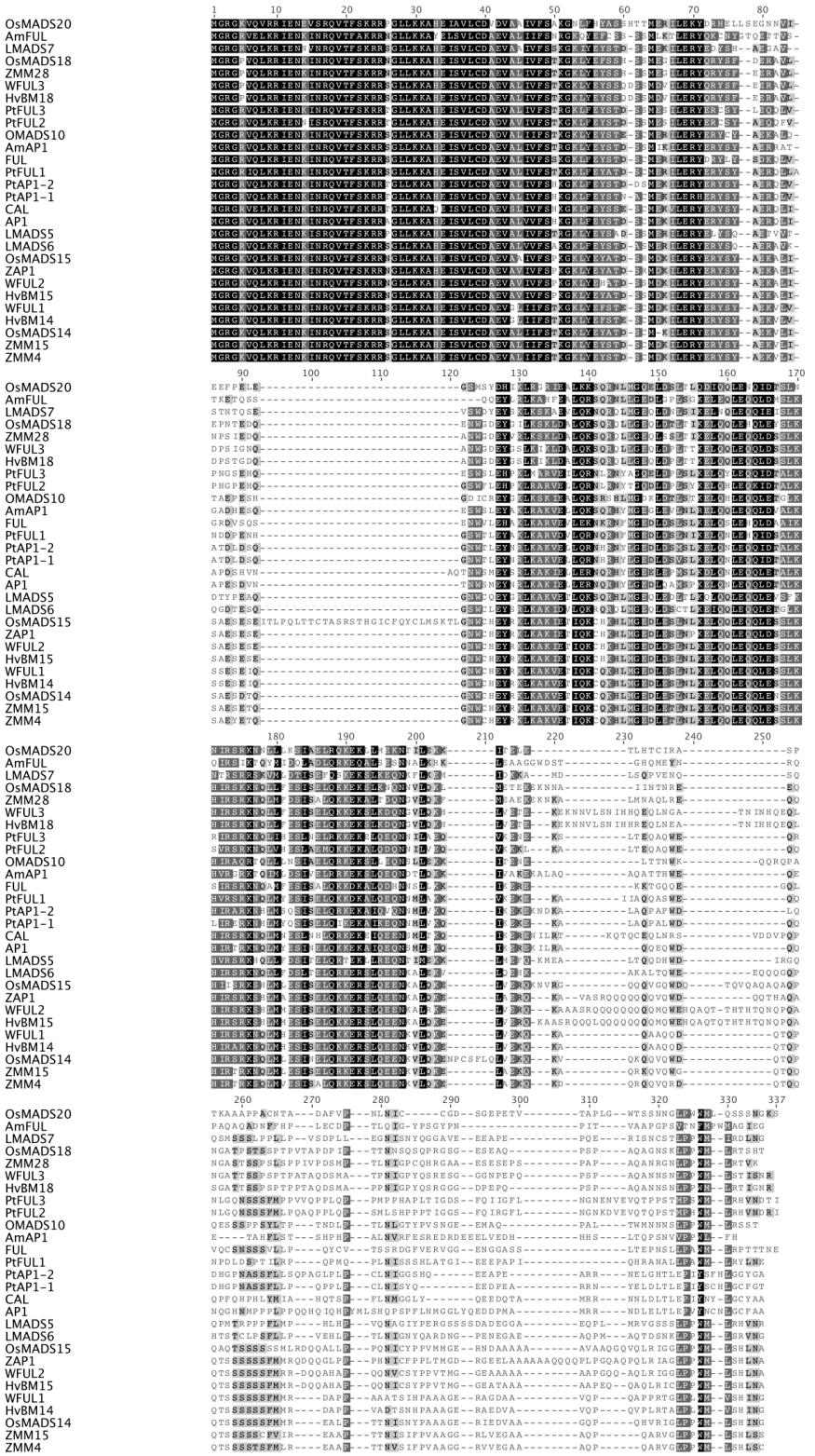
**Zhang D, Yuan Z, An G, Dreni L, Hu J, Kater MM.** 2013. Panicle development. In: Zhang Q, Wing AR, eds. Genetics and genomics of rice. New York: Springer New York, 279–295.

**Zhao Q, Weber AL, McMullen MD, Guill K, Doebley J.** 2011. MADS-box genes of maize: frequent targets of selection during domestication. Genetics Research **93,** 65–75.

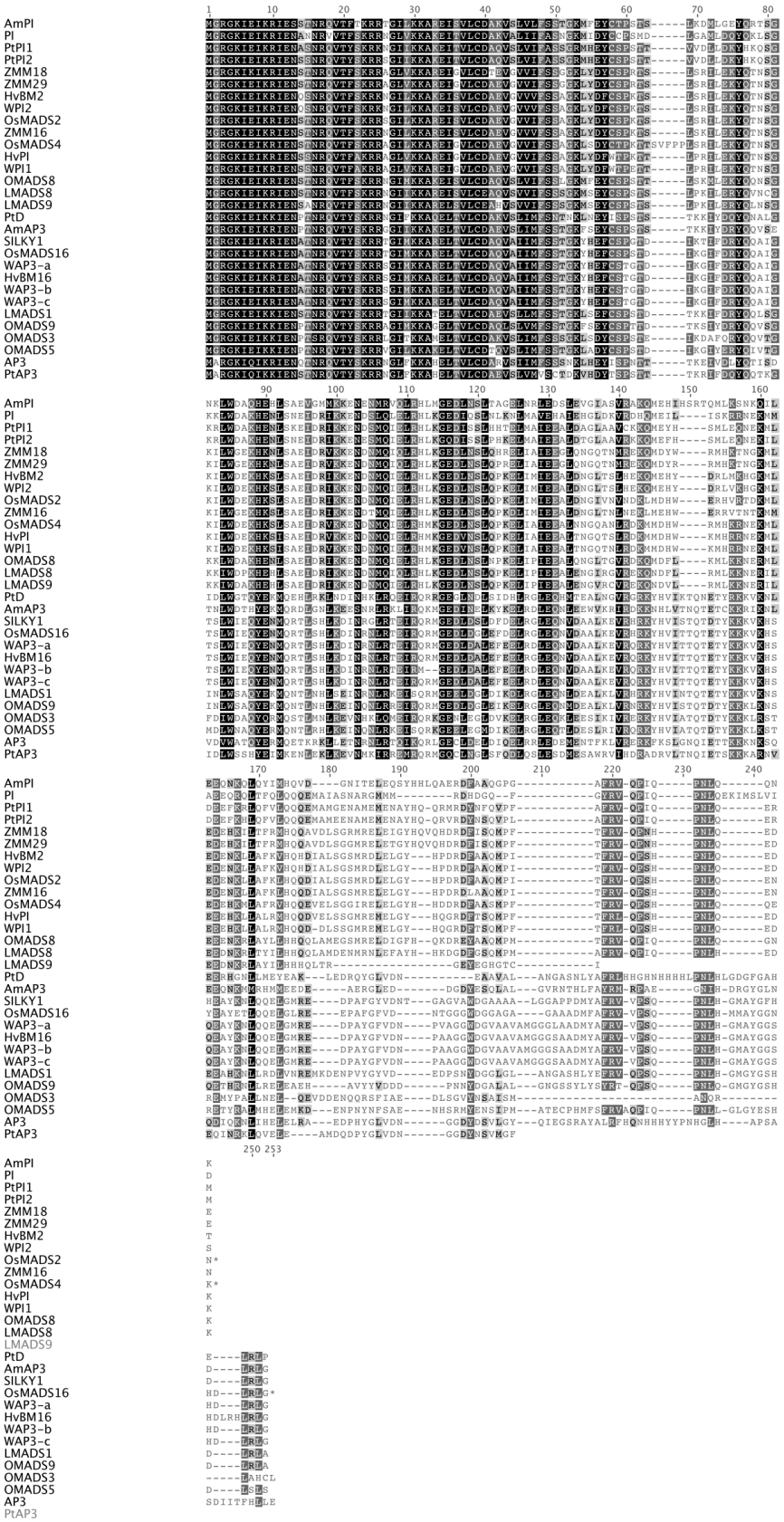
**Zhao T, Ni Z, Dai Y, Yao Y, Nie X, Sun Q.** 2006. Characterization and expression of 42 MADS-box genes in wheat (*Triticum aestivum* L.). Molecular Genetics and Genomics **276,** 334–350.

**Zhao XY, Cheng ZJ, Zhang XS.** 2006. Overexpression of TaMADS1, a SEPALLATA-like gene in wheat, causes early flowering and the abnormal development of floral organs in Arabidopsis. Planta **223,** 698–707.

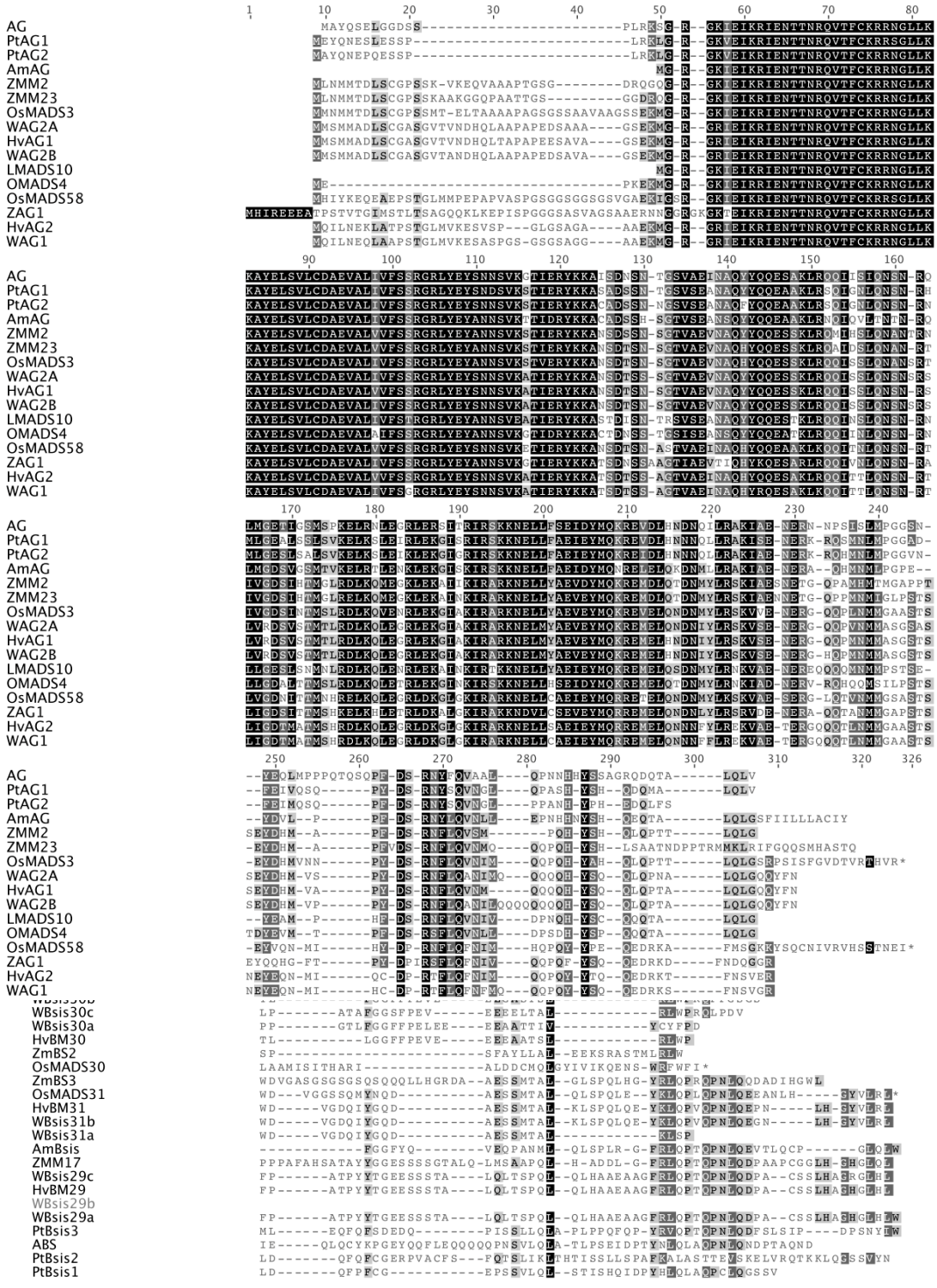
# Chapter 1: Supplementary files



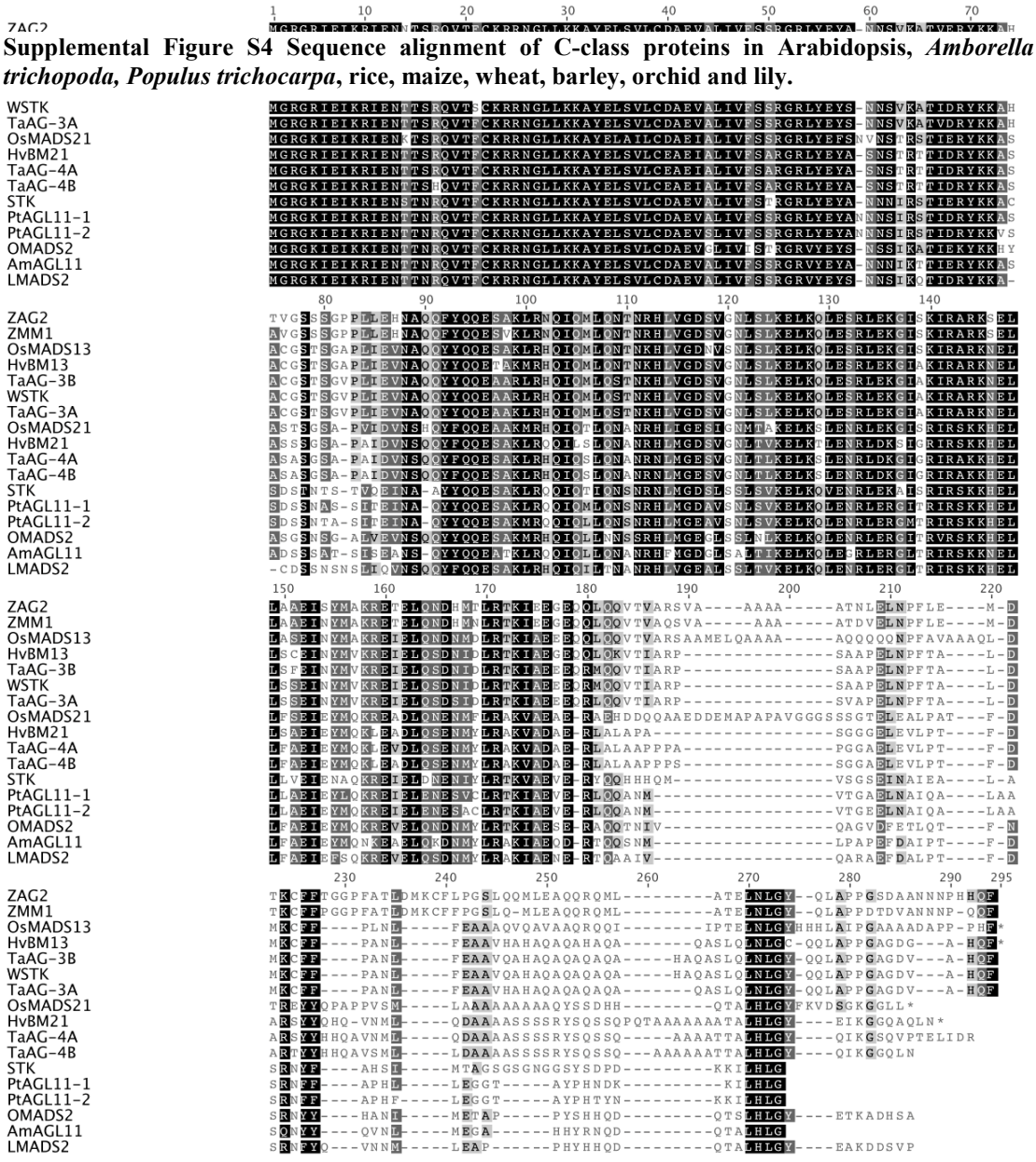

**Supplemental Figure S1 Sequence alignment of A-class proteins in Arabidopsis, *Amborella trichopoda, Populus trichocarpa*, rice, maize, wheat, barley, orchid and lily.**



**Supplemental Figure S2 Sequence alignment of B-class proteins in Arabidopsis, *Amborella trichopoda, Populus trichocarpa*, rice, maize, wheat, barley, orchid and lily.**



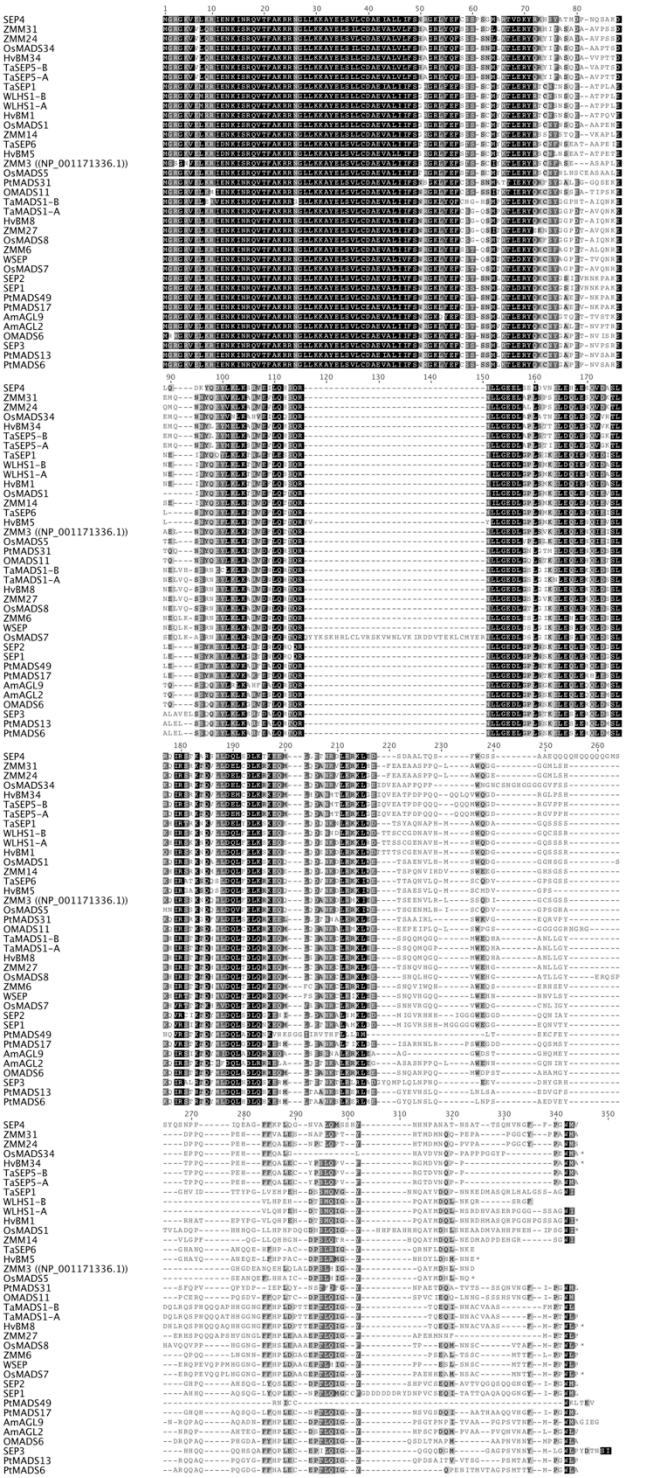

**Supplemental Figure S3 Sequence alignment of $B_{sister}$-class proteins in Arabidopsis, *Amborella trichopoda, Populus trichocarpa*, rice, maize, wheat, barley, orchid and lily.**



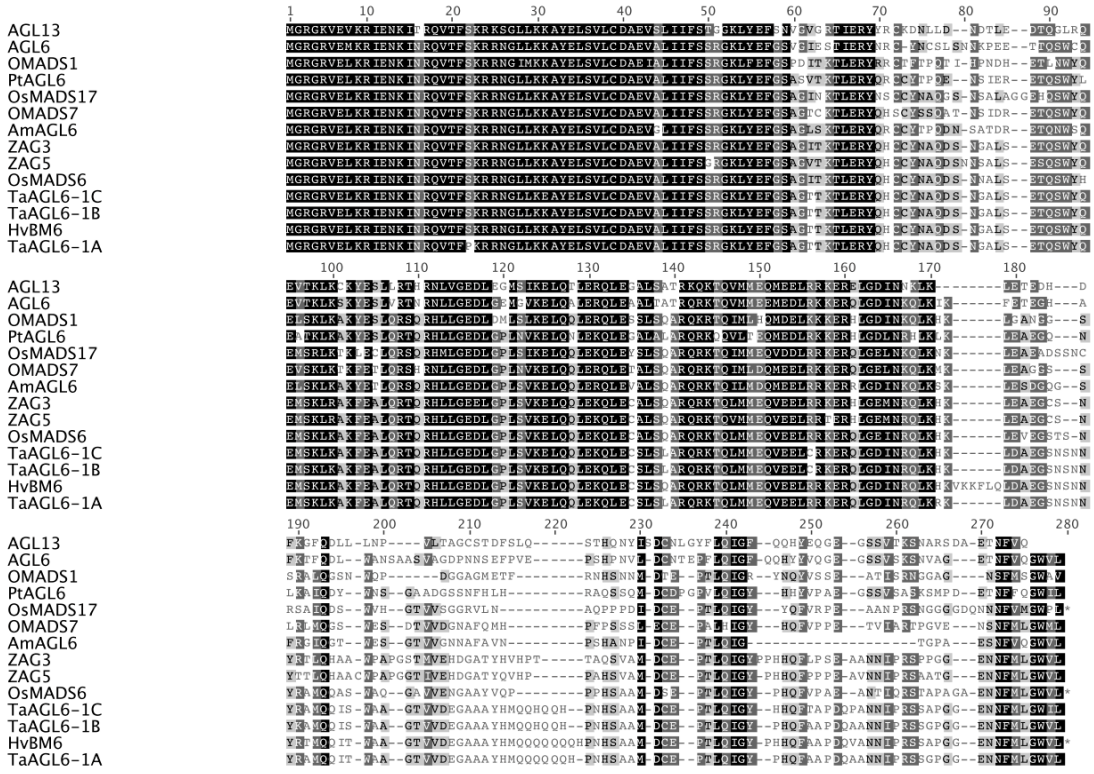
**Supplemental Figure S4 Sequence alignment of C-class proteins in Arabidopsis, *Amborella trichopoda, Populus trichocarpa*, rice, maize, wheat, barley, orchid and lily.**



**Supplemental Figure S5 Sequence alignment of D-class proteins in Arabidopsis, *Amborella trichopoda, Populus trichocarpa*, rice, maize, wheat, barley, orchid and lily.**



**Supplemental Figure S6 Sequence alignment of E-class proteins in Arabidopsis, *Amborella trichopoda, Populus trichocarpa*, rice, maize, wheat, barley, orchid and lily.**




**Supplemental Figure S7 Sequence alignment of AGL6-class proteins in Arabidopsis, *Amborella trichopoda, Populus trichocarpa*, rice, maize, wheat, barley, orchid and lily.**

## Aims and objectives

The ABCDE model of floral development hasn't been extensively investigated in barley (*Hordeum vulgare*). I aimed to provide thorough, tissue-specific expression patterns of all the ABCDE-model MADS-box genes in barley throughout reproductive development by qRT-PCR. The developmental stages examined start at the stem elongation and the formation of the primary sporogenous cells in the anthers, and end at anthesis. In situ hybridization analysis was used to provide a more specific localisation of expression of the ABCDE-model MADS-box genes (Chapter 2). A functional analysis using the CRES-T dominant repression system focused on the B-class DEF/GLO MADS-box genes. These genes are known to be involved in lodicule and stamens development in other species and are therefore crucial for fertility of the barley florets (Chapter 3). No functional analysis has been carried out on these genes to date. The expression profiles and functional analysis of the ABCDE-model MADS-box genes were investigated to better our understanding of their role in the ABCDE model in barley and their evolutionary conservation or differences.

MADS-box genes had been shown to be involved in abiotic stress response and tolerance. Prior to investigating the role of the ABCDE-model MADS-box in abiotic stress response in barley, I aimed to investigate the effects of heat stress on the reproductive development in barley (Chapter 4). Three commercial European spring barley varieties (Optic, Moonshine and RGT Planet) were subjected to high temperature conditions at two vulnerable reproductive stages: meiosis and mitosis. The pollen viability was investigated using potassium iodide staining and fertility assays were carried out on the number of mature and aborted seeds to establish the effects of high temperatures at meiosis or mitosis on fertility in all three varieties. 3D X-ray imaging was used as a non-destructive method of phenotyping combined with dissection of florets to visualise morphological changes in the reproductive organs. Immunolabeling was used to provide insight into the cellular morphological changes of the anthers and the ovule of heat-stressed florets. Lastly, expression of heat shock proteins in mitosis heat-stressed florets were compared to expression in control florets. I aimed to use all these results to find tolerant and/or susceptible varieties that could in future be used to find underlying mechanisms, of which the MADS-box genes might be a part, providing tolerance to heat stress.

# Chapter 2: Expression analysis and protein-protein interactions of the DEF/GLO-like MADS-box genes in barley (*Hordeum vulgare*)

Cindy Callens[1,2], Neil J. Shirley[2], Xiujuan Yang[2], Matthew R. Tucker[2], Dabing Zhang[2,3] and Zoe A. Wilson[1]

[1] School of Biosciences, University of Nottingham, Sutton Bonington Campus, Loughborough, Leicestershire LE12 5RD, UK
[2] School of Agriculture, Food and Wine, University of Adelaide, Waite Campus, Urrbrae, SA, Australia
[3] School of Life Sciences and Biotechnology, Shanghai Jiao Tong University, Shanghai 200240, China

# Introduction to Chapter 2: Expression analysis and protein-protein interactions of the DEF/GLO-like MADS-box genes in barley (*Hordeum vulgare*)

Mapping the expression levels of genes of unknown function is a valuable tool to gain an initial understanding of their potential role or importance in the plant. Comparing these expression levels to those of orthologues identified in closely related species can highlight evolutionary changes and hint at potential mutations and divergent functions.
Clustering expression patterns of genes that are known to work in complexes can also give a first indication of which potential complexes might be at play.

In this chapter the expression patterns of the ABCDE MADS-box genes were investigated using quantitative reverse transcription PCR and In Situ Hybridization. Samples from different tissues at various stages were collected to be able to give an accurate and detailed representation of the expression of all the genes throughout development. For the staging, the method described by Gómez and Wilson (2012) was used because this methods was well known in the lab. Additional staging methods, like those of Zadoks *et al.* (1974) and Waddington *et al.* (1983), were used to have as many morphological indicators of the stages as possible. Staging proved difficult in certain instances; different expression levels were found between biological replicates for two particular stages, indicating that either a mistake was made during staging or that the expression level varies at different time points during this stage.

qRT-PCR expression analysis gives a good overview of the relative expression of genes based on an average of technical replicates from the same cDNA and biological replicates, cDNA from different florets. In Situ Hybridization analysis provides a more specific look at where genes are expressed in the tissue and can indicate localised or general expression. In this chapter, only *HvBM2* is investigated through In Situ Hybridization. Issues with the probe for *HvBM4* delayed the analysis of that particular gene. The In Situ Hybridization analysis of *HvBM16* was carried out by a fellow PhD student investigating this gene. *HvBM16* seemed expressed in

the very early stages of flower development which fell outside the scope of the qRT-PCR analysis. It was therefore decided not to include the In situ Hybridization Analysis of *HvBM16*.

Protein-protein interactions of the B-class ABCDE MADS-box genes were meant to be investigated using Bimolecular Fluorescent Complementation. Constructs were made for all the B-class ABCDE MADS-box genes. Due to several persistent pests in the glasshouse, the tobacco plants needed to perform the experiment were unable to grow healthily and the experiment had to be postponed.

The results in this chapter show that it is important to have many different tissues at many time points throughout floral development to provide an accurate overview of the expression levels of the ABCDE MADS-box genes. These expression patterns can give a good first indication of the function of the ABCDE MADS-box proteins and their place in the ABCDE model.

## 2.1 Introduction

### *2.1.1 Expression patterns of ABCDE MADS-box genes in grasses*

The expression patterns of the ABCDE MADS-box genes have been investigated in crops such as rice, maize and wheat. An overview of the expression patterns across these economically important grasses (see Chapter 1) and other grasses such as *Brachypodium distachyon* shows an overall conservation of expression patterns with only a few exceptions. An in-depth expression analysis can provide a first indication of the functional importance of genes. Comparison of the expression pattern of MADS-box genes of the ABCDE model among different plant species can provide hint of functional conservation and divergence. For barley, an economically important crop, there is no tissue-specific expression data across developmental stages currently available for all the classes. However, recent work indicates that the expression patterns of the ABCDE MADS-box genes in rice and wheat are generally conserved in barley during meristem development (Digel *et al.*, 2015; Liu *et al.*, 2019). In this chapter the expression pattern of the ABCDE MADS-box genes in barley in specific tissues at different developmental stages was investigated and compared to that in closely related species.

*A-class expression in rice, maize, wheat and brachypodium*

In rice, *OsMADS15* is expressed in the apical region of the floral meristem, while *OsMADS14* is expressed in the whole floral meristem. *OsMADS15* and subsequently *OsMADS14* accumulates in the developing lemma, palea and lodicules, with *OsMADS14* also showing expression in the primordia of the glumes (Kyozuka *et al.*, 2000; Pelucchi *et al.*, 2002). *OsMADS18* is expressed in roots, leaves and flowers except for the lodicules and sterile glumes, with expression levels increasing when reproductive stage is reached (Fornara *et al.*, 2003; Masiero *et al.*, 2002; Pelucchi *et al.*, 2002). *OsMADS20* is expressed in shoots and seeds (Lee *et al.*, 2003). Maize *Zea mays APETALA 1* (*ZAP1*) is expressed in male and female inflorescences and the husk leaves that surround the developing ear and more specifically in lemma, palea and lodicules in the flowers (Li *et al.*, 2014; Mena *et al.*, 1996). Low levels of *Zea mays MADS-box 14* (*ZMM4*) and *ZMM15* (*OsMADS14* orthologues) expression were found in developing apical and lateral inflorescences and later in husk, stalk, mature leaf and root (Danilevskaya *et al.*, 2008).

In barley, *HvBM15* is strongly expressed at the awn primordium stage (Schmitz *et al.*, 2000). *HvBM14* and *HvBM15* are expressed in all organ primordia and the vascular system of the barley floret, while *HvBM18* is also expressed in all other tissues (Schmitz *et al.*, 2000). *HvBM14* shows an increase in expression during the induction of the reproductive phase (Fornara *et al.*, 2004). In wheat, *Wheat FRUITFUL 3* (*WFUL3*) (*OsMADS18* orthologue) is expressed in the spikelet primordia and throughout the spikelet meristem. *WFUL1* (*OsMADS14* orthologue) and *WFUL2* (*OsMADS15* orthologue) are only expressed in the basal part of the spikelet meristem, with *WFUL1* subsequently expressed in leaves at the vegetative phase, in young spikes and in all floral organs after floral organ development. *WFUL2* expression is low in stamens and undetectable in pistils (Kinjo *et al.*, 2012). In Brachypodium *BdMADS3*, *10* and *33* are expressed in the lodicule, lemma, palea, stamen and in the young seed (Wei *et al.*, 2014). *BdMADS31* is weakly expressed in the leaf.

*B-class expression in rice, maize, wheat, barley and brachypodium*

In rice, the *APETALA 3* (AP3)-like *OsMADS16* is expressed in lodicule and stamen primordia (Fornara *et al.*, 2003; Moon *et al.*, 1999; Nagasawa *et al.*, 2003). The maize gene *SILKY1* is expressed in the centre of the floral meristem and in lodicules and stamens throughout their development (Ambrose *et al.*, 2000). In wheat, the homeologue *WAP3/TaMADS#51* is only expressed in young spikes at the floral organ development stage, while the *WAP3/TaMADS#82* homeologue expression is higher in spikes at heading stage (Hama *et al.*, 2004). *BdMADS5* in Brachypodium is expressed in lodicules and stamen (Wei *et al.*, 2014).

In rice the *PISTILLATA* (PI)-like genes *OsMADS2* and *OsMADS4* are mainly expressed in lodicules, stamens and carpels (Chung *et al.*, 1995; Fornara *et al.*, 2003; Kyozuka *et al.*, 2000). The maize genes *ZMM18*, *ZMM29* and *ZMM16* are expressed in lodicules, stamens and carpel primordia in male and female inflorescences and later are restricted only to stamen and lodicules (Whipple *et al.*, 2004). *ZMM16* was also weakly detected in vegetative organs (Munster *et al.*, 2001). In wheat, *WPI1* (*OsMADS4* orthologue) is expressed in the primordia of the stamen and lodicules (Hama *et al.*, 2004). Brachypodium *BdMADS20* is strongly expressed in the lodicules and stamen and weakly expressed in the palea (Wei *et al.*, 2014).

*BdMADS16* has a similar expression pattern and is also expressed in the carpel and the young seed.

*$B_{sister}$ expression in rice, maize, wheat and brachypodium*

Expression analysis in rice showed that *OsMADS29* expression is restricted to developing seeds, while *OsMADS30* is expressed throughout all organs in the plant (Yang *et al.*, 2012). In maize *ZMM17* is expressed in all organ primordia of the female spikelet, but later restricted to the ovule and the developing silk (Becker *et al.*, 2002; Yang *et al.*, 2012). *WBsis* is expressed in the endothelial layer of the inner integument of the ovule, weak expression is also detected in the nucellus and the outer integument (Mizzotti *et al.*, 2012; Yamada *et al.*, 2009; Yang *et al.*, 2012). It has also been shown that $B_{sister}$ gene expression might be upregulated in response to stress conditions (Puig *et al.*, 2013; Schilling *et al.*, 2019). Brachypodium has three $B_{sister}$ genes: *BdMADS17* and *BdMADS23* is weakly detectable in the palea and in the young seed and *BdMADS38* has weak expression in the stamen (Wei *et al.*, 2014). In contrast to the phylogenetically closely related B-class genes the expression and function of the $B_{sister}$-like genes seems to be restricted to the ovule and the developing seed.

*C-class expression in rice, maize, wheat and brachypodium*

In rice, one of the C genes, *OsMADS3* is strongly expressed in stamen primordia, while the other, *OsMADS58*, is expressed at a lower level uniformly throughout the floral meristem (Dreni *et al.*, 2011). Later in development *OsMADS3* and *OsMADS58* are expressed in the filament and the anther wall and in the carpel and ovule primordia (Dreni *et al.*, 2011). In wheat, C-class genes *WAG1* and *WAG2* are expressed in the stamen, carpel and ovule (Yamada *et al.*, 2009). The maize gene *ZAG1* (*OsMADS58* orthologue) is expressed early in stamen and carpel primordia, while *ZMM2* (*OsMADS3* orthologue) is mainly expressed in the anthers (Schmidt *et al.*, 1993) (Li *et al.*, 2014; Mena *et al.*, 1996). *BdMADS14* in Brachypodium is expressed in stamen and the young seed, while *BdMADS18* is expressed in stamen, carpel, lodicule, palea and in the young seed (Wei *et al.*, 2014).

*D-class expression in rice, maize, wheat and brachypodium*

Rice D-class gene *OsMADS13* is expressed in the ovule primordium and the inner cell layer of the carpel wall. During development it is expressed in the ovule, mainly

in the integuments (Lopez-Dee *et al.*, 1999). *OsMADS21* is expressed at low levels in the inner two whorls of the flower and it is highly expressed in developing kernels (Arora *et al.*, 2007; Dreni *et al.*, 2007). The D-class gene in wheat, *WSTK*, is expressed in pistils with strong expression in the developing ovule (Yamada *et al.*, 2009). *TaAG-4* (closest relative to *OsMADS21*) has weak expression in stamens and very high expression in pistils (Paolacci *et al.*, 2007). Expression of maize D-class gene *ZAG2* is largely restricted to the developing ovules and the inner carpel face (Schmidt *et al.*, 1993). In Brachypodium *BdMADS2* is strongly expressed in the carpel, while *BdMADS4* has weaker expression in the carpel (Wei *et al.*, 2013; Wei *et al.*, 2014).

*E-class expression in rice, maize, wheat, barley and brachypodium LOFSEP-lineage*

Expression of *OsMADS1* is detected in the floral meristem during early flower development, and later in the palea, lemma and weakly in the carpel (Chung *et al.*, 1994; Kobayashi *et al.*, 2010; Prasad *et al.*, 2001). The expression of two maize homologs of *OsMADS1*, *ZMM8* and *ZMM14* was only detectable in the upper floret, but not in the lower floret of the developing spike (Cacharrón *et al.*, 1995; Cacharrón *et al.*, 1999). *ZMM14* expression is lower than that of *ZMM8* and is stronger in the carpels than in the other tissues (Cacharrón *et al.*, 1999). The expression of *HvBM1* in barley is seen in the floret meristem at the distal part of the awn primordium. Expression is later in development detected in the lemma and palea, in the lodicules and the ovule, but not in the anther (Schmitz *et al.*, 2000). The expression of the wheat gene *WLHS1* is initially detectable in the inflorescence axis at inflorescence meristem initiation and later in the spikelet axis at the most proximal position (Shitsukawa *et al.*, 2007). In mature flowers their expression was observed in the glume, lemma and palea (Shitsukawa *et al.*, 2007). *BdMADS11* in Brachypodium is expressed in all floral organ tissues (Wei *et al.*, 2014).

T*aSEP-6* (*OsMADS5* orthologue) in wheat is expressed in all floral organs, but at very high levels in glumes, lemma and palea (Paolacci *et al.*, 2007). In Brachypodium, *BdMADS7* is expressed in the lemma, stamen and carpel (Wei *et al.*, 2014). Two maize homologues of *OsMADS34*, *ZMM24* and *ZMM31* are expressed in early developing tassels and ears, and *ZMM24* shows high expression throughout ear

development (Danilevskaya *et al.*, 2008). *TaSEP-5* has high expression levels at the early spike developmental stages and in spikes at the booting and heading stages, which high expression in glumes, lemma and palea (Paolacci *et al.*, 2007).

*SEP3-lineage*

*OsMADS7* and *OsMADS8* are expressed in lodicule and stamen primordia and subsequently in lodicules, stamen and carpel (Kang *et al.*, 1997; Pelucchi *et al.*, 2002). *ZMM6* (*OsMADS7* orthologue) in maize is weakly expressed in all organs of the upper and lower floret during the inflorescence development and strongly expressed in the endosperm transfer cell region and the embryo during maize kernel development (Cacharrón *et al.*, 1995; Cacharrón *et al.*, 1999; Lid *et al.*, 2004). In barley, *HvBM7* expression has been found in anthers, but not in the lemma or palea and later also in lodicules and the carpel (Schmitz *et al.*, 2000). Wheat *WSEP* expression is detected in whorls 2, 3 and 4 in early development and subsequently expands into all four whorls (Shitsukawa *et al.*, 2007). Similar to *BdMADS11* in Brachypodium, *BdMADS26* is also expressed in all the floral organ tissues (Wei *et al.*, 2014).

*ZMM27* (*OsMADS8* orthologue) in maize shows weak expression during development of the inflorescence and strong expression during maize kernel development (Lid *et al.*, 2004). *TaMADS1* (*OsMADS8* orthologue) in wheat is expressed uniformly in the spikelet primordia and later confined to the carpels and stamens (Zhao *et al.*, 2006). *BdMADS32* in Brachypodium is not expressed in the lemma and palea, but is expressed in all other floral organs (Wei *et al.*, 2014).

*AGL6-like expression in rice, maize and brachypodium*

*OsMADS6* in rice is expressed in the floral meristem at early stages and later in the emerging palea primordium, the developing palea, lodicules, ovule integuments, carpels and weakly in the lemma (Dreni and Zhang, 2016; Li *et al.*, 2010). *OsMADS17* is expressed in the floral meristem and later becomes restricted to the lodicule primordia and is also detected in the anther wall (Reinheimer and Kellogg, 2009). Maize *ZAG3* (orthologue of *OsMADS6*) is expressed in both the upper and lower floral meristems and was later in development found in developing lodicules, palea, carpel and the inner integument of the ovule (Dreni and Zhang, 2016; Mena *et al.*, 1995; Reinheimer and Kellogg, 2009; Thompson *et al.*, 2009). In Brachypodium

*BdMADS28* expression is weakly detectable in the stamen and lodicules (Wei *et al.*, 2014).

*2.1.2 Protein-protein interactions of B-class MADS-box genes in grasses*

All MADS-box transcription factors bind DNA as obligate dimers. They all recognise a CArG box motif (CC[A/T]$_6$GG) (Tilly *et al.*, 1998). Type II MADS-box transcription factors have three domains that are involved in protein-protein interactions: the I-domain, which is a short helical domain that confers dimerization specificity, the K-domain, a keratin-like domain that has a predicted coiled-coil important for tetramerization, and the C-domain, which is involved in transactivation and/or the recruitment of other factors (Lai *et al.*, 2019). These domains, together with the diversity of them created by alternative splicing, has led to a large and complex protein-protein interaction (PPI) network (Lai *et al.*, 2019). ABCDE MADS-box genes are well known to form tetramers, or 'floral quartets', to carry out their function (Theissen and Saedler, 2001). Tetrameric complexes made by MIKC$^c$ MADS-box genes, to which the ABCDE MADS-box genes belong, are plant specific and can bind DNA cooperatively at two sites (Jetha *et al.*, 2014; Melzer *et al.*, 2008).

The structure of the K-domain has been well conserved throughout evolution in the MIKC MADS-box transcription factors, consisting of three subdomains: K1, K2 and K3.The K-domain folds into two α-helices (K1 and K2+K3) connected by a kink region (Figure 2.1) (Rümpler *et al.*, 2018). Hydrophobic residues in the K-domain have been shown to be highly important for dimerization and tetramerization of ABCDE MADS-box transcription factors (Lai *et al.*, 2019). Although the structure of the K-domain has been conserved, there is still a marked difference in the probability to form coiled coils between the different MADS-box transcriptions factors (Lai *et al.*, 2019). SEP3, previously identified as the 'glue' or the 'hub' for MADS-box transcription factor complex formation, has the highest probability of forming coiled coils (Immink *et al.*, 2009; Lai *et al.*, 2019). AP1 and PI show medium probability, while AG and AP3 only show low probability to form coiled coils (Lai *et al.*, 2019). It was hypothesised by Lai *et al.* (2019) that at least one monomer in the floral quartet must have a strong probability to form coiled coils in the α2 helix to be able to drive tetramerization. Even small changes in these 'hubs',

like SEP3, can lead to destabilisation of the complex or completely abolish the tetramerization (Rümpler *et al.*, 2018).

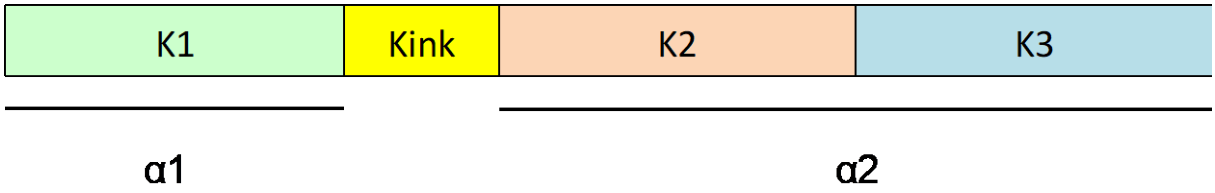



**Figure 2.1 Structure of the K-box domain in MIKC$^c$ MADS-box genes.**
The K-box domain in MIKC$^c$ MADS-box genes consists of three subdomains: K1, K2 and K3.The K-domain folds into two α-helices (α1 and α2) connected by a kink region. The α1 helix is thought to be important for dimerization and the α2 helix for dimerization and tetramerization.

DEF- and GLO-like proteins form obligate heterodimers, which have been hypothesised to have originated after the gymnosperm-angiosperm split but before the monocot-eudicot split (Davies *et al.*, 1996; Goto and Meyerowitz, 1994; Winter *et al.*, 2002b). Yang *et al.* (2003) and Yang and Jack (2004) showed that leucine-zipper motifs in the K1 and K2 helices of the K-domain were important for DEF/GLO heterodimerization. OsMADS16 has been shown to form heterodimers with OsMADS4 and OsMADS2 in rice, confirming the conservation of the interaction between GLO- and DEF-clade proteins in rice (Moon *et al.*, 1999; Yao *et al.*, 2008). This has previously been shown in Arabidopsis, where AP3 and PI form obligate heterodimers (Krizek and Meyerowitz, 1996). Whipple *et al.* (2004) showed that ZMM16 in maize also forms obligate heterodimers to bind DNA. They also showed that neither SILKY1, nor ZMM16 alone could bind DNA, while SILKY1 and ZMM16 together could bind DNA, indicating that the heterodimer is necessary for DNA binding.

A better understanding of the complexes that are formed between the different classes can help us further elucidate the workings of the model and understand the way these proteins function.

## 2.2 Materials and methods

*2.2.1 Plant materials, growth conditions and sample preparation*

*Hordeum vulgare cv. Golden Promise* seeds were sown in Cocopeat compost in 13cm diameter pots and grown in a controlled environment growth chamber with a continuous temperature of 18°C and 12 hour photoperiod. Samples were collected from spikes, florets and floral organs at different growth stages according to the staging system established by Zadoks *et al.* (1974), Waddington *et al.* (1983) and Gómez and Wilson (2012) and flash frozen in liquid nitrogen (Table 2.1).

| Stage | Size of the spike | Plant characteristics and reproductive developmental stage |
|---|---|---|
| 31 | 0.6 cm | First node detectable on the stem.<br>Primary sporogenous cells. Three cell layers surrounding the anther locule. |
| 32 | 0.7 - 1.6 cm | Second node detectable on the stem.<br>Secondary sporogenous cells to pollen mother cells. Four layers surrounding the anther locule: epidermis, endothecium, middle layer, and tapetum. |
| 33 | 2 - 3.1 cm | Third node detectable on the stem.<br>Pollen mother cells undergo meiosis. Tapetum layer is prominent. |
| 34 | 3.3 - 4 cm | Fourth node detectable on the stem.<br>Microspores released from the tetrad. Tapetum vacuolated. |
| 35 | 4.2 cm | Fifth node detectable on the stem.<br>Free microspores. Middle layer undergoes crushing. The prominent tapetum layer starts to degenerate. |
| 36 | 5.5 cm | Sixth node detectable on the stem.<br>Microspores become vacuolated. Tapetum degenerating.<br>Stigmatic branches of the carpel are elongating. |
| 37 | 7 cm | Flag leaf just visible.<br>Mitosis I. Tapetum degenerating, but still present.<br>Hairs on the ovary wall are just differentiating. |
| LFE2 | 7 - 7.5 cm | Last flag sheath extended 5–10 cm. Boot swelling obvious. Awns may be visible. Spike still inside the sheath, rachis has not started elongating.<br>Mitosis I. Tapetum degenerating, but still present.<br>Stigmatic branches and hairs on the ovary wall are elongating. |
| LFE3 | 7.5 – 8.5 cm | The last flag leaf opening and awns being clearly visible.<br>Mitosis II. Binuclear pollen.<br>Style and stigmatic branches erect. Stigmatic hairs differentiating. |
| LFE4 | 8.5 - 9 cm | Spike has completed its upward movement and was entirely localized within the last flag sheath. Heading is imminent.<br>Trinuclear pollen. Septum breakage.<br>Styles and stigmatic branches of the carpel are spreading. |

**Table 2.1 Developmental staging and spike size for samples collected from *Hordeum vulgare cv. Golden Promise*.** Explanation of the different stages collected for the expression analysis of the ABCDE MADS-box genes based on the staging by Zadoks *et al.* (1974), Waddington *et al.* (1983) and Gómez and Wilson (2012).

For In situ Hybridization Analysis florets of *Hordeum vulgare cv. Golden Promise* were harvested at LFE3 stage, characterized by the last flag leaf opening and awns being clearly visible, and fixed in 4% (w/v) paraformaldehyde in phosphate-buffered saline (PBS) with 0.1% (v/v) Triton X-100 and 0.1% (v/v) Tween 20. A vacuum treatment of 15min was performed before leaving overnight at 4°C. Samples were then washed three times with 70% (v/v) EtOH for 10min each. Dehydration with an EtOH series of 95% (v/v) and 2x100% (v/v) was followed by a 2:1 EtOH-HistoChoice mix overnight. Incubation in 1:1 and 1:2 mixes of EtOH and HistoChoice were then followed with overnight incubation in 100% HistoChoice. After another incubation in 100% HistoChoice a 1:1 mix of HistoChoice/Paraplast was added at 42°C, followed by an overnight incubation in 100% Paraplast at 56-60°C. Paraplast was replaced twice at 56-60°C and then replaced a last time at room temperature and left to solidify. Samples in Paraplast blocks were stored at 4°C.

*2.2.2 Quantitative reverse transcription PCR (qRT-PCR)*

RNA was extracted with the Spectrum™ Plant Total RNA kit (Sigma-Aldrich, Germany). cDNA was synthesised from total RNA using SuperScript™ III reverse transcriptase (ThermoFisher Scientific, UK) and checked for quality by RT-PCR of the barley housekeeping gene *HvGAP*. Real-time quantitative PCR was performed at the University of Adelaide by Dr. Neil Shirley with primers, designed by Nicolaas Kuijer, Dr. Laura Wilkinson and Cindy Callens, for all ABCDE MADS-box genes (Table 2.2) on three technical replicates and analysed using the CFX384 qPCR system (Bio-Rad). Expression values relative to the barley *α-Tubulin* gene (*HvTUB*), barley *HSP70* gene (*HvHSP70*) and barley *Cycolphilin* gene (*HvCyc*) as control housekeeping genes were calculated. These genes were routinely used by Dr. Neil Shirley in barley and have been extensively tested. All housekeeping genes were expressed continuously at similar levels in all samples. Extra primers were designed for *HvBM2* and *HvBM4* due to the presence of receptor kinases on the reverse strand of both genes, amplifying either both genes or the receptor kinases separately (Figure 2.2). All amplified gene fragments were verified by sequencing.

*2.2.3 Clustering analysis*

A hierarchical clustering analysis using Manhattan distance was carried out through the Multi Experiment Viewer (MeV) software (Tm4) on all the relative expression values obtained from the quantitative RT-PCR (Saeed *et al.*). The values were normalised to the highest expression value for each gene.

| Gene | ABCDE class | Gene identifier | Forward primer (5'-3') | Reverse primer (5'-3') |
|---|---|---|---|---|
| *HvBM14* | A | HORVU5Hr1G095630.3 | CAGCGGCGGCAGGCGAGAG | CCAGGCTGGCCGCTGCAAC |
| *HvBM15* | A | HORVU2Hr1G063800.7 | ATATGCCTACCGCCATGGAT | ATACAGCGAACCAGCATTCC |
| *HvBM18* | A | HORVU2Hr1G069820.2 | CCAGCATGATATCGCCTTG | TCGAGCCAGTGGTGGATAA |
| *HvBM2* | B | HORVU3Hr1G091000.8 | CCAATCTGCAGGAGGACAC | TCGGCACATCATCAAGCTAC |
| *Receptor Kinase 2* | | HORVU3Hr1G090990.3 | / | CAACAAATCAAGATTTTCCACA |
| *HvBM4* | B | HORVU1Hr1G063620.2 | ATGGAGCTCGGGTACCATC | CCTGCAGGTAGATGGAGCA |
| *Receptor Kinase 3* | | HORVU1Hr1G063610.4 | TTCTCGTGTTTGTTCTGGTCA | ATGCCAAGATGTTCCTGGTC |
| *HvBM16* | B | AK373398.1 | TCACCACACAGACTGAAACCT | TGGAGATATGCGGTGCACAAG |
| *HvBM29* | $B_{sister}$ | HORVU6Hr1G032220.8 | GAAGAGATTAACCACGAT | TCCAAGATATGCTCCTT |
| *HvBM30* | $B_{sister}$ | HORVU7Hr1G108280.4 | GACCAGAACAGCTTCCTTCG | GCTTCCGTCCAATTTCGTCA |
| *HvBM31* | $B_{sister}$ | HORVU2Hr1G098930.2 | ATGAACCCGAAGCTGTTCC | AAGCTCCGATCATCCATCC |
| *HvBM3* | C | HORVU3Hr1G026650.1 | GCAGCAGCAGCATTACTCC | ACACATGCACGCGACAGTA |
| *HvBM58* | C | HORVU1Hr1G029220.1 | ATCATGCAGCAGCCTCAGT | GGTGTGGCCAAGCCTTAAT |
| *HvBM13* | D | HORVU1Hr1G023620.1 | TCAGCTGAACCTAGGCTGC | TTTGACAGGAATAGTTGAGTAC TGGT |
| *HvBM21* | D | HORVU1Hr1G064150.2 | CTCTTCACCTCGGCTACGA | TCTTCACAACACGCACACG |
| *HvBM1* | E | HORVU4Hr1G067680.2 | TCGTCTGCAGGTTGGATATG | CAGCGTACAACGCAGCTTAG |
| *HvBM5* | E | HORVU7Hr1G025700.6 | CCTGGATCACATGAACAATGA | CGAAATGCGCACATGTCTAT |
| *HvBM7* | E | HORVU7Hr1G054220.1 | ACCCTCCTGAGTCCCTGAA | ACGAAAGTTGCACGCAAAA |
| *HvBM8* | E | HORVU5Hr1G076400.1 | CTCAGGAGCAGATAAACAACG | GTACGCGAACGCGGTACTA |
| *HvBM34* | E | HORVU5Hr1G095710.1 | ATTTCGTGGCATGGATGTG | AACACAAAAGCAGCCGAGTT |
| *HvBM6* | AGL6 | HORVU6Hr1G066140.9 | ATGCTGGGGTGGGTTCTT | GCCACGCAGGGTACTTCTC |

**Table 2.2 Gene specific primers designed for the ABCDE MADS-box genes for Real-time quantitative PCR analysis.**

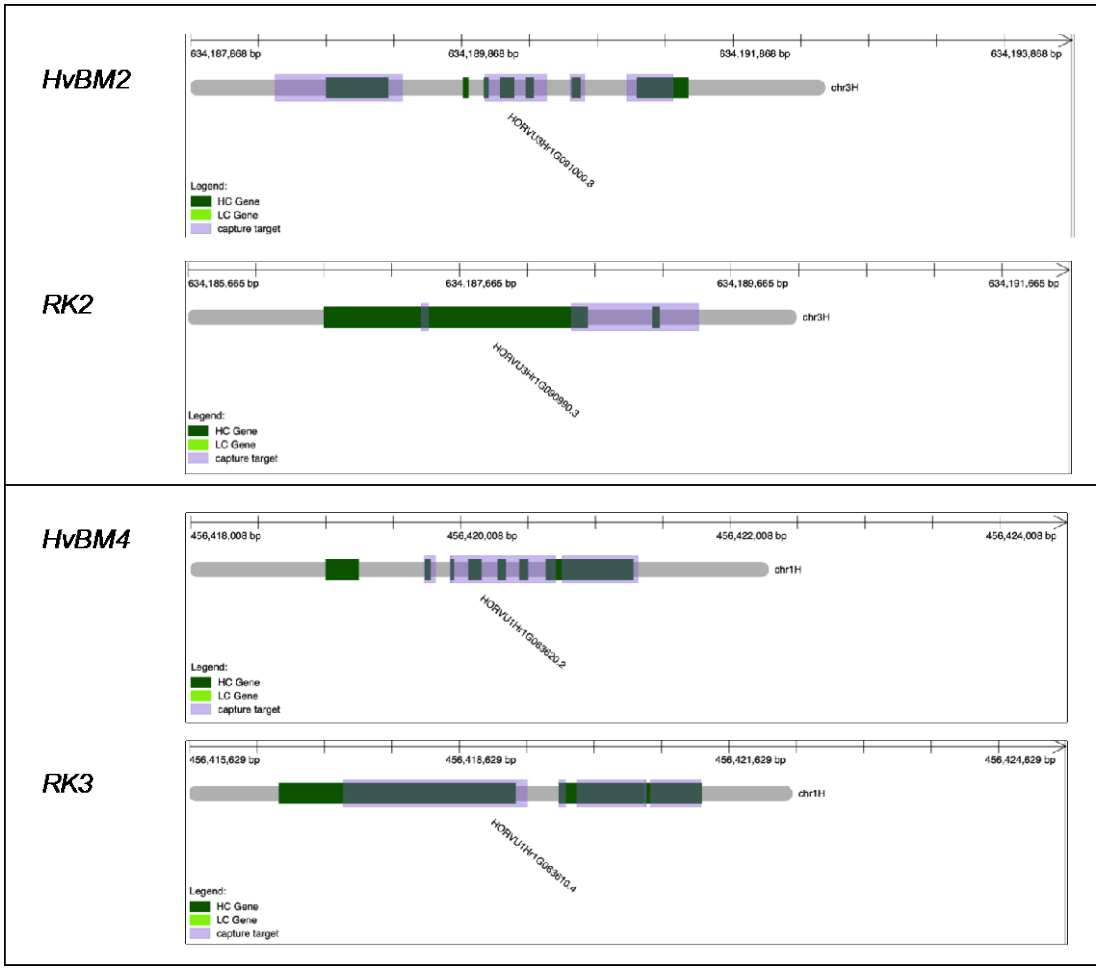



**Figure 2.2 B-class genes *HvBM2* and *HvBM4* on the reverse strand and the presence of *Receptor Kinase 2* and *3* on the forward strand.**
The expression analysis of the B-class MADS-box genes *HvBM2* and *HVBM4*, present on the reverse strand, was made difficult by the presence of *receptor kinase 2* and *3*, respectively, being on the forward strand. A specific set of three primers was designed for these genes to eliminate the expression data from the receptor kinase genes.

*2.2.4 In Situ Hybridization*

All the In Situ Hybridization work was carried out at the University of Adelaide by Dr. Xiujuan Yang. The probe for the B-class gene *HvBM2* was amplified from a DNA template (From 5'-CAGGAGGACACCTAG... to …GAATAGTTTGTAATGACAAC-3'). The probe was transcribed from the DNA template for 2 hours at 37°C and then went through DNase digestion for 15-30min at 37°C. To 50µl probe product, 9µl of 0.5M EDTA, 24µl 4M LiCl and 600µl chilled ethanol was added and left at -20°C overnight. The probe was then centrifuged at high speed for 10min and the pellet was washed with 200µl chilled ethanol. The probe was again centrifuged at 13.000 rpm for 10min and the supernatant was removed. After air drying on ice 50µl DEPC-treated water was added to dissolve the probe.

Samples fixed and embedded in paraffin (Paraplast) were sectioned at 6-8µm thickness by a rotary microtome and stretched in water on glass slides at 37°C. All glassware used from here on was washed with water, RNAse-away and autoclaved before use. The slides were dewaxed with 100% HistoChoice and rehydrated with 100% EtOH followed by 95% EtOH (v/v) and a mix of 85% EtOH (v/v) and 0.85% NaCl (w/v). The slides and covers were put in a glass box filled with 85% EtOH(v/v)/0.85% NaCl (w/v) and secured in the slide holder which was then loaded into the slide tray. Hybridisation was carried out using Intavis InsituPro robot (Intavis GmBH, Germany).

## 2.3 Results

*2.3.1 Expression analysis of the ABCDE MADS-box genes in barley*

*2.3.1.1 Relative expression of the ABCDE MADS-box genes in barley by qRT-PCR*

To investigate the expression pattern of the ABCDE MADS-box genes in barley, qRT-PCR was performed on different floral tissues across different developmental stages. The stages examined range from first node being visible on the stem and primary sporogenous cells being formed in the anther (stage 31), to immediately before anthesis when heading is imminent (stage LFE4). The relative expression values obtained by qRT-PCR were visualised in a heatmap (Figure 2.3).

*HvBM15* was the most abundant A-class gene in all tissues throughout development with the exception of the reproductive tissues (Figure 2.4.A). *HvBM14* was also expressed throughout development with higher expression in LFE2 and LFE4. In the

reproductive tissues *HvBM14* was the most abundantly expressed gene (Figure 2.4.B). *HvBM18* had very low expression in all tissues and throughout development.

The expression analysis of the B-class MADS-box genes had the added difficulty of *HvBM2* and *HVBM4* both being on the reverse strand of two receptor kinase genes (Figure 2.2). A specific set of three primers was designed for these genes to eliminate the expression data from the receptor kinase genes (Table 2.2). One primer pair was designed to amplify across the stop codon of *HvBM2*/*HvBM4* with a forward primer in the CDS and the reverse primer in the 3'UTR. This primer pair amplified both the PI-like B-class gene and the receptor kinase. The same forward primer was combined with a reverse primers in the receptor kinase, outside of the 3'UTR of the PI-like B-class gene. This primer pair only amplified the receptor kinase. Expression levels for both these fragments could then be subtracted to obtain the accurate expression level of the PI-like B-class genes. This showed that *HvBM2* was the most abundantly expressed of the B-class genes and was predominantly expressed in stage 36-LFE4 and in the reproductive organs (Figure 2.5.A). *HvBM4* is expressed in the reproductive organs, but not as abundantly as *HvBM2*. *HvBM16* is not highly expressed throughout floral organ development.

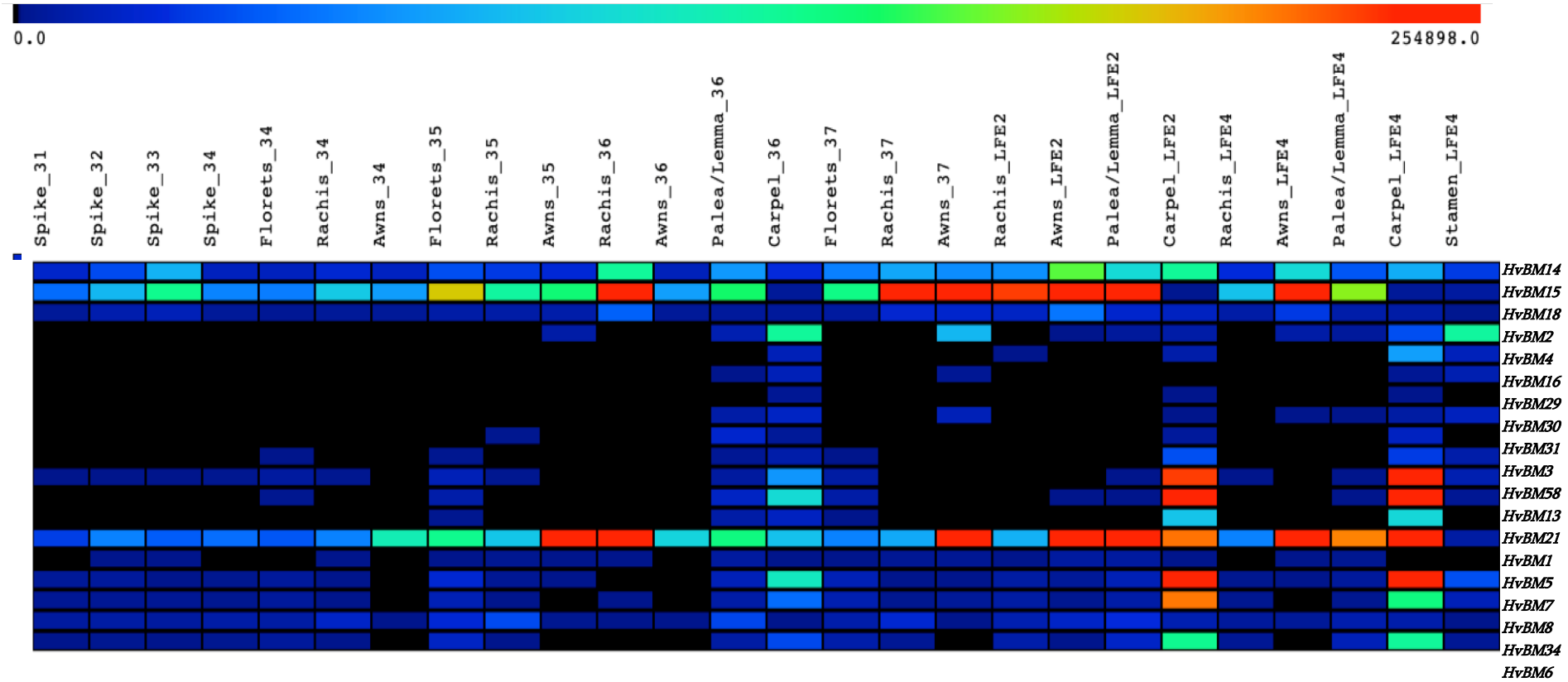



**Figure 2.3 Heat map showing relative expression of the ABCDE MADS-box genes in barley.**
Heat map of the relative expression values obtained through qRT-PCR for different tissues and stages (columns) and all the ABCDE MADS-box genes (rows). High relative expression is shown in red and low relative expression is shown in black. Made with the Multi Experiment Viewer (MeV) software (Tm4).

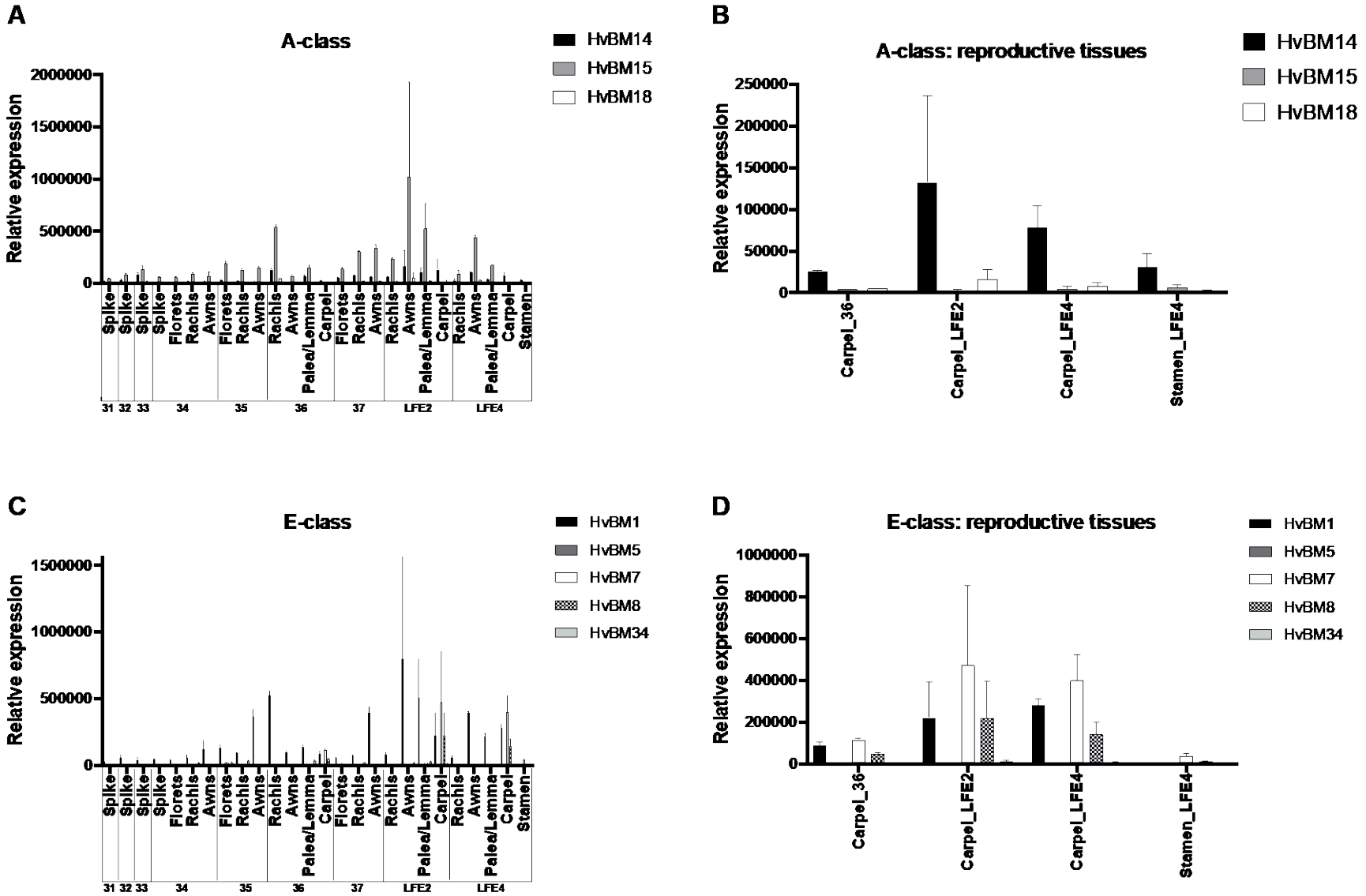



**Figure 2.4 Real-time quantitative PCR expression analysis of A-class and B-class MADS-box genes.**
(A) Relative expression analysis of A-class genes in different floral tissues, at different developmental stages (B) relative expression of the A-class genes in only the reproductive tissues at stage 36, LFE2 and LFE4. (C) Relative expression analysis of E-class genes in different floral tissues, at different developmental stages, (D) relative expression of the E-class genes in only the reproductive tissues at stage 36, LFE2 and LFE4 (D).

The barley $B_{sister}$ genes are not highly expressed in the organs examined. They are all predominantly expressed in the carpel, but there is also high expression of *HvBM30* and *HvBM31* in the palea and lemma and of *HvBM30* in the awns and stamen (Figure 2.5.B). Sequencing of *HvBM30* amplified from compiled cDNA from different tissues and different stages shows several different isoforms of the gene were recovered. These aberrant forms might have been picked up in the qPCR.

Expression of the C-class MADS-box genes is detected in the carpel when the stigmatic branches of the carpel are elongating and gets stronger in the later stages, peaking immediately before anthesis (Figure 2.5.C). *HvBM58* is the most abundantly expressed, with *HvBM3* barely showing any expression.
The D-class MADS-box genes are expressed in the carpel in later stages of development, when the stigmatic branches and hairs on the ovary wall are elongating (LFE2) and when the styles and stigmatic branches start spreading (LFE4) (Figure 2.5.D). *HvBM13* is most abundantly expressed, while *HvBM21* only has low expression.

*HvBM1* is the most abundantly expressed E-class gene and is expressed throughout development and in all tissues (Figure 2.4.C). However, in the reproductive tissues, *HvBM7*, *HvBM8* and *HvBM6* have a higher expression level than *HvBM1* (Figure 2.4.D and Figure 2.6.A). *HvBM5* and *HvBM34* are barely expressed in any tissues throughout development.

A large difference was noticed between gene expression in biological replicates in the later stages (LFE2 and LFE4). The spikes of the biological replicates for LFE2 measured 7cm (LFE2_1) and 7.5cm (LFE2_2). These samples will be at different stages of mitosis I of the pollen development and during elongation of the stigmatic branches and hairs on the ovary wall. The length of the spikes of the biological replicates of LFE4 measured 8.5cm (LFE4_1) and 9cm (LFE4_2). These samples were collected immediately before anthesis and will be at the last stages of pollen development, where trinuclear pollen is present. Comparing the relative expression levels of certain genes in the reproductive tissues, awns and palea/lemma between these biological replicates uncovered a change in gene expression within the stage (Figure 2.6.B-D).

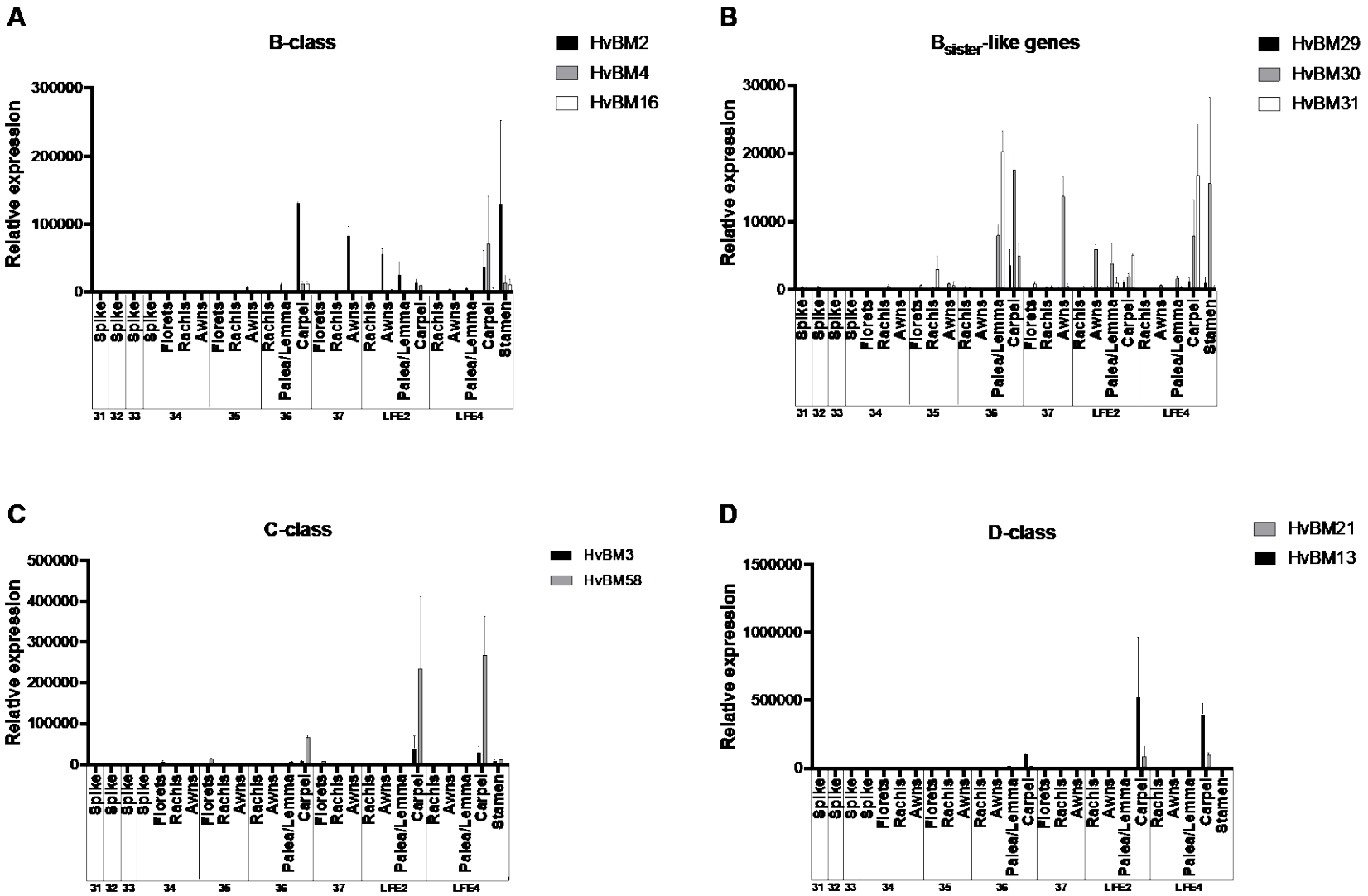



**Figure 2.5 Real-time quantitative PCR expression analysis of B-class, $B_{sister}$-like, C-class and D-class MADS-box genes.**
Relative expression analysis of B-class genes (A), $B_{sister}$-like genes (B), C-class genes (C) and D-class genes (D) in different floral tissues, at different developmental stages.

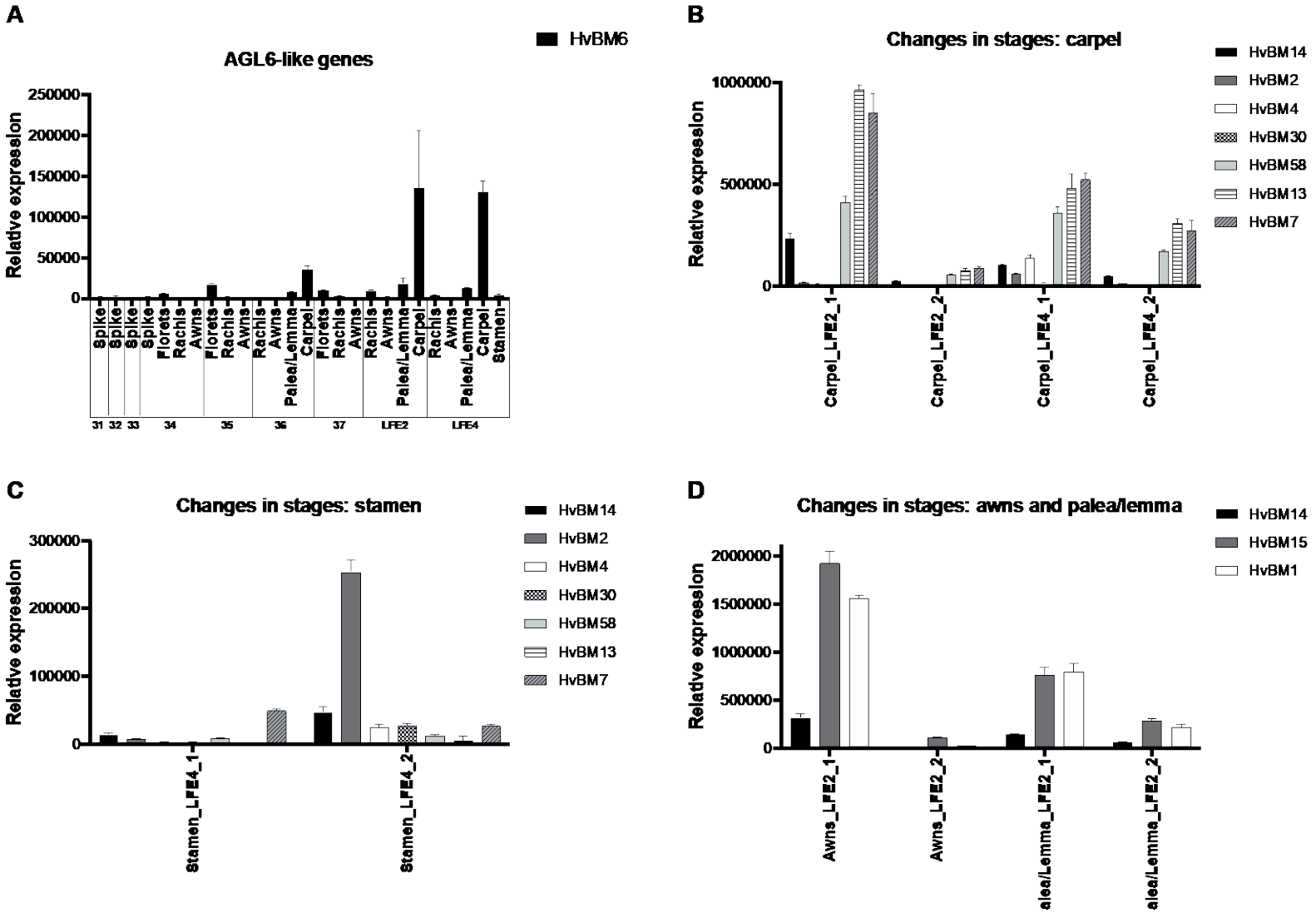



**Figure 2.6 Real-time quantitative PCR expression analysis of AGL6-like MADS-box genes and changes in expression between biological replicates in stages LFE2 and LFE4.**

Relative expression analysis of AGL6-like genes (A) in different floral tissues, at different developmental stages. Differences between biological replicates in LFE2 and LFE4 in the carpel(B), in LFE4 in the stamen (C) and in LFE2 and LFE4 in awns and palea/lemma (D), indicated that the exact staging at these developmental points in time were more difficult. Graphs B, C and D show the results of three technical replicates: three samples from the same cDNA.

Genes specific to reproductive tissues are down-regulated in the carpel between beginning and end of LFE2 and LFE4 and up-regulated in the stamen between beginning and end of LFE4. In awns and palea/lemma the prominent A- and E-class genes are down-regulated between beginning and end of LFE2.

*2.3.1.2 Clustering of expression patterns*

Hierarchical clustering analysis highlights various clusters of genes that are highly expressed in different tissues of the floret at different stages (Figure 2.7). *HvBM34* is expressed early in development in the rachis and florets at stage 34 and in the rachis at stage 35. In the palea and lemma at stage 36 a cluster with *HvBM31* and *HvBM5* is formed. A first big cluster can be seen in the rachis of stage 36 with *HvBM14*, *HvBM15*, *HvBM18* and *HvBM1*, A- and E-class genes. Early carpel development, when the stigmatic branches start elongating (stage 36), is dominated by a cluster of B-class and $B_{sister}$ genes: *HvBM2*, *HvBM16*, *HvBM29* and *HvBM30*. Later carpel development, when the stigmatic branches and hairs on the ovary wall are elongating (stage LFE2), shows a shift towards A-, C-, D-, E-class and AGL6-like genes: *HvBM14*, *HvBM3*, *HvBM58*, *HvBM13*, *HvBM21*, *HvBM7*, *HvBM8* and *HvBM6*. In LFE4 the B-class gene *HvBM4* is added to that cluster. In the stamen at stage LFE4, at the last stages of pollen development and the spreading of the styles and stigmatic branches in the carpel, there is a cluster of B- and $B_{sister}$ gene expression: *HvBM2*, *HvBM16* and *HvBM30*. The awns in LFE2 have a cluster of the highest expression of A- and E-class genes.

*2.3.1.3 In Situ Hybridization analysis of the DEF/GLO-like MADS-box genes*

The mRNA in situ hybridization results show signal of the *HvBM2* transcript in the ovule, the carpel and in the anther wall and filament at stage LFE3 (Figure 16). The sense probe shows that there is some background signal in the anther walls and in the pollen.

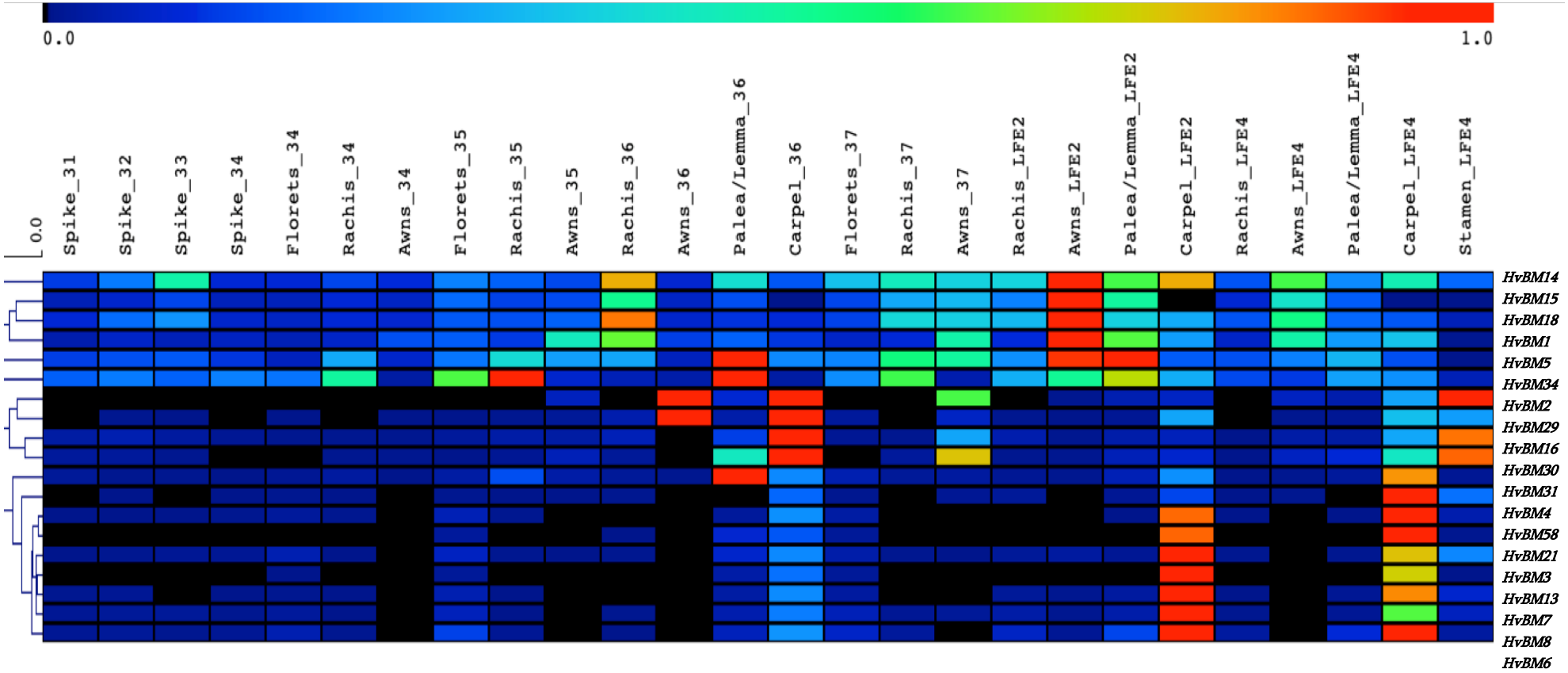



**Figure 2.7 Heat map showing hierarchical clustering of the relative expression values of the ABCDE MADS-box genes in barley.**
A hierarchical clustering analysis using Manhattan distance was carried out through the Multi Experiment Viewer (MeV) software (Tm4) on all the relative expression values obtained from the quantitative RT-PCR. The values were normalised to the highest expression value for each gene, giving an indication of which tissues and stages have the highest expression for each specific gene and which genes might play a specific role in certain tissues at certain stages.

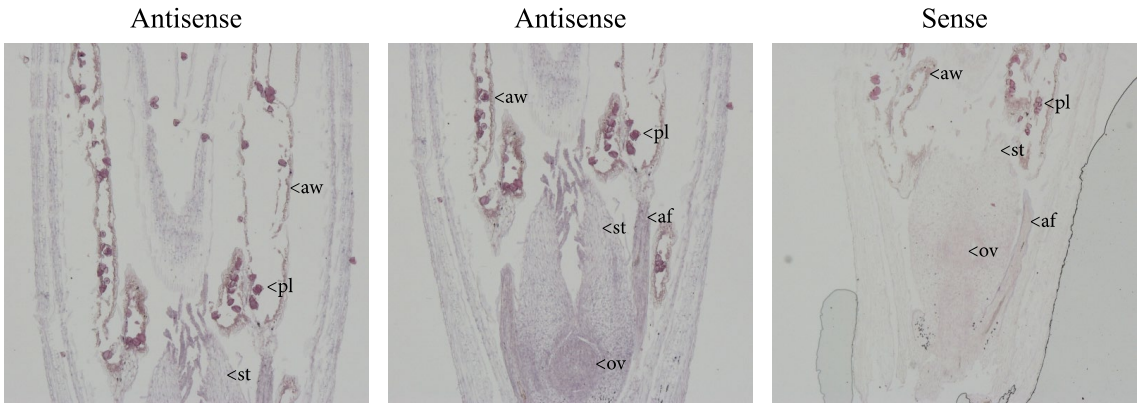



**Figure 2.8 mRNA in situ hybridization of the *HvBM2* transcript**
In florets of *Hordeum vulgare cv. Golden Promise* at stage LFE3 the mRNA in situ hybridization results show some signal of the *HvBM2* transcript in the ovule, the carpel and in the anther wall and filament. The sense probe shows that there is some background signal in the anther walls and in the pollen. (aw = anther wall, pl = pollen, st = style, af = anther filament, ov = ovule)

## 2.4 Discussion

We have carried out a tissue-specific expression analysis throughout a wide range of developmental stages in *Hordeum vulgare cv. Golden Promise* to generate an overview of the expression patterns of all the ABCDE MADS-box genes in barley (Figure 2.3).

The results for the A-class genes are similar to those reported in barley by Schmitz *et al.* (2000). *HvBM15* is the most abundantly expressed gene of all the classes, showing expression in all stages of development and in all tissues except the reproductive tissues. *HvBM14* is the most abundant A-class gene in the reproductive tissues, indicating a possible role for *HvBM14* in carpel and stamens development, while *HvBM15* is more likely to be involved in development of palea, lemma, rachis and awns. This corresponds to what has previously been reported in rice and wheat (Kinjo *et al.*, 2012; Kyozuka *et al.*, 2000; Pelucchi *et al.*, 2002).

The expression analysis of the B-class genes *HvBM2* and *HvBM4* was made difficult by the presence of receptor kinase 2 and 3, respectively, on the reverse strands of both genes. An extra primer pair was designed to extract the relative expression values derived from the receptor kinases from the overall relative expression values detected. However, this proved to be quite difficult and not entirely accurate because of discrepancies of values detected for both genes compared to only the receptor

kinase gene in certain tissues. Expression analysis of the receptor kinases showed that they are not expressed in the reproductive tissues, meaning that the qPCR results are likely to reflect specific amplification of *HvBM2* and *HvBM4*. Specific expression in the carpel and the stamen was detected for these two genes, which corresponds to the expression patterns found in rice (Chung *et al.*, 1995; Fornara *et al.*, 2003; Kyozuka *et al.*, 2000). The in situ hybridization results show that *HvBM2* expression is more specifically located in the carpel and the anther wall and filaments. These results might indicate a function for HvBM2 and HvBM4 in stamen and carpel development. *HvBM16* shows low expression compared to the PI-like genes, which might indicate a function in a specific part of the stamen and carpel function that might be revealed by in situ hybridization.

The $B_{sister}$ genes in barley are overall not highly expressed. They are most abundant in the carpel and two, *HvBM30* and *HvBM31*, also show expression in palea/lemma and in the awns, which is consistent with rice and wheat (Mizzotti *et al.*, 2012; Yamada *et al.*, 2009; Yang *et al.*, 2012). $B_{sister}$ genes have been shown in other species to be involved in seed development and the low expression observed here might be an indication of a more important role in the seed, at a developmental stage not included in the sample set collected for this expression analysis.

The C-class genes *HvBM3* and *HvBM58* are only expressed in the carpel and late in development also in the stamen. This is similar to what previously has been described in rice and wheat (Dreni *et al.*, 2011; Yamada *et al.*, 2009). *HvBM58* is significantly more abundant than *HvBM3* which might indicate that HvBM3 doesn't play a dominant role in carpel and stamens morphogenesis. Similar to rice, HvBM3 might be involved in slightly different floral developmental processes at different stages due to sub-functionalization of the genes after gene duplication (Yamaguchi *et al.*, 2006). Knock-out mutants of *HvBM3* and *HvBM58* separately compared to a double knock-out of *HvBM3* and *HvBM58* combined with in situ hybridization analysis of both genes in early and later stages of development might help validate this hypothesis.

Similarly, the D-class genes *HvBM13* and *HvBM21* are only expressed in the carpel, more or less corresponding to the expression patterns of D-class genes in rice, maize

and wheat (Arora *et al.*, 2007; Dreni *et al.*, 2007; Lopez-Dee *et al.*, 1999; Paolacci *et al.*, 2007; Schmidt *et al.*, 1993; Yamada *et al.*, 2009). Low expression of *HvBM21* during these developmental stages might indicate that, like OsMADS21, HvBM21 plays a more important role in developing seeds.

Expression analysis of the E-class genes in barley shows that *HvBM1* is the most abundant gene, expressed in all tissues across developmental stages, except for the reproductive tissues where it is absent in the stamen and only has low expression in the carpel. This corresponds to earlier reported data (Schmitz *et al.*, 2000). This might indicate that HvBM1 is involved in development of the outer whorls. *HvBM7* and *HvBM8* might play a more important role in reproductive development, shown by their abundant expression in the carpel and to a lesser degree in the stamen. Similarly *HvBM6* is most abundantly expressed in the carpel, indicating a role in reproductive development. This corresponds to the results found in rice and maize (Dreni and Zhang, 2016; Li *et al.*, 2010; Mena *et al.*, 1995; Reinheimer and Kellogg, 2009).

Comparing the hierarchical clustering analysis and the relative expression values obtained by qRT-PCR potential interacting ABCDE MADS-box proteins in specific tissues at different developmental stages can be hypothesised (Figure 2.9). The developmental stages deemed to have the most significant expression patterns range from tapetum degeneration in the anthers and elongating styles with stigmatic branches just differentiating in the carpel (stage 35), to anthesis (stage LFE4). HvBM1 could potentially be a hub protein as was described for SEP3 in *Arabidopsis*, because of its prominent expression throughout the developmental stages investigated here and in all the different floral tissues (Immink et al., 2009). Together with *HvBM1*, *HvBM15* is expressed highly in all tissues throughout the developmental stages presented here, except for the carpel and the stamens. It is likely that a HvBM1-HvBM15 heterodimer acts as a hub for tetramers involved in the development of all tissues except for the carpel and the stamens. In the carpel at stage 36, when the stigmatic branches start elongating, HvBM2, HvBM1, HvBM7, HvBM58 and HvBM13 are likely involved in carpel development. In the carpel at stage LFE2, when the stigmatic branches and the hairs on the ovary are elongating, HvBM1, HvBM14, HvBM7, HvBM58, HvBM13, HvBM8, HvBM6 and HvBM21

are found to be potentially involved in carpel development. The same combination of the genes is found in the carpel at stage LFE4, when the styles and stigmatic branches are spreading, with the exception of HvBM14. It is likely that different complexes are formed out of these proteins to determine and/or develop different parts of the carpel: ovule, ovary, styles and the stigmatic branches, at these three different stages. In the stamens at stage LFE4, when trinuclear pollen is formed and the septum is about to break, only *HvBM2* is highly expressed. Although *HvBM16* and *HvBM30* have high expression in the stamens at this stage, their relative expression is significantly lower than that of *HvBM2* and they therefore might not play a significant role in comparison to HvBM2.

| 35 | | | 36 | | | | 37 | | | LFE2 | | | | LFE4 | | | | |
|---|---|---|---|---|---|---|---|---|---|---|---|---|---|---|---|---|---|---|
| Florets | Rachis | Awns | Rachis | Awns | Palea/ Lemma | Carpel | Florets | Rachis | Awns | Rachis | Awns | Palea/ Lemma | Carpel | Rachis | Awns | Palea /Lemma | Carpel | Stamens |
| HvBM15 | HvBM15 | HvBM15 | HvBM15 | HvBM15 | HvBM15 | | HvBM15 | HvBM15 | HvBM15 | HvBM15 | HvBM15 | HvBM15 | | HvBM15 | HvBM15 | HvBM15 | | |
| HvBM1 | HvBM1 | HvBM1 | HvBM1 | HvBM1 | HvBM1 | HvBM1 | HvBM1 | HvBM1 | HvBM1 | HvBM1 | HvBM1 | HvBM1 | HvBM1 | HvBM1 | HvBM1 | HvBM1 | HvBM1 | |
| | | | HvBM14 | | HvBM14 | | | | | HvBM14 | HvBM14 | HvBM14 | HvBM14 | | HvBM14 | | | |
| | | | | | | | | | | | HvBM18 | | | | | | | |
| | | | | | | HvBM2 | | | | | | | | | | | | HvBM2 |
| | | | | | | HvBM7 | | | | | | | HvBM7 | | | | HvBM7 | |
| | | | | | | HvBM58 | | | | | | | HvBM58 | | | | HvBM58 | |
| | | | | | | HvBM13 | | | | | | | HvBM13 | | | | HvBM13 | |
| | | | | | | | | | | | | | HvBM8 | | | | HvBM8 | |
| | | | | | | | | | | | | | HvBM6 | | | | HvBM6 | |
| | | | | | | | | | | | | | HvBM21 | | | | HvBM21 | |

**Figure 2.9 Schematic overview of potential interacting ABCDE MADS-box proteins in development of floral tissues at different developmental stages.**
Based on the relative expression values obtained by qRT-PCR and the hierarchical clustering analysis potential interacting partners of the ABCDE MADS-box proteins were schematically represented in floral tissues at developmental stages ranging from tapetum degeneration in the anthers and the presence of the style primordia on the carpel before style elongation, to anthesis. (Green = A-class, red = E-class, blue = B-class, purple = C-class, yellow = D-class, orange = AGL6-like)

## 2.5 References


**Ambrose BA, Lerner DR, Ciceri P, Padilla CM, Yanofsky MF, Schmidt RJ**. 2000. Molecular and genetic analyses of the silky1 gene reveal conservation in floral organ specification between eudicots and monocots. *Molecular Cell* **5**, 569-579.

**Arora R, Agarwal P, Ray S, Singh AK, Singh VP, Tyagi AK, Kapoor S**. 2007. MADS-box gene family in rice: genome-wide identification, organization and expression profiling during reproductive development and stress. *BMC Genomics* **8**, 242.

**Becker A, Kaufmann K, Freialdenhoven A, Vincent C, Li M-A, Saedler H, Theissen G**. 2002. A novel MADS-box gene subfamily with a sister-group relationship to class B floral homeotic genes. *Molecular Genetics and Genomics* **266**, 942-950.

**Cacharrón J, Fischer A, Saedler H, Theissen G**. 1995. Expression patterns of MADS-box genes as studied by in situ hybridization. *Maize Genetics Cooperation Newsletter* **69**, 37-38.

**Cacharrón J, Saedler H, Theissen G**. 1999. Expression of MADS box genes ZMM8 and ZMM14 during inflorescence development of Zea mays discriminates between the upper and the lower floret of each spikelet. *Development Genes and Evolution* **209**, 411-420.

**Chung Y-Y, Kim S-R, Finkel D, Yanofsky MF, An G**. 1994. Early flowering and reduced apical dominance result from ectopic expression of a rice MADS box gene. *Plant Molecular Biology* **26**, 657-665.

**Chung Y-Y, Kim S-R, Kang H-G, Noh Y-S, Park MC, Finkel D, An G**. 1995. Characterization of two rice MADS box genes homologous to GLOBOSA. *Plant Science* **109**, 45-56.

**Danilevskaya ON, Meng X, Selinger DA, Deschamps S, Hermon P, Vansant G, Gupta R, Ananiev EV, Muszynski MG**. 2008. Involvement of the MADS-box gene ZMM4 in floral induction and inflorescence development in maize. *Plant Physiology* **147**, 2054-2069.

**Davies B, Egea-Cortines M, de Andrade Silva E, Saedler H, Sommer H**. 1996. Multiple interactions amongst floral homeotic MADS box proteins. *The EMBO Journal* **15**, 4330-4343.

**Digel B, Pankin A, von Korff M**. 2015. Global Transcriptome Profiling of Developing Leaf and Shoot Apices Reveals Distinct Genetic and Environmental Control of Floral Transition and Inflorescence Development in Barley. *The Plant Cell* **27**, 2318.

**Dreni L, Jacchia S, Fornara F, Fornari M, Ouwerkerk PB, An G, Colombo L, Kater MM**. 2007. The D-lineage MADS-box gene OsMADS13 controls ovule identity in rice. *The Plant Journal* **52**, 690-699.

**Dreni L, Pilatone A, Yun D, Erreni S, Pajoro A, Caporali E, Zhang D, Kater MM**. 2011. Functional Analysis of All AGAMOUS Subfamily Members in Rice Reveals Their Roles in Reproductive Organ Identity Determination and Meristem Determinacy. *The Plant Cell* **23**, 2850.

**Dreni L, Zhang D**. 2016. Flower development: the evolutionary history and functions of the AGL6 subfamily MADS-box genes. *The Journal of Experimental Botany* **67**, 1625-1638.

**Fornara F, Marziani G, Mizzi L, Kater M, Colombo L**. 2003. MADS-Box Genes Controlling Flower Development in Rice. *Plant Biology* **5**, 16-22.

**Fornara F, Parenicova L, Falasca G, Pelucchi N, Masiero S, Ciannamea S, Lopez-Dee Z, Altamura MM, Colombo L, Kater MM**. 2004. Functional characterization of OsMADS18, a member of the AP1/SQUA subfamily of MADS box genes. *Plant Physiology* **135**, 2207-2219.
**Gómez JF, Wilson ZA**. 2012. Non-destructive staging of barley reproductive development for molecular analysis based upon external morphology. *Journal of Experimental Botany* **63**, 4085-4094.
**Goto K, Meyerowitz EM**. 1994. Function and regulation of the Arabidopsis floral homeotic gene PISTILLATA. *Genes and Development* **8**, 1548-1560.
**Hama E, Takumi S, Ogihara Y, Murai K**. 2004. Pistillody is caused by alterations to the class-B MADS-box gene expression pattern in alloplasmic wheats. *Planta* **218**, 712-720.
**Immink RGH, Tonaco IAN, de Folter S, Shchennikova A, van Dijk ADJ, Busscher-Lange J, Borst JW, Angenent GC**. 2009. SEPALLATA3: the 'glue' for MADS box transcription factor complex formation. *Genome Biology* **10**, R24.
**Jetha K, Theißen G, Melzer R**. 2014. Arabidopsis SEPALLATA proteins differ in cooperative DNA-binding during the formation of floral quartet-like complexes. *Nucleic Acids Research* **42**, 10927-10942.
**Kang HG, Jang S, Chung JE, Cho YG, An G**. 1997. Characterization of two rice MADS box genes that control flowering time. *Molecules and Cells* **7**, 559-566.
**Kinjo H, Shitsukawa N, Takumi S, Murai K**. 2012. Diversification of three APETALA1/FRUITFULL-like genes in wheat. *Molecular Genetics and Genomics* **287**, 283-294.
**Kobayashi K, Maekawa M, Miyao A, Hirochika H, Kyozuka J**. 2010. PANICLE PHYTOMER2 (PAP2), encoding a SEPALLATA subfamily MADS-box protein, positively controls spikelet meristem identity in rice. *Plant and Cell Physiology* **51**, 47-57.
**Kyozuka J, Kobayashi T, Morita M, Shimamoto K**. 2000. Spatially and temporally regulated expression of rice MADS box genes with similarity to Arabidopsis class A, B and C genes. *Plant and Cell Physiology* **41**, 710-718.
**Lai X, Daher H, Galien A, Hugouvieux V, Zubieta C**. 2019. Structural Basis for Plant MADS Transcription Factor Oligomerization. *Computational and Structural Biotechnology Journal* **17**, 946-953.
**Lee S, Kim J, Son J-S, Nam J, Jeong D-H, Lee K, Jang S, Yoo J, Lee J, Lee D-Y, Kang H-G, An G**. 2003. Systematic Reverse Genetic Screening of T-DNA Tagged Genes in Rice for Functional Genomic Analyses: MADS-box Genes as a Test Case. *Plant and Cell Physiology* **44**, 1403-1411.
**Li H, Liang W, Jia R, Yin C, Zong J, Kong H, Zhang D**. 2010. The AGL6-like gene OsMADS6 regulates floral organ and meristem identities in rice. *Cell Research* **20**, 299-313.
**Li N, Liu Y, Zhong M, Li H**. 2014. Thinking out of the box: MADS-box genes and maize spikelet development. *AFRICAN JOURNAL OF BIOTECHNOLOGY* **13**.
**Lid SE, Meeley RB, Min Z, Nichols S, Olsen O-A**. 2004. Knock-out mutants of two members of the AGL2 subfamily of MADS-box genes expressed during maize kernel development. *Plant Science* **167**, 575-582.
**Liu H, Li G, Yang X, Kuijer HNJ, Liang W, Zhang D**. 2019. Transcriptome profiling reveals phase-specific gene expression in the developing barley inflorescence. *The Crop Journal*.

**Lopez-Dee ZP, Wittich P, Enrico Pe M, Rigola D, Del Buono I, Gorla MS, Kater MM, Colombo L**. 1999. OsMADS13, a novel rice MADS-box gene expressed during ovule development. *Developmental Genetics* **25**, 237-244.
**Masiero S, Imbriano C, Ravasio F, Favaro R, Pelucchi N, Gorla MS, Mantovani R, Colombo L, Kater MM**. 2002. Ternary complex formation between MADS-box transcription factors and the histone fold protein NF-YB. *The Journal of Biological Chemistry* **277**, 26429-26435.
**Melzer R, Verelst W, Theißen G**. 2008. The class E floral homeotic protein SEPALLATA3 is sufficient to loop DNA in 'floral quartet'-like complexes in vitro. *Nucleic Acids Research* **37**, 144-157.
**Mena M, Ambrose BA, Meeley RB, Briggs SP, Yanofsky MF, Schmidt RJ**. 1996. Diversification of C-Function Activity in Maize Flower Development. *Science* **274**, 1537.
**Mena M, Mandel MA, Lerner DR, Yanofsky MF, Schmidt RJ**. 1995. A characterization of the MADS-box gene family in maize. *The Plant Journal* **8**, 845-854.
**Mizzotti C, Mendes MA, Caporali E, Schnittger A, Kater MM, Battaglia R, Colombo L**. 2012. The MADS box genes SEEDSTICK and ARABIDOPSIS Bsister play a maternal role in fertilization and seed development. *The Plant Journal* **70**, 409-420.
**Moon Y-H, Jung J-Y, Kang H-G, An G**. 1999. Identification of a rice APETALA3 homologue by yeast two-hybrid screening. *Plant Molecular Biology* **40**, 167-177.
**Munster T, Wingen LU, Faigl W, Werth S, Saedler H, Theissen G**. 2001. Characterization of three GLOBOSA-like MADS-box genes from maize: evidence for ancient paralogy in one class of floral homeotic B-function genes of grasses. *Gene* **262**, 1-13.
**Nagasawa N, Miyoshi M, Sano Y, Satoh H, Hirano H, Sakai H, Nagato Y**. 2003. SUPERWOMAN1 and DROOPING LEAF genes control floral organ identity in rice. *Development* **130**, 705.
**Paolacci AR, Tanzarella OA, Porceddu E, Varotto S, Ciaffi M**. 2007. Molecular and phylogenetic analysis of MADS-box genes of MIKC type and chromosome location of SEP-like genes in wheat (Triticum aestivum L.). *Molecular Genetics and Genomics* **278**, 689-708.
**Pelucchi N, Fornara F, Favalli C, Masiero S, Lago C, Pè E, Colombo L, Kater M**. 2002. Comparative analysis of rice MADS-box genes expressed during flower development. *Sexual Plant Reproduction* **15**, 113-122.
**Prasad K, Sriram P, Kumar CS, Kushalappa K, Vijayraghavan U**. 2001. Ectopic expression of rice OsMADS1 reveals a role in specifying the lemma and palea, grass floral organs analogous to sepals. *Development Genes and Evolution* **211**, 281-290.
**Puig J, Meynard D, Khong GN, Pauluzzi G, Guiderdoni E, Gantet P**. 2013. Analysis of the expression of the AGL17-like clade of MADS-box transcription factors in rice. *Gene Expression Patterns* **13**, 160-170.
**Reinheimer R, Kellogg EA**. 2009. Evolution of AGL6-like MADS box genes in grasses (Poaceae): ovule expression is ancient and palea expression is new. *The Plant Cell* **21**, 2591-2605.
**Rümpler F, Theißen G, Melzer R**. 2018. A conserved leucine zipper-like motif accounts for strong tetramerization capabilities of SEPALLATA-like MADS-domain transcription factors. *Journal of Experimental Botany* **69**, 1943-1954.

**Saeed AI, Sharov V Fau - White J, White J Fau - Li J, Li J Fau - Liang W, Liang W Fau - Bhagabati N, Bhagabati N Fau - Braisted J, Braisted J Fau - Klapa M, Klapa M Fau - Currier T, Currier T Fau - Thiagarajan M, Thiagarajan M Fau - Sturn A, Sturn A Fau - Snuffin M, Snuffin M Fau - Rezantsev A, Rezantsev A Fau - Popov D, Popov D Fau - Ryltsov A, Ryltsov A Fau - Kostukovich E, Kostukovich E Fau - Borisovsky I, Borisovsky I Fau - Liu Z, Liu Z Fau - Vinsavich A, Vinsavich A Fau - Trush V, Trush V Fau - Quackenbush J, Quackenbush J**. TM4: a free, open-source system for microarray data management and analysis.

**Schilling S, Kennedy A, Pan S, Jermiin LS, Melzer R**. 2019. Genome-wide analysis of MIKC-type MADS-box genes in wheat: pervasive duplications, functional conservation and putative neofunctionalization. *New Phytologist*.

**Schmidt RJ, Veit B, Mandel MA, Mena M, Hake S, Yanofsky MF**. 1993. Identification and molecular characterization of ZAG1, the maize homolog of the Arabidopsis floral homeotic gene AGAMOUS. *The Plant Cell* **5**, 729-737.

**Schmitz J, Franzen R, Ngyuen TH, Garcia-Maroto F, Pozzi C, Salamini F, Rohde W**. 2000. Cloning, mapping and expression analysis of barley MADS-box genes. *Plant Molecular Biology* **42**, 899-913.

**Shitsukawa N, Tahira C, Kassai K, Hirabayashi C, Shimizu T, Takumi S, Mochida K, Kawaura K, Ogihara Y, Murai K**. 2007. Genetic and epigenetic alteration among three homoeologous genes of a class E MADS box gene in hexaploid wheat. *The Plant Cell* **19**, 1723-1737.

**Theissen G, Saedler H**. 2001. Plant biology. Floral quartets. *Nature* **409**, 469-471.

**Thompson BE, Bartling L, Whipple C, Hall DH, Sakai H, Schmidt R, Hake S**. 2009. bearded-ear Encodes a MADS Box Transcription Factor Critical for Maize Floral Development. *The Plant Cell* **21**, 2578.

**Tilly JJ, Allen DW, Jack T**. 1998. The CArG boxes in the promoter of the Arabidopsis floral organ identity gene APETALA3 mediate diverse regulatory effects. *Development* **125**, 1647.

**Waddington SR, Cartwright PM, Wall PC**. 1983. A Quantitative Scale of Spike Initial and Pistil Development in Barley and Wheat. *Annals of Botany* **51**, 119-130.

**Wei B, Liu D, Guo J, Leseberg CH, Zhang X, Mao L**. 2013. Functional divergence of two duplicated D-lineage MADS-box genes BdMADS2 and BdMADS4 from Brachypodium distachyon. *Journal of Plant Physiology* **170**, 424-431.

**Wei B, Zhang R-Z, Guo J-J, Liu D-M, Li A-L, Fan R-C, Mao L, Zhang X-Q**. 2014. Genome-Wide Analysis of the MADS-Box Gene Family in Brachypodium distachyon. *PLoS One* **9**, e84781.

**Whipple CJ, Ciceri P, Padilla CM, Ambrose BA, Bandong SL, Schmidt RJ**. 2004. Conservation of B-class floral homeotic gene function between maize and Arabidopsis. *Development* **131**, 6083.

**Winter K-U, Weiser C, Kaufmann K, Bohne A, Kirchner C, Kanno A, Saedler H, Theißen G**. 2002. Evolution of Class B Floral Homeotic Proteins: Obligate Heterodimerization Originated from Homodimerization. *Molecular Biology and Evolution* **19**, 587-596.

**Yamada K, Saraike T, Shitsukawa N, Hirabayashi C, Takumi S, Murai K**. 2009. Class D and B(sister) MADS-box genes are associated with ectopic ovule

formation in the pistil-like stamens of alloplasmic wheat (Triticum aestivum L.). *Plant Molecular Biology* **71**, 1-14.
**Yamaguchi T, Lee DY, Miyao A, Hirochika H, An G, Hirano H-Y**. 2006. Functional Diversification of the Two C-Class MADS Box Genes OSMADS3 and OSMADS58 in Oryza sativa. *The Plant Cell* **18**, 15.
**Yang X, Wu F, Lin X, Du X, Chong K, Gramzow L, Schilling S, Becker A, Theissen G, Meng Z**. 2012. Live and let die - the B(sister) MADS-box gene OsMADS29 controls the degeneration of cells in maternal tissues during seed development of rice (Oryza sativa). *PLoS One* **7**, e51435.
**Yang Y, Fanning L, Jack T**. 2003. The K domain mediates heterodimerization of the Arabidopsis floral organ identity proteins, APETALA3 and PISTILLATA. *The Plant Journal* **33**, 47-59.
**Yang Y, Jack T**. 2004. Defining subdomains of the K domain important for protein–protein interactions of plant MADS proteins. *Plant Molecular Biology* **55**, 45-59.
**Yao S-G, Ohmori S, Kimizu M, Yoshida H**. 2008. Unequal Genetic Redundancy of Rice PISTILLATA Orthologs, OsMADS2 and OsMADS4, in Lodicule and Stamen Development. *Plant and Cell Physiology* **49**, 853-857.
**Zadoks JC, Chang TT, Konzak CF**. 1974. A decimal code for the growth stages of cereals. *Weed Research* **14**, 415-421.
**Zhao XY, Cheng ZJ, Zhang XS**. 2006. Overexpression of TaMADS1, a SEPALLATA-like gene in wheat, causes early flowering and the abnormal development of floral organs in Arabidopsis. *Planta* **223**, 698-707.

# Chapter 3: Functional analysis of the DEF/GLO-like MADS-box genes in barley (*Hordeum vulgare*)

Cindy Callens[1,2], Matthew R. Tucker[2], Dabing Zhang[2,3] and Zoe A. Wilson[1]

[1] School of Biosciences, University of Nottingham, Sutton Bonington Campus, Loughborough, Leicestershire LE12 5RD, UK
[2] School of Agriculture, Food and Wine, University of Adelaide, Waite Campus, Urrbrae, SA, Australia
[3] School of Life Sciences and Biotechnology, Shanghai Jiao Tong University, Shanghai 200240, China

# Introduction to Chapter 3: Functional analysis of the DEF/GLO-like MADS-box genes in barley (*Hordeum vulgare*)

To better understand the function of the DEF/GLO-like MADS-box genes two approaches were considered: the Chimeric Repressor Silencing technology (CRES-T) and the CRISPR/Cas9 approach. The CRES-T system is presented in this chapter and uses an EAR-motif repression domain, also known as SRDX, attached to the gene of interest to transform the transcription factor into a repressor (Fig 3). It is a relatively easy system and can show phenotypes in the first generation of transformed plants due to the overexpression of the constructs. However, varying expression of the constructs contributes to a wide variety of phenotypes with low expression of the constructs showing no or a minor phenotype. MADS-box genes are also known to work in complexes and their C-domain can mediate both activation and repression of target genes dependent on the complexes formed. These factors should all be taken into account when making conclusions based on the observed phenotypes.

Single dominant repression constructs for the CRES-T system were made for all the B-class genes (*HvBM2*, *HvBM4* and *HvBM16*) as well as the $B_{sister}$-like genes (*HvBM29*, *HvBM30*, *HvBM31*). Triple constructs for the CRISPR/Cas9 approach were made with three different targets for all three B-class genes. Due to a lack of time it was decided to only generate transgenic lines with the dominant repression constructs for the B-class genes. Transformations with the CRISPR/Cas9 constructs did not lead to any transgenic plants and lack of time meant a second round of barley embryo transformations was not possible.

Barley embryos were inoculated with *Agrobacterium tumefaciens* containing either one of the dominant repression constructs, a combination of two of the constructs, or all three of the constructs. Genotyping revealed that all transformations with a single constructs and some with a combination of two constructs were successful. No transgenic plants containing all three constructs were identified.
As control, florets from wild type *Hordeum vulgare* var. *Golden Promise* were grown from seeds because tissue culture of wild type plants was not successful.

Control florets were always at the same stage as the florets examined from the CRES-T transgenic plants.

The CRES-T system resulted in a variety of phenotypes due to different levels op expression of the constructs. The resulting phenotypes were largely as expected with some additional, new phenotypes. More generations of the transgenic plants are needed to confirm the results and crosses between the plants will provide transgenic plants with all three dominant repression constructs (*HvBM2*, *HvBM4* and *HvBM16*). Other methods like CRISPR/Cas9 need to be considered to have stable knock-out mutants of the three genes separately and in combination.

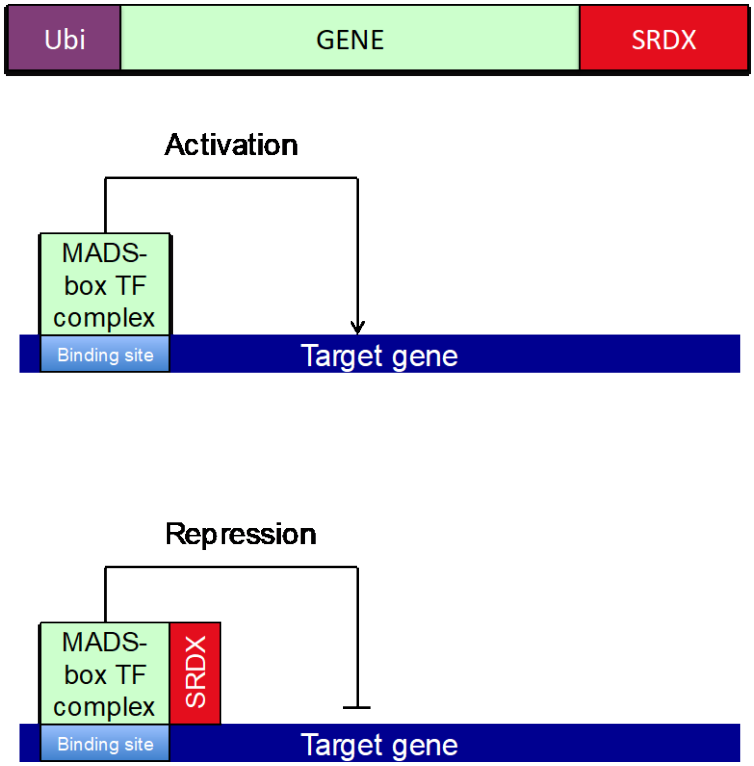



**Figure 3 Schematic representation of the SRDX mode of action.** An EAR-motif repression domain is attached to the gene of interest and placed under a ubiquitin promotor. MADS-box transcription factors with an added EAR-motif, or SRDX, repression domain will repress target genes instead of activating them.

## 3.1 Introduction

In *Arabidopsis*, it has been shown that the B-class genes determine the identity of petals and stamens (Fornara *et al.*, 2003). The B-class genes are thought to have split from the $B_{sister}$-like genes following a gene duplication event after the diversifications of ferns, but before the divergence between gymnosperms and angiosperms (Becker *et al.*, 2002; Gioppato and Dornelas, 2019; Goremykin *et al.*, 1997; Münster *et al.*, 1997; Theissen *et al.*, 2000). The B-class clade has two lineages: the DEF-like lineage (AP3-like proteins) and the GLO-like lineage (PI-like proteins), that are the result of another gene duplication event close to the base of the crown group angiosperms between 260 and 290 MYA (Becker and Theissen, 2003; Hernández-Hernández *et al.*, 2006; Kim *et al.*, 2004; Winter *et al.*, 2002a; Zahn *et al.*, 2005). The B-class genes have been hypothesised to be involved in the morphological diversification of angiosperm flower morphologies, more specifically the perianth (Gioppato and Dornelas, 2019; Irish, 2017; Theißen *et al.*, 2016).

In Arabidopsis, mutants of the B-class genes *PI* and *AP3*, have sepals in the second whorl and carpeloid organs or carpels instead of stamens (Bowman *et al.*, 1989, 1991; Hill and Lord, 1989; Jack *et al.*, 1992). Ectopic expression of AP3 leads to partial conversion of carpels to stamens and expression of PI in the fourth whorl (Jack *et al.*, 1994). Ectopic expression of both *AP3* and *PI* results in flowers with petals in whorl one and two, and stamens in whorls three and four (Krizek and Meyerowitz, 1996). Depending on the specific whorl, *AP3* has also been shown to differentially regulate the production of intercellular signals (Jenik and Irish, 2001). The loss-of-function mutants of the AP3-like *OsMADS16* in rice, known as *spw1 (superwoman1)*, and *SILKY1* in maize show the homeotic transformation of stamens into carpels and lodicules into palea-like organs (Ambrose *et al.*, 2000; Nagasawa *et al.*, 2003). These results suggest that *OsMADS16* and *SILKY1* are well conserved between rice, maize and *Arabidopsis* (Yamaguchi and Hirano, 2006). RNAi knock-down lines of the PI-like *OsMADS2* in rice showed continued growth of the distal region of the lodicules forming an elongated bract-like structure, but no apparent changes in stamen shape (Yadav *et al.*, 2007; Yao *et al.*, 2008; Yoshida *et al.*, 2007). RNAi lines of *OsMADS4* showed no phenotypic alterations (Yao *et al.*, 2008; Yoshida *et al.*, 2007). In the double knock-down mutants of *OsMADS2* and

*OsMADS4* the stamens were transformed into carpel-like organs and the lodicules showed a complete homeotic conversion to bract-like organs (Yao *et al.*, 2008; Yoshida *et al.*, 2007). The alloplasmic wheat with a deficiency of *WPI1*, the *OsMADS4* orthologue, showed pistillody, the change of stamens into pistil-like structures (Hama *et al.*, 2004).

To date, a functional analysis of the B-class genes in barley has not been carried out. In this chapter we use the chimeric repressor silencing technology (CRES-T) system to investigate the function of the PI-like B-class genes *HvBM2* and *HvBM4*, and the AP3-like B-class gene *HvBM16* by attaching the plant-specific EAR (ERF-associated amphiphilic repression) motif repression domain (SRDX), which lends repressor activity to transcription factors (Ohta *et al.*, 2001). The EAR motif was initially identified in class II ERFs and TFIIIA-type zinc finger proteins. In these proteins it has a consensus sequence of (L/F)DLN(L/F)xP (Ohta *et al.*, 2001). Phylogenetic analysis showed that the EAR motif is conserved in a lot of species and is in fact the predominant form of transcriptional repression motif in plants identified to date (Kagale and Rozwadowski, 2011). The consensus sequence of the EAR motif across species is either LxLxL or DLNxxP (Kagale and Rozwadowski, 2011). The EAR motif facilitates epigenetic regulation of gene expression by recruiting chromatin remodelling factors and co-repressors (Kagale and Rozwadowski, 2011).
In previous studies, chimeric repressor with an SRDX domain was shown to suppress expression of target genes even when there was a redundant transcription factor present (Hiratsu *et al.*, 2003). The phenotypes that were obtained using the CRES-T system were similar to those of a loss-of-function allele (Hiratsu *et al.*, 2003).

## 3.2 Materials and methods

### *3.2.1 Design of SRDX pBract214 dominant repression constructs*

SRDX dominant repression lines were created for the B-class (*HvBM2*, *HvBM4* and *HvBM16)* in barley (*Hordeum vulgare cv. Golden promise*). Accurate sequences were identified based on the extensive phylogenetic analysis shown in Figure 1.4. Identifiers for these sequences can be found in Table 2. Primers were designed to amplify the complete CDS sequence of the genes. An additional reverse primer with

the SRDX sequence (5'-AGCGAAACCCAAACGGAGTTCTAGATCCAGATCCAG-3') was designed to add the SRDX sequence to the CDS of the gene (Table 4).

| Gene | Forward primer | Reverse primers without stopcodon | Reverse primers with SRDX |
|---|---|---|---|
| *HvBM2* | ATG GGG CGC GGG AAG ATC | GGT GTC CTC CTG CAG AT | CTA –SRDX- GGT GTC CTC CTG CAG AT |
| *HvBM4* | ATG GGG CGC GGC AAG AT | CTT GTC TTC CTG CAA GT | CTA –SRDX- CTT GTC TTC CTG CAA GT |
| *HvBM16* | ATG GGG CGG GGG AAG AT | TCC GAG GCG CAG GTG | TTA –SRDX- TCC GAG GCG CAG GTG |

**Table 3.1 Primers used for the design of *HvBM2*, *HvBM4* and *HvBM16* SRDX dominant repression constructs.**

The complete CDS sequence of both genes was amplified from floret cDNA of relevant growth stages. Using a nested PCR, the SRDX sequence with a stop codon was attached to the 3' end of the CDS sequence without stop codon, and loaded on a 0.8% (w/v) agarose gel to verify the size. The DNA was then extracted from the gel using the Wizard® SV Gel and PCR Clean Up System (Promega, UK). The construct was introduced into the pCR8GW TOPO TA vector and transformed in Dh5α *E.coli* competent cells. Positive colonies were identified by sequencing. Using Gateway cloning the constructs were then introduced in the pBract214 vector (John Innes Centre, Norwich, UK), which contains a CaMV pUBI promoter. Positive constructs were transformed into AGL1 *Agrobacterium tumefaciens* together with the pSOUP vector.

*3.2.2 Agrobacterium-mediated barley transformation*

Agrobacterium-mediated transformation was carried out following the protocol as described by Harwood *et al.* (2009). Seeds from *Hordeum vulgare cv. Golden Promise* with immature embryos of 1.5-2mm in diameter were removed from the spike and sterilised by washing with 70% (v/v) ethanol for 30 seconds followed by three washes in sterile distilled water. The seeds were then further sterilised in a solution of sodium hypochlorite diluted 50:50 with water for four minutes. Lastly, the seeds were washed four times with sterile distilled water.

The immature embryos were removed from the sterilised seed in a laminar flow hood under sterile conditions. The embryos were then plated scutellem side up on callus induction medium and stored overnight at 23-24°C in the dark.

*Agrobacterium* cultures were prepared by adding a standard inoculum to 10mL of LB medium without antibiotics. This was incubated on a shaker at 180rpm at 28°C overnight. The culture was then used to inoculate the embryos by dropping a small amount of *Agrobacterium* onto each embryo. The embryos were gently removed from the plates and transferred to a fresh callus induction plate, scutellum side down. Plates were sealed with Micropore$^{TM}$ surgical tape and incubated at 23-24°C for three days.

The embryos were then transferred to fresh callus induction plates containing 50µg/ml (w/v) hygromycin (Roche) as the selective agent and 160 µg/ml (w/v) timentin (Duchefa) to remove *Agrobacterium* from the cultures. The plates were sealed with Micropore$^{TM}$ surgical tape and incubated at 23-24°C in the dark for two weeks. This selection step was repeated two more times. After six weeks of selection, the embryo-derived callus was transferred to transition medium containing hygromycin and timentin and incubated at 24°C at low light (75 $\mu mol.m^{-2}.s^{-1}$) for two weeks. The callus was then transferred to regeneration medium containing hygromycin and timentin. Once shoots were 2-3 cm in length and roots had formed, the plantlets were removed from the plates and transferred to glass culture tubes containing 12mL of callus induction medium containing hygromycin and timentin. Once rooted plants reached the top of the tubes, they were transferred to John Innes N°3 soil.

*3.2.3 Plant materials and growth conditions*

Plants were grown in controlled environment chamber with a constant temperature of 16°C and 16 hour photoperiod. Leaf samples were collected and flash frozen for genotyping. Florets were collected at the LFE3 stage before full heading and flash frozen for RNA extraction or fixed in 4% paraformaldehyde (w/v) in phosphate-buffered saline (PBS) with 0.1% (v/v) Triton X-100 and 0.1% (v/v) Tween 20 for embedding.

*3.2.4 Genotyping*

gDNA was extracted from leaf tissue of all lines with the Isolate II Genomic DNA Kit (Bioline, UK). Presence of the SRDX constructs was verified by RT-PCR with specific primers for the gene, the SRDX construct and the vector (Table 5).

| | Forward primer | Reverse primer | Reverse pBract214 |
|---|---|---|---|
| *HvBM2* | GAGAACAAGTTGCTGGCCTTT | AGCGAAACCCAAACGGAGTTC | CGCGCAATTAACCCTCACTA |
| *HvBM4* | GATGCACAGGAGGAATGAGA | AGCGAAACCCAAACGGAGTTC | CGCGCAATTAACCCTCACTA |
| *HvBM16* | ACC CGG CGT ACG GGT TC | AGCGAAACCCAAACGGAGTTC | CGCGCAATTAACCCTCACTA |

**Table 3.2 Primers designed for genotyping of the *HvBM2*, *HvBM4* and *HvBM16* SRDX pBract214 constructs in transformed barley plants.**

*3.2.5 Phenotyping*

Three florets were collected from each line that was positively genotyped for the SRDX constructs and from control plants at stage LFE3-LFE4 and dissected. Images were taken using a Zeiss Stemi SV6 microscope and a Axiocam ERc Rev 2.0 camera.

*3.2.6 Pollen viability assay with Fluorescein Diacetate (FDA) stain*

Fluorescein diacetate (FDA) is an apolar and non-fluorescent molecule that can penetrate cells. Within the pollen grain it can be hydrolysed by pollen esterases which yields fluorescein. Fluorescein appears fluorescent in blue light. When the cell membrane is intact and the pollen is viable, the fluorescein will accumulate within the pollen grain (Li, 2011).

1µl of FDA stock solution (2mg FDA in 1ml acetone) was added to 1ml of BK buffer S15 MOPS (7.5g sucrose, 5ml 100mM MOPS pH7.5, 6.35µl 1M $Ca(NO_3)_2$, 4.05µl 1M $MgSO_4$, 5 µl 1M $KNO_3$). A few drops of the FDA-buffer mixture were added to a slide with pollen grains and pollen viability was observed with the Leica DM5000B microscope in blue light (wavelength = 495nm). Images were taken with the Leica DFC420 C camera.

**3.2.7 Embedding and sectioning**

Florets fixed in 4% (w/v) paraformaldehyde in phosphate-buffered saline (PBS) with 0.1% (v/v) Triton X-100 and 0.1% (v/v) Tween 20 were dehydrated with an ethanol series (30%, 50%, 70% and 100% (v/v)) and propylene oxide (TAAB, 50% and

100% (v/v)). The florets were then pre-infiltrated with a 1:1 mixture of 100% propylene oxide and Spurr resin (TAAB) and infiltrated overnight at 4°C with pure Spurr resin and embedded in moulds at 70-75°C.

Floret were sectioned using the Microtome and sections (5 µm) were mounted on slides at 42°C and stained with x% (w/v) toluidine blue in x (w/v).

### *3.2.8 Quantitative reverse transcription (qRT) PCR*

Expression levels of the SRDX pBract214 construct were determined by real-time quantitative reverse transcription PCR using specific primers (Table 5).

RNA was extracted with the RNeasy Plant Mini Kit (QIAGEN, UK). cDNA was synthesised from total RNA using SuperScript$^{TM}$ IV reverse transcriptase (ThermoFisher Scientific, UK) and checked for quality through RT-PCR of the barley housekeeping gene *HvTUB*. Real-time quantitative PCR was performed on three technical replicates and analysed using the LightCycler® 480 (Roche Life Science, UK). Expression values relative to the barley *α-Tubulin* gene (*HvTUB*) were calculated.

### *3.2.9 Evaluation of sterility in barley transformants expressing pUBI:HvBM2-SRDX*

All tillers from four different lines expression the *pUBI:HvBM2-SRDX* construct were harvested (Lines 2, 3, 7 and 8). For every spike the number of total spikelets and the number of spikelets that developed into seeds were counted. The percentage of "sterility per tiller" was calculated by dividing the number of seeds by the total number of spikelets and multiplying by 100.

## 3.3 Results

### *3.3.1 Barley transformants expressing pUBI:HvBM2-SRDX*

A total of 40 embryos were extracted from immature *Golden Promise* seeds and inoculated with the Agrobacterium inoculum containing the pBract214 *pUBI:HvBM2-SRDX* construct and the helper plasmid pSOUP. After tissue culture nine lines were transferred to pots. Genotyping confirmed that all lines contained the *pUBI:HvBM2-SRDX* construct.

Three lines showed varying degrees of changes in stamen and lodicule development. Stamens showed partial conversion to carpel-like structures, exhibiting stigma-like trichomes (Figure 3.1). Lodicules were elongated and showed partial conversion to a

palea-like structure. The anthers of the lines showing a phenotype contain no or very little viable pollen and showed therefore extreme sterility (Figure 3.2).

Lines exhibiting a fertility phenotype (Lines 2, 3 and 8) had little to no seeds compared to transformed lines that didn't exhibit a phenotype (Line 7) (Figure 3.3). Florets that did get fertilised in lines 2, 3 and 8 had aborted seeds, which were counted as sterile florets.

### *3.3.2 Barley transformants expressing pUBI:HvBM4-SRDX*

A total of 40 embryos were extracted from immature *Golden Promise* seeds and inoculated with the Agrobacterium inoculum containing the pBract214 *pUBI:HvBM4-SRDX* construct and the helper plasmid pSOUP. After tissue culture seven lines were transferred to pots. Genotyping confirmed that all lines examined contained the *pUBI:HvBM4-SRDX* construct.

One line showed a conversion of stamens to carpeloid structures and lodicules to small bract-like structures without trichomes (Figure 3.4). The stamen did not contain any pollen. The carpel was small and underdeveloped showing only limited stigmatic branches (Figure 3.4).




**Figure 3.1 Phenotype of carpel, stamens and lodicules in barley transformants expressing *pUBI:HvBM2-SRDX* (Line 2) compared to control florets.**
Carpels, stamens and lodicules dissected from florets from barley transformants expressing *pUBI:HvBM2-SRDX* and control florets. In florets expressing the *pUBI:HvBM2-SRDX* construct stamens showed partial conversion to carpel-like structures, exhibiting stigma-like trichomes. Lodicules were elongated and showed partial conversion to a palea-like structure.

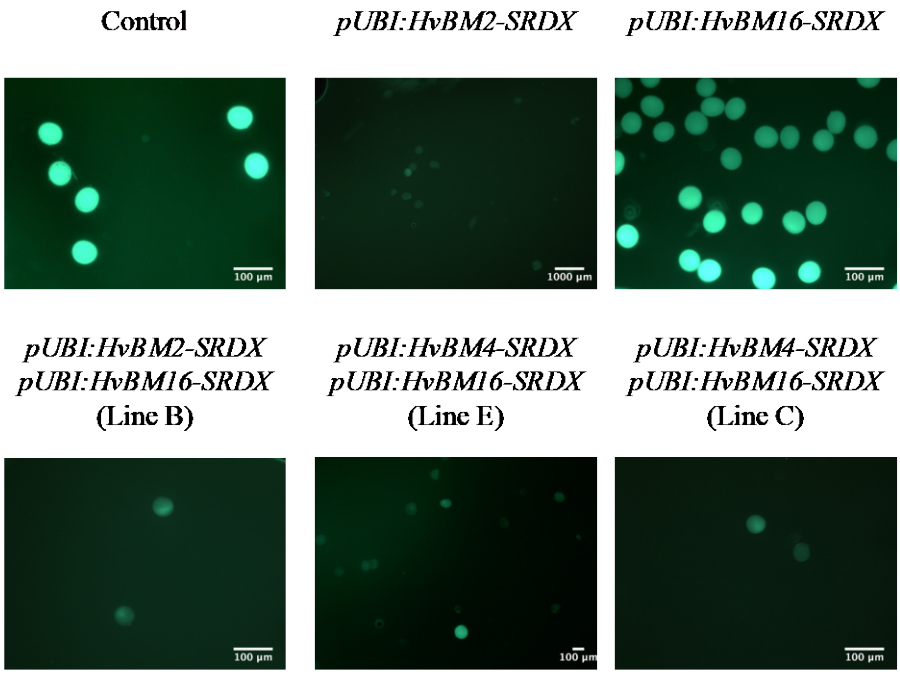



**Figure 3.2 Pollen viability of barley transformants expression *pUBI:HvBM2-SRDX*, *pUBI:HvBM4-SRDX* or *pUBI:HvBM16-SRDX* compared to control**
Pollen viability in mature anthers of barley transformants was visualised using Fluorescein Diacetate (FDA) stain. Viable pollen accumulates fluorescein and will show fluorescence. Non-viable pollen has no fluorescence. Low numbers of pollen reflect the lack of pollen in the mature anthers. Pollen viability was observed in blue light (wavelength = 495nm).

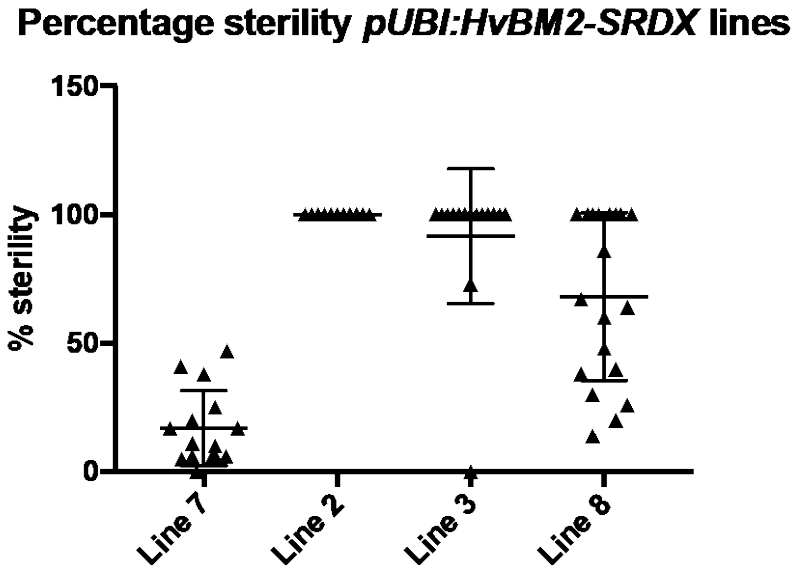



**Figure 3.3 Sterility in barley transformants expressing *pUBI:HvBM2-SRDX***
Percentage of sterility was calculated for all tillers for four barley transformant lines expressing the *HvBM2-SRDX* construct. Line 7 showed no phenotype, while line 2, line 3 and line 8 showed varying degrees of phenotype. Kruskal-Wallis test was used to determine significance of difference between the lines.

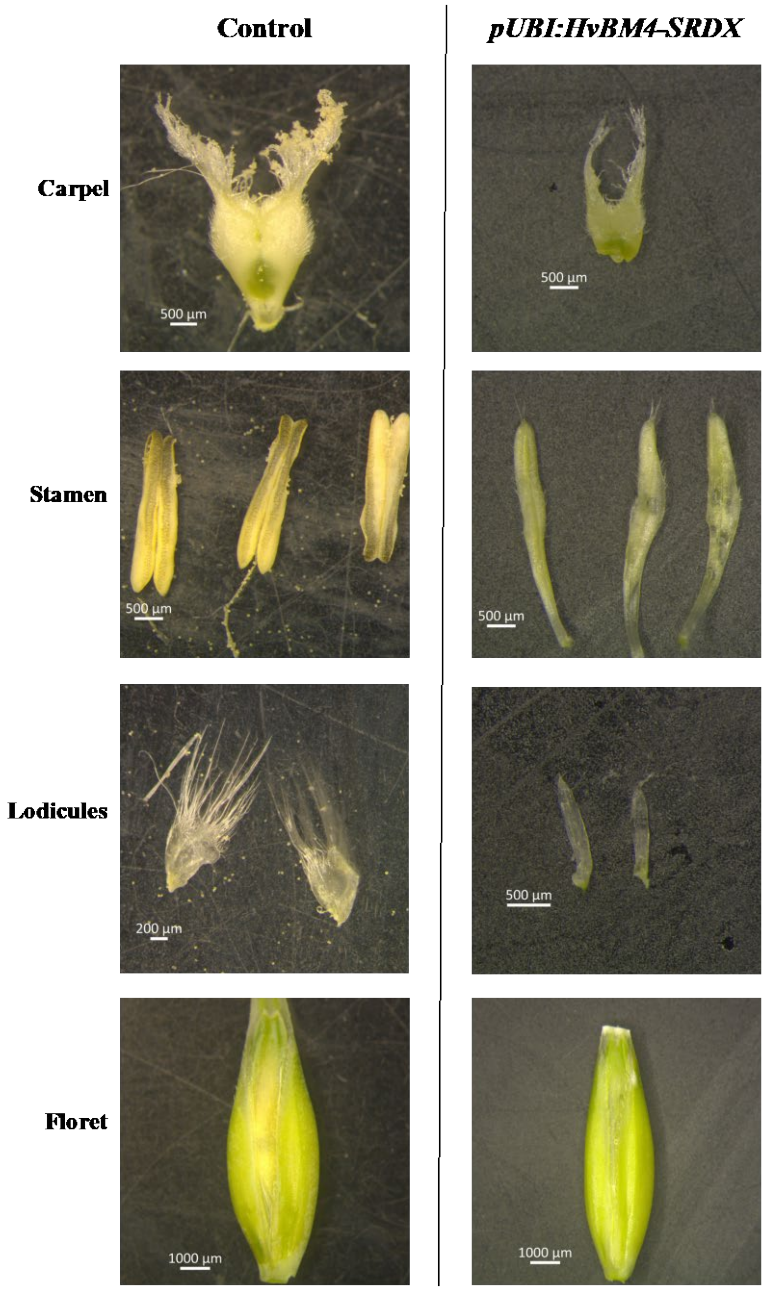



**Figure 3.4 Phenotype of carpel, stamens and lodicules in barley transformants expressing *pUBI:HvBM4-SRDX* compared to control florets.**
Carpels, stamens and lodicules dissected from florets from barley transformants expressing *pUBI:HvBM4-SRDX* and control florets. The most severe phenotype was found in these florets. There was a conversion of stamens to carpeloid structures and lodicules to small bract-like structures without trichomes. The carpel was small and underdeveloped showing only limited stigmatic branches.

### *3.3.3 Barley transformants expressing pUBI:HvBM16-SRDX*

A total of 40 embryos were extracted from immature *Golden Promise* seeds and inoculated with the Agrobacterium inoculum containing the pBract214 *pUBI:HvBM16-SRDX* construct and the helper plasmid pSOUP. After tissue culture four lines were transferred to pots, but only three lines survived. No phenotype was discovered in any of the three lines expressing the *pUBI:HvBM16-SRDX* pBract214 construct (Figure 3.5). All the pollen was viable and fully developed (Figure 3.2).

### *3.3.4 Embryos transformed with pUBI:HvBM2-SRDX, pUBI:HvBM4-SRDX and pUBI:HvBM16-SRDX*

A total of 50 embryos were extracted from immature *Golden Promise* seeds and inoculated with the Agrobacterium inoculum containing the pBract214 *pUBI:HvBM2-SRDX, pUBI:HvBM4-SRDX* and *pUBI:HvBM16-SRDX* constructs and the helper plasmid pSOUP. After tissue culture twenty lines were transferred to pots. All twenty lines contained a combination of two B-class MADS-box SRDX constructs, but never all three constructs. Six lines containing a combination of either *pUBI:HvBM2-SRDX* or *pUBI:HvBM4-SRDX* with *pUBI:HvBM16-SRDX* showed a phenotype.

#### *3.3.4.1 Barley transformants expressing pUBI:HvBM2-SRDX and pUBI:HvBM16-SRDX*

Two lines were confirmed to express the *pUBI:HvBM2-SRDX* and the *pUBI:HvBM16-SRDX* pBract214 construct. Roughly half of all florets on each spike had an emaciated carpel, but normal stamens and lodicules (Figure 3.6). Although the stamen looked to be well developed, there was little viable pollen inside (Figure 3.2). The *pUBI:HvBM2-SRDX* construct was expressed highly in one of these lines compared to the other lines expressing the construct (Figure 20, Line B).

#### *3.3.4.2 Barley transformants expressing pUBI:HvBM4-SRDX and pUBI:HvBM16-SRDX*

Four lines expressing both the *pUBI:HvBM4-SRDX* and the *pUBI:HvBM16-SRDX* pBract214 construct showed a phenotype. The phenotypes of three of the lines was significantly different compared to the fourth line.

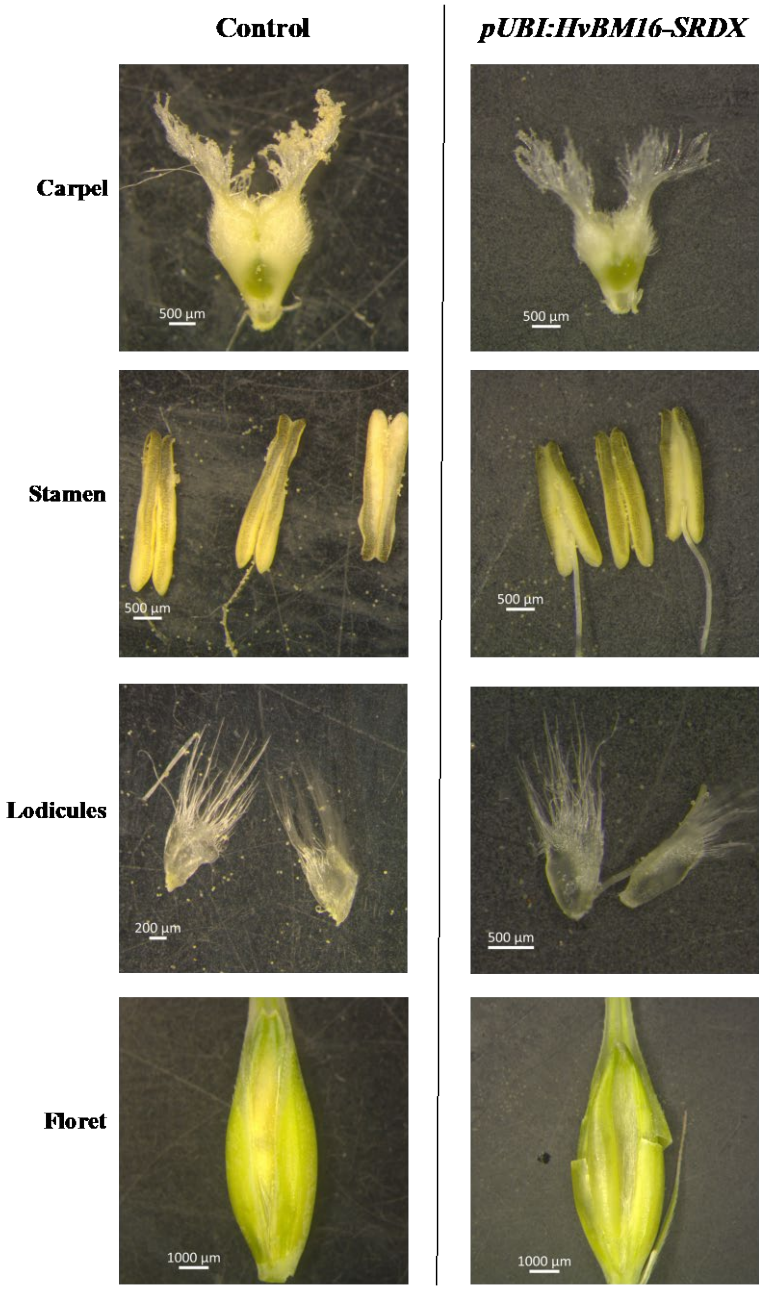



**Figure 3.5 Phenotype of carpel, stamens and lodicules in barley transformants *pUBI:HvBM16-SRDX* compared to control florets.**
Carpels, stamens and lodicules dissected from florets from barley transformants expressing *pUBI:HvBM16-SRDX* and control florets. No phenotypes were found in florets expressing the *pUBI:HvBM16-SRDX* construct.




**Figure 3.6 Phenotype of carpel, stamens and lodicules in barley transformants expressing a combination of *pUBI:HvBM2-SRDX* and *pUBI:HvBM16-SRDX* (Line C) constructs compared to control florets.**
Carpels, stamens and lodicules dissected from florets from barley transformants expressing a combination of *pUBI:HvBM2-SRDX* and *pUBI:HvBM16-SRDX* constructs and control florets. Carpels in line B were emaciated, though all other floral organs seemed to have developed normally.

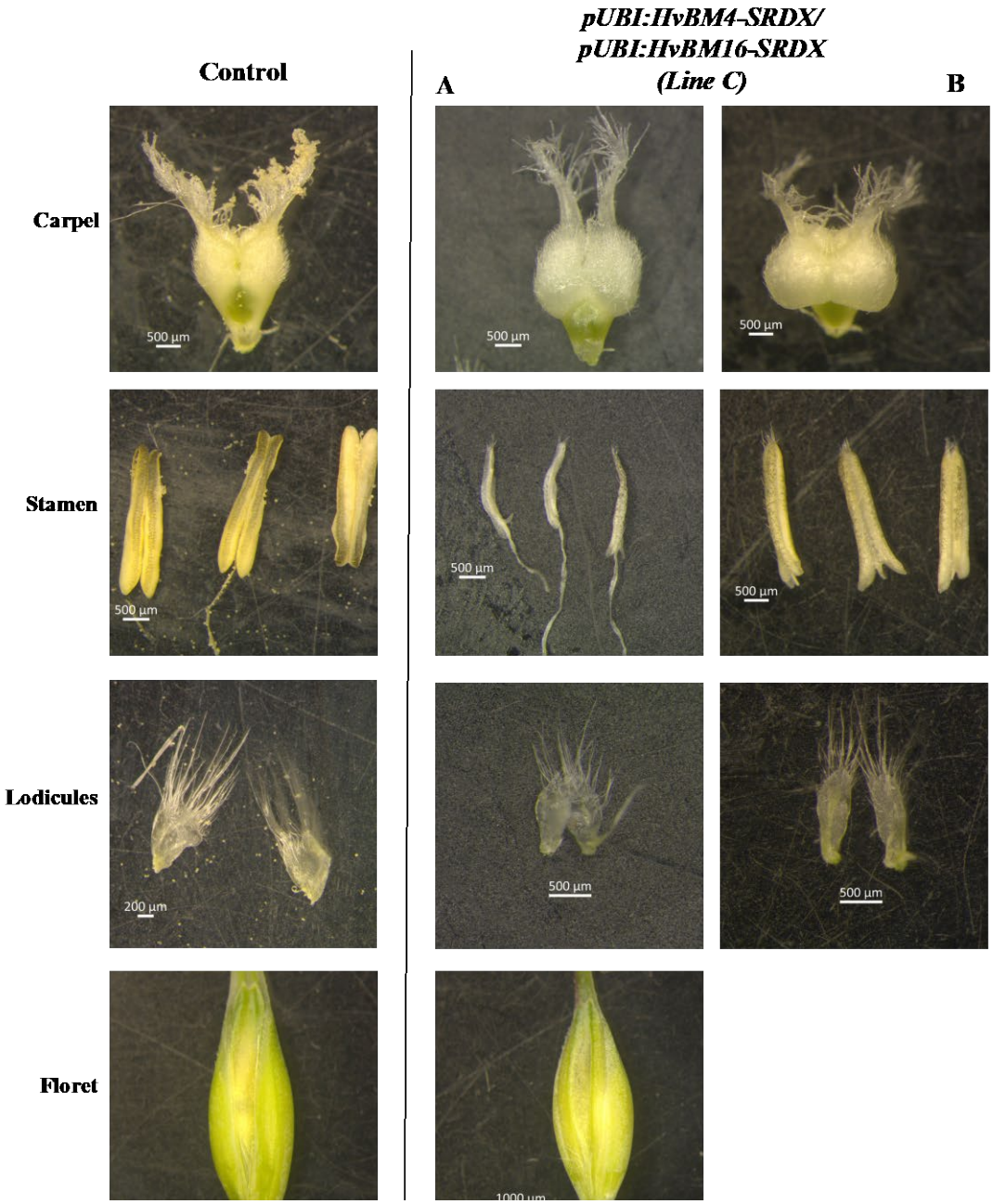



**Figure 3.7 Phenotype of carpel, stamens and lodicules in barley transformants expressing a combination of *pUBI:HvBM4-SRDX* and *pUBI:HvBM16-SRDX* (Line C) constructs compared to control florets.**

Carpels, stamens and lodicules dissected from florets from barley transformants expressing a combination of *pUBI:HvBM4-SRDX* and *pUBI:HvBM16-SRDX* constructs and control florets. Line C shows a partial conversion of the stamen to carpeloid structures and the carpel had an elongated phenotype. Even though the lodicules seemed similar in appearance to the control lodicules (A), in other tillers with a less severe anther phenotype the lodicules were slightly elongated (B).

In one line all tillers showed changes in stamen structure of varying severity, with the most severe showing a partial conversion of the stamen to carpeloid structures (Figure 3.7). The anthers had stigma-like hairs and had lost all colour compared to the control. No pollen was found inside the anthers. The carpel had an elongated phenotype, no longer exhibiting the 'heart' shape of the characteristic of carpels in wheat, rice and barley. Even though the lodicules seemed similar in appearance to the control lodicules, in other tillers with a less severe anther phenotype, the lodicules were slightly elongated (Figure 3.7, A and B). Anthers from these florets contained some viable pollen, although significantly less than the control (Figure 3.2). Two other lines also showed this phenotype. Surprisingly, the line with the most severe anther conversion (Line C) showed lower expression of the *pUBI:HvBM4-SRDX* than another line exhibiting a less severe anther phenotype (Line D) (Figure 3.8).

Florets of another line were noticeably bigger and spikes were shorter, carrying less florets than the control. The carpel and the lodicules of these florets were also bigger than the control, but showed no changes in structure (Figure 3.9). Pollen found inside the anthers was viable, but there was significantly less viable pollen than the control (Figure 3.2). Pollen found inside the anthers was also found to be sticking together (Figure 3.9). Expression of the *pUBI:HvBM4-SRDX* construct was very low in these florets (Figure 3.8, Line E).

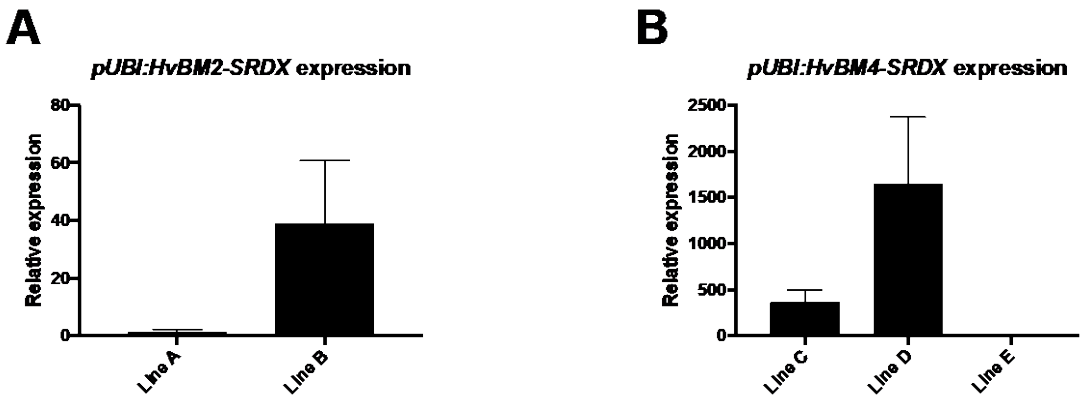



**Figure 3.8 Expression analysis of the *pUBI:HvBM2-SRDX* (A) and *pUBI:HvBM4-SRDX* (B) constructs in plants exhibiting a phenotype.**
(A) Line B expresses the *pUBI:HvBM2-SRDX* construct more highly than Line A. (B) Line D has the highest expression of the *pUBI:HvBM4-SRDX* construct even though Line C exhibits a much more pronounced phenotype. The expression in Line E is negligable compared to the other two lines.

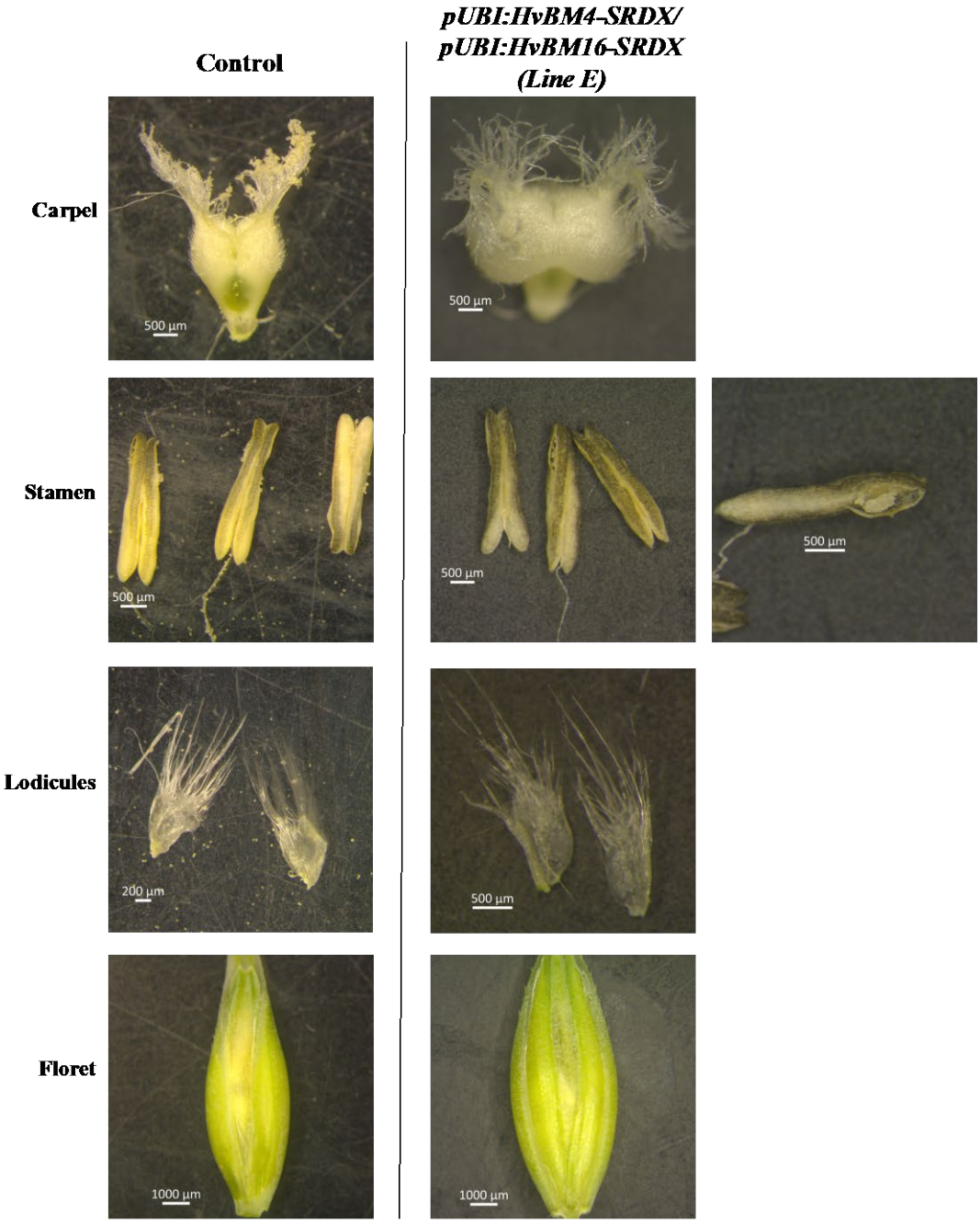



**Figure 3.9 Phenotype of carpel, stamens and lodicules in barley transformants expressing a combination of *pUBI:HvBM4-SRDX* and *pUBI:HvBM16-SRDX* (Line E) constructs compared to control florets.**

Carpels, stamens and lodicules dissected from florets from barley transformants expressing a combination of *pUBI:HvBM4-SRDX* and *pUBI:HvBM16-SRDX* constructs and control florets. Line E has bigger florets that contain bigger carpels and lodicules, but no apparent changes in anther structure. Pollen inside the anthers was found to be clumped together.

## 3.4 Discussion

In *Arabidopsis* the B-class genes determine the identity of the petals and the stamens (Fornara *et al.*, 2003). In grasses they are thought to determine the identity of the lodicules, the equivalent of petals, and the stamens. A functional analysis of the B-class MADS-box genes in barley is still lacking. By using the CRES-T system of dominant repression by attaching an EAR motif domain, also known as SRDX, to the CDS of the B-class genes we generated dominant repression lines.

Dominant repression of single PI-like genes resulted in beginning to partial conversion of stamens into carpeloid structures. In the transformants examined, the *pUBI:HvBM4-SRDX* line showed the most severe phenotype. Stamens were converted into carpeloid structures, the carpels were small and underdeveloped. The lodicules were small and had lost their rounded shape and the presence of trichomes. These results are contrary to what has previously been reported in rice, where there was no phenotype observed in the *OsMADS4* RNAi lines (Yao *et al.*, 2008; Yoshida *et al.*, 2007). However, the stamen and lodicule phenotype correspond to those observed in the *WPI1* mutant in wheat (Hama *et al.*, 2004). Curiously, the carpel phenotype observed in the *pUBI:HvBM4-SRDX* line has not been described in any other crops or in *Arabidopsis*. This might indicate an indirect role of *HvBM4* in carpel development.

The phenotypes observed in *pUBI:HvBM2-SRDX* lines showed more similarity to those observed in rice *OsMADS2* RNAi lines (Yadav *et al.*, 2007; Yao *et al.*, 2008; Yoshida *et al.*, 2007). In both the rice and our barley lines, elongated and bract-like lodicules were found. In the rice *OsMADS2* RNAi lines, however, no phenotype was observed in the stamens, whereas stamens in our barley *pUBI:HvBM2-SRDX* lines showed changes in stamens shape and the appearance of trichomes on the top of the stamens.

Both the sterility data from the *pUBI:HvBM2-SRDX* lines and the lack of viable pollen in the majority of the other SRDX lines shows that pollen development is also severely impacted. This could be and indirect effect or due to the changes in structure of the anthers, or it could indicate that the B-class genes are involved in pollen development. Unpublished RNAseq data produced by Dr. Matthew Aubert has shown that *HvBM2* is also expressed after fertilisation of the carpel in the

nucellar projection. The aborted seeds in the *pUBI:HvBM2-SRDX* lines could point to an as of yet unknown function in seed production.

The *pUBI:HvBM16-SRDX* lines showed no phenotype, which is contrary to what was seen in rice and maize (Ambrose *et al.*, 2000; Nagasawa *et al.*, 2003). The different phenotypes and degrees of severity or the lack of phenotypes are likely due to the expression levels of the SRDX construct. If the expression of the construct is very low, the repressor SRDX MADS-box gene can still be outcompeted by the native MADS-box gene.

The results of these dominant repression lines show that HvBM2 and HvBM4 have a conserved function in stamens and lodicule development. A carpel phenotype that hasn't been described before and the aborted seeds in the lines with a phenotype point to a potential function in the carpel and in the developing seed. HvBM2 and HvBM4 might have a redundant function in stamens and lodicule development, shown by the less severe phenotype in *pUBI:HvBM2-SRDX* lines, which is similar to what was found in rice, though in rice HvBM4 seems to have a lesser function (Yao *et al.*, 2008; Yoshida *et al.*, 2007).

| **Construct** | **Line** | **Phenotype** |
|---|---|---|
| *pUBI:HvBM2-SRDX* | 2 | Partial conversion of stamens to carpel-like structures. Stigma-like trichomes on stamens. Elongated lodicules, partial conversion to palea-like structure. |
| *pUBI:HvBM4-SRDX* | | Conversion of stamens to carpeloid structures. Conversion of lodicules to small bract-like structures without trichomes. Carpel small and underdeveloped showing limited stigmatic branching. |
| *pUBI:HvBM16-SRDX* | | No phenotypes found. |
| *pUBI:HvBM2-SRDX* + *pUBI:HvBM16-SRDX* | B | Emaciated carpels. |
| *pUBI:HvBM4-SRDX* + *pUBI:HvBM16-SRDX* | C | Partial conversion stamen to carpeloid structures. Elongated carpel. Lodicules slightly elongated. |
| | E | Bigger florets, carpels and lodicules. |

**Table 3.3 Overview of the constructs transformed in the transgenic plants and the resulting phenotypes.**

## 3.5 References

**Ambrose BA, Lerner DR, Ciceri P, Padilla CM, Yanofsky MF, Schmidt RJ**. 2000. Molecular and genetic analyses of the silky1 gene reveal conservation in floral organ specification between eudicots and monocots. *Molecular Cell* **5**, 569-579.

**Becker A, Kaufmann K, Freialdenhoven A, Vincent C, Li M-A, Saedler H, Theissen G**. 2002. A novel MADS-box gene subfamily with a sister-group relationship to class B floral homeotic genes. *Molecular Genetics and Genomics* **266**, 942-950.

**Becker A, Theissen G**. 2003. The major clades of MADS-box genes and their role in the development and evolution of flowering plants. *Mol Phylogenet Evol* **29**, 464-489.

**Bowman JL, Smyth DR, Meyerowitz EM**. 1989. Genes directing flower development in Arabidopsis. *The Plant Cell Online* **1**, 37.

**Bowman JL, Smyth DR, Meyerowitz EM**. 1991. Genetic interactions among floral homeotic genes of Arabidopsis. *Development* **112**, 1.

**Fornara F, Marziani G, Mizzi L, Kater M, Colombo L**. 2003. MADS-Box Genes Controlling Flower Development in Rice. *Plant Biology* **5**, 16-22.

**Gioppato HA, Dornelas MC**. 2019. When Bs Are Better than As: the Relationship between B-Class MADS-Box Gene Duplications and the Diversification of Perianth Morphology. *Tropical Plant Biology* **12**, 1-11.

**Goremykin VV, Hansmann S, Martin WF**. 1997. Evolutionary analysis of 58 proteins encoded in six completely sequenced chloroplast genomes: Revised molecular estimates of two seed plant divergence times. *Plant Systematics and Evolution* **206**, 337-351.

**Hama E, Takumi S, Ogihara Y, Murai K**. 2004. Pistillody is caused by alterations to the class-B MADS-box gene expression pattern in alloplasmic wheats. *Planta* **218**, 712-720.

**Harwood WA, Bartlett JG, Alves SC, Perry M, Smedley MA, Leyl N, Snape JW**. 2009. Barley Transformation Using Agrobacterium-Mediated Techniques. In: Jones HD, Shewry PR, eds. *Transgenic Wheat, Barley and Oats: Production and Characterization Protocols*. Totowa, NJ: Humana Press, 137-147.

**Hernández-Hernández T, Martínez-Castilla LP, Alvarez-Buylla ER**. 2006. Functional Diversification of B MADS-Box Homeotic Regulators of Flower Development: Adaptive Evolution in Protein–Protein Interaction Domains after Major Gene Duplication Events. *Molecular Biology and Evolution* **24**, 465-481.

**Hill JP, Lord EM**. 1989. Floral development in Arabidopsis thaliana: a comparison of the wild type and the homeotic pistillata mutant. *Canadian Journal of Botany* **67**, 2922-2936.

**Hiratsu K, Matsui K, Koyama T, Ohme-Takagi M**. 2003. Dominant repression of target genes by chimeric repressors that include the EAR motif, a repression domain, in Arabidopsis. *The Plant Journal* **34**, 733-739.

**Irish V**. 2017. The ABC model of floral development. *Current Biology* **27**, R887-R890.

**Jack T, Brockman LL, Meyerowitz EM**. 1992. The homeotic gene APETALA3 of Arabidopsis thaliana encodes a MADS box and is expressed in petals and stamens. *Cell* **68**, 683-697.

**Jack T, Fox GL, Meyerowitz EM**. 1994. Arabidopsis homeotic gene APETALA3 ectopic expression: Transcriptional and posttranscriptional regulation determine floral organ identity. *Cell* **76**, 703-716.
**Jenik PD, Irish VF**. 2001. The Arabidopsis floral homeotic gene APETALA3 differentially regulates intercellular signaling required for petal and stamen development. *Development* **128**, 13.
**Kagale S, Rozwadowski K**. 2011. EAR motif-mediated transcriptional repression in plants. *Epigenetics* **6**, 141-146.
**Kim S, Yoo M-J, Albert VA, Farris JS, Soltis PS, Soltis DE**. 2004. Phylogeny and diversification of B-function MADS-box genes in angiosperms: evolutionary and functional implications of a 260-million-year-old duplication. *American Journal of Botany* **91**, 2102-2118.
**Krizek BA, Meyerowitz EM**. 1996. The Arabidopsis homeotic genes APETALA3 and PISTILLATA are sufficient to provide the B class organ identity function. *Development* **122**, 11.
**Li X**. 2011. Pollen Fertility/viability Assay Using FDA Staining. *Bio-protocol* **1**, e75.
**Münster T, Pahnke J, Di Rosa A, Kim JT, Martin W, Saedler H, Theissen G**. 1997. Floral homeotic genes were recruited from homologous MADS-box genes preexisting in the common ancestor of ferns and seed plants. *Proceedings of the National Academy of Sciences* **94**, 2415.
**Nagasawa N, Miyoshi M, Sano Y, Satoh H, Hirano H, Sakai H, Nagato Y**. 2003. SUPERWOMAN1 and DROOPING LEAF genes control floral organ identity in rice. *Development* **130**, 705.
**Ohta M, Matsui K, Hiratsu K, Shinshi H, Ohme-Takagi M**. 2001. Repression Domains of Class II ERF Transcriptional Repressors Share an Essential Motif for Active Repression. *The Plant Cell* **13**, 1959.
**Theissen G, Becker A, Di Rosa A, Kanno A, Kim JT, Münster T, Winter K-U, Saedler H**. 2000. A short history of MADS-box genes in plants. *Plant Molecular Biology* **42**, 115-149.
**Theißen G, Melzer R, Rümpler F**. 2016. MADS-domain transcription factors and the floral quartet model of flower development: linking plant development and evolution. *Development* **143**, 3259.
**Winter K-U, Saedler H, Theißen G**. 2002. On the origin of class B floral homeotic genes: functional substitution and dominant inhibition in Arabidopsis by expression of an orthologue from the gymnosperm Gnetum. *The Plant Journal* **31**, 457-475.
**Yadav SR, Prasad K, Vijayraghavan U**. 2007. Divergent regulatory OsMADS2 functions control size, shape and differentiation of the highly derived rice floret second-whorl organ. *Genetics* **176**, 283-294.
**Yamaguchi T, Hirano HY**. 2006. Function and diversification of MADS-box genes in rice. *The Scientific World Journal* **6**, 1923-1932.
**Yao S-G, Ohmori S, Kimizu M, Yoshida H**. 2008. Unequal Genetic Redundancy of Rice PISTILLATA Orthologs, OsMADS2 and OsMADS4, in Lodicule and Stamen Development. *Plant and Cell Physiology* **49**, 853-857.
**Yoshida H, Itoh J-I, Ohmori S, Miyoshi K, Horigome A, Uchida E, Kimizu M, Matsumura Y, Kusaba M, Satoh H, Nagato Y**. 2007. superwoman1-cleistogamy, a hopeful allele for gene containment in GM rice. *Plant Biotechnology Journal* **5**, 835-846.

**Zahn LM, Leebens-Mack J, dePamphilis CW, Ma H, Theissen G**. 2005. To B or Not to B a Flower: The Role of DEFICIENS and GLOBOSA Orthologs in the Evolution of the Angiosperms. *Journal of Heredity* **96**, 225-240.

# Chapter 4: Effects of heat stress on reproductive development in three European barley varieties

Cindy Callens[1,2], José Fernandez Goméz[1], Matthew R. Tucker[2], Dabing Zhang[2,3] and Zoe A. Wilson[1]

[1] School of Biosciences, University of Nottingham, Sutton Bonington Campus, Loughborough, Leicestershire LE12 5RD, UK
[2] School of Agriculture, Food and Wine, University of Adelaide, Waite Campus, Urrbrae, SA, Australia
[3] School of Life Sciences and Biotechnology, Shanghai Jiao Tong University, Shanghai 200240, China

Submitted for publication to Journal of Experimental Botany on 23/07/2019

# Introduction to Chapter 4: Effects of heat stress on reproductive development in three European barley varieties.

MADS-box genes have been shown to be important in abiotic stress tolerance in several studies on various crops (Castelán-Muñoz *et al.*, 2019). In this chapter heat stress experiments were used to investigate the impact of heat stress on the reproductive organs of three commercial European spring barley varieties. Heat stress was applied at two critical stages in floret development: meiosis and mitosis. These two particular time points were chosen to see if early heat stress, simulating heat waves in spring in Europe, has an effect on the reproductive development, as well as comparing these results to the effects of heat stress in the later stages of development. A day temperature of 30°C was chosen to mimic abnormal heat in Northern Europe.

Fertility assays looking at pollen viability were used to have a first look at sterility in the different varieties. 3D X-ray CT scans were carried out as a non-destructive method to visualise the morphology of florets and floret organs without manipulation. This is a promising new method to give a more representative image and accurate volume measurements calculated by the X-ray software VG Studio Max 2.2 based on the regions of interest segmented out of the scan. However, it involves many hours of work, understanding of the software and precision work segmenting the desired regions of interest, in this case the reproductive organs, out of the X-ray CT scans to obtain the 3D images represented in this chapter. Immunolabeling was used to visualise changes in the cell walls in anthers and ovules.

The heat stress experiment was repeated to confirm the results observed in the first experiment. All results presented in this chapter were obtained in the second experiment, due to the fact that the X-ray CT scans were only able performed during the second experiment. However, all other results were similar between both experiments.

These experiments were to be combined with a genetic analysis of the ABCDE MADS-box genes in the heat stress plants compared to the control to investigate if these genes could be of interest for abiotic stress tolerance in barley. However, due

to a lack of time and a shift of focus to the functional and expression analysis of the ABCDE MADS-box this genetic analysis was not carried out. Further research into the effect of heat stress on the ABCDE MADS-box genes and investigating their role in abiotic stress tolerance in barley might be interesting for future breeding strategies.

# Effects of heat stress on reproductive development in three European barley varieties

Cindy Callens[1,2], José Fernandez Goméz[1], Matthew R. Tucker[2], Dabing Zhang[2,3] and Zoe A. Wilson[1,4]

[1]School of Biosciences, University of Nottingham, Sutton Bonington Campus, Loughborough, Leicestershire, LE12 5RD, United Kingdom
[2]School of Agriculture, Food and Wine, University of Adelaide, Waite Campus, Urrbrae, SA, Australia.
[3]Joint International Research Laboratory of Metabolic & Developmental Sciences, State Key Laboratory of Hybrid Rice, School of Life Sciences and Biotechnology, Shanghai Jiao Tong University, Shanghai 200240, China
[4]Authors for correspondence: Email zoe.wilson@nottingham.ac.uk; Tel: +44(0)115 9513235

cindy.callens@nottingham.ac.uk
matthew.tucker@adelaide.edu.au
dabing.zhang@adelaide.edu.au

Date of Submission: 22/07/2019
Number of Tables: 1  Number of Figures: 5
Word Count (introduction to the end of acknowledgements): 5037

Running Title: **Heat stress on barley reproduction**

**Highlight:** Using fertility assays, 3-dimensional modelling, cytology and immunolabelling, cultivar and stage-dependent variations in male fertility were identified in response to high temperature stress.

**Key words:** barley, heat stress, reproductive development, meiosis, mitosis

## 4.1 Abstract

The Poaceae, or grasses, include many agriculturally important crops such as rice (*Oryza sativa*), maize (*Zea mays*), barley (*Hordeum vulgare*) and wheat (*Triticum aestivum*). Barley is a widely grown cereal crop used for stock feed, malting and brewing. Abiotic stresses, particularly global warming, are the major causes of crop yield losses by affecting normal fertility and seed set. However, effects of heat stress on reproductive structures and fertility in barley have not been extensively investigated. In this study we examined three commercial European spring barley varieties under high temperature conditions to investigate the effects on floret development. Using a combination of fertility assays, 3-dimensional modelling, cytology and immunolabelling, we observed that male reproductive organs are severely impacted by increased temperature, while the female reproductive organs are less susceptible. Importantly, the timing of stress relative to reproductive development had a significant impact on fertility in a cultivar-dependent manner. This work provides insight into how heat stress, when applied during male meiosis and mitosis, affects crop fertility and seed set, and also describes complementary invasive and non-invasive techniques to investigate floret development. This information will be used to identify and study barley cultivars that are less susceptible to heat stress at specific stages of floral development.

## 4.2 Introduction

The world is facing an exponentially increasing population, with associated increased demands for food, and all major climate models predict a higher average temperature globally with larger temperature fluctuations and more frequent heat waves (Christidis *et al.*, 2014; IPCC, 2014). Abiotic stresses are, individually or in combination, one of the major reasons for crop yield loss. These stresses cause morphological, physiological, biochemical and molecular changes that impair plant development (Bita and Gerats, 2013). Lesk *et al.* (2016) has shown that extreme heat significantly reduced national cereal production globally by 9-10%. Wheat, maize and barley have been shown to have the strongest negative yield impacts due to the changing climate in the last two decades with an estimated annual combined loss for these three crops of roughly $5 billion per year since 2002 (David and Christopher, 2007). In particular the increased frequency of heat stress over the last 40 years, has led to a greater frequency of yield anomalies in wheat (Zampieri *et al.*, 2017). Wheat

yields, which account for 21% of food production, could decrease significantly with an increase in temperature in regions where temperatures are currently optimal (Delphine *et al.*, 2014; Ortiz *et al.*, 2008). Experiments in rice also showed that heat stress has an adverse effect on important yield components especially fertile spikelets and 1000 grain weight, decreasing the yield significantly (Aghamolki *et al.*, 2016). This serves as a warning for future global food security.

Reproductive organs are significantly more vulnerable to high temperatures than other plant organs. Planting of crops is typically timed to minimise high temperature exposure during the reproductive stages, however the fluctuations and extremes of temperature that are now occurring mean that there is an increasing probability that peaks of high temperature will overlap with the flowering period (Teixeira *et al.*, 2013). Seed set requires many developmental steps to be successfully completed; for example, pollen must be produced, viable pollen grains must be released and the pollen tubes must grow properly to ensure functional signalling mechanisms with the style and the ovule. Concurrently, the ovule must develop within the ovary to produce and nourish the embryo sac, producing a female gamete and a suitable environment for the downstream events of seed development (Wilkinson *et al.*, 2018). Once fertilization is completed, the embryo must then develop normally to ensure successful seed set (Barnabas *et al.*, 2008; Maestri *et al.*, 2002; Wilson and Zhang, 2009). Nevertheless, these developmental processes show variable sensitivity to heat stress.

Saini *et al.* (1983) reported that one third of ovaries in wheat that experienced heat stress during meiosis exhibited abnormal development. Pollen, in contrast, shows much higher levels of abortion after heat stress and has been shown to be one of the most heat-sensitive developmental stages in cereals (Prasad *et al.*, 2008; Saini *et al.*, 1983; Stone and Basra, 2001). At the pre-meiotic stage, high temperatures caused development of short anthers possessing no pollen grains in barley (Sakata *et al.*, 2000). Heat stress during meiosis resulted in pollen grains that possessed exine, but showed little starch accumulation (Sakata *et al.*, 2000). Draeger and Moore (2017) also showed that exposure of wheat to high temperatures affected the progression of pollen mother cell (PMC) meiosis. Disruption of synapsis is one of the most commonly reported meiotic failures under high temperatures and this can lead to

unpaired univalents that segregate randomly or are lost (Bomblies *et al.*, 2015). In addition, at mitosis 1 and 2 both wheat and barley pollen grains have been shown to be highly sensitive to elevated temperatures (Barnabas *et al.*, 2008; Saini *et al.*, 1984). This has been proposed as due to an inability to synthesize all required Heat Shock Proteins (HSPs) necessary to survive during heat stress conditions (Barnabas *et al.*, 2008; Cooper *et al.*, 1984; Mascarenhas and Crone, 1996). A causal involvement of HSPs in thermotolerance in plants has been shown in non-cereal species (Hong and Vierling, 2000). Genotypes that express HSPs are better able to withstand heat stress as they minimise heat-induced protein aggregation and thus during the recovery period, facilitate their refolding (Farooq *et al.*, 2011; Feder and Hofmann, 1999; Nguyen *et al.*, 1994). In many cases, expression of HSPs is developmentally regulated and they are thus present prior to heat stress (Maestri *et al.*, 2002). Heat stress during the early periods of grain filling in maize has also been shown to cause a reduction in grain weight which was attributed to a lower number of endosperm cells (Nicolas *et al.*, 1985).

In this study, we analysed the effects of heat stress on reproductive development of three European spring barley varieties under controlled environmental conditions. One of these varieties, RGT Planet, has recently been identified as a variety of considerable promise for high yield and malt quality in Australian conditions (SeedForce, 2017). We found that after heat stress anthers from all varieties showed abnormal development, whilst ovules were less severely affected. The three varieties showed differences in sterility, confirming their varying tolerance to heat stress, with Moonshine being most tolerant overall. RGT Planet exhibited excellent yield under control conditions, but suffered significantly after heat stress. In contrast to Moonshine and RGT Planet, Optic was the most severely affected by heat stress during mitosis in reproductive development.

## 4.3 Materials and methods

### *4.3.1 Plant materials and growth conditions*

Seeds from three different spring barley varieties (*Hordeum vulgare*; Optic, RAGT Moonshine and RGT Planet) were provided by the Wilson lab (University of Nottingham) and were sown in John Innes Potting Compost No.3 in 13cm diameter pots. Optic is a variety created by Syngenta, RAGT Moonshine and RGT Planet are

varieties created by RAGT Seeds. RGT Planet is a relatively new variety that has been shown to be one of the highest yielding spring varieties on the AHDB Recommended List that is fully approved for brewing use (AHDB, 2017). RAGT Moonshine and Optic were removed from the AHDB Recommended List in 2016 (AHDB, 2016). All three are two-row varieties and are primarily grown in the United Kingdom, although RGT Planet is becoming popular in Australia. Temperatures of ~20°C are considered optimal for growth and development of spring barley varieties (Kruszka *et al.*, 2014). The pots were placed in a controlled environment growth chamber with a continuous temperature of 17°C and 16 hour photoperiod. After one week, the plants were transferred to CSNG (General Container Nursery Stock compost, Levington Advance) compost in 13cm diameter pots. Heat stress was applied to two stages of reproductive development (meiosis and mitosis, Supplemental Figure 1) according to the non-destructive staging described in Gómez and Wilson (2012) and these plants were compared to plants grown in control conditions. Male as well as female reproductive development were simultaneously targeted because the onset of the pollen mother cells (PMCs) in anthers coincides approximately with meiosis in the megaspore mother cell (Saini *et al.*, 1983). Twelve plants of each variety were used for each condition: 1) meiosis heat stress, 2) mitosis heat stress and 3) control. The periods of heat stress were carried out in a controlled environment growth room with a day/night temperature of 30/25°C and a 16 hour photoperiod to mimic extreme heat stress conditions. The temperatures were chosen to mimic heat waves occurring more frequently in Europe. Tillers of a similar age were selected at the beginning of meiosis or mitosis, and were tagged for analysis before being submitted to heat stress. All pots were monitored daily and watered to avoid any water stress. Plants undergoing meiosis heat treatment were submitted to heat stress for two days, while plants undergoing the mitosis heat treatment remained in the heat stress for five days to ensure completion of mitosis I and II, before being transferred back to control conditions.

*4.3.2 Pollen viability assay*

Pollen viability in control and heat stressed plants was assayed using 0.2% (w/v) potassium iodide and 1% (w/v) iodine (Chang *et al.*, 2014). Normal mature pollen grains that contain starch granules stain black, whilst immature pollen grains or

deformed pollen grains appear orange or red. Pollen viability images were taken with a Nikon Eclipse 50i microscope and a Nikon DS-Fi1 camera.

*4.3.3 Immunolabelling*

Florets were harvested from the tillers tagged for heat stress during meiosis immediately before anthesis, fixed in 4% (w/v) paraformaldehyde in phosphate-buffered saline (PBS) with 0.1% (v/v) Triton X-100 and 0.1% (v/v) Tween 20 and embedded in paraffin. Floret sections (8μm) were mounted on slides at 42°C, the paraffin was removed from the sections using 100% Histoclear (v/v) and tissue was rehydrated by using an ethanol series (100%, 90%, 70% and 30% (v/v)) and water. Slides were washed with 1xPBS and treated subsequently with glycine to inactivate residual aldehyde groups. They were then washed with Incubation buffer (1% (w/v) bovine serum albumin (BSA)) in 1xPBS (Burton *et al.*, 2011). Primary antibody was added to the sections and incubated in a humidity chamber for 1h: BG1 murine monoclonal antibodies raised against barley (1,3;1,4)-β-d-glucan (diluted 1:50; Biosupplies Australia, Parkville, Vic., Australia) and LM19 monoclonal antibodies raised against homogalacturonan (Burton *et al.*, 2011; Meikle *et al.*, 1994; Verhertbruggen *et al.*, 2009). After three washes with Incubation buffer the slides were dried and the secondary antibodies added. Goat anti-mouse Alexa Fluor® 488 IgG (H+L) (diluted 1:200, Invitrogen, Australia) was used for BG1 and Dylight 550 Goat anti-rat IgM (diluted 1:200, Invitrogen, Australia) was used for LM19. The slides were incubated for 2h and then washed with Incubation buffer. 0.1% (w/v) Calcofluor white was added and washed off before imaging with the Zeiss Axio Imager 2 as described in Aditya et al., (2015).

*4.3.4 3D X-ray imaging*

The Phoenix Nanotom S, a nanofocus Computed Tomography system was used to scan barley florets of the three varieties at the Hounsfield Facility in Nottingham as previously described (Tracy *et al.* (2017). One control floret and one heat stressed floret (heat stress applied during meiosis) were scanned and the scans were segmented and analysed using VG Studio Max 2.2.

*4.3.5 Phenotyping*

Five different, randomly chosen florets were harvested immediately before anthesis after the heat treatments and in control conditions from all varieties and dissected to

observe the morphology of the anthers. Images were taken with a Zeiss Stemi SV6 microscope and an Axiocam ERc Rev. 2.0 camera.

*4.3.6 Evaluation of sterility*

All tillers from control and heat stressed plants were harvested (Table 1). For every spike the number of total spikelets and the number of spikelets that developed into seeds were counted. The percentage of "sterility per tiller" was calculated by dividing the number of seeds by the total number of spikelets and multiplying by 100.

## 4.4 Results

*4.4.1 Anther morphology in barley varieties after heat stress*

Anthers were dissected from at least three randomly selected florets for the different varieties (Optic, RAGT Moonshine and RGT Planet) that had been exposed to heat treatment at meiosis and mitosis, and compared to those from the control conditions. All of the heat-treated lines showed effects on anther morphology, with alterations in anther shape and a change in colour from yellow to white (Figure 4.1). In all three varieties, the effect on anther morphology was more severe after heat stress during meiosis compared to mitosis, but both treatments showed impacts on anther shape and colour. In particular, Optic and RGT Planet showed a severe change in meiosis heat stressed anthers (Figure 4.1).

Anther morphology was investigated further using 3D images obtained from X-ray micro-CT scans of Optic and RGT Planet. The resulting X-ray micro-CT scans (Figure 4.3) of all six florets (one control floret and one meiosis heat stressed floret for each variety) were carefully segmented to obtain individual 3D images of the anthers and carpels (Figure 4.2).

Anther volume, calculated by the software VG Studio Max 2.2 from the segmented CT scans of the floral organs, varied significantly; control non-stressed anthers were approximately 0.9mm$^3$ (4.33mm length, 1.98mm width, 1.43mm depth) in Optic and 1.1 mm$^3$ (4.49 mm length. 2.83 mm width, 1.37 mm depth) in RGT Planet. Whereas the meiosis heat stressed anthers were smaller: 0.29 mm$^3$ (3.91 mm length, 3.01 mm width, 1.82 mm depth) in Optic and 0.71 mm$^3$ (3.1 mm length, 2.35 mm width, 1.01

mm depth) in RGT Planet (Figure 4.2). The septum in the heat-stressed anthers could be observed as broken in the micro-CT scans, while this was not the case for the control anthers (Figure 4.2).




**Figure 4.1 Anther development in barley cultivars Optic, Moonshine and RGT Planet.**
Anthers dissected from control and heat stressed florets (heat stress during meiosis and mitosis of pollen development) show differences in anther development under the different conditions.

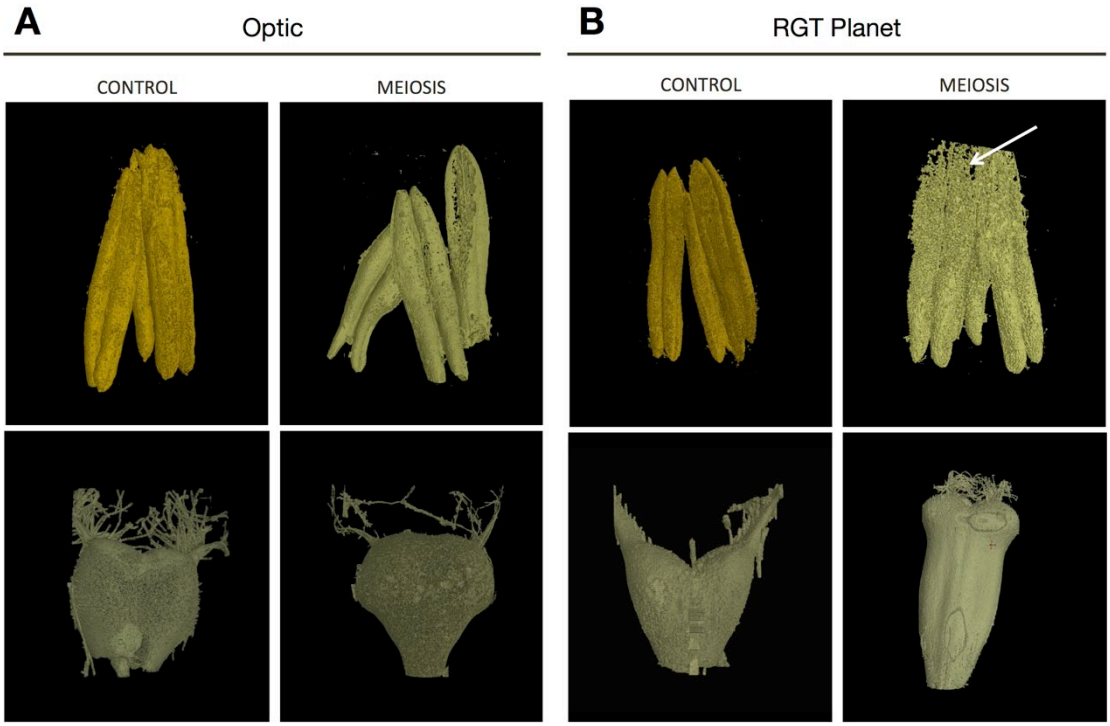



**Figure 4.2 X-ray CT images of (A) anther and (B) carpel development in control and heat stress conditions for Optic and Planet.**
X-ray images of the anthers and carpels obtained by X-ray CT were compared for control environment and heat stress environment (heat stress during meiosis of pollen development) immediately before anthesis. Arrow indicates the broken septum in RGT Planet heat stressed anther.

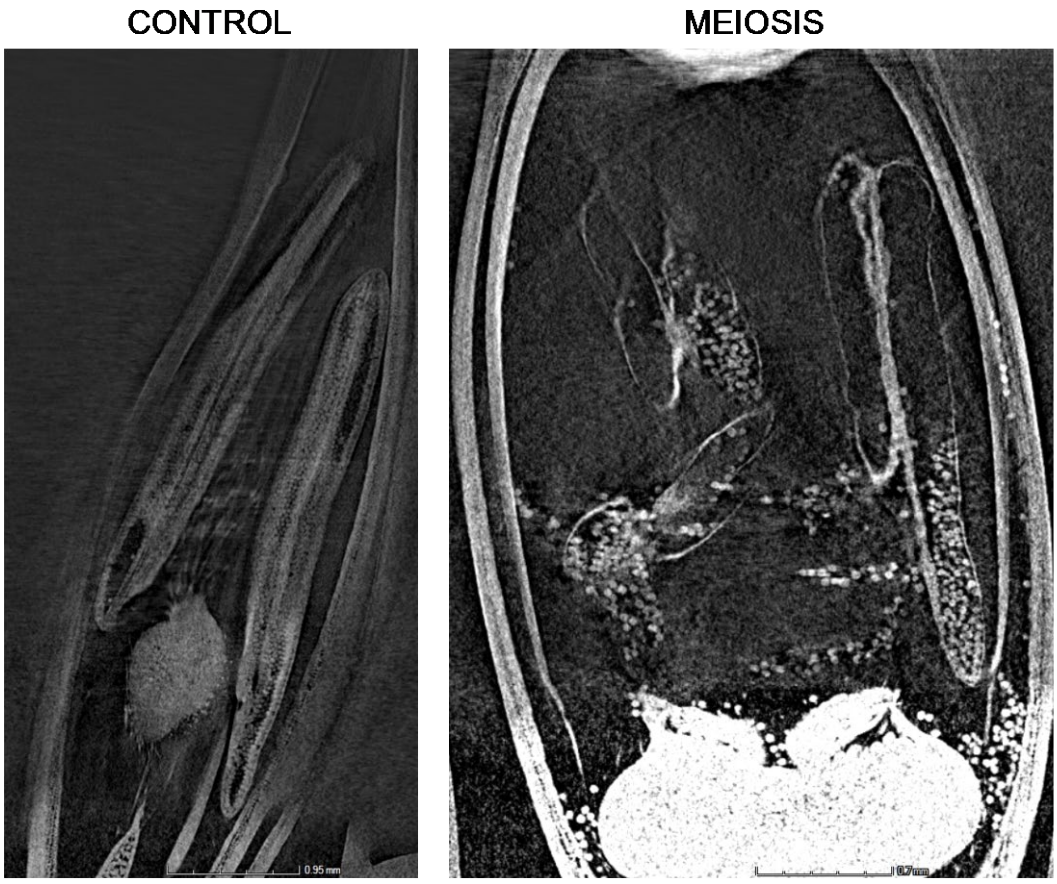



**Figure 4.3 X-ray CT images of anther and carpel development in control and heat stress conditions for Moonshine.** X-ray images of the anthers and carpels obtained by X-ray CT are compared for control environment and heat stress environment (heat stress during meiosis of pollen development) right before anthesis.

Immunolabelling was subsequently used to observe sections of the anthers and highlight cell wall components such as 1,3;1,4-β-glucan, de-esterified pectin and cellulose (Figure 4.3). Calcofluor white stained β-glycan polysaccharides in the outer layers of the anther, the filament vascular tissue and the pollen grains (Figure 4.3A). Some autofluorescence was detected in the pollen grains, particularly in the 1,3;1,4-β-glucan channel (Figure 4.3B), but positive controls confirmed 1,3;1,4-β-glucan and de-esterified pectin labelling (Figure 4.3C). The results clearly indicated that the meiosis heat-stressed anthers of all the lines were significantly impacted by the stress (Figure 4.3). In Optic (Figure 4.3D, E), pollen was visible in the control anthers, but not in the meiosis heat-stressed anthers. The epidermal cells of the anther wall were intact, but the endothecium had degraded. Both tissue layers were intact and visible in the Optic control anthers (Supplementary Figure S4). In Moonshine (Figure 4.3F, G), no pollen was visible in the meiosis heat-stressed anthers despite it being

observed in the micro-CT scanned images (Supplementary Figure S3). The epidermis was also intact, but the endothecium had degraded in the heat stressed anthers (Supplementary Figure S5). Similar to the other two varieties, while pollen grains were visible in the control anthers, there was none visible in the heat stressed anthers in RGT Planet (Figure 4.3H, I). The anther wall in the heat stressed anthers seemed to have collapsed, which agrees with the observations from the micro-CT scan (Figure 4.2; Supplementary Figure S5). In all heat stressed anthers, the vascular tissue was less well developed than in the control anthers.

*4.4.2 Carpel morphology in barley varieties after heat stress*

The 3D images of the carpels from Optic showed no significant changes in morphology between heat-stressed and control florets, but there was a difference in size (Figure 4.2; Supplementary Figure S4). Calculated by VG Studio Max 2.2 from the segmented CT scans of the floral organs, the control carpel measured 1.31mm$^3$ (2.71mm length, 2.35mm width, 1.45mm depth), which is smaller than the heat stressed carpel, which measured 2.58mm$^3$ (2.86 length, 2.77mm width, 1.34 depth). The X-ray imaging also showed a significantly enlarged carpel in the RGT Planet heat stressed floret with a volume of 4.46mm$^3$ (5.37mm length, 2.51mm width, 1.57mm depth) compared to the control which had a volume of 1.37mm$^3$ (2.42mm length, 2.22mm width, 1.13mm depth) (Figure 4.2).

The immunolabelling of ovule sections in Optic only showed slight differences between control and heat stressed florets (Figure 4.3J, K): the embryo sac was present, but there seemed to be less cell layers between the embryo sac and the integument, and nucellus cells appeared larger. This could be due to regional nucellar degeneration and faster development of heat-stressed ovules. Similarly, embryo sac morphology in the heat-stressed ovules of Moonshine did not show any significant difference compared to control ovules (Figure 4.3L, M). The ovules in the heat-stressed florets of RGT Planet seemed to be further developed than the controls (Figure 4.3N, O), but no clear irregularities in the morphology of the embryo sacs could be identified.

*4.4.3 Male fertility after heat stress*

Meiosis and mitosis stages are known to be stages vulnerable to heat stress during pollen development, therefore pollen viability was assessed using potassium iodide/iodine solution in anthers from all three varieties with and without heat

treatment. Using this method, viable pollen stains black due to starch deposition whilst non-viable pollen stains orange-red. Pollen was still able to develop in the florets after heat stress at meiosis and mitosis, but there was a lack of starch staining indicating a high level of sterility (Supplementary Figure S1B). Pollen could be observed in the Optic and RGT Planet anthers, after both meiosis and mitosis heat stress, but this was less than in the control plants, and none was viable. Moonshine was even more strongly affected with no pollen present after the meiosis heat stress. After heat stress during mitosis viable pollen was observed but at a lower amount than in the control anthers.

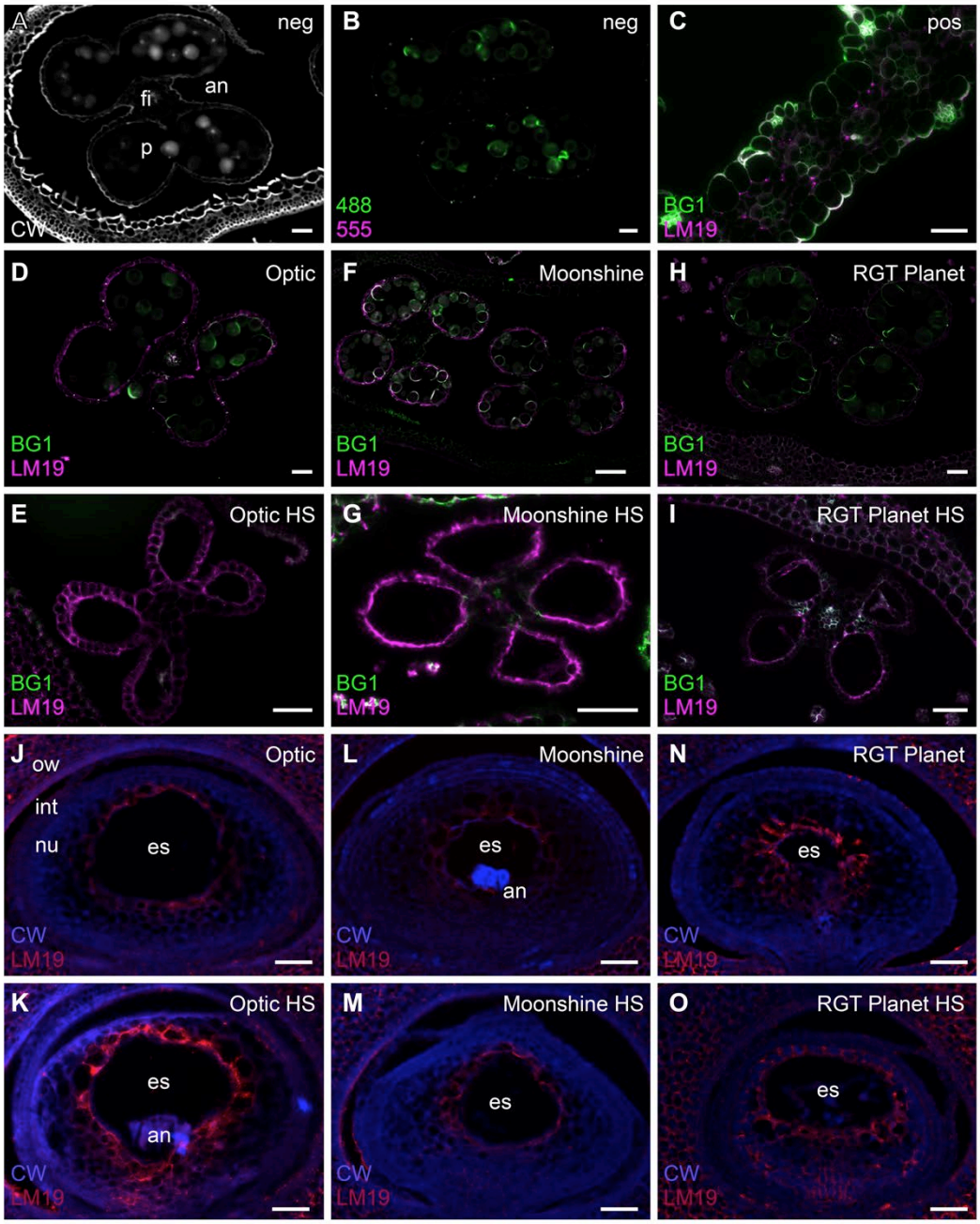



**Figure 4.4 Immunolabelling of cell wall components in anthers and ovules in Optic, Moonshine and Planet at meiosis stage.**
(A) Calcofluor white staining (CW, white colour) of a control anther (an). The filament (fi) and pollen (p) are indicated. (B) The same anther shown in A, showing autofluorescence (green) in the Alexafluor-488 channel. (C) A barley leaf sample showing positive labelling of (1,3;1,4)-β-glucan (BG1, green) and de-esterified pectin (LM19, magenta). (D-O) Comparison of control and heat stressed anthers and ovules in barley florets of the three varieties. Merged images of the antibody labelling patterns are shown. (D) Optic control anther. (E) Optic heat-stressed anther. (F) Moonshine control anther. (G) Moonshine heat-stressed anther. (H) Planet control anther. (I) Planet heat-stressed anther. (J) Optic control ovule. The ovary wall (ow), integuments (int), nucellus (nu) and embryo sac (es) are indicated. (K) Optic heat-stressed ovule. In this ovule the antipodals (an) are also evident. (L) Moonshine control ovule. (M) Moonshine heat-stressed ovule. (N) Planet control ovule. (O) Planet heat-stressed ovule. Bar = 50µm in all images.

*4.4.4 Seed set after heat stress*

The number of tillers and seeds per spike was determined for all three varieties after both treatments and in control conditions (Table 4.1). In Optic, there was no significant difference between the average number of seeds per spike after meiosis heat stress and the control. However, there was a significant reduction of average seed number per spike after mitosis heat stress compared to the control, from 19 to 6 seeds per spike. In Moonshine there was a significant decrease in seed set after both meiosis and mitosis heat treatments, from 25 in the control conditions to 16 and 14 respectively. The same could be observed in RGT Planet where a significant decrease was identified after both heat treatments. In control conditions, there was an average of 28 seeds per spike, while after meiosis heat stress this was reduced to 12 and after mitosis heat stress to 13.

| Variety | Treatment | Average number of tillers/plant | Number of tagged tillers | Average number of seeds/spike |
|---|---|---|---|---|
| **Optic** | Control | 7±1.8 | | 19±2.8 |
| | Meiosis | 6±0.7 | 8 | 14±4.6 |
| | Mitosis | 5±0.9 | 12 | 6±3.8* |
| **Moonshine** | Control | 7±1 | | 25±2.0 |
| | Meiosis | 6±0.7 | 5 | 16±3.4* |
| | Mitosis | 6±1.1 | 16 | 14±2.4* |
| **RGT Planet** | Control | 6±1.2 | | 28±2.8 |
| | Meiosis | 6±1.6 | 12 | 12±3.4* |
| | Mitosis | 6±1.3 | 13 | 13±4.1* |

**Table 4.1** Average number of tillers per plant and seeds per spike, and number of tagged tillers for the three different varieties in control conditions, after meiosis heat treatment or after mitosis heat treatment ± standard deviation. Stars indicate a p -value <0.05.

## 4.5 Discussion

Three barley varieties were assessed for their resilience to heat stress during reproductive stages. Plants that experienced heat stress at two key stages in their reproductive development (meiosis and mitosis) showed severe deficiencies in anther development, and these are likely to be the leading cause of sterility due to high temperature stress. A short period of heat stress during early development led to significantly smaller and deformed anthers. Although the anthers were harvested at the same time from heat stressed and control plants, the septa in the heat stressed anthers had already broken, suggesting a more rapid developmental progression in the heat stressed lines and or a change in the physical properties of the anther walls. It has been suggested that thick locule walls and well-developed cavities in the septa may be responsible for the tolerance to high temperatures in rice (Matsui *et al.*, 2001). The cavities are hypothesised to enable easy rupture of the septa in response to the swelling of the pollen grains while the thick locule walls promote the swelling of the pollen grains by retaining water in the locules (Matsui *et al.*, 2001). The locule walls and cavities seemed less developed in the heat stressed anthers, which might be another reason why the pollen grains did not develop correctly. Saini *et al.* (1984) described two types of anther defects after heat stress in wheat. Type 1 typically had premature tapetal degeneration which resulted in periplasmodial invasion of the locule at meiosis and ultimately led to sterility. Degeneration of the outer layers of the anther wall was also observed. The second type was characterised by microspores that completed pollen grain mitosis I (PGM1), but a proportion of which became disoriented from the tapetum and developed no further. The breaking of the septa identified in heat-stressed barley might be attributed to the fragility of the anther walls, as we can see some degeneration of anther wall layers in the immunolabelled images from RGT Planet.

Pollen development was severely affected by heat stress during both meiosis and mitosis, with decreased viability and a reduced accumulation of starch. However, as shown by the X-ray CT images of Moonshine florets after meiosis heat stress, and by the presence of viable pollen in Optic after meiosis heat stress, pollen is still formed in some heat-stressed florets and some may be viable. It has been suggested that stresses such as water stress could inhibit starch deposition in rice and wheat pollen, either by decreasing the availability of assimilates or by impairing the activities of

enzymes involved in starch biosynthesis (Ji *et al.*, 2010; Sheoran and Saini, 1996). Pressman *et al.* (2002) found that continuous high temperatures prevented the transient increase in starch concentration in tomato pollen grains which led to decreases in the concentrations of soluble sugars in the anther walls and the pollen grains. They concluded that this might contribute to decreased pollen viability in tomato after heat stress. This has been confirmed in other species, such as sorghum (Jain *et al.*, 2007) and has been supported by evidence that barley grains from heat stressed plants accumulated less starch than grains from control plants due to reduced conversion of sucrose to starch (Wallwork *et al.*, 1998). Heat stress has been reported to have a negative effect on the activities of enzymes involved in the sucrose-to-starch metabolism in cereals which might explain the reduction in starch content (Duke and Doehlert, 1996; Hurkman *et al.*, 2003; Wilhelm *et al.*, 1999).

The female reproductive organs did not show any significant differences in embryo sac phenotypes after heat stress. However, the carpels were bigger and the ovules appeared to have developed faster than the controls. This suggests that in the three varieties under examination, the female reproductive organs are not as severely impacted by heat stress as anthers at the meiotic and mitotic stages of development. The immunohistology presented in this paper and previous research shows that the cell walls in the anthers, specifically the tapetum, are very vulnerable to heat stress. The developmental program of the tapetum has been shown to be disrupted by abiotic stress (Parish *et al.*, 2012). In contrast, little is known about the effects of abiotic stress on cellular morphology and the regulatory developmental network of the carpel and ovule. Several studies indicate that both pre- and post-fertilisation stages of ovary development are sensitive to stress, but this varies depending on the species and genotype (Bac-Molenaar *et al.*, 2015a; Onyemaobi *et al.*, 2017; Sun *et al.*, 2004; Zinn *et al.*, 2010). In wheat, plants exposed to severe heat stress at the start of meiosis experienced disrupted nucellus and integument development, and complete ovule abortion at a frequency of 30% (Saini *et al.*, 1983). The nucellar cells in all three barley cultivars examined here, particularly Optic, appeared to be somewhat disorganised and enlarged after heat stress relative to controls. However, in all cases, similar immunolabelling patterns for de-esterified pectin were observed around what appeared to be an intact embryo sac. Barley only has one ovule per floret and therefore needs to safeguard its one chance of survival. The multi-layered

nucellus might be one of the reasons the developmental program of the ovule is more robust than that of the anther (Wilkinson *et al.*, 2018). The larger size of the carpels could be due to swelling of unfertilized ovaries resulting in a second opening to promote cross-pollination (Okada *et al.*, 2018). The broken septa in the anthers in the heat stressed plants might indicate that plants exposed to short pulse of heat stress around meiosis might respond by speeding up reproductive organ development. A similar phenomenon was previously been reported where heat stress hastened spike development and reduced spike number, thus impacting the number of grains per spike (Halse and Weir, 1974; Johnson and Kanemasu, 1983; Saini and Aspinall, 1982). This is consistent with the reduction in seeds per spike we observed in the three varieties after both heat stress treatments.

The differences in heat stress sensitivity between the three varieties could be due to a difference in genetic composition or stress response factors, which may be the consequence of altered gene expression leading to differential resilience or alternatively altered developmental progression so that stress exposure is minimised.

## 4.6 Conclusions

A short period of heat stress during the reproductive phase in barley is detrimental for the development of the male reproductive organs, but less so for the female reproductive organs. Results indicate that after heat stress, floret development was generally hastened, which might reflect an overall stress response from the plant to ensure seed set, albeit with a smaller amount of seeds. Prolonged heat stress at a later stage in development (mitosis) showed more severe effects in the male reproductive organs in Optic than in the other two varieties, with no viable pollen and significantly more sterility. The female reproductive organs of the three cultivars showed no severe effects after heat stress, at least in terms of embryo sac expansion. Overall, RGT Planet performed worst compared to the control conditions and Moonshine performed best. However, there were less florets per spike in the heat stressed plants across all three varieties compared to control plants. Further investigation will be required to identify the traits that contribute to Moonshine being more heat tolerant than the other two varieties. The data provided here provides a basis for further studies into differential heat stress responses during key stages of barley reproductive development. Moreover, the use of X-ray imaging is a promising

new method to visualise the morphology of floret organs without dissection and manipulation with chemicals, giving a more representative image and accurate volume measurements.

## 4.7 Acknowledgements

CC is studying on a Dual PhD Degree at The University of Nottingham and University of Adelaide, and is funded from a PhD Scholarship from The University of Nottingham. The Hounsfield Facility received funding from ERC (FUTUREROOTS; Brussels, Belgium), BBSRC (Swindon, UK), and the Wolfson Foundation (London, UK). Special thanks to Dr. Brian Atkinson for help with the X-ray imaging, Dr. Jamal Faraj for help with the sterility assessment and Laura Wilkinson for providing advice regarding use of the LM19 antibody.

## 4.8 References


**Aghamolki MTK, Yusop MK, Oad FC, Jaafar HZ, Khalatbari AM, Kharidah S, Musa MH**. 2016. Impact of heat stress on growth and yield of rice (Oryza sativa L.) cultivars. *Journal of Food, Agriculture & Environment* **14**, 111-116.

**AHDB**. 2016. AHDB Recommended Lists 2016-2017.

**AHDB**. 2017. Spring Barley Harvest Results 2017.

**Bac-Molenaar JA, Fradin EF, Becker FFM, Rienstra JA, van der Schoot J, Vreugdenhil D, Keurentjes JJB**. 2015. Genome-Wide Association Mapping of Fertility Reduction upon Heat Stress Reveals Developmental Stage-Specific QTLs in Arabidopsis thaliana. *The Plant Cell* **27**, 1857-1874.

**Barnabas B, Jager K, Feher A**. 2008. The effect of drought and heat stress on reproductive processes in cereals. *Plant Cell Environ* **31**, 11-38.

**Bita CE, Gerats T**. 2013. Plant tolerance to high temperature in a changing environment: scientific fundamentals and production of heat stress-tolerant crops. *Front Plant Sci* **4**, 273.

**Bomblies K, Higgins JD, Yant L**. 2015. Meiosis evolves: adaptation to external and internal environments. *New Phytologist* **208**, 306-323.

**Burton RA, Collins HM, Kibble NA, Smith JA, Shirley NJ, Jobling SA, Henderson M, Singh RR, Pettolino F, Wilson SM, Bird AR, Topping DL, Bacic A, Fincher GB**. 2011. Over-expression of specific HvCslF cellulose synthase-like genes in transgenic barley increases the levels of cell wall (1,3;1,4)-beta-d-glucans and alters their fine structure. *Plant Biotechnol J* **9**, 117-135.

**Chang F, Zhang Z, Jin Y, Ma H**. 2014. Cell Biological Analyses of Anther Morphogenesis and Pollen Viability in Arabidopsis and Rice. In: Riechmann JL, Wellmer F, eds. *Flower Development: Methods and Protocols*. New York, NY: Springer New York, 203-216.

**Christidis N, Jones GS, Stott PA**. 2014. Dramatically increasing chance of extremely hot summers since the 2003 European heatwave. *Nature Climate Change* **5**, 46.

**Cooper P, Ho T-HD, Hauptmann RM**. 1984. Tissue Specificity of the Heat-Shock Response in Maize. *Plant Physiology* **75**, 431.

**David BL, Christopher BF**. 2007. Global scale climate–crop yield relationships and the impacts of recent warming. *Environmental Research Letters* **2**, 014002.

**Delphine D, Declan C, Navin R, Jeff P, Rachel W**. 2014. Global crop yield response to extreme heat stress under multiple climate change futures. *Environmental Research Letters* **9**, 034011.

**Draeger T, Moore G**. 2017. Short periods of high temperature during meiosis prevent normal meiotic progression and reduce grain number in hexaploid wheat (Triticum aestivum L.). *Theoretical and Applied Genetics* **130**, 1785-1800.

**Duke ER, Doehlert DC**. 1996. Effects of heat stress on enzyme activities and transcript levels in developing maize kernels grown in culture. *Environmental and Experimental Botany* **36**, 199-208.

**Farooq M, Bramley H, Palta JA, Siddique KHM**. 2011. Heat Stress in Wheat during Reproductive and Grain-Filling Phases. *Critical Reviews in Plant Sciences* **30**, 491-507.

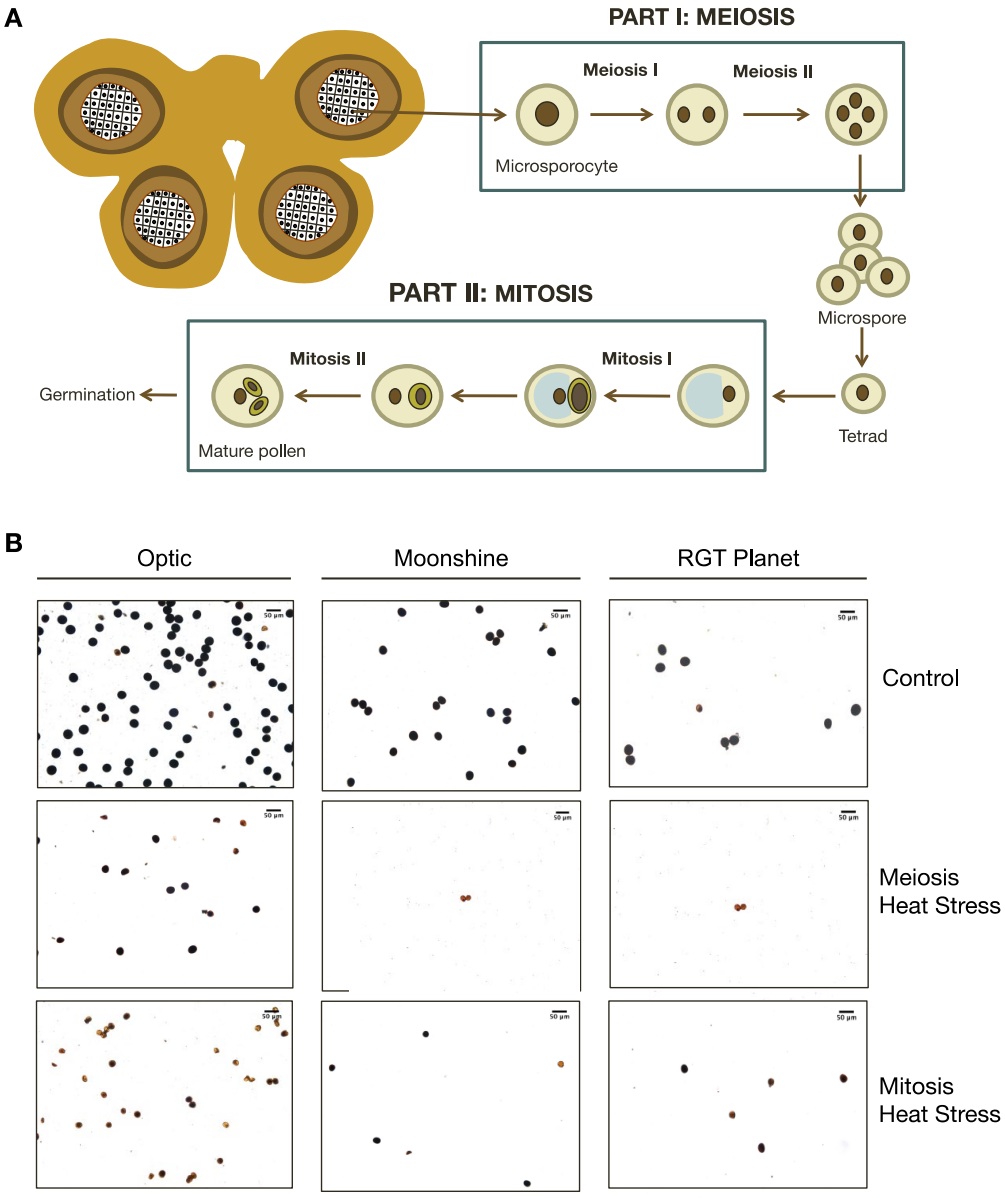
**Feder ME, Hofmann GE**. 1999. HEAT-SHOCK PROTEINS, MOLECULAR CHAPERONES, AND THE STRESS RESPONSE: Evolutionary and Ecological Physiology. *Annual Review of Physiology* **61**, 243-282.

**Gómez JF, Wilson ZA**. 2012. Non-destructive staging of barley reproductive development for molecular analysis based upon external morphology. *Journal of Experimental Botany* **63**, 4085-4094.
**Guo P, Baum M, Grando S, Ceccarelli S, Bai G, Li R, von Korff M, Varshney RK, Graner A, Valkoun J**. 2009. Differentially expressed genes between drought-tolerant and drought-sensitive barley genotypes in response to drought stress during the reproductive stage. *Journal of Experimental Botany* **60**, 3531-3544.
**Halse NJ, Weir RN**. 1974. Effects of temperature on spikelet number of wheat. *Australian Journal of Agricultural Research* **25**, 687-695.
**Hartl FU**. 1996. Molecular chaperones in cellular protein folding. *Nature* **381**, 571.
**Hong S-W, Vierling E**. 2000. Mutants of Arabidopsis thaliana defective in the acquisition of tolerance to high temperature stress. *Proceedings of the National Academy of Sciences of the United States of America* **97**, 4392-4397.
**Hurkman WJ, McCue KF, Altenbach SB, Korn A, Tanaka CK, Kothari KM, Johnson EL, Bechtel DB, Wilson JD, Anderson OD, DuPont FM**. 2003. Effect of temperature on expression of genes encoding enzymes for starch biosynthesis in developing wheat endosperm. *Plant Science* **164**, 873-881.
**IPCC**. 2014. Climate Change 2014: Mitigation of Climate Change. Contribution of Working Group III to the Fifth Assessment Report of the Intergovernmental Panel on Climate Change. In: Edenhofer O, R. Pichs-Madruga, Y. Sokona, E. Farahani, S. Kadner, K. Seyboth, A. Adler, I. Baum, S. Brunner, P. Eickemeier, B. Kriemann, J. Savolainen, S. Schlömer, C. von Stechow, T. Zwickel and J.C. Minx (eds.), ed. *Cambridge University Press*. Cambridge, United Kingdom and New York, NY, USA.
**Jain M, Prasad PV, Boote KJ, Hartwell AL, Jr., Chourey PS**. 2007. Effects of season-long high temperature growth conditions on sugar-to-starch metabolism in developing microspores of grain sorghum (Sorghum bicolor L. Moench). *Planta* **227**, 67-79.
**Ji X, Shiran B, Wan J, Lewis DC, Jenkins CLD, Condon AG, Richards RA, Dolferus R**. 2010. Importance of pre-anthesis anther sink strength for maintenance of grain number during reproductive stage water stress in wheat. *Plant, Cell & Environment* **33**, 926-942.
**Johnson RC, Kanemasu ET**. 1983. Yield and Development of Winter Wheat at Elevated Temperatures1. *Agronomy Journal* **75**, 561-565.
**Kruszka K, Pacak A, Swida-Barteczka A, Nuc P, Alaba S, Wroblewska Z, Karlowski W, Jarmolowski A, Szweykowska-Kulinska Z**. 2014. Transcriptionally and post-transcriptionally regulated microRNAs in heat stress response in barley. *J Exp Bot* **65**, 6123-6135.
**Lesk C, Rowhani P, Ramankutty N**. 2016. Influence of extreme weather disasters on global crop production. *Nature* **529**, 84.
**Maestri E, Klueva N, Perrotta C, Gulli M, Nguyen HT, Marmiroli N**. 2002. Molecular genetics of heat tolerance and heat shock proteins in cereals. *Plant Mol Biol* **48**, 667-681.
**Mascarenhas JP, Crone DE**. 1996. Pollen and the heat shock response. *Sexual Plant Reproduction* **9**, 370-374.

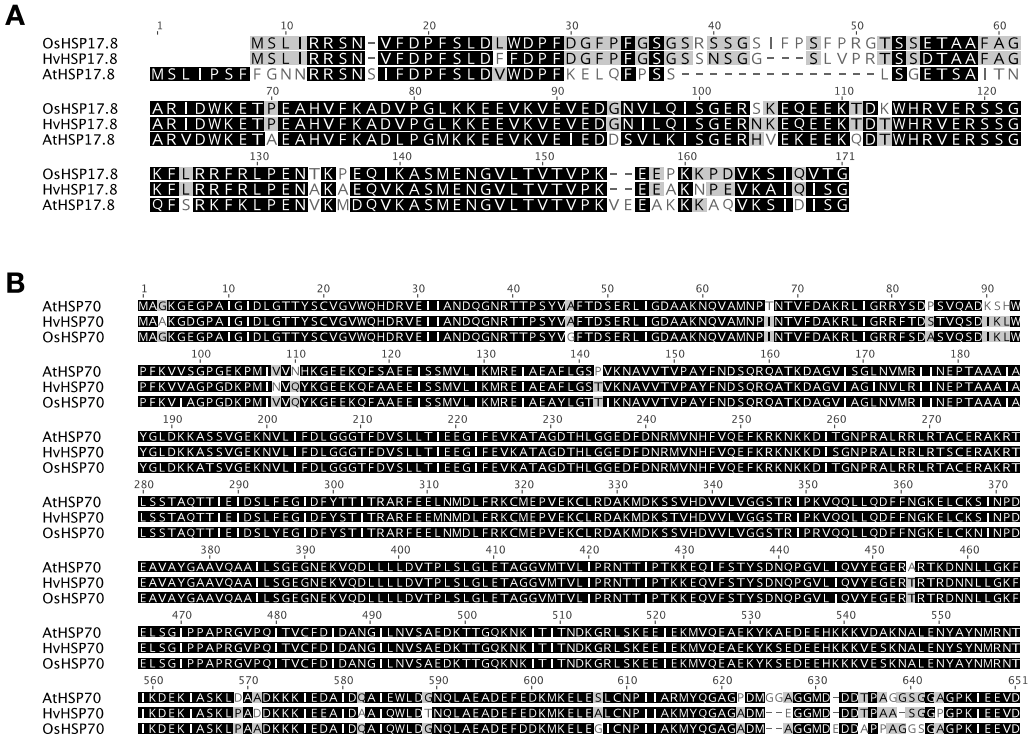
**Matsui T, Omasa K, Horie T**. 2001. The Difference in Sterility due to High Temperatures during the Flowering Period among Japonica-Rice Varieties. *Plant Production Science* **4**, 90-93.
**Meikle PJ, Hoogenraad NJ, Bonig I, Clarke AE, Stone BA**. 1994. A (1-->3,1-->4)-beta-glucan-specific monoclonal antibody and its use in the quantitation and immunocytochemical location of (1-->3,1-->4)-beta-glucans. *Plant J* **5**, 1-9.
**Montero-Barrientos M, Hermosa R, Cardoza RE, Gutiérrez S, Nicolás C, Monte E**. 2010. Transgenic expression of the Trichoderma harzianum hsp70 gene increases Arabidopsis resistance to heat and other abiotic stresses. *Journal of Plant Physiology* **167**, 659-665.
**Nguyen HT, Joshi CP, Klueva N, Weng J, Hendershot KL, Blum A**. 1994. The Heat-Shock Response and Expression of Heat-Shock Proteins in Wheat Under Diurnal Heat Stress and Field Conditions. *Functional Plant Biology* **21**, 857-867.
**Nicolas ME, Gleadow RM, Dalling MJ**. 1985. Effect of Post-anthesis Drought on Cell Division and Starch Accumulation in Developing Wheat Grains. *Annals of Botany* **55**, 433-444.
**Okada T, Jayasinghe JEARM, Nansamba M, Baes M, Warner P, Kouidri A, Correia D, Nguyen V, Whitford R, Baumann U**. 2018. Unfertilized ovary pushes wheat flower open for cross-pollination. *Journal of Experimental Botany* **69**, 399-412.
**Onyemaobi I, Liu H, Siddique KHM, Yan G**. 2017. Both Male and Female Malfunction Contributes to Yield Reduction under Water Stress during Meiosis in Bread Wheat. *Frontiers in Plant Science* **7**.
**Ortiz R, Sayre KD, Govaerts B, Gupta R, Subbarao GV, Ban T, Hodson D, Dixon JM, Iván Ortiz-Monasterio J, Reynolds M**. 2008. Climate change: Can wheat beat the heat? *Agriculture, Ecosystems & Environment* **126**, 46-58.
**Parish RW, Phan HA, Iacuone S, Li SF**. 2012. Tapetal development and abiotic stress: a centre of vulnerability. *Functional Plant Biology* **39**, 553-559.
**Prasad PVV, Pisipati SR, Mutava RN, Tuinstra MR**. 2008. Sensitivity of Grain Sorghum to High Temperature Stress during Reproductive Development All rights reserved. No part of this periodical may be reproduced or transmitted in any form or by any means, electronic or mechanical, including photocopying, recording, or any information storage and retrieval system, without permission in writing from the publisher. Permission for printing and for reprinting the material contained herein has been obtained by the publisher. *Crop Science* **48**, 1911-1917.
**Pressman E, Peet MM, Pharr DM**. 2002. The Effect of Heat Stress on Tomato Pollen Characteristics is Associated with Changes in Carbohydrate Concentration in the Developing Anthers. *Annals of Botany* **90**, 631-636.
**Saini H, Sedgley M, Aspinall D**. 1983. Effect of Heat Stress During Floral Development on Pollen Tube Growth and Ovary Anatomy in Wheat (<I>Triticum aestivum</I> L.). *Functional Plant Biology* **10**, 137-144.
**Saini HS, Aspinall D**. 1982. Abnormal Sporogenesis in Wheat (Triticum aestivum L.) Induced by Short Periods of High Temperature. *Annals of Botany* **49**, 835-846.
**Saini HS, Sedgley M, Aspinall D**. 1984. Development Anatomy in Wheat of Male Sterility Induced by Heat Stress, Water Deficit or Abscisic Acid. *Functional Plant Biology* **11**, 243-253.

**Sakata T, Takahashi H, Nishiyama I, Higashitani A**. 2000. Effects of High Temperature on the Development of Pollen Mother Cells and Microspores in Barley Hordeum vulgare L. *Journal of Plant Research* **113**, 395-402.
**SeedForce**. 2017.
**Sheoran IS, Saini HS**. 1996. Drought-induced male sterility in rice: Changes in carbohydrate levels and enzyme activities associated with the inhibition of starch accumulation in pollen. *Sexual Plant Reproduction* **9**, 161-169.
**Stone P, Basra A**. 2001. The effects of heat stress on cereal yield and quality. *Crop responses and adaptations to temperature stress*. Binghampton: NY Food Products Press, 179-187.
**Sun K, Hunt K, Hauser BA**. 2004. Ovule Abortion in Arabidopsis Triggered by Stress. *Plant Physiology* **135**, 2358-2367.
**Sung DY, Vierling E, Guy CL**. 2001. Comprehensive Expression Profile Analysis of the Arabidopsis Hsp70 Gene Family. *Plant Physiology* **126**, 789-800.
**Teixeira EI, Fischer G, van Velthuizen H, Walter C, Ewert F**. 2013. Global hot-spots of heat stress on agricultural crops due to climate change. *Agricultural and Forest Meteorology* **170**, 206-215.
**Tracy SR, Gómez JF, Sturrock CJ, Wilson ZA, Ferguson AC**. 2017. Non-destructive determination of floral staging in cereals using X-ray micro computed tomography (μCT). *Plant Methods* **13**, 9.
**Verhertbruggen Y, Marcus SE, Haeger A, Ordaz-Ortiz JJ, Knox JP**. 2009. An extended set of monoclonal antibodies to pectic homogalacturonan. *Carbohydrate Research* **344**, 1858-1862.
**Wallwork MAB, Logue SJ, MacLeod LC, Jenner CF**. 1998. Effect of high temperature during grain filling on starch synthesis in the developing barley grain. *Functional Plant Biology* **25**, 173-181.
**Wang W, Vinocur B, Shoseyov O, Altman A**. 2004. Role of plant heat-shock proteins and molecular chaperones in the abiotic stress response. *Trends in Plant Science* **9**, 244-252.
**Wilhelm EP, Mullen RE, Keeling PL, Singletary GW**. 1999. Heat Stress during Grain Filling in Maize: Effects on Kernel Growth and Metabolism The research was funded as a joint collaboration between ICI Seeds (presently Garst Seed Co.), 2369 330th St., P.O. Box 500, Slater, IA 50244 and Iowa State University. Journal Paper no. J-18085 of the Iowa Agric. and Home Econ. Exp. Sta., Ames, IA, Project no. 2775, and supported by Hatch Act and State of Iowa. *Crop Science* **39**, 1733-1741.
**Wilkinson LG, Bird DC, Tucker MR**. 2018. Exploring the Role of the Ovule in Cereal Grain Development and Reproductive Stress Tolerance. *Annual Plant Reviews online*.
**Wilson ZA, Zhang D-B**. 2009. From Arabidopsis to rice: pathways in pollen development. *Journal of Experimental Botany* **60**, 1479-1492.
**Zampieri M, Ceglar A, Dentener F, Toreti A**. 2017. Wheat yield loss attributable to heat waves, drought and water excess at the global, national and subnational scales. *Environmental Research Letters* **12**, 064008.
**Zinn KE, Tunc-Ozdemir M, Harper JF**. 2010. Temperature stress and plant sexual reproduction: uncovering the weakest links. *Journal of Experimental Botany* **61**, 1959-1968.

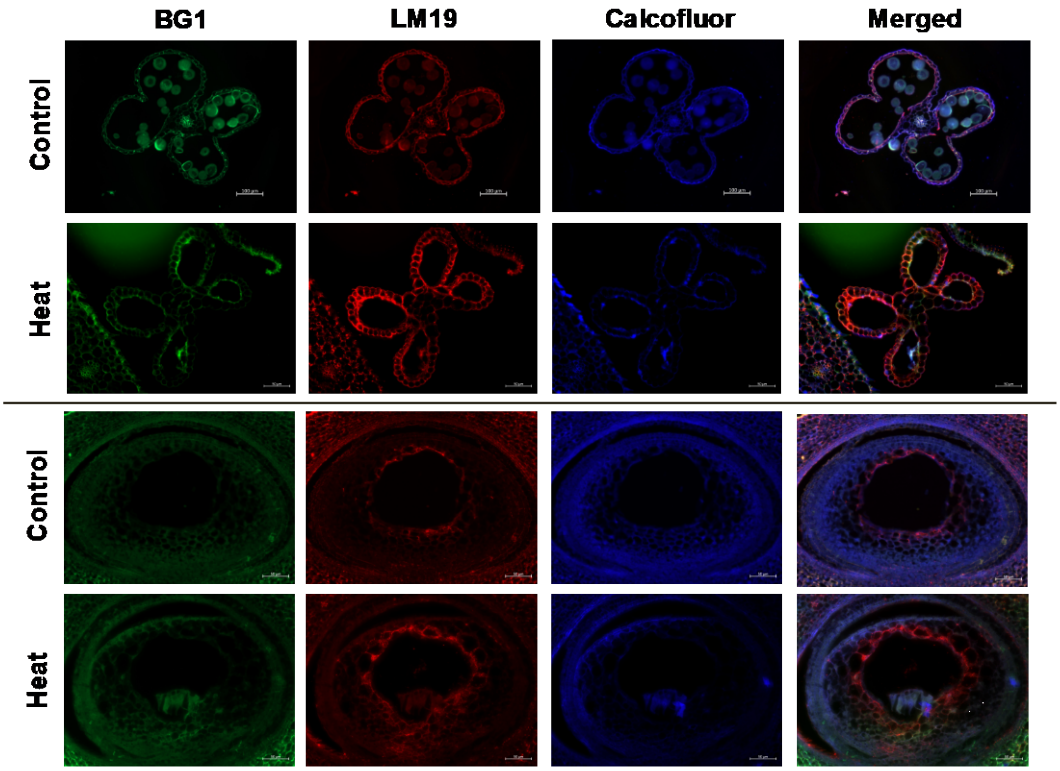
# Chapter 4: Supplementary files



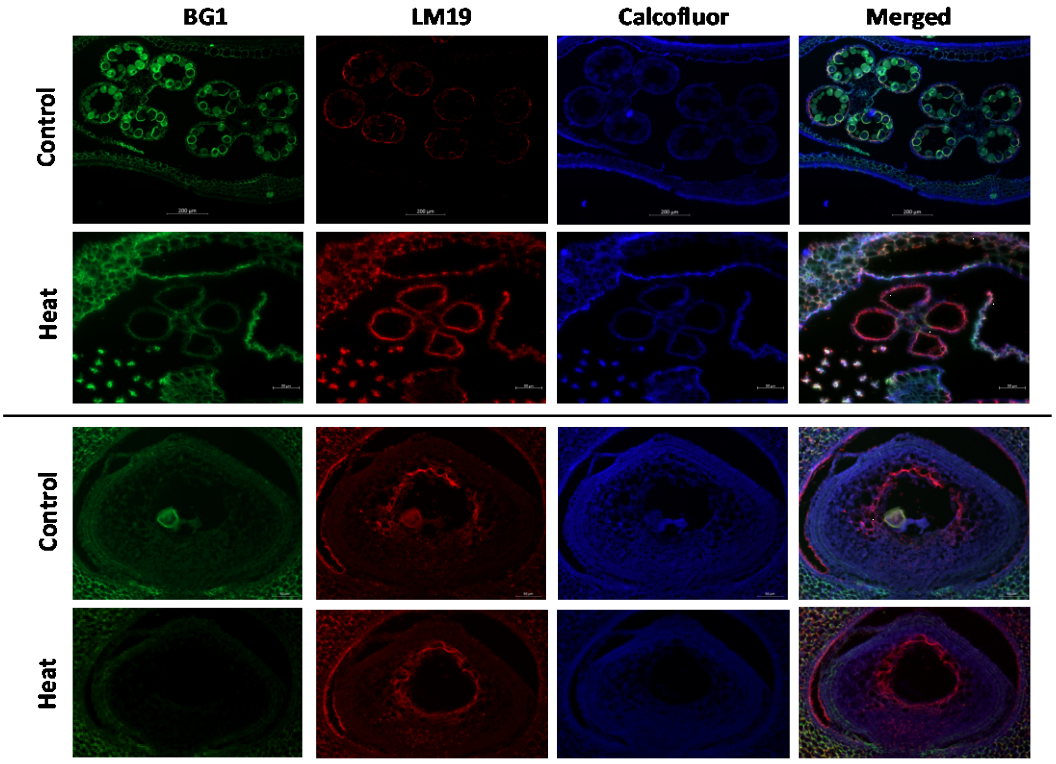

**Supplementary Figure S1 Schematic of heat stress treatments during pollen development for barley varieties and pollen viability in barley cultivars Optic, Moonshine and RGT Planet.** (A) Two pots with four plants each of the three varieties were submitted to either meiosis heat stress during meiosis I and II of pollen development, or mitosis heat stress during mitosis I and II of pollen development. (B) Pollen viability is shown from a randomly selected floret right before anthesis from heat stressed plants and control plants. Black pollen is viable, while yellow/brown pollen is not viable; low numbers of pollen reflect the lack of pollen in the mature anthers.



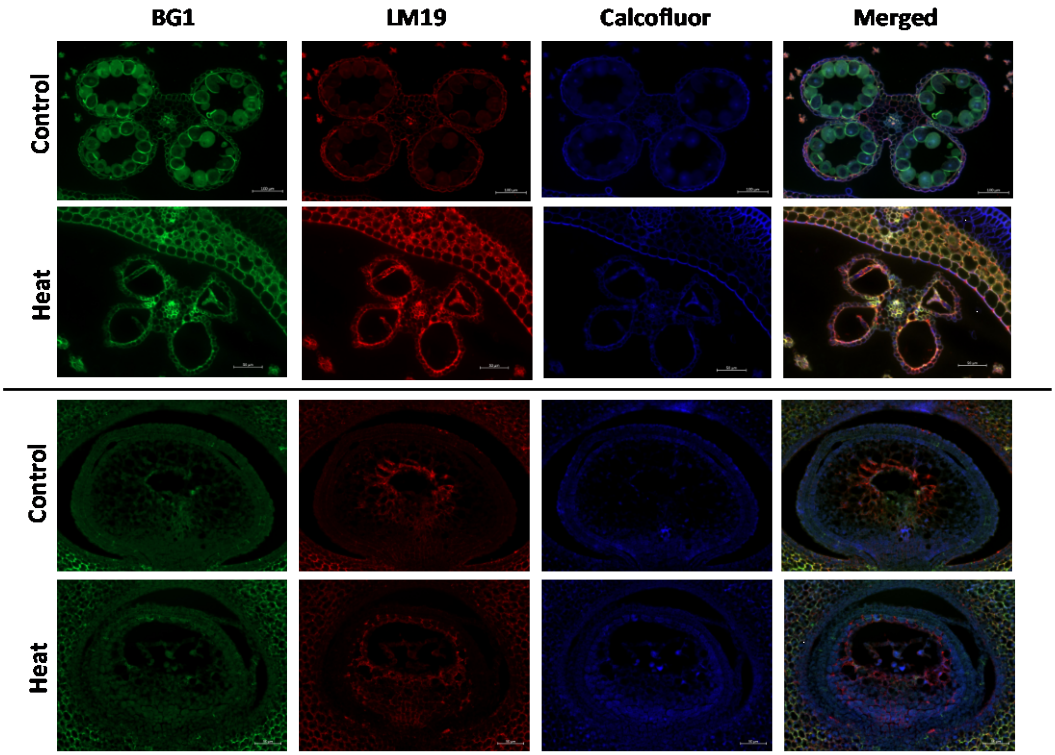

**Supplementary Figure S2 Phylogenetic analysis of rice, Arabidopsis and barley HSP17.8 (A) and HSP70 orthologs (B).** The alignments were constructed using the Geneious alignment method and the Blosum62 cost matrix in Geneious.



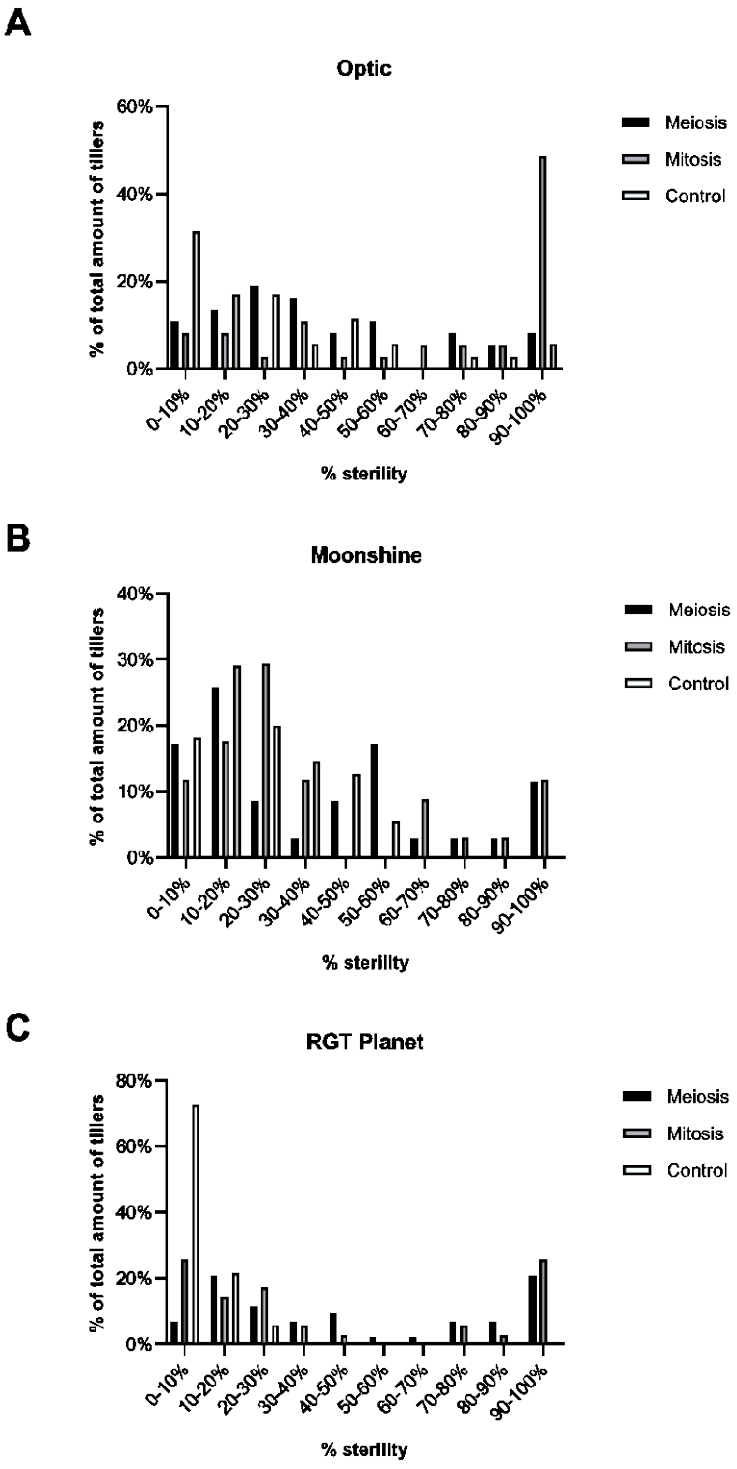

**Supplementary Figure S4 Immunolabelling of cell wall components in anthers and ovules in Optic.** Comparison of control and heat stressed anthers and ovules in barley florets of the variety RGT Planet. Antibodies include BG1 (1,3;1,4-β-glucan, green) and LM19 (low methylesterified pectin, red). Calcofluor White counterstain was used to detect cellulose and mixed-linkage glucan (blue).




**Supplementary Figure S5 Immunolabelling of cell wall components in anthers and ovules in Moonshine.** Comparison of control and heat stressed anthers and ovules in barley florets of the variety RGT Planet. Antibodies include BG1 (1,3;1,4-β-glucan, green) and LM19 (low methylesterified pectin, red). Calcofluor White counterstain was used to detect cellulose and mixed-linkage glucan (blue).




**Supplementary Figure S6 Immunolabelling of cell wall components in anthers and ovules in RGT Planet.** Comparison of control and heat stressed anthers and ovules in barley florets of the variety RGT Planet. Antibodies include BG1 (1,3;1,4-β-glucan, green) and LM19 (low methylesterified pectin, red). Calcofluor White counterstain was used to detect cellulose and mixed-linkage glucan (blue).




**Supplementary Figure S7 Frequency distribution of sterility in heat stressed and control conditions in three European barley varieties.** The percentage sterility (florets that did not produce seed) was calculated for all three varieties in control conditions and after meiosis or mitosis heat treatment for all pots (A, B, C).

# Chapter 5: Discussion

Cindy Callens[1,2], Matthew R. Tucker[2], Dabing Zhang[2,3] and Zoe A. Wilson[1]

[1] School of Biosciences, University of Nottingham, Sutton Bonington Campus, Loughborough, Leicestershire LE12 5RD, UK
[2] School of Agriculture, Food and Wine, University of Adelaide, Waite Campus, Urrbrae, SA, Australia
[3] School of Life Sciences and Biotechnology, Shanghai Jiao Tong University, Shanghai 200240, China

In this thesis tissue-specific expression patterns of all the ABCDE-model MADS-box genes in barley were presented at developmental stages starting from stem elongation and the formation of the primary sporogenous cells in the anthers, and ending at anthesis. In situ hybridization analysis of the B-class gene *HvBM2* was carried out to localise the expression more specifically. The CRES-T dominant repression system was used to investigate the function of the B-class DEF/GLO MADS-box proteins HvBM2, HvBM4 and HvBM16. Although the sequences, the expression patterns and the functions of the ABCDE MADS-box genes are conserved between species, gene duplication throughout evolution can lead to non-functionalization, sub-functionalization or neo-functionalization (Schilling *et al.*, 2015). These changes can affect the ABCDE model and can ultimately lead to new flower morphologies. Understanding the ABCDE model in different species can provide a clearer understanding of how the flower morphology in particular species evolved and how it might still change in the future.

MADS-box genes had been shown to be involved in abiotic stress response. We investigated the effects of high temperature conditions on the reproductive development in three commercial European spring barley varieties at two vulnerable reproductive stages: meiosis and mitosis. Understanding the effects of heat stress on barley floral organ morphology and fertility in different varieties is important to find tolerant and susceptible varieties that can be used to investigate the underlying mechanism of heat stress tolerance.

## 5.1 Expression of the A-, Bsister-like, C-, D-, E- and AGL6-like MADS-box genes in barley

The ABCDE-model MADS-box genes can be divided in five different classes based on their homeotic function: class A, B, C, D and E genes (Bowman *et al.*, 1989, 1991; Coen and Meyerowitz, 1991; Theissen and Saedler, 2001; Weigel and Meyerowitz, 1994). Two classes, phylogenetically related to the B-class and the E-class respectively have also been added: the $B_{sister}$-like genes and the AGL6-like genes (Becker *et al.*, 2002; Becker and Theissen, 2003). The A- and E-class protein complexes specify sepals in the first whorl. Complexes of A-, B- and E-class proteins specify petals in the second whorl (Honma and Goto, 2001). B-, C- and E-class complexes specify stamens in the third whorl and C- and E-class protein complexes specify carpels in the fourth whorl (Coen and Meyerowitz, 1991; Honma

and Goto, 2001). D-class proteins specify ovules (Colombo *et al.*, 1995). The $B_{sister}$-like genes function in the ovule, while the AGL6-like genes are thought to function in all four whorls (Becker and Theissen, 2003; Munster *et al.*, 2001; Reinheimer and Kellogg, 2009).

The tissue-specific expression analysis from early stem elongation to heading in *Hordeum vulgare cv. Golden Promise* presented in this thesis gives us a first idea of the possible functions of the ABCDE MADS-box genes in barley. The two most abundantly expressed genes are *HvBM15* and *HvBM1*. The A-class gene *HvBM15* shows expression in all stages of development and in all tissues except the stamens and carpel. *HvBM1* is the most abundant gene in the E-class and is, similar to *HvBM15*, expressed in all tissues across developmental stages, except for the reproductive tissues where it is absent in the stamen and only has low expression in the carpel. Both of these genes are most likely to be involved in early development and development in whorls 1 and 2.

*HvBM14* is the most abundant A-class gene in the reproductive tissues. The E-class genes *HvBM7* and *HvBM8* might also play a more important role in reproductive development, shown by their expression in the carpel and the stamen. *HvBM6* is most abundantly expressed in the carpel in later stages of development. Clustering of these genes shows that *HvBM14* might play a minor role in carpel development, while *HvBM7*, *HvBM8* and *HvBM6* might be part of the floral quartets determining the carpel identity and development. The other classes are more specifically expressed in the inner whorls. The B-class genes are known to be expressed in the reproductive organs and the lodicules, while the C-class genes are expressed in both stamens and carpels. D-class and $B_{sister}$-like genes are usually expressed in the ovule.

The $B_{sister}$ genes in barley are most abundant in the carpel and two of them are also expressed in the palea/lemma and in the awns. *HvBM30* expression has also been found in stamens late in development. All three of them are however overall not highly expressed, which could indicate a function in tissues or at developmental stages not examined here, for example in the developing seed. The C-class genes are expressed in the carpel and later in development also in the stamen. *HvBM58* is more abundant than *HvBM3* which might indicate that HvBM3 doesn't play an important role in carpel and stamens development. HvBM3 might be involved in different

floral development processes at different stages as a result of sub-functionalization due to gene duplication, as has been shown for OsMADS3 and OsMADS58 in rice (Yamaguchi *et al.*, 2006). Knock-out mutants of *HvBM3* and *HvBM58* and a double knock-out of *HvBM3* and *HvBM58* might provide more answers.
Similarly, D-class genes are only expressed in the carpel. The low expression of *HvBM21* is similar to the low expression of *OsMADS21* in rice and might indicate that the gene plays a more important role in the developing seeds as was shown for OsMADS21 (Arora *et al.*, 2007; Dreni *et al.*, 2007).

Overall, there are a lot of similarities between the expression patterns found in barley for the ABCDE MADS-box genes and those found in rice, wheat or maize. Rice has a fourth A-class gene, *OsMADS20*, which is lacking in barley, wheat and maize. However, RNAi lines of OsMADS20 showed no observable phenotype and the quadruple mutant *osmads14/15/18/20* does not show a more severe phenotype than the double mutant *osmads14/15* (Wu *et al.*, 2017). This might indicate that OsMADS20 has no role in floral organ development and is therefore not found in other closely related species. These results also indicate that OsMADS18 has no function in floral organ development, but other studies have shown that it may be involved in promoting the differentiation of the vegetative shoot or in seed development (Fornara *et al.*, 2004; Wu *et al.*, 2017). This is supported by the low expression values found for *HvBM18* in barley, indicating that HvBM18 might have a similar role as OsMADS18. The $B_{sister}$-like genes seem conserved in rice, maize, wheat and barley. However, in rice OsMADS30 was found to lack the characteristic $B_{sister}$ motifs and a mobile element was found to be inserted in the C-domain of the gene (Becker *et al.*, 2002; Schilling *et al.*, 2015; Yang *et al.*, 2012). This changed the expression pattern and the function of OsMADS30 (Schilling *et al.*, 2015). This change seems to have no effect on reproductive development, which might indicate that OsMADS29 and OsMADS31 are sufficient for the $B_{sister}$ function. Functional analysis of the $B_{sister}$-like genes in maize, wheat and barley might confirm this hypothesis. Expression patterns and functions of the C- and D-class genes seem to be well conserved between rice, wheat and barley. However, the relative expression values shown in this thesis indicate that HvBM58 plays a more important role than HvBM3 in stamens and carpel development, which is the complete opposite of what has been shown in rice (Yamaguchi *et al.*, 2006). The E-class genes are also well

conserved in rice, barley and wheat. Although SEPALLATA3 (SEP3) has been identified as a 'hub' protein in Arabidopsis, the expression patterns shown here indicate that HvBM1, orthologue of SEP1, acts as a 'hub' protein in barley (Figure 2.9) (Immink *et al.*, 2009). Similar to the A-class, rice has an second AGL6-like gene that is not present in maize, barley or wheat. Although maize has two AGL6-like genes, they are both orthologues of *OsMADS6* and have arisen through gene duplication (Dreni and Zhang, 2016). RNAi lines of *OsMADS17* did not result in a phenotype, suggesting that *OsMADS17* is a redundant gene and is not necessary for floral development (Ohmori *et al.*, 2009).

## 5.2 Expression and protein-protein interactions of the B-class MADS-box genes in barley

Gene duplications are thought to have shaped the diversification of angiosperms (Theissen and Saedler, 2001). The B-class genes have been hypothesised to be involved in the morphological diversification of the perianth (Gioppato and Dornelas, 2019; Lamb and Irish, 2003). The observation of the more broadly expressed B-class genes and the spirally arranged floral organs with a gradual transition between them in basal angiosperms have lead to the 'fading borders' model (Buzgo *et al.*, 2004; Kim *et al.*, 2005; Soltis *et al.*, 2007; Soltis *et al.*, 2006). The 'fading borders' model suggests that in basal angiosperms the functions of floral transcription factors are not restricted to only one whorl of the floret. The model hypothesises that there is a gradual transition from the periphery to the centre of the flower (Buzgo *et al.*, 2004; Soltis *et al.*, 2007; Soltis *et al.*, 2006). Proof for this model was also found in the basal monocot *Triglochin Maritima* (Buzgo *et al.*, 2006). The B-class genes are believed to have gone through multiple gene duplication events (Stellari *et al.*, 2004). The first has led to the $B_{sister}$-like genes branching off from the main B-class genes (Becker *et al.*, 2002). Both lineages are still present, which points to an important function of both in floral organ development (Becker *et al.*, 2002; De Folter *et al.*, 2006).

In many monocots, these duplication events are apparent in the amount of B-class genes present. Multiple duplication events in the B-class in orchids has been hypothesised to have resulted in the formation of the labellum (Chang *et al.*, 2010). In contrast to *Arabidopsis*, grasses have multiple PI-like B-class genes (Chapter 1, Table 1). The B-class genes seem to play an important role in evolutionary floral

morphological diversification and are therefore an interesting class to explore further in different species. Not a lot is known about the B-class genes in barley. The expression analysis and functional analysis of these genes presented here helps shed more light on their role in the floral architecture in barley.

Although the expression analysis of the PI-like B-class genes was made difficult by other genes (receptor kinase 2 and 3) on the reverse strand, additional analysis showed no expression of the receptor kinases in the reproductive organs. Expression of the PI-like genes *HvBM2* and *HvBM4* was detected in the carpel and in the stamens. The *in situ* hybridization results shows that *HvBM2* expression is more specifically located in the carpel and the anther wall and filaments. *HvBM16* shows low expression compared to the PI-like genes. Due to its role in the conserved obligate heterodimers between the PI-like and the AP3-like B-class genes, it is unlikely that crops like barley are losing the *HvBM16* function. The clustering analysis showed that *HvBM2* and *HvBM16* might play a more important role in early carpel development and late stamens development, while *HvBM4* is more involved in later carpel development.

### 5.3 Function of the B-class genes in flower development in barley

To further understand the role of the B-class MADS-box genes in barley, a functional analysis was carried out. Dominant repression constructs were made using the chimeric repressor silencing technology (CRES-T) system, attaching an EAR-motif repression domain, also known as SRDX, to the gene of interest.

It has been shown that the SRDX repression domain can convert a transcriptional complex into a repressor via transrepression. Through protein-protein interactions the protein that contains the SRDX repression domain transfers repression activity to interacting proteins (Matsui and Ohme-Takagi, 2010). The MADS-box transcription factors are known to function through complex protein-protein interaction networks and help determine the four whorls of the floral architecture by forming so called ‘floral quartets’. Based on the findings from Matsui and Ohme-Takagi (2010), attaching the SRDX repression domain to one ABCDE MADS-box transcription factor will therefore transform the whole tetramer into a repressor complex.

AP3-like and PI-like B-class MADS-box genes form obligate heterodimers (Davies *et al.*, 1996). Attaching an SRDX repression domain to either the AP3-like or the PI-

like B-class gene would therefore result in turning the whole B-class centred complexes into a repressor, possibly yielding the same phenotype. The difference in observed phenotypes can thus in all possibility partly be due to the other interaction partners of the B-class genes and the associated functions of these complexes in determining different parts of the floral architecture.

Dominant repression of *HvBM4* by introducing *pUBI:HvBM4-SRDX* showed the most severe phenotype among the transformants examined. Stamens were converted into carpeloid structures and the carpel was small and underdeveloped, with the trichomes concentrated on the tip of the styles. The lodicules were small and had lost the rounded shape seen in the control lodicules. They also completely lacked trichomes. Continuing on from the consistency in the amount of gene duplications in the ABCDE MADS-box genes and in the expression patterns, barley shows the most similarity with wheat and shows some significant differences with rice (Table 5.1). *OsMADS4* RNAi lines in rice resulted in no phenotypic alterations, whereas a *WPI1* mutant in wheat showed carpeloid organs instead of stamens (Hama *et al.*, 2004; Yao *et al.*, 2008; Yoshida *et al.*, 2007). The carpel phenotype observed in the *pUBI:HvBM4-SRDX* line has not been described in any other crops or in *Arabidopsis*. The expression of *HvBM4* in the carpel later in development and the clustering analysis already suggested a potential important role for *HvBM4* in carpel development. The underdevelopment of the carpel in the *pUBI:HvBM4-SRDX* line now adds more certainty to this hypothesis.

The phenotypes observed in the *pUBI:HvBM2-SRDX* lines partly correspond to those observed in rice *OsMADS2* RNAi lines (Yadav *et al.*, 2007; Yao *et al.*, 2008; Yoshida *et al.*, 2007). Elongated, bract-like lodicules were observed but, contrary to the results in the OsMADS2 RNAi lines, stamens in our barley *pUBI:HvBM2-SRDX* lines showed changes in stamens shape and the appearance of trichomes on the top of the stamens. Aside from the morphological differences in the floral organs, pollen development was also severely impacted in SRDX lines exhibiting a phenotype, as shown by the sterility data from the *pUBI:HvBM2-SRDX* lines and the lack of viable pollen in the other SRDX lines. This could be due to the changes in anther morphology, or it could indicate that the B-class genes are involved in pollen development. A possible function for *HvBM2* in seed development is supported by

its expression in the nucellar projection and by the presence of aborted seeds in the *pUBI:HvBM2-SRDX* lines.

In contrast to the AP3-like mutants in rice (*OsMADS16* or *superwoman*) and maize (*SILKY*), no phenotype was observed in any of the *pUBI:HvBM16-SRDX* (Ambrose *et al.*, 2000; Nagasawa *et al.*, 2003). The lack of phenotype when a very strong phenotype was found in closely related crops, could be due to low expression of the *pUBI:HvBM16-SRDX* constructs in the lines or could point to a diminished role for *HvBM16* in barley.

| | Rice | Maize | Wheat | Barley |
|---|---|---|---|---|
| **A-class** | | | | |
| Palea/Lemma | OsMADS14, -15, -18 | ZMM4, -15, ZAP1 | WFUL1, -2, -3 | HvBM14, -15 |
| Lodicules | OsMADS14, -15, -18 | ZMM4, -15, ZAP1 | WFUL1, -2, -3 | HvBM14 |
| Carpel | OsMADS14, -18 | | WFUL1, -3 | HvBM14 |
| Stamens | OsMADS14, -18 | | WFUL1, -3 | HvBM14 |
| **B-class** | | | | |
| Lodicules | OsMADS2, -4, -16 | SILKY1, ZMM16, -18, -29 | WPI1, -2 | HvBM2, -4 |
| Carpel | OsMADS2, -4 | | | HvBM2 |
| Stamens | OsMADS2, -4, -16 | SILKY1, ZMM16, -18, -29 | WPI1, -2 | HvBM2, -4 |
| **$B_{sister}$-like** | | | | |
| Palea/Lemma | OsMADS30 | | | |
| Lodicules | OsMADS30 | | | |
| Carpel | OsMADS30 | ZMM17 | Wbsis | |
| Stamens | OsMADS30 | | | |
| **C-class** | | | | |
| Carpel | OsMADS3, -58 | | WAG1, -2 | HvBM3, -58 |
| Stamens | OsMADS3, -58 | ZMM2, -23 | WAG1, -2 | |
| **D-class** | | | | |
| Carpel | OsMADS13, -21 | ZMM1 | WSTK, TaAG-4 | HvBM13, -21 |
| Stamens | OsMADS21 | | WSTK, TaAG-4 | |
| **E-class** | | | | |
| Palea/Lemma | OsMADS1, -34 | ZMM24 | WLHS1, WSEP, TaSEP-6, -5 | HvBM1 |
| Lodicules | OsMADS7, -8 | ZMM24 | WSEP, TaSEP-6 | HvBM1, -7 |
| Carpel | OsMADS1, -7, -8 | ZMM14, -24 | WSEP, TaSEP-6, TaMADS1 | HvBM1, -7, -8 |
| Stamens | OsMADS7, -8, -34 | | WSEP, TaSEP-6, TaMADS1 | HvBM7 |
| **AGL6-like** | | | | |
| Palea/Lemma | OsMADS6 | ZAG3 | | |
| Lodicules | OsMADS6 | ZAG3 | | |
| Carpel | OsMADS6 | ZAG3 | | HvBM6 |
| Stamens | OsMADS6 | | | |

**Table 5.1 Comparison of expression patterns in rice, maize, wheat and barley in different floral organ tissues.**

## 5.4 MADS-box genes and abiotic stress

MADS-box genes are not only important for floral organ development. Several studies have shown that they might also be involved in abiotic stress tolerance (Castelán-Muñoz *et al.*, 2019). In tomato, cold stress altered the expression of several MADS-box genes involved in flower development, one of them the AP3-like B-class gene, which could be the cause of severely affected flower and fruit development (Lozano *et al.*, 1998). Under continuous mild heat two B-class genes were down-regulated in tomato anthers, while two pistil-specific genes were ectopically expressed in the anthers instead, explaining the partial conversion of anthers to pistil-like structures under continuous mild heat (Müller *et al.*, 2016). Cold, salt and/or drought stress also lead to differential expression of seven MADS-box genes in rice (Arora *et al.*, 2007). A number of flower development genes were also identified as responsive to abiotic stress in wheat (Tardif *et al.*, 2007). In *Brassica rapa*, eleven genes from the MIKC$^{c}$ MADS-box genes were shown to be differentially expressed after cold, salt and/or drought stress (Saha *et al.*, 2015). Comparison between cold-tolerant and cold-susceptible varieties showed more up-regulation of MADS-box genes in the cold-tolerant line than in the cold-susceptible line (Saha *et al.*, 2015). Several differentially expressed MADS-box genes were also found in *Brachypodium distachyon* after abiotic stress treatment (Wei *et al.*, 2014). A MADS-box gene of the AGL2-clade was also up-regulated by abiotic stresses in maize (Zhang *et al.*, 2012). MADS-box genes were also found to be induced by cold and salt stress in sheepgrass (*Leymus chinensis*) (Jia *et al.*, 2018).

The response of ABCDE MADS-box genes to abiotic stress in barley has not been investigated yet, however prior to analysis of the specific impact of abiotic stress on the MADS-box genes, it is important to understand the effects of abiotic stress on barley per se. Heat stress is a growing climatological problem that has a severe impact on cereal yield and production globally (IPCC, 2014; Lesk *et al.*, 2016), therefore understanding the impact of temperature stress and developing mitigation strategies is important for maintaining crop yield.

Three European spring barley varieties were subjected to heat stress conditions at two important stages in their reproductive development (meiosis and mitosis). A

short period of heat stress during early development (meiosis) led to significantly smaller and deformed anthers (section 4.4.1). Severe deficiencies in anther development are likely to be the leading cause of sterility due to high temperature stress, which was illustrated by the deformed and sterile pollen found in the heat stressed anthers (section 4.4.3). The septa in the heat stressed anthers was prematurely broken, whilst those in the control anthers were still closed. This suggests a more rapid developmental progression in the heat stressed lines and/or a change in the physical properties of the anther walls. The locule walls and cavities seemed less developed in the heat stressed anthers, which might be another reason why the pollen grains did not develop correctly. The premature breaking of the septa identified in heat-stressed barley might also be attributed to the fragility of the anther walls, as we can see some degeneration of anther wall layers in the immunolabelled images from RGT Planet, which corresponds to the types of anther deficiencies described by Saini *et al.* (1984). The immunohistology and previous research shows that the cell walls in the anthers, specifically the tapetum, are very vulnerable to heat stress. The developmental program of the tapetum has been shown to be disrupted by abiotic stress (Parish *et al.*, 2012). Tapetal degradation in the anthers failed to occur after exposure to high temperatures in rice (Endo *et al.*, 2009). In barley, the progression of anther development to the meiotic prophase was accelerated in the pollen mother cells. Other responses to high temperature conditions included premature degeneration of tapetum cells, cell-proliferation arrest and increased vacuolization in developing anther cells (Oshino *et al.*, 2007).

Pollen development was also severely affected by heat stress during both meiosis and mitosis. However some pollen is still formed in a few heat-stressed florets and some may be viable. In tomato and sorghum, high temperatures have been shown to prevent transient increase in starch concentration in pollen grains which led to decreases in the concentrations of soluble sugars in the anther walls and the pollen grains, which might lead to decreased pollen viability (Jain *et al.*, 2007; Pressman *et al.*, 2002). In barley, grains from heat stressed plants accumulated less starch than grains from control plants due to reduced conversion of sucrose to starch (Wallwork *et al.*, 1998). This is most likely due to heat stress having a negative effect on the activities of enzymes involved in the sucrose-to-starch metabolism in cereals (Duke and Doehlert, 1996; Hurkman *et al.*, 2003; Wilhelm *et al.*, 1999).

The carpels in the three varieties were bigger and the ovules appeared to have developed faster after heat stress treatment than in the plants in control conditions (Section 4.4.2). This suggests that in these three varieties the female reproductive organs are not as severely impacted by heat stress as the anthers at the two vulnerable developmental stages examined here. The larger size of the carpels could be due to swelling of unfertilized ovaries resulting in a second opening to promote cross-pollination (Okada *et al.*, 2018). It has been shown that both pre- and post-fertilisation stages of ovary development are sensitive to stress, but this varies depending on the species and genotype (Bac-Molenaar *et al.*, 2015b; Onyemaobi *et al.*, 2017; Sun *et al.*, 2004; Zinn *et al.*, 2010). In wheat, disrupted nucellus and integument development was observed after severe heat stress treatment and 30% showed complete ovule abortion (Saini *et al*., 1983). The nucellar cells of Moonshine, RGT Planet and particularly Optic, appeared to be somewhat disorganised and enlarged after heat stress compared to controls. However, in all three varieties, similar immunolabelling patterns for de-esterified pectin were observed around what appeared to be an intact embryo sac. The multi-layered nucellus might be one of the reasons the developmental program of the ovule is more robust than that of the anther (Wilkinson *et al.*, 2018).

In control conditions Optic showed variable fertility, but this variety seemed to be most vulnerable to prolonged heat stress during mitosis than the other varieties, as shown by the high percentage of sterile seeds. When compared to the control conditions, Moonshine seemed to perform best at both stages and in control conditions it also produced significantly better results than Optic. RGT Planet had the best yield of all three varieties, which supports its reputation as the joint best yielding fully approved malting variety grown today. Moonshine was introduced to the malting and brewing community in 2011, outcompeting previously approved varieties in terms of yield and grain quality. It also matured earlier than previously approved varieties at the time (Scotsman, 2011). This early maturation might be one of the reasons Moonshine is less susceptible to high temperature conditions.

Further investigation is needed to confirm the reasons for the differences in heat stress sensitivity between the three varieties, but these could be due to a difference in genetic composition or stress response factors, which may be the consequence of altered gene expression leading to differential resilience or alternatively altered developmental progression so that stress exposure is minimised.

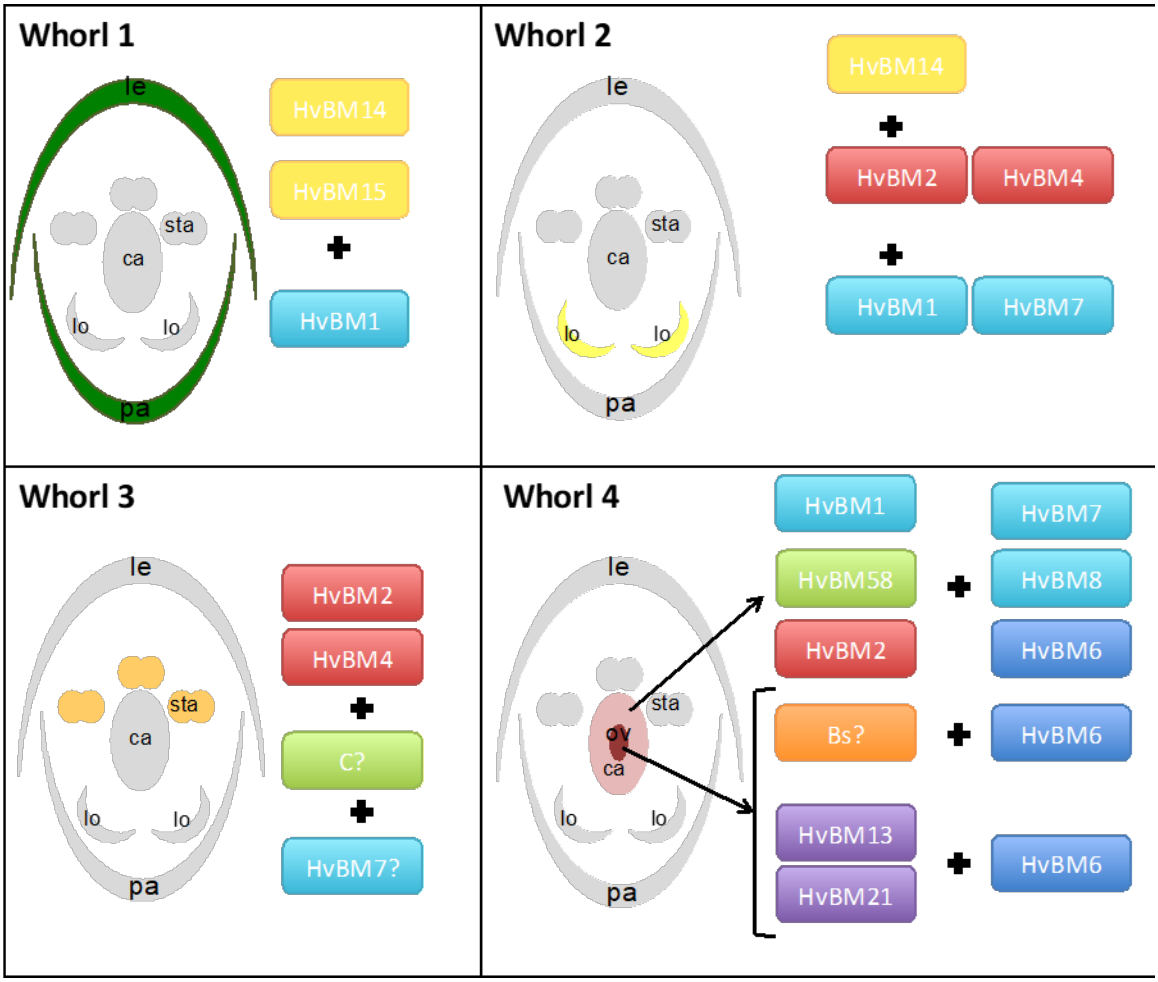



**Figure 5.1 Hypothetical ABCDE model in barley based on expression analysis, hierarchical clustering and functional analysis of the B-class genes.**
A hypothetical ABCDE model is proposed for the four whorls of the floret in barley. The A-class proteins HvBM15 and HvBM14 (yellow) are involved in determining the palea and the lemma together with the E-class protein HvBM1 (blue). Expression of *HvBM14* was detected in carpel tissue at stage LFE2, which is most likely due to lodicule tissue being present. It is therefore likely that HvBM14, together with the B-class proteins HvBM2 and HvBM4 (red) and the E-class proteins HvBM1 and HvBM7. Only high expression of *HvBM2* was detected in the stamens, but phenotypes of the *pUBI:HvBM4-SRDX* suggest that HvBM4 also plays a significant role in stamens development. No high expression of a C-class gene (green) was detected, but based on the hypothetical models of closely related species and *Arabidopsis*, we can't rule out the involvement of a C-class protein in stamens development. The only E-class gene showing expression in the stamens is *HvBM7* and it is therefore likely it plays a role in stamens development. Carpel development is likely controlled by the C-class protein HvBM58, the E-class proteins HvBM1, HvBM7 and HvBM8 and the AGL6-like protein HvBM6. Due to the carpel phenotype found in transformants expressing the *pUBI:HvBM2-SRDX* construct and the expression of *HvBM2* found in carpel tissue at stage 36, it is possible that HvBM2 also plays a role in carpel development. The $B_{sister}$-like genes had only very low expression in the carpel tissue, indicating that they might not be as important for ovule development as has been proposed in other hypothetical ABCDE models. Both the D-class proteins HvBM13 and HvBM21 and the AGL6-like protein HvBM6 seems to play a role in ovule development.

## 5.5 Conclusions and future work

To understand the function of MADS-box genes in abiotic stress tolerance in barley, expression analysis of these genes after different heat treatments and in tolerant and susceptible varieties needs to be carried out. If the ABCDE MADS-box genes are involved in abiotic stress tolerance, quantitative real-time PCR could show differential expression of these genes after stress treatments and could highlight differences between tolerant and susceptible varieties.

To further investigate the ABCDE model in barley several experiments involving the different genes in all the classes could be carried out. More protein-protein interaction experiments with all the ABCDE MADS-box genes could lead to a better understanding of the floral quartets functioning in floral organ development in barley.

Functional analysis of the other ABCDE MADS-box genes will further expand an accurate ABCDE model in barley and in grasses in general. With the emergence of the CRISPR/Cas9 system, making targeted knock-out mutants has been made more accessible. The CRISPR/Cas9 system has been used successfully in barley and could now be used for the functional analysis of the MADS-box genes (Lawrenson *et al.*, 2015). The CRES-T dominant repression system used in this thesis has the advantage of relatively easy constructs and showing phenotypes in the first generation of transformed plants due to the overexpression of the construct. However, the system has limitation. Transformed plants with low expression of the construct will show no phenotype or only a minor phenotype. Varying expression levels of the construct also contribute to a wide variety of phenotypes, as has been shown in this thesis. Reversing the role of a transcription factor from activator to repressor can also not be seen as a complete loss-of-function, even though it has been described as such before (Hiratsu *et al.*, 2003). It has been shown that the C-domain of MADS-box genes is important in mediating both activation and repression of target genes dependent on the interaction partners and the complexes formed (Cho *et al.*, 1999; Gioppato and Dornelas, 2019; Sridhar *et al.*, 2006). Although the CRISPR/Cas9 is more labour intensive due to designing and testing working targets and the genotyping of the transformed lines, the insertions or deletions created by this system produce stable knock-out lines.

Future work for the B-class SRDX lines includes sectioning of the florets expressing the SRDX constructs and exhibiting a phenotype. The cell types found in floral organs that have changed morphological structure could provide more certainty about the new identity of these whorls and indicate which genes might have taken over in the absence of a well-functioning B-class gene. Overexpression of the B-class genes might yield phenotypes that complement the phenotypes observed in the SRDX transformants, further solidifying their role in floral organ development. Crosses of SRDX transformants expressing the *pUBI:HvBM4-SRDX/pUBI:HvBM16-SRDX* constructs with transformants expressing the *pUBI:HvBM2-SRDX* construct might lead to triple B-class SRDX lines, which might give an indication of the role of all B-class genes together in the ABCDE model.

With a combination of the tissue-specific expression patterns in different developmental stages, hierarchical clustering analysis and functional analysis of the B-class genes presented here a hypothetical model of the barley ABCDE model for the four floral organ whorls can be proposed (Figure 5.1). The A-class proteins HvBM15 and HvBM14 are involved in determining the palea and the lemma together with the E-class protein HvBM1. Expression of *HvBM14* was detected in carpel tissue at stage LFE2, which is most likely due to lodicule tissue being present. It is therefore likely that HvBM14, together with the B-class proteins HvBM2 and HvBM4 and the E-class proteins HvBM1 and HvBM7. Only high expression of *HvBM2* was detected in the stamens, but phenotypes of the *pUBI:HvBM4-SRDX* suggest that HvBM4 also plays a significant role in stamens development. No high expression of a C-class gene was detected, but based on the hypothetical models of closely related species and *Arabidopsi*s, we can't rule out the involvement of a C-class protein in stamens development. The only E-class gene showing expression in the stamens is *HvBM7* and it is therefore likely it plays a role in stamens development. Carpel development is likely controlled by the C-class protein HvBM58, the E-class proteins HvBM1, HvBM7 and HvBM8 and the AGL6-like protein HvBM6. Due to the carpel phenotype found in transformants expressing the *pUBI:HvBM2-SRDX* construct and the expression of *HvBM2* found in carpel tissue at stage 36, it is possible that HvBM2 also plays a role in carpel development. The

$B_{sister}$-like genes had only very low expression in the carpel tissue, indicating that they might not be as important for ovule development as has been proposed in other hypothetical ABCDE models. Both the D-class proteins HvBM13 and HvBM21 and the AGL6-like protein HvBM6 seems to play a role in ovule development.
Protein-protein interaction analysis could help determine the validity of the complexes presented in the model. Functional analysis of the other ABCDE MADS-box genes through CRISPR/Cas9 mutation or with the use of the SRDX repression domain can further verify the functions proposed in the hypothetical model.

To further understand the underlying genetic pathways controlling floral organ development, the target genes of the different ABCDE-model MADS-box genes could be investigated by using for example RNAseq analysis of ABCDE knock-out mutants compared to the wild type.

## 5.6 References

**Aghamolki MTK, Yusop MK, Oad FC, Jaafar HZ, Khalatbari AM, Kharidah S, Musa MH**. 2016. Impact of heat stress on growth and yield of rice (Oryza sativa L.) cultivars. *Journal of Food, Agriculture & Environment* **14**, 111-116.

**AHDB**. 2016. AHDB Recommended Lists 2016-2017.

**AHDB**. 2017. Spring Barley Harvest Results 2017.

**Ambrose BA, Lerner DR, Ciceri P, Padilla CM, Yanofsky MF, Schmidt RJ**. 2000. Molecular and genetic analyses of the silky1 gene reveal conservation in floral organ specification between eudicots and monocots. *Molecular Cell* **5**, 569-579.

**Arora R, Agarwal P, Ray S, Singh AK, Singh VP, Tyagi AK, Kapoor S**. 2007. MADS-box gene family in rice: genome-wide identification, organization and expression profiling during reproductive development and stress. *BMC Genomics* **8**, 242.

**Bac-Molenaar JA, Fradin EF, Becker FFM, Rienstra JA, van der Schoot J, Vreugdenhil D, Keurentjes JJB**. 2015a. Genome-Wide Association Mapping of Fertility Reduction upon Heat Stress Reveals Developmental Stage-Specific QTLs in Arabidopsis thaliana. *The Plant Cell* **27**, 1857-1874.

**Bac-Molenaar JA, Fradin EF, Becker FFM, Rienstra JA, van der Schoot J, Vreugdenhil D, Keurentjes JJB**. 2015b. Genome-Wide Association Mapping of Fertility Reduction upon Heat Stress Reveals Developmental Stage-Specific QTLs in Arabidopsis thaliana. *The Plant Cell* **27**, 1857-1874.

**Barnabas B, Jager K, Feher A**. 2008. The effect of drought and heat stress on reproductive processes in cereals. *Plant Cell Environ* **31**, 11-38.

**Becker A, Kaufmann K, Freialdenhoven A, Vincent C, Li M-A, Saedler H, Theissen G**. 2002. A novel MADS-box gene subfamily with a sister-group relationship to class B floral homeotic genes. *Molecular Genetics and Genomics* **266**, 942-950.

**Becker A, Theissen G**. 2003. The major clades of MADS-box genes and their role in the development and evolution of flowering plants. *Mol Phylogenet Evol* **29**, 464-489.

**Bita CE, Gerats T**. 2013. Plant tolerance to high temperature in a changing environment: scientific fundamentals and production of heat stress-tolerant crops. *Front Plant Sci* **4**, 273.

**Bomblies K, Higgins JD, Yant L**. 2015. Meiosis evolves: adaptation to external and internal environments. *New Phytologist* **208**, 306-323.

**Bowman JL, Smyth DR, Meyerowitz EM**. 1989. Genes directing flower development in Arabidopsis. *The Plant Cell Online* **1**, 37.

**Bowman JL, Smyth DR, Meyerowitz EM**. 1991. Genetic interactions among floral homeotic genes of Arabidopsis. *Development* **112**, 1.

**Burton RA, Collins HM, Kibble NA, Smith JA, Shirley NJ, Jobling SA, Henderson M, Singh RR, Pettolino F, Wilson SM, Bird AR, Topping DL, Bacic A, Fincher GB**. 2011. Over-expression of specific HvCslF cellulose synthase-like genes in transgenic barley increases the levels of cell wall (1,3;1,4)-beta-d-glucans and alters their fine structure. *Plant Biotechnol J* **9**, 117-135.

**Buzgo M, Soltis DE, Soltis PS, Sangate K, Ma H, Hauser BA, Leebens-Mack J, Johansen B**. 2006. PERIANTH DEVELOPMENT IN THE BASAL MONOCOT TRIGLOCHIN MARITIMA (JUNCAGINACEAE). *Aliso* **22**, 107-125.

**Buzgo M, Soltis Pamela S, Soltis Douglas E**. 2004. Floral Developmental Morphology of Amborella trichopoda (Amborellaceae). *International Journal of Plant Sciences* **165**, 925-947.
**Cacharrón J, Fischer A, Saedler H, Theissen G**. 1995. Expression patterns of MADS-box genes as studied by in situ hybridization. *Maize Genetics Cooperation Newsletter* **69**, 37-38.
**Cacharrón J, Saedler H, Theissen G**. 1999. Expression of MADS box genes ZMM8 and ZMM14 during inflorescence development of Zea mays discriminates between the upper and the lower floret of each spikelet. *Development Genes and Evolution* **209**, 411-420.
**Castelán-Muñoz N, Herrera J, Cajero-Sánchez W, Arrizubieta M, Trejo C, García-Ponce B, Sánchez MdlP, Álvarez-Buylla ER, Garay-Arroyo A**. 2019. MADS-Box Genes Are Key Components of Genetic Regulatory Networks Involved in Abiotic Stress and Plastic Developmental Responses in Plants. *Frontiers in Plant Science* **10**.
**Chang F, Zhang Z, Jin Y, Ma H**. 2014. Cell Biological Analyses of Anther Morphogenesis and Pollen Viability in Arabidopsis and Rice. In: Riechmann JL, Wellmer F, eds. *Flower Development: Methods and Protocols*. New York, NY: Springer New York, 203-216.
**Chang YY, Kao NH, Li JY, Hsu WH, Liang YL, Wu JW, Yang CH**. 2010. Characterization of the possible roles for B class MADS box genes in regulation of perianth formation in orchid. *Plant Physiology* **152**, 837-853.
**Cho S, Jang S, Chae S, Chung KM, Moon Y-H, An G, Jang SK**. 1999. Analysis of the C-terminal region of Arabidopsis thaliana APETALA1 as a transcription activation domain. *Plant Molecular Biology* **40**, 419-429.
**Christidis N, Jones GS, Stott PA**. 2014. Dramatically increasing chance of extremely hot summers since the 2003 European heatwave. *Nature Climate Change* **5**, 46.
**Chung Y-Y, Kim S-R, Finkel D, Yanofsky MF, An G**. 1994. Early flowering and reduced apical dominance result from ectopic expression of a rice MADS box gene. *Plant Molecular Biology* **26**, 657-665.
**Chung Y-Y, Kim S-R, Kang H-G, Noh Y-S, Park MC, Finkel D, An G**. 1995. Characterization of two rice MADS box genes homologous to GLOBOSA. *Plant Science* **109**, 45-56.
**Coen ES, Meyerowitz EM**. 1991. The war of the whorls: genetic interactions controlling flower development. *Nature* **353**, 31.
**Colombo L, Franken J, Koetje E, van Went J, Dons HJ, Angenent GC, van Tunen AJ**. 1995. The petunia MADS box gene FBP11 determines ovule identity. *The Plant Cell* **7**, 1859-1868.
**Cooper P, Ho T-HD, Hauptmann RM**. 1984. Tissue Specificity of the Heat-Shock Response in Maize. *Plant Physiology* **75**, 431.
**Danilevskaya ON, Meng X, Selinger DA, Deschamps S, Hermon P, Vansant G, Gupta R, Ananiev EV, Muszynski MG**. 2008. Involvement of the MADS-box gene ZMM4 in floral induction and inflorescence development in maize. *Plant Physiology* **147**, 2054-2069.
**David BL, Christopher BF**. 2007. Global scale climate–crop yield relationships and the impacts of recent warming. *Environmental Research Letters* **2**, 014002.

**Davies B, Egea-Cortines M, de Andrade Silva E, Saedler H, Sommer H**. 1996. Multiple interactions amongst floral homeotic MADS box proteins. *The EMBO Journal* **15**, 4330-4343.
**De Folter S, Shchennikova AV, Franken J, Busscher M, Baskar R, Grossniklaus U, Angenent GC, Immink RGH**. 2006. A Bsister MADS-box gene involved in ovule and seed development in petunia and Arabidopsis. *The Plant Journal* **47**, 934-946.
**Delphine D, Declan C, Navin R, Jeff P, Rachel W**. 2014. Global crop yield response to extreme heat stress under multiple climate change futures. *Environmental Research Letters* **9**, 034011.
**Digel B, Pankin A, von Korff M**. 2015. Global Transcriptome Profiling of Developing Leaf and Shoot Apices Reveals Distinct Genetic and Environmental Control of Floral Transition and Inflorescence Development in Barley. *The Plant Cell* **27**, 2318.
**Draeger T, Moore G**. 2017. Short periods of high temperature during meiosis prevent normal meiotic progression and reduce grain number in hexaploid wheat (Triticum aestivum L.). *Theoretical and Applied Genetics* **130**, 1785-1800.
**Dreni L, Jacchia S, Fornara F, Fornari M, Ouwerkerk PB, An G, Colombo L, Kater MM**. 2007. The D-lineage MADS-box gene OsMADS13 controls ovule identity in rice. *The Plant Journal* **52**, 690-699.
**Dreni L, Pilatone A, Yun D, Erreni S, Pajoro A, Caporali E, Zhang D, Kater MM**. 2011. Functional Analysis of All AGAMOUS Subfamily Members in Rice Reveals Their Roles in Reproductive Organ Identity Determination and Meristem Determinacy. *The Plant Cell* **23**, 2850.
**Dreni L, Zhang D**. 2016. Flower development: the evolutionary history and functions of the AGL6 subfamily MADS-box genes. *The Journal of Experimental Botany* **67**, 1625-1638.
**Duke ER, Doehlert DC**. 1996. Effects of heat stress on enzyme activities and transcript levels in developing maize kernels grown in culture. *Environmental and Experimental Botany* **36**, 199-208.
**Endo M, Tsuchiya T, Hamada K, Kawamura S, Yano K, Ohshima M, Higashitani A, Watanabe M, Kawagishi-Kobayashi M**. 2009. High Temperatures Cause Male Sterility in Rice Plants with Transcriptional Alterations During Pollen Development. *Plant and Cell Physiology* **50**, 1911-1922.
**Farooq M, Bramley H, Palta JA, Siddique KHM**. 2011. Heat Stress in Wheat during Reproductive and Grain-Filling Phases. *Critical Reviews in Plant Sciences* **30**, 491-507.
**Feder ME, Hofmann GE**. 1999. HEAT-SHOCK PROTEINS, MOLECULAR CHAPERONES, AND THE STRESS RESPONSE: Evolutionary and Ecological Physiology. *Annual Review of Physiology* **61**, 243-282.
**Fornara F, Marziani G, Mizzi L, Kater M, Colombo L**. 2003. MADS-Box Genes Controlling Flower Development in Rice. *Plant Biology* **5**, 16-22.
**Fornara F, Parenicova L, Falasca G, Pelucchi N, Masiero S, Ciannamea S, Lopez-Dee Z, Altamura MM, Colombo L, Kater MM**. 2004. Functional characterization of OsMADS18, a member of the AP1/SQUA subfamily of MADS box genes. *Plant Physiology* **135**, 2207-2219.

**Gioppato HA, Dornelas MC**. 2019. When Bs Are Better than As: the Relationship between B-Class MADS-Box Gene Duplications and the Diversification of Perianth Morphology. *Tropical Plant Biology* **12**, 1-11.
**Gómez JF, Wilson ZA**. 2012. Non-destructive staging of barley reproductive development for molecular analysis based upon external morphology. *Journal of Experimental Botany* **63**, 4085-4094.
**Goremykin VV, Hansmann S, Martin WF**. 1997. Evolutionary analysis of 58 proteins encoded in six completely sequenced chloroplast genomes: Revised molecular estimates of two seed plant divergence times. *Plant Systematics and Evolution* **206**, 337-351.
**Goto K, Meyerowitz EM**. 1994. Function and regulation of the Arabidopsis floral homeotic gene PISTILLATA. *Genes and Development* **8**, 1548-1560.
**Halse NJ, Weir RN**. 1974. Effects of temperature on spikelet number of wheat. *Australian Journal of Agricultural Research* **25**, 687-695.
**Hama E, Takumi S, Ogihara Y, Murai K**. 2004. Pistillody is caused by alterations to the class-B MADS-box gene expression pattern in alloplasmic wheats. *Planta* **218**, 712-720.
**Harwood WA, Bartlett JG, Alves SC, Perry M, Smedley MA, Leyl N, Snape JW**. 2009. Barley Transformation Using Agrobacterium-Mediated Techniques. In: Jones HD, Shewry PR, eds. *Transgenic Wheat, Barley and Oats: Production and Characterization Protocols*. Totowa, NJ: Humana Press, 137-147.
**Hernández-Hernández T, Martínez-Castilla LP, Alvarez-Buylla ER**. 2006. Functional Diversification of B MADS-Box Homeotic Regulators of Flower Development: Adaptive Evolution in Protein–Protein Interaction Domains after Major Gene Duplication Events. *Molecular Biology and Evolution* **24**, 465-481.
**Hill JP, Lord EM**. 1989. Floral development in Arabidopsis thaliana: a comparison of the wild type and the homeotic pistillata mutant. *Canadian Journal of Botany* **67**, 2922-2936.
**Hiratsu K, Matsui K, Koyama T, Ohme-Takagi M**. 2003. Dominant repression of target genes by chimeric repressors that include the EAR motif, a repression domain, in Arabidopsis. *The Plant Journal* **34**, 733-739.
**Hong S-W, Vierling E**. 2000. Mutants of Arabidopsis thaliana defective in the acquisition of tolerance to high temperature stress. *Proceedings of the National Academy of Sciences of the United States of America* **97**, 4392-4397.
**Honma T, Goto K**. 2001. Complexes of MADS-box proteins are sufficient to convert leaves into floral organs. *Nature* **409**, 525.
**Hurkman WJ, McCue KF, Altenbach SB, Korn A, Tanaka CK, Kothari KM, Johnson EL, Bechtel DB, Wilson JD, Anderson OD, DuPont FM**. 2003. Effect of temperature on expression of genes encoding enzymes for starch biosynthesis in developing wheat endosperm. *Plant Science* **164**, 873-881.
**Immink RGH, Tonaco IAN, de Folter S, Shchennikova A, van Dijk ADJ, Busscher-Lange J, Borst JW, Angenent GC**. 2009. SEPALLATA3: the 'glue' for MADS box transcription factor complex formation. *Genome Biology* **10**, R24.
**IPCC**. 2014. Climate Change 2014: Mitigation of Climate Change. Contribution of Working Group III to the Fifth Assessment Report of the Intergovernmental Panel on Climate Change. In: Edenhofer O, R. Pichs-Madruga, Y. Sokona, E. Farahani, S. Kadner, K. Seyboth, A. Adler, I. Baum, S. Brunner, P. Eickemeier, B. Kriemann, J. Savolainen, S. Schlömer, C. von Stechow, T. Zwickel and J.C. Minx

(eds.), ed. *Cambridge University Press*. Cambridge, United Kingdom and New York, NY, USA.
**Irish V**. 2017. The ABC model of floral development. *Current Biology* **27**, R887-R890.
**Jack T, Brockman LL, Meyerowitz EM**. 1992. The homeotic gene APETALA3 of Arabidopsis thaliana encodes a MADS box and is expressed in petals and stamens. *Cell* **68**, 683-697.
**Jack T, Fox GL, Meyerowitz EM**. 1994. Arabidopsis homeotic gene APETALA3 ectopic expression: Transcriptional and posttranscriptional regulation determine floral organ identity. *Cell* **76**, 703-716.
**Jain M, Prasad PV, Boote KJ, Hartwell AL, Jr., Chourey PS**. 2007. Effects of season-long high temperature growth conditions on sugar-to-starch metabolism in developing microspores of grain sorghum (Sorghum bicolor L. Moench). *Planta* **227**, 67-79.
**Jenik PD, Irish VF**. 2001. The Arabidopsis floral homeotic gene APETALA3 differentially regulates intercellular signaling required for petal and stamen development. *Development* **128**, 13.
**Jetha K, Theißen G, Melzer R**. 2014. Arabidopsis SEPALLATA proteins differ in cooperative DNA-binding during the formation of floral quartet-like complexes. *Nucleic Acids Research* **42**, 10927-10942.
**Ji X, Shiran B, Wan J, Lewis DC, Jenkins CLD, Condon AG, Richards RA, Dolferus R**. 2010. Importance of pre-anthesis anther sink strength for maintenance of grain number during reproductive stage water stress in wheat. *Plant, Cell & Environment* **33**, 926-942.
**Jia J, Zhao P, Cheng L, Yuan G, Yang W, Liu S, Chen S, Qi D, Liu G, Li X**. 2018. MADS-box family genes in sheepgrass and their involvement in abiotic stress responses. *BMC Plant Biology* **18**, 42.
**Johnson RC, Kanemasu ET**. 1983. Yield and Development of Winter Wheat at Elevated Temperatures1. *Agronomy Journal* **75**, 561-565.
**Kagale S, Rozwadowski K**. 2011. EAR motif-mediated transcriptional repression in plants. *Epigenetics* **6**, 141-146.
**Kang HG, Jang S, Chung JE, Cho YG, An G**. 1997. Characterization of two rice MADS box genes that control flowering time. *Molecules and Cells* **7**, 559-566.
**Kim S, Koh J, Yoo M-J, Kong H, Hu Y, Ma H, Soltis PS, Soltis DE**. 2005. Expression of floral MADS-box genes in basal angiosperms: implications for the evolution of floral regulators. *The Plant Journal* **43**, 724-744.
**Kim S, Yoo M-J, Albert VA, Farris JS, Soltis PS, Soltis DE**. 2004. Phylogeny and diversification of B-function MADS-box genes in angiosperms: evolutionary and functional implications of a 260-million-year-old duplication. *American Journal of Botany* **91**, 2102-2118.
**Kinjo H, Shitsukawa N, Takumi S, Murai K**. 2012. Diversification of three APETALA1/FRUITFULL-like genes in wheat. *Molecular Genetics and Genomics* **287**, 283-294.
**Kobayashi K, Maekawa M, Miyao A, Hirochika H, Kyozuka J**. 2010. PANICLE PHYTOMER2 (PAP2), encoding a SEPALLATA subfamily MADS-box protein, positively controls spikelet meristem identity in rice. *Plant and Cell Physiology* **51**, 47-57.

**Krizek BA, Meyerowitz EM**. 1996. The Arabidopsis homeotic genes APETALA3 and PISTILLATA are sufficient to provide the B class organ identity function. *Development* **122**, 11.
**Kruszka K, Pacak A, Swida-Barteczka A, Nuc P, Alaba S, Wroblewska Z, Karlowski W, Jarmolowski A, Szweykowska-Kulinska Z**. 2014. Transcriptionally and post-transcriptionally regulated microRNAs in heat stress response in barley. *J Exp Bot* **65**, 6123-6135.
**Kyozuka J, Kobayashi T, Morita M, Shimamoto K**. 2000. Spatially and temporally regulated expression of rice MADS box genes with similarity to Arabidopsis class A, B and C genes. *Plant and Cell Physiology* **41**, 710-718.
**Lai X, Daher H, Galien A, Hugouvieux V, Zubieta C**. 2019. Structural Basis for Plant MADS Transcription Factor Oligomerization. *Computational and Structural Biotechnology Journal* **17**, 946-953.
**Lamb RS, Irish VF**. 2003. Functional divergence within the <em>APETALA3/PISTILLATA</em> floral homeotic gene lineages. *Proceedings of the National Academy of Sciences* **100**, 6558.
**Lawrenson T, Shorinola O, Stacey N, Li C, Østergaard L, Patron N, Uauy C, Harwood W**. 2015. Induction of targeted, heritable mutations in barley and Brassica oleracea using RNA-guided Cas9 nuclease. *Genome Biology* **16**, 258.
**Lee S, Kim J, Son J-S, Nam J, Jeong D-H, Lee K, Jang S, Yoo J, Lee J, Lee D-Y, Kang H-G, An G**. 2003. Systematic Reverse Genetic Screening of T-DNA Tagged Genes in Rice for Functional Genomic Analyses: MADS-box Genes as a Test Case. *Plant and Cell Physiology* **44**, 1403-1411.
**Lesk C, Rowhani P, Ramankutty N**. 2016. Influence of extreme weather disasters on global crop production. *Nature* **529**, 84.
**Li H, Liang W, Jia R, Yin C, Zong J, Kong H, Zhang D**. 2010. The AGL6-like gene OsMADS6 regulates floral organ and meristem identities in rice. *Cell Research* **20**, 299-313.
**Li N, Liu Y, Zhong M, Li H**. 2014. Thinking out of the box: MADS-box genes and maize spikelet development. *AFRICAN JOURNAL OF BIOTECHNOLOGY* **13**.
**Li X**. 2011. Pollen Fertility/viability Assay Using FDA Staining. *Bio-protocol* **1**, e75.
**Lid SE, Meeley RB, Min Z, Nichols S, Olsen O-A**. 2004. Knock-out mutants of two members of the AGL2 subfamily of MADS-box genes expressed during maize kernel development. *Plant Science* **167**, 575-582.
**Liu H, Li G, Yang X, Kuijer HNJ, Liang W, Zhang D**. 2019. Transcriptome profiling reveals phase-specific gene expression in the developing barley inflorescence. *The Crop Journal*.
**Lopez-Dee ZP, Wittich P, Enrico Pe M, Rigola D, Del Buono I, Gorla MS, Kater MM, Colombo L**. 1999. OsMADS13, a novel rice MADS-box gene expressed during ovule development. *Developmental Genetics* **25**, 237-244.
**Lozano R, Angosto T, Gómez P, Payán C, Capel J, Huijser P, Salinas J, Martínez-Zapater JM**. 1998. Tomato Flower Abnormalities Induced by Low Temperatures Are Associated with Changes of Expression of MADS-Box Genes. *Plant Physiology* **117**, 91-100.
**Maestri E, Klueva N, Perrotta C, Gulli M, Nguyen HT, Marmiroli N**. 2002. Molecular genetics of heat tolerance and heat shock proteins in cereals. *Plant Mol Biol* **48**, 667-681.

**Mascarenhas JP, Crone DE**. 1996. Pollen and the heat shock response. *Sexual Plant Reproduction* **9**, 370-374.
**Masiero S, Imbriano C, Ravasio F, Favaro R, Pelucchi N, Gorla MS, Mantovani R, Colombo L, Kater MM**. 2002. Ternary complex formation between MADS-box transcription factors and the histone fold protein NF-YB. *The Journal of Biological Chemistry* **277**, 26429-26435.
**Matsui K, Ohme-Takagi M**. 2010. Detection of protein–protein interactions in plants using the transrepressive activity of the EAR motif repression domain. *The Plant Journal* **61**, 570-578.
**Matsui T, Omasa K, Horie T**. 2001. The Difference in Sterility due to High Temperatures during the Flowering Period among Japonica-Rice Varieties. *Plant Production Science* **4**, 90-93.
**Meikle PJ, Hoogenraad NJ, Bonig I, Clarke AE, Stone BA**. 1994. A (1-->3,1-->4)-beta-glucan-specific monoclonal antibody and its use in the quantitation and immunocytochemical location of (1-->3,1-->4)-beta-glucans. *Plant J* **5**, 1-9.
**Melzer R, Verelst W, Theißen G**. 2008. The class E floral homeotic protein SEPALLATA3 is sufficient to loop DNA in 'floral quartet'-like complexes in vitro. *Nucleic Acids Research* **37**, 144-157.
**Mena M, Ambrose BA, Meeley RB, Briggs SP, Yanofsky MF, Schmidt RJ**. 1996. Diversification of C-Function Activity in Maize Flower Development. *Science* **274**, 1537.
**Mena M, Mandel MA, Lerner DR, Yanofsky MF, Schmidt RJ**. 1995. A characterization of the MADS-box gene family in maize. *The Plant Journal* **8**, 845-854.
**Mizzotti C, Mendes MA, Caporali E, Schnittger A, Kater MM, Battaglia R, Colombo L**. 2012. The MADS box genes SEEDSTICK and ARABIDOPSIS Bsister play a maternal role in fertilization and seed development. *The Plant Journal* **70**, 409-420.
**Moon Y-H, Jung J-Y, Kang H-G, An G**. 1999. Identification of a rice APETALA3 homologue by yeast two-hybrid screening. *Plant Molecular Biology* **40**, 167-177.
**Müller F, Xu J, Kristensen L, Wolters-Arts M, de Groot PFM, Jansma SY, Mariani C, Park S, Rieu I**. 2016. High-Temperature-Induced Defects in Tomato (Solanum lycopersicum) Anther and Pollen Development Are Associated with Reduced Expression of B-Class Floral Patterning Genes. *PLoS One* **11**, e0167614.
**Münster T, Pahnke J, Di Rosa A, Kim JT, Martin W, Saedler H, Theissen G**. 1997. Floral homeotic genes were recruited from homologous MADS-box genes preexisting in the common ancestor of ferns and seed plants. *Proceedings of the National Academy of Sciences* **94**, 2415.
**Munster T, Wingen LU, Faigl W, Werth S, Saedler H, Theissen G**. 2001. Characterization of three GLOBOSA-like MADS-box genes from maize: evidence for ancient paralogy in one class of floral homeotic B-function genes of grasses. *Gene* **262**, 1-13.
**Nagasawa N, Miyoshi M, Sano Y, Satoh H, Hirano H, Sakai H, Nagato Y**. 2003. SUPERWOMAN1 and DROOPING LEAF genes control floral organ identity in rice. *Development* **130**, 705.
**Nguyen HT, Joshi CP, Klueva N, Weng J, Hendershot KL, Blum A**. 1994. The Heat-Shock Response and Expression of Heat-Shock Proteins in Wheat Under Diurnal Heat Stress and Field Conditions. *Functional Plant Biology* **21**, 857-867.

**Nicolas ME, Gleadow RM, Dalling MJ**. 1985. Effect of Post-anthesis Drought on Cell Division and Starch Accumulation in Developing Wheat Grains. *Annals of Botany* **55**, 433-444.
**Ohmori S, Kimizu M, Sugita M, Miyao A, Hirochika H, Uchida E, Nagato Y, Yoshida H**. 2009. MOSAIC FLORAL ORGANS1, an AGL6-like MADS box gene, regulates floral organ identity and meristem fate in rice. *The Plant Cell* **21**, 3008-3025.
**Ohta M, Matsui K, Hiratsu K, Shinshi H, Ohme-Takagi M**. 2001. Repression Domains of Class II ERF Transcriptional Repressors Share an Essential Motif for Active Repression. *The Plant Cell* **13**, 1959.
**Okada T, Jayasinghe JEARM, Nansamba M, Baes M, Warner P, Kouidri A, Correia D, Nguyen V, Whitford R, Baumann U**. 2018. Unfertilized ovary pushes wheat flower open for cross-pollination. *Journal of Experimental Botany* **69**, 399-412.
**Onyemaobi I, Liu H, Siddique KHM, Yan G**. 2017. Both Male and Female Malfunction Contributes to Yield Reduction under Water Stress during Meiosis in Bread Wheat. *Frontiers in Plant Science* **7**.
**Ortiz R, Sayre KD, Govaerts B, Gupta R, Subbarao GV, Ban T, Hodson D, Dixon JM, Iván Ortiz-Monasterio J, Reynolds M**. 2008. Climate change: Can wheat beat the heat? *Agriculture, Ecosystems & Environment* **126**, 46-58.
**Oshino T, Abiko M, Saito R, Ichiishi E, Endo M, Kawagishi-Kobayashi M, Higashitani A**. 2007. Premature progression of anther early developmental programs accompanied by comprehensive alterations in transcription during high-temperature injury in barley plants. *Molecular Genetics and Genomics* **278**, 31-42.
**Paolacci AR, Tanzarella OA, Porceddu E, Varotto S, Ciaffi M**. 2007. Molecular and phylogenetic analysis of MADS-box genes of MIKC type and chromosome location of SEP-like genes in wheat (Triticum aestivum L.). *Molecular Genetics and Genomics* **278**, 689-708.
**Parish RW, Phan HA, Iacuone S, Li SF**. 2012. Tapetal development and abiotic stress: a centre of vulnerability. *Functional Plant Biology* **39**, 553-559.
**Pelucchi N, Fornara F, Favalli C, Masiero S, Lago C, Pè E, Colombo L, Kater M**. 2002. Comparative analysis of rice MADS-box genes expressed during flower development. *Sexual Plant Reproduction* **15**, 113-122.
**Prasad K, Sriram P, Kumar CS, Kushalappa K, Vijayraghavan U**. 2001. Ectopic expression of rice OsMADS1 reveals a role in specifying the lemma and palea, grass floral organs analogous to sepals. *Development Genes and Evolution* **211**, 281-290.
**Prasad PVV, Pisipati SR, Mutava RN, Tuinstra MR**. 2008. Sensitivity of Grain Sorghum to High Temperature Stress during Reproductive Development All rights reserved. No part of this periodical may be reproduced or transmitted in any form or by any means, electronic or mechanical, including photocopying, recording, or any information storage and retrieval system, without permission in writing from the publisher. Permission for printing and for reprinting the material contained herein has been obtained by the publisher. *Crop Science* **48**, 1911-1917.

**Pressman E, Peet MM, Pharr DM**. 2002. The Effect of Heat Stress on Tomato Pollen Characteristics is Associated with Changes in Carbohydrate Concentration in the Developing Anthers. *Annals of Botany* **90**, 631-636.
**Puig J, Meynard D, Khong GN, Pauluzzi G, Guiderdoni E, Gantet P**. 2013. Analysis of the expression of the AGL17-like clade of MADS-box transcription factors in rice. *Gene Expression Patterns* **13**, 160-170.
**Reinheimer R, Kellogg EA**. 2009. Evolution of AGL6-like MADS box genes in grasses (Poaceae): ovule expression is ancient and palea expression is new. *The Plant Cell* **21**, 2591-2605.
**Rümpler F, Theißen G, Melzer R**. 2018. A conserved leucine zipper-like motif accounts for strong tetramerization capabilities of SEPALLATA-like MADS-domain transcription factors. *Journal of Experimental Botany* **69**, 1943-1954.
**Saeed AI, Sharov V Fau - White J, White J Fau - Li J, Li J Fau - Liang W, Liang W Fau - Bhagabati N, Bhagabati N Fau - Braisted J, Braisted J Fau - Klapa M, Klapa M Fau - Currier T, Currier T Fau - Thiagarajan M, Thiagarajan M Fau - Sturn A, Sturn A Fau - Snuffin M, Snuffin M Fau - Rezantsev A, Rezantsev A Fau - Popov D, Popov D Fau - Ryltsov A, Ryltsov A Fau - Kostukovich E, Kostukovich E Fau - Borisovsky I, Borisovsky I Fau - Liu Z, Liu Z Fau - Vinsavich A, Vinsavich A Fau - Trush V, Trush V Fau - Quackenbush J, Quackenbush J**. TM4: a free, open-source system for microarray data management and analysis.
**Saha G, Park J-I, Jung H-J, Ahmed NU, Kayum MA, Chung M-Y, Hur Y, Cho Y-G, Watanabe M, Nou I-S**. 2015. Genome-wide identification and characterization of MADS-box family genes related to organ development and stress resistance in Brassica rapa. *BMC Genomics* **16**, 178.
**Saini H, Sedgley M, Aspinall D**. 1983. Effect of Heat Stress During Floral Development on Pollen Tube Growth and Ovary Anatomy in Wheat (<I>Triticum aestivum</I> L.). *Functional Plant Biology* **10**, 137-144.
**Saini HS, Aspinall D**. 1982. Abnormal Sporogenesis in Wheat (Triticum aestivum L.) Induced by Short Periods of High Temperature. *Annals of Botany* **49**, 835-846.
**Saini HS, Sedgley M, Aspinall D**. 1984. Development Anatomy in Wheat of Male Sterility Induced by Heat Stress, Water Deficit or Abscisic Acid. *Functional Plant Biology* **11**, 243-253.
**Sakata T, Takahashi H, Nishiyama I, Higashitani A**. 2000. Effects of High Temperature on the Development of Pollen Mother Cells and Microspores in Barley Hordeum vulgare L. *Journal of Plant Research* **113**, 395-402.
**Schilling S, Gramzow L, Lobbes D, Kirbis A, Weilandt L, Hoffmeier A, Junker A, Weigelt-Fischer K, Klukas C, Wu F, Meng Z, Altmann T, Theissen G**. 2015. Non-canonical structure, function and phylogeny of the Bsister MADS-box gene OsMADS30 of rice (Oryza sativa). *The Plant Journal* **84**, 1059-1072.
**Schilling S, Kennedy A, Pan S, Jermiin LS, Melzer R**. 2019. Genome-wide analysis of MIKC-type MADS-box genes in wheat: pervasive duplications, functional conservation and putative neofunctionalization. *New Phytologist*.
**Schmidt RJ, Veit B, Mandel MA, Mena M, Hake S, Yanofsky MF**. 1993. Identification and molecular characterization of ZAG1, the maize homolog of the Arabidopsis floral homeotic gene AGAMOUS. *The Plant Cell* **5**, 729-737.

**Schmitz J, Franzen R, Ngyuen TH, Garcia-Maroto F, Pozzi C, Salamini F, Rohde W**. 2000. Cloning, mapping and expression analysis of barley MADS-box genes. *Plant Molecular Biology* **42**, 899-913.
**Scotsman T**. 2011. Moonshine is being pushed for the growing malting industry. *The Scotsman*.
**SeedForce**. 2017.
**Sheoran IS, Saini HS**. 1996. Drought-induced male sterility in rice: Changes in carbohydrate levels and enzyme activities associated with the inhibition of starch accumulation in pollen. *Sexual Plant Reproduction* **9**, 161-169.
**Shitsukawa N, Tahira C, Kassai K, Hirabayashi C, Shimizu T, Takumi S, Mochida K, Kawaura K, Ogihara Y, Murai K**. 2007. Genetic and epigenetic alteration among three homoeologous genes of a class E MADS box gene in hexaploid wheat. *The Plant Cell* **19**, 1723-1737.
**Soltis DE, Chanderbali AS, Kim S, Buzgo M, Soltis PS**. 2007. The ABC Model and its Applicability to Basal Angiosperms. *Annals of Botany* **100**, 155-163.
**Soltis PS, Soltis DE, Kim S, Chanderbali A, Buzgo M**. 2006. Expression of Floral Regulators in Basal Angiosperms and the Origin and Evolution of ABC-Function. *Advances in Botanical Research*, Vol. 44: Academic Press, 483-506.
**Sridhar VV, Surendrarao A, Liu Z**. 2006. APETALA1 and SEPALLATA3 interact with SEUSS to mediate transcription repression during flower development. *Development* **133**, 3159.
**Stellari GM, Jaramillo MA, Kramer EM**. 2004. Evolution of the APETALA3 and PISTILLATA Lineages of MADS-Box–Containing Genes in the Basal Angiosperms. *Molecular Biology and Evolution* **21**, 506-519.
**Stone P, Basra A**. 2001. The effects of heat stress on cereal yield and quality. *Crop responses and adaptations to temperature stress*. Binghampton: NY Food Products Press, 179-187.
**Sun K, Hunt K, Hauser BA**. 2004. Ovule Abortion in Arabidopsis Triggered by Stress. *Plant Physiology* **135**, 2358-2367.
**Tardif G, Kane NA, Adam H, Labrie L, Major G, Gulick P, Sarhan F, Laliberté J-F**. 2007. Interaction network of proteins associated with abiotic stress response and development in wheat. *Plant Molecular Biology* **63**, 703-718.
**Teixeira EI, Fischer G, van Velthuizen H, Walter C, Ewert F**. 2013. Global hot-spots of heat stress on agricultural crops due to climate change. *Agricultural and Forest Meteorology* **170**, 206-215.
**Theissen G, Becker A, Di Rosa A, Kanno A, Kim JT, Münster T, Winter K-U, Saedler H**. 2000. A short history of MADS-box genes in plants. *Plant Molecular Biology* **42**, 115-149.
**Theißen G, Melzer R, Rümpler F**. 2016. MADS-domain transcription factors and the floral quartet model of flower development: linking plant development and evolution. *Development* **143**, 3259.
**Theissen G, Saedler H**. 2001. Plant biology. Floral quartets. *Nature* **409**, 469-471.
**Thompson BE, Bartling L, Whipple C, Hall DH, Sakai H, Schmidt R, Hake S**. 2009. bearded-ear Encodes a MADS Box Transcription Factor Critical for Maize Floral Development. *The Plant Cell* **21**, 2578.

**Tilly JJ, Allen DW, Jack T**. 1998. The CArG boxes in the promoter of the Arabidopsis floral organ identity gene APETALA3 mediate diverse regulatory effects. *Development* **125**, 1647.
**Tracy SR, Gómez JF, Sturrock CJ, Wilson ZA, Ferguson AC**. 2017. Non-destructive determination of floral staging in cereals using X-ray micro computed tomography (μCT). *Plant Methods* **13**, 9.
**Verhertbruggen Y, Marcus SE, Haeger A, Ordaz-Ortiz JJ, Knox JP**. 2009. An extended set of monoclonal antibodies to pectic homogalacturonan. *Carbohydrate Research* **344**, 1858-1862.
**Waddington SR, Cartwright PM, Wall PC**. 1983. A Quantitative Scale of Spike Initial and Pistil Development in Barley and Wheat. *Annals of Botany* **51**, 119-130.
**Wallwork MAB, Logue SJ, MacLeod LC, Jenner CF**. 1998. Effect of high temperature during grain filling on starch synthesis in the developing barley grain. *Functional Plant Biology* **25**, 173-181.
**Wei B, Liu D, Guo J, Leseberg CH, Zhang X, Mao L**. 2013. Functional divergence of two duplicated D-lineage MADS-box genes BdMADS2 and BdMADS4 from Brachypodium distachyon. *Journal of Plant Physiology* **170**, 424-431.
**Wei B, Zhang R-Z, Guo J-J, Liu D-M, Li A-L, Fan R-C, Mao L, Zhang X-Q**. 2014. Genome-Wide Analysis of the MADS-Box Gene Family in Brachypodium distachyon. *PLoS One* **9**, e84781.
**Weigel D, Meyerowitz EM**. 1994. The ABCs of floral homeotic genes. *Cell* **78**, 203-209.
**Whipple CJ, Ciceri P, Padilla CM, Ambrose BA, Bandong SL, Schmidt RJ**. 2004. Conservation of B-class floral homeotic gene function between maize and Arabidopsis. *Development* **131**, 6083.
**Wilhelm EP, Mullen RE, Keeling PL, Singletary GW**. 1999. Heat Stress during Grain Filling in Maize: Effects on Kernel Growth and Metabolism The research was funded as a joint collaboration between ICI Seeds (presently Garst Seed Co.), 2369 330th St., P.O. Box 500, Slater, IA 50244 and Iowa State University. Journal Paper no. J-18085 of the Iowa Agric. and Home Econ. Exp. Sta., Ames, IA, Project no. 2775, and supported by Hatch Act and State of Iowa. *Crop Science* **39**, 1733-1741.
**Wilkinson LG, Bird DC, Tucker MR**. 2018. Exploring the Role of the Ovule in Cereal Grain Development and Reproductive Stress Tolerance. *Annual Plant Reviews online*.
**Wilson ZA, Zhang D-B**. 2009. From Arabidopsis to rice: pathways in pollen development. *Journal of Experimental Botany* **60**, 1479-1492.
**Winter K-U, Saedler H, Theißen G**. 2002a. On the origin of class B floral homeotic genes: functional substitution and dominant inhibition in Arabidopsis by expression of an orthologue from the gymnosperm Gnetum. *The Plant Journal* **31**, 457-475.
**Winter K-U, Weiser C, Kaufmann K, Bohne A, Kirchner C, Kanno A, Saedler H, Theißen G**. 2002b. Evolution of Class B Floral Homeotic Proteins: Obligate Heterodimerization Originated from Homodimerization. *Molecular Biology and Evolution* **19**, 587-596.

**Wu F, Shi X, Lin X, Liu Y, Chong K, Theißen G, Meng Z**. 2017. The ABCs of flower development: mutational analysis of AP1/FUL-like genes in rice provides evidence for a homeotic (A)-function in grasses. *The Plant Journal* **89**, 310-324.
**Yadav SR, Prasad K, Vijayraghavan U**. 2007. Divergent regulatory OsMADS2 functions control size, shape and differentiation of the highly derived rice floret second-whorl organ. *Genetics* **176**, 283-294.
**Yamada K, Saraike T, Shitsukawa N, Hirabayashi C, Takumi S, Murai K**. 2009. Class D and B(sister) MADS-box genes are associated with ectopic ovule formation in the pistil-like stamens of alloplasmic wheat (Triticum aestivum L.). *Plant Molecular Biology* **71**, 1-14.
**Yamaguchi T, Hirano HY**. 2006. Function and diversification of MADS-box genes in rice. *The Scientific World Journal* **6**, 1923-1932.
**Yamaguchi T, Lee DY, Miyao A, Hirochika H, An G, Hirano H-Y**. 2006. Functional Diversification of the Two C-Class MADS Box Genes OSMADS3 and OSMADS58 in Oryza sativa. *The Plant Cell* **18**, 15.
**Yang X, Wu F, Lin X, Du X, Chong K, Gramzow L, Schilling S, Becker A, Theissen G, Meng Z**. 2012. Live and let die - the B(sister) MADS-box gene OsMADS29 controls the degeneration of cells in maternal tissues during seed development of rice (Oryza sativa). *PLoS One* **7**, e51435.
**Yang Y, Fanning L, Jack T**. 2003. The K domain mediates heterodimerization of the Arabidopsis floral organ identity proteins, APETALA3 and PISTILLATA. *The Plant Journal* **33**, 47-59.
**Yang Y, Jack T**. 2004. Defining subdomains of the K domain important for protein–protein interactions of plant MADS proteins. *Plant Molecular Biology* **55**, 45-59.
**Yao S-G, Ohmori S, Kimizu M, Yoshida H**. 2008. Unequal Genetic Redundancy of Rice PISTILLATA Orthologs, OsMADS2 and OsMADS4, in Lodicule and Stamen Development. *Plant and Cell Physiology* **49**, 853-857.
**Yoshida H, Itoh J-I, Ohmori S, Miyoshi K, Horigome A, Uchida E, Kimizu M, Matsumura Y, Kusaba M, Satoh H, Nagato Y**. 2007. superwoman1-cleistogamy, a hopeful allele for gene containment in GM rice. *Plant Biotechnology Journal* **5**, 835-846.
**Zadoks JC, Chang TT, Konzak CF**. 1974. A decimal code for the growth stages of cereals. *Weed Research* **14**, 415-421.
**Zahn LM, Leebens-Mack J, dePamphilis CW, Ma H, Theissen G**. 2005. To B or Not to B a Flower: The Role of DEFICIENS and GLOBOSA Orthologs in the Evolution of the Angiosperms. *Journal of Heredity* **96**, 225-240.
**Zampieri M, Ceglar A, Dentener F, Toreti A**. 2017. Wheat yield loss attributable to heat waves, drought and water excess at the global, national and subnational scales. *Environmental Research Letters* **12**, 064008.
**Zhang Z, Li H, Zhang D, Liu Y, Fu J, Shi Y, Song Y, Wang T, Li Y**. 2012. Characterization and expression analysis of six MADS-box genes in maize (Zea mays L.). *Journal of Plant Physiology* **169**, 797-806.
**Zhao XY, Cheng ZJ, Zhang XS**. 2006. Overexpression of TaMADS1, a SEPALLATA-like gene in wheat, causes early flowering and the abnormal development of floral organs in Arabidopsis. *Planta* **223**, 698-707.

**Zinn KE, Tunc-Ozdemir M, Harper JF**. 2010. Temperature stress and plant sexual reproduction: uncovering the weakest links. *Journal of Experimental Botany* **61**, 1959-1968.